b140 925 78

U.O.V.S. BIBLIOTEEK

ERDIE EKSEMPLAAR MAG ONDER
EEN OMSTANDIGHEDE UIT DIE
BLIOTEEK VERWYDER WORD NIE

University Free State
34300001167646
Universiteit Vrystaat

AQUIFER PARAMETER ESTIMATION IN FRACTURED-ROCK AQUIFERS USING A COMBINATION OF HYDRAULIC AND TRACER TESTS

BY

KORNELIUS RIEMANN

Submitted in fulfilment of the requirements for the degree of Doctor of Philosophy in the Faculty of Natural and Agricultural Sciences, Department of Geohydrology at the University of the Free State, Bloemfontein, South Africa

August 2002

Promoter: Prof. G.J. van Tonder

I dedicate this thesis to my lovely and dear friend, who had a hard time due to my decision to study in South Africa.

Without your love, support and understanding during these two years it would have been impossible to finish the thesis.

ACKNOWLEDGEMENTS

I have to express my thanks to many people for their support and encouragement during the process of my thesis. The acknowledgements given below are just a small choice of the whole.

My special thanks go to Prof. Wen-Hsing Chiang and Prof. Gerrit van Tonder, who offered me the possibility to study at the IGS and to write my Ph.D. Thesis. During the whole time they were supporting and encouraging me.

I thank all the students and the staff at the IGS for their support, especially Panganai Dzanga, Jaco Hough and Thilivhali Phophi for their help in conducting the field tests, and Ingrid van der Voort for her support during the project.

The financial support of the Water Research Commission of South Africa (WRC) for the projects "Decision Tool for establishing a Strategy for protecting groundwater resources: Data requirements, Assessment and Pollution Risk" and "Guidelines for Aquifer Parameter Estimation with Computer Models" is acknowledged. Without this support it would not be possible to finish the study.

My special acknowledgement goes to Diganta Sarma and Blessing Mudzingwa from the Water Resources Consulting cc. in Gaborone, Botswana and to the Department of Water Affairs, Botswana that I could be involved in the investigation for groundwater resources in the area of Tsabong. I appreciate the teamwork and the permission to use the field data of both hydraulic and tracer tests for my thesis.

Very special thanks go to Randall Roberts from the Sandia National Laboratory in Albuquerque, USA. He allowed me to use his software nSIGHTS as a beta tester and to use results obtained with this software in the thesis. The discussions with him via e-mail and telephone were always a challenge.

I thank Reinie Meyer from the CSIR in Pretoria for giving me the idea to search for a new methodology for estimating the kinematc porosity from tracer tests and for the permission to use the data from the field experiment in the case studies. The CSIR and the WRC funded the fieldwork, which is highly acknowledged.

At last but not least I thank my family in Germany for their understanding and support during my absence, especially my mother, my sister with her family and my brother with his family.

TABLE OF CONTENTS

CHAPTER 1 THEORY OF FLOW IN FRACTURED AQUIFERS 3

1.1. Introduction 3

1.2. Flow Characteristics in Fractured Aquifers 5

1.3. Flow Behaviour in Fractured Media 7

1.3.1. Linear Flow 7
1.3.2. Radial Flow 7
1.3.3. Spherical Flow 9

1.4. Well and Reservoir Effects 9

1.4.1. Well Bore Storage 10
1.4.2. Well Bore Skin 10
1.4.3. Partial Penetration Skin 12
1.4.4. Fracture Skin 12
1.4.5. Pseudo-Skin 14
1.4.6. Fracture Dewatering 14
1.4.7. Reservoir Boundaries 15

CHAPTER 2 THEORY OF TRANSPORT IN FRACTURED AQUIFERS .. 16

2.1. Mass Transport in Saturated Media 16

2.1.1. Transport by Advection 16
2.1.2. Transport by Concentration Gradients 17
2.1.3. Influence of Dispersion 18
2.1.4. Influence of Chemical or Biological Reactions 20

2.2. Governing Equations 21

2.3. Transport in Fractured Media 23

2.3.1. Influence of Fracture Geometry 23
2.3.2. Influence of Flow Geometry 24
2.3.3. Influence of Matrix Diffusion 25

CHAPTER 3 THEORY OF NON-INTEGER FLOW DIMENSION 27

3.1. Introduction 27

3.2. Fractal Reservoir Model 30

3.2.1. Mathematics of Fractals 30
3.2.2. Fractal Reservoir Model 31

3.3. Generalised Radial Flow Model 33

3.3.1. GRF-Model (Barker, 1988) 33
3.3.2. Extended GRF-Model (Roberts and Beauheim, 2001) 36

3.4. Comparison FR Model – GRF Model 38

CHAPTER 4 PARAMETER ESTIMATION 39

4.1. Hydraulic Parameters 41
4.1.1. Hydraulic Tests 41
4.1.1.1. Slug Tests 41
4.1.1.2. Multirate Tests 42
4.1.1.3. Constant Head Tests 42
4.1.1.4. Constant Discharge Tests 42
4.1.2. Analysing Methods 43
4.1.2.1. Diagnostic Tools 43
4.1.2.2. Analytical Methods 46
4.1.2.3. Numerical Models 56
4.1.2.4. Uncertainties of Numerical Models 65
4.1.2.5. Analytical vs. Numerical Models 69
4.1.3. Parameter Estimation 72
4.1.3.1. Thickness 72
4.1.3.2. Fracture Extent 77
4.1.3.3. Flow Dimension 78
4.1.3.4. Transmissivity 81
4.1.3.5. Hydraulic Conductivity 84
4.1.3.6. Storativity 88
4.1.3.7. Hydraulic Gradient 94
4.1.4. Discussion 96

4.2. Transport Parameters 97
4.2.1. Tracers 97
4.2.2. Tracer Tests and Analysing Methods 100
4.2.2.1. Single-well Tracer Tests, Natural Gradient 100
4.2.2.2. Single-well Tracer Tests, Forced Gradient 105
4.2.2.3. Multiple-well Tracer Tests, Natural Gradient 106
4.2.2.4. Multiple-well Tracer Tests, Forced Gradient 108
4.2.3. Parameter Estimation 112
4.2.3.1. Flow Velocity 112
4.2.3.2. Dispersion 121
4.2.3.3. Matrix Diffusion 124
4.2.3.4. Porosity 125
4.2.4. Discussion 127

CHAPTER 5 PROPOSED PROCEDURE FOR CONDUCTING HYDRAULIC AND TRACER TESTS 128

5.1. Procedure for Hydraulic Tests 128
5.1.1. Planning of Hydraulic Test 128
5.1.2. Conducting Hydraulic Tests in the Field 129
5.1.3. Data Measurement and Interpretation 130

5.2. Procedure for Tracer Tests 131
5.2.1. Planning of Tracer Test 131
5.2.1.1. Type of Test 131
5.2.1.2. Tracer 132
5.2.1.3. Flow Rate 135

5.2.1.4. Duration of Test ... 136
5.2.2. Conducting Tracer Tests in the Field ... 137
5.2.2.1. Installing the Equipment ... 137
5.2.2.2. Conducting the Test ... 141
5.2.2.3. Measurement Tools ... 143
5.2.3. Data Measurement and Interpretation ... 145

5.3. Combination of Hydraulic and Tracer Test ... 147
5.3.1. Radial Convergent Tracer Test – Hydraulic Test ... 147
5.3.2. Single-Well Tracer Test – Hydraulic Test ... 147

5.4. Developed Software for Tracer Test Analysis ... 148
5.4.1. TRACER-PLAN ... 148
5.4.2. TRACER ... 151

CHAPTER 6 CASE STUDIES ... 159

6.1. Campus Test Site ... 159
6.1.1. Geology ... 159
6.1.1.1. General ... 159
6.1.1.2. Borehole Construction ... 162
6.1.2. Hydraulic Tests ... 165
6.1.3. Tracer Tests ... 186
6.1.3.1. Single-Well Tests ... 186
6.1.3.2. Multiple-Well Tests ... 190

6.2. Meadhurst Test Site ... 194
6.2.1. Geology ... 194
6.2.2. Hydraulic Tests ... 197
6.2.3. Tracer Tests ... 202

6.3. Farm Griesel ... 203
6.3.1. Tracer Tests ... 203

6.4. Tsabong Botswana ... 205
6.4.1. Geology ... 205
6.4.2. Hydraulic Tests ... 207
6.4.3. Tracer Tests ... 213

CHAPTER 7 CONCLUSION AND RECOMMENDATION ... 221

7.1. Conclusion ... 221

7.2. Recommendation ... 224

CHAPTER 8 REFERENCES ... 225

APPENDICES ... 230

LIST OF FIGURES

Figure 1-1 Fracture networks embedded in different matrices, (a) impermeable, (b) micro fissured, (c) porous matrix (Krusemann and De Ridder, 1991)
Figure 1-2 The representative elementary volume REV of a fractured rock
Figure 1-3 Fracture flow domains and corresponding friction factors (after Louis, 1967)
Figure 1-4 Absolute and relative roughness of a parallel plate fracture model
Figure 1-5 Different flow phases observed in a single fracture of finite extension embedded in an infinite formation (adapted from Horne, 1997)
Figure 1-6 REV for a single vertical fracture with infinite conductivity. An observation point beyond the grey area would show only radial-acting flow behaviour (Van Tonder *et al.*, 2001)
Figure 1-7 Spherical flow behaviour in a bounded aquifer under isotropic (Kr = Kv) and anisotropic (Kr > Kv) conditions (Van Tonder *et al.*, 2001)
Figure 1-8 Relationship between gradient changes in the reservoir and well bore storage (Van Tonder *et al.*, 2001)
Figure 1-9 Well bore skin and its effect on the drawdown in a pumped well (Van Tonder *et al.*, 2001)
Figure 1-10 Flow to a fully penetrating (left) and a partial penetrating well (right), (Van Tonder *et al.*, 2001)
Figure 1-11 Drawdown in a single vertical fracture caused by a skin between fracture and matrix (Van Tonder *et al.*, 2001)
Figure 1-12 Effect of a fracture skin on the drawdown of the matrix and fracture system in a double porosity aquifer (Van Tonder *et al.*, 2001)
Figure 1-13 Effects of recharge and no-flow boundaries on drawdown curves (after Krusemann and de Ridder, 1991)
Figure 2-1 Spreading of a solute slug with time due to diffusion (Fetter, 1999)
Figure 2-2 Factors causing longitudinal dispersion at the scale of individual pores
Figure 2-3 Factors for dispersion at different scales (after Kinzelbach, 1992)
Figure 2-4 Illustration of the effect of retardation by comparing the breakthrough curve of a conservative solute (solid line) with the breakthrough curve of a retarded solute (dashed line); after Fetter (1999)
Figure 2-5 Flow and transport in a single fracture, showing zones of mobile and immobile water (Fetter, 1999)
Figure 2-6 Conceptual representation of channeling in the fracture plane (John and Roberts, 1991)
Figure 2-7 Schematic illustration of the effect of matrix diffusion (van der Voort, 2001)
Figure 3-1 Flow dimension definition in well testing (after Doe, 1991)
Figure 3-2 (a) parallel, orthogonal and acute fracture-wellbore intersections along a vertical wellbore; (b) corresponding intersection outlines (linear, circular, elliptical) and streamline patterns (parallel, radial, general); (after Aydin, 1997)
Figure 3-3 Power law properties of fractal networks; a) linear system D = 1, b) fractal network 1 < D < 2, c) radial system D = 2 (Acuna and Yortsos, 1995)
Figure 3-4 Characteristic fractal pressure transient behaviour in the abstraction borehole for a) $\delta < 1$ and b) $\delta > 1$ (Acuna and Yortsos, 1995)
Figure 3-5 Type curves for different flow dimensions (n), (Van Tonder *et al.*, 2001)
Figure 3-6 Influence of a bounded system (stars) compared to an infinite radial system (solid line) on a) flow area and b) flow dimension (Roberts and Beauheim, 2001)
Figure 4-1 Log-log and semi-log plots of theoretical time-drawdown relationships of consolidated fractured aquifers; (A) double-porosity aquifer; (B) single vertical fracture; (C) permeable dyke in a low permeable aquifer (after Kruseman and deRidder, 1991)

Figure 4-2 Effects of different conditions on drawdown and drawdown-derivative log-log plots (Roberts and Beauheim, 2001)
Figure 4-3 Natural fracture systems and their simplification into spherical-shaped blocks and slab-shaped blocks (van Tonder *et al.*, 2001)
Figure 4-4 Groundwater flow in an idealised double porosity aquifer (van Tonder *et al.*, 2001)
Figure 4-5 Example log-log plot of pressure change derivative showing the late-time straight line for flow dimension of n = 1.2, 2.0 and 2.7 (Roberts and Beauheim, 2001)
Figure 4-6 Semilog plot of the scaled second derivative of pressure change for constant rate tests with different flow dimension (Roberts and Beauheim, 2001)
Figure 4-7 The wedge-shaped slice taken from a full three-dimensional aquifer. Groundwater in this slice is assumed to be two-dimensional (after Verwey *et al.*, 1995)
Figure 4-8 System graph for dual-porosity system with 11 radial nodes and 3 matrix nodes (Roberts *et al.*, 2001)
Figure 4-9 Conceptual model of the flow in the sandstone aquifer of the Campus Test Site with the relevant parameters (explanation of the abbreviations in Table 4-2)
Figure 4-10 Model discretisation in three dimensions
Figure 4-11 Result of inverse modelling with vertical K-matrix higher than horizontal K-matrix
Figure 4-12 Comparison observed and calculated data for the UO5 test (2 l/s). Forward run with estimated values from UO5 test (0.5 l/s); a) Fracture piezometers, b) matrix piezometers above (bold = calibrated, fine = observed)
Figure 4-13 Required thickness for parameter estimation depending on geological set-up and aquifer test
Figure 4-14 Definition of the vertical width of a fracture, intersected in a borehole
Figure 4-15 Cone of depression during constant discharge test with the real hydraulic gradient (solid line) and averaged hydraulic gradient (dashed line) at observation points
Figure 4-16 Typical Time-Concentration relationship during a Point-Dilution Test
Figure 4-17 Movement of a tracer pulse during drift phase and pumpback phase (after Leap and Kaplan, 1988)
Figure 4-18 Velocity as a function of dimensionless time (t / t_*), applying Leap and Kaplan (1988) and Borowczyk *et al.* (1966)
Figure 4-19 Tracer plume movement in a natural flow field with influence of longitudinal and transversal dispersion and changing flow direction (after Fetter, 1999)
Figure 4-20 Radial flow field in a single fracture; a) possible flow paths due to heterogeneity, b) idealised flow paths in homogeneous medium (Shapiro and Nicholas, 1989).
Figure 4-21 Schematic view of capture and discharge zones in the vicinity of the injection well (Zlotnik and Logan, 1996)
Figure 4-22 Typical Dilution curve of a tracer test, (a) without subtracted background and (b) with subtracted background (Van Wyk, 1998)
Figure 4-23 Distortion of the flow field causes increased flux through the well (after Freeze and Cherry, 1970)
Figure 4-24 Applying one-dimensional and two-dimensional solutions to observation boreholes of natural flow tracer test; a) in the flow direction, b) normal to flow direction
Figure 4-25 Breakthrough curve from a radial convergent tracer test (dots) and relative recovery (triangle) with best fit (lines)
Figure 4-26 Theoretically simulated breakthrough curves showing the influence of dispersivity (Van Wyk *et al.*, 2001)
Figure 4-27 Influence of transversal dispersivity on shape of contamination plume (Fetter, 1999)

Figure 4-28 Influence of transversal dispersivity and heterogeneity on a tracer plume (after Fetter, 1999)
Figure 5-1 Tracer Movement in radial flow field (Zlotnik & Logan)
Figure 5-2 Equipment installing at injection and abstraction borehole; a) submersible pumps with a flow rate of 0.3 to 1 L/s, b) mono pump rigs, discharging up to 20 L/s
Figure 5-3 Required equipment and borehole installation for the injection borehole
Figure 5-4 Proposed design of an open container for tracer injection
Figure 5-5 Equipment and borehole installation for abstraction borehole
Figure 5-6 Different steps during the withdrawal part of the Injection-Withdrawal tracer test (values for concentration and time are examples)
Figure 5-7 Through-flow cell for measurement tracer concentration and physico-chemical properties of the water using electrodes (e.g. EC, pH, Ion sensitive Sensor)
Figure 5-8 Influence of calibration and recalculating on Darcy velocity, obtained from a Point-Dilution test; a) field data, b) calibrated and recalculated data
Figure 5-9 Influence of sampling on Darcy velocity, obtained from Point-Dilution test
Figure 5-10 Input Screen 'Basic Information' of software TRACER-PLAN
Figure 5-11 Input and output screen 'Test Set-Up' of software TRACER-PLAN
Figure 5-12 Output screen 'Simulation' of software TRACER-PLAN
Figure 5-13 Input screen 'Main' of software TRACER
Figure 5-14 Input and output screen 'Barker' of software TRACER
Figure 5-15 Inputscreen 'Calibration' of software TRACER
Figure 5-16 Input and output screen 'Point Dilution' of software TRACER
Figure 5-17 Input and output screen 'Radial Convergent' of software TRACER
Figure 5-18 Input and output screen 'Injection Withdrawal' of software TRACER
Figure 5-19 Input and output screen 'Natural Flow' of software TRACER
Figure 5-20 Output screen 'Results' of software TRACER
Figure 6-1 Locations of the boreholes at Campus Test Site
Figure 6-2 Lithology of boreholes on the Campus Test Site (after Botha *et al.*, 1998)
Figure 6-3 Borehole video of the fracture zone in borehole UO5 at a depth of between 20.9 – 21.1 m below surface, showing a fracture zone thickness of about 200 mm
Figure 6-4 Borehole Conductivity Log of UO28, showing the position of the fractures at 20.5m and 22m
Figure 6-5 Scheme of installing the piezometers into the boreholes
Figure 6-6 Drawdown in the abstraction and observation boreholes during the constant rate test at UO26. The values in parenthesis give the distance between individual boreholes and UO26, which was the abstraction borehole (at 0.7 L/s).
Figure 6-7 Measured drawdown after 2 minutes vs. distance of observation during constant rate test at UO26
Figure 6-8 Barker-method applied to the abstraction borehole UO26, yielding a flow dimension of 1.85. For comparison the simulated drawdown curve with a flow dimension of 2 is included.
Figure 6-9 UO5 pumping test, showing the drawdown behaviour in boreholes. UO5 was the abstraction borehole (rate of 1.25 l/s).
Figure 6-10 Cooper-Jacob II applied to the data of the UO5-test resulting in a T = 700 m^2/d for the fracture zone
Figure 6-11 Barker-method applied to the abstraction borehole UO5, yielding a flow dimension of 1.75. For comparison the simulated drawdown curve with a flow dimension of 2 is included.
Figure 6-12 Simulation result for UO5-test, using drawdown in abstraction borehole
Figure 6-13 Simulation result for UO5-test, using drawdown in observation borehole UP16
Figure 6-14 Jacobian Matrix for simulation UO5-test for observation borehole UP16
Figure 6-15 Simulation result for UO5-test, using drawdown in observation borehole UP16 and leaky aquifer model

Figure 6-16 Drawdown in the fracture-piezometers during constant discharge test UO5, July 2000
Figure 6-17 Drawdown in the matrix-piezometers below the fracture zone during the constant discharge test UO5, July 2000
Figure 6-18 Measured drawdown in UO5 (dots) during constant rate test at UO5, July 2000 and fitted curve with Gringarten-method, parameter values from table 3.4.3
Figure 6-19 Measured drawdown after 20 minutes vs. distance of observation during constant rate test at UO5, July 2000 (The estimated S-value is far too low for the fracture system. If neglecting the abstraction borehole UO5, an S-value of E-10 can be computed, which is even lower than expected)
Figure 6-20 Measured drawdown in the matrix-piezometer after 3000 minutes vs. distance of observation during constant rate test at UO5, July 2000
Figure 6-21 Best result of inverse modelling with observation data of fracture and matrix;
Figure 6-22 Drawdown in the fracture-piezometers during constant discharge test UO5, September 2000
Figure 6-23 Drawdown in the matrix-piezometers during constant discharge test UO5, September 2000
Figure 6-24 Comparison observed and calculated data for the UO5 test September 2000. Forward run with estimated values from UO5 test July 2000 a) Fracture piezometers, b) matrix piezometers above (bold = calibrated, fine = observed)
Figure 6-25 Point dilution measurements obtained in borehole UO20 under natural conditions
Figure 6-26 Tracer measurements measured during the pump back phase of the single-well injection-withdrawal test in borehole UO20. The large dot shows the tracer mass centre
Figure 6-27 Point dilution measurements obtained in borehole UO28 under natural conditions
Figure 6-28 Tracer measurements measured during the pump back phase of the single-well injection-withdrawal test in borehole UO28. The large dot shows the tracer mass centre
Figure 6-29 Point dilution measurements obtained during the UO5-tracer test in the injection borehole UO20
Figure 6-30 NaBr breakthrough curve and best fit obtained in the abstraction borehole (UO5) during the radial convergent UO5-tracer test. Fitted parameters obtained were v=51 m/d, dispersivity = 5.4 m and thickness = 0.15 m.
Figure 6-31 Point dilution measurements obtained during the UO26-tracer test in the injection borehole UO28
Figure 6-32 Uranine breakthrough curve and fit obtained during the UO26-tracer test (radial convergent). Fitted parameters obtained were v=51 m/d; dispersivity = 0.5 m and thickness = 0.16 m.
Figure 6-33 Position of boreholes, pitlatrines and septic tanks at Meadhurst test site
Figure 6-34 Borehole logs of M1 and M11, intersecting the dolerite dyke
Figure 6-35 Conceptual model of the flow in the Meadhurst aquifer, intersected by an abstraction borehole (after Barnard, 2001)
Figure 6-36 Drawdown in the abstraction borehole M1 and the observation borehole M2 during the constant rate test with 1.4 l/s at Meadhurst Test Site
Figure 6-37 Drawdown behaviour of the observation boreholes M2 and M3
Figure 6-38 Drawdown-distance plot of the constant rate test at Meadhurst Test Site
Figure 6-39 Comparison observed (fine line) and calculated drawdown (bold line) of the best fit; using the observation boreholes M2, M5 and M6. a) Observation borehole M2, b) Abstraction borehole M1 (data not used for calibration), c) Observation boreholes M5 and M6
Figure 6-40 Pumping test results and water strike information of borehole M11 on the Meadhurst Test Site

Figure 6-41 Breakthrough curve of fluorescein in borehole FP1 during Radial Convergent Tracer Test, including simulations of various peaks
Figure 6-42 Comparison of the porosity estimation from NMR (solid line; after Meyer, 2001) and single-well tracer tests, showing the geology
Figure 6-43 Geological map of the Tsabong area with detailed study areas (after Resources Services, 2001)
Figure 6-44 Time-Drawdown plot of long-term constant rate test at BH 9414, including simulated drawdown with Barker-method (solid line) and straight-line method of Cooper-Jacob (dashed line)
Figure 6-45 Time-Drawdown plot for observation borehole BH 9276 (15m away from abstraction), including simulated drawdown with Barker-method, yielding a flow dimension of 1.96
Figure 6-46 Time-Drawdown plot for observation borehole BH 9411 (100m away from abstraction), including simulated drawdown with Barker-method, yielding a flow dimension of 1.97
Figure 6-47 Drawdown-Distance method of Cooper-Jacob, applied to long-term constant rate test at BH 9414, yielding a transmissivity value of 220 m2/day and a storativity of 2.8 E-05
Figure 6-48 Time-Drawdown plot of long-term constant rate test at BH 9447, including simulated drawdown with Barker-method (solid line) and straight-line method of Cooper-Jacob (dashed line)
Figure 6-49 Time-Drawdown plot for observation borehole BH 9391 (5m away from abstraction), including simulated drawdown with Barker-method, yielding a flow dimension of 1.6
Figure 6-50 Time-Drawdown plot for observation borehole BH 9459 (1km away from abstraction), including simulated drawdown with Barker-method, yielding a flow dimension of 1.47
Figure 6-51 Drawdown-Distance method of Cooper-Jacob, applied to long-term constant rate test at BH 9447, yielding a transmissivity value of 555 m^2/day and a storativity of 3,6 E-06
Figure 6-52 Dilution in injection borehole BH 9391 during single-well test at BH 9391
Figure 6-53 Dilution in injection borehole BH 9391 during first radial convergent tracer test at BH 9447
Figure 6-54 Dilution in injection borehole BH 9391 during second radial convergent tracer test at BH 9447
Figure 6-55 Breakthrough curve for fluorescein during first radial convergent tracer test at BH 9447
Figure 6-56 Breakthrough curve for fluorescein during second radial convergent tracer test at BH 9447
Figure 6-57 Dilution in injection borehole BH 9276 during first radial convergent tracer test at BH 9414
Figure 6-58 Dilution in injection borehole BH 9276 during second radial convergent tracer test at BH 9414
Figure 6-59 Breakthrough curve for fluorescein during first radial convergent tracer test at BH 9414
Figure 6-60 Breakthrough curve for fluorescein during second radial convergent tracer test at BH 9414
Figure 6-61 Comparison of measurements of fluorescein (solid line) and salt (dots) during second radial convergent tracer test at borehole BH 9414

LIST OF TABLES

Table 4-1 Methods to estimate the different Flow and Transport Parameter
Table 4-2 Complete list of parameters for PEST-calibration
Table 4-3 Influence of the geometry of the model (a: best fit, b: Thickness below fracture is halved, c: Area of the fracture is halved, d: Area of the fracture is doubled)
Table 4-4 Comparison of the estimated parameter values for the UO5 tests, July and September 2000, obtained from the best fit of inverse modelling (July 2000) and the geometric mean of reasonable runs of inverse modelling (September 2000)
Table 4-5 Comparison of the results from analytical and numerical models for a aquifer with single, horizontal fracture zone in a sandstone matrix
Table 4-6 Comparison of estimated transmissivities and their geometric mean values, obtained from the numerical model application and the analytical methods
Table 4-7 Parameter values obtained from the UO20 point dilution test (injection for the UO5 radial convergent test) with different approaches.
Table 4-8 Parameter values obtained from the UO28 point dilution test (injection for the UO26 radial convergent test) with different approaches.
Table 4-9 Estimated flow velocities obtained from both the UO5 and UO26 tracer test, using different approaches.
Table 5-1 Suggested tracers and their possible application
Table 5-2 Assumed values for dispersion and diffusion for different geological structures
Table 5-3 Measurement tools for proposed tracer substances
Table 6-1 Test Sites for the case studies and their hydrogeological flow regime
Table 6-2 Depth of the fracture zone in the new boreholes (m under surface)
Table 6-3 Conditions for the constant discharge test UO26, conducted at Campus Test Site
Table 6-4 Results of the evaluated aquifer parameter for the constant rate test UO26
Table 6-5 Parameter values for the UO26-test obtained from the Barker model
Table 6-6 Parameter values for the UO5-test obtained from the Barker model
Table 6-7 Hydraulic parameters for the aquifer on the Campus Test Site as estimated with the three-dimensional model (Khm=horizontal matrix K; Kvm=vertical matrix K; Khf=fracture K; Ssm=matrix specific storativity)
Table 6-8 Estimated parameter values for the UO5-test, obtained from applying the nSIGHTS program
Table 6-9 Conditions for the constant discharge test UO5, conducted at Campus Test Site
Table 6-10 Results of the evaluated aquifer parameter for the constant rate test UO5, July 2000, obtained from the fracture-piezometers
Table 6-11 Estimated and assumed parameter values from the Gringarten-method for the constant rate test UO5, July 2000
Table 6-12 Results of the evaluated aquifer parameter for the constant rate test UO5, July 2000, obtained from the matrix-piezometers
Table 6-13 Estimated parameter values of the best fit of inverse modelling with observation data of the fracture and matrix (comparison of observed and calculated drawdown shown in Figure 6-21)
Table 6-14 Statistical data for the best fit of inverse modelling
Table 6-15 Minimum, maximum and mean values of the estimated parameters, obtained from all reasonable calibration runs compared with the results of the best fit
Table 6-16 Conditions for the constant discharge test UO5, conducted at Campus Test Site
Table 6-17 Results of the evaluated aquifer parameter for the constant rate test UO5, September 2000, obtained from the fracture- and the matrix-piezometers
Table 6-18 Comparison of the estimated parameter values for the UO5 tests, July and September 2000, obtained from the best fit of inverse modelling (July 2000) and the geometric mean of reasonable runs of inverse modelling (September 2000)

Table 6-19 Parameter values obtained from the UO20 point dilution and single-well injection-withdrawal tests by using a flow dimension n = 1.75 and n = 2 respectively
Table 6-20 Parameter values obtained from the UO28 point dilution and single-well injection-withdrawal tests by using a flow dimension n = 1.85 and n = 2 respectively
Table 6-21 Parameter values obtained from the UO5-tracer test by using a flow dimension n = 1.75 and n = 2 respectively
Table 6-22 Parameter values obtained from the UO26-tracer test by using a flow dimension n = 1.85 and n = 2 respectively
Table 6-23 Conditions for the constant discharge tests, conducted at Meadhurst Test Site
Table 6-24 Results from the Constant Rate Test at Meadhurst Test Site, using the standard methods of Cooper-Jacob and Theis.
Table 6-25 Estimated parameter values of forward modelling (best fit) with observation data of boreholes M2, M5 and M6 (comparison of observed and calculated drawdown shown in Figure 6-39)
Table 6-26 Conducted Tracer Tests at Test Site Griesel
Table 6-27 Results from Single Well Tracer Tests at Test Site Griesel
Table 6-28 Estimated aquifer parameters for constant rate test at BH 9414, applying the GRF-method and Cooper-Jacob-methods
Table 6-29 Estimated aquifer parameters for constant rate test at BH 9414, applying the GRF-method and Cooper-Jacob-method
Table 6-30 Results of radial convergent tracer tests at BH 9414
Table 6-31 Results of radial convergent tracer tests at BH 9414

NOTATIONS

A	Cross sectional area normal to the direction of flow	L^2
b	Extent of the flow domain	L
2b	Equivalent aperture of the fracture	L
C	Concentration of the tracer in the injection borehole at time = t	M/L^3
C_0	Concentration of the tracer in the injection borehole at t = 0	M/L^3
c (r,t)	Concentration of the tracer at time = t and distance = r	M/L^3
d	Length of the tested section in the borehole	L
D	Aquifer thickness	L
D_L	Longitudinal dispersion coefficient (= α_L v)	L^2/T
D_T	Transversal dispersion coefficient (= α_L v)	L^2/T
i	Horizontal hydraulic gradient	-
K	Hydraulic conductivity	L/T
K_f	Hydraulic conductivity of the fracture zone	L/T
K_{hm}	Horizontal hydraulic conductivity of the matrix	L/T
K_{vm}	Vertical hydraulic conductivity of the matrix	L/T
n	Flow dimension	-
N	Defined as 1-n/2	-
q	Darcy velocity under natural conditions	L/T
q_f	Darcy velocity under forced flow conditions	L/T
Q	Pumping rate of the well during abstraction phase	L^3/T
r	Distance along the flow path between the abstraction and observation borehole, or between the injection and abstraction borehole	L
r_f	Extent of a horizontal fracture, expressed as radius	L
r_W	Radius of the well	L
s (r,t)	Drawdown in borehole at distance = r and time = t	L
S	Storativity	-
S_{sf}	Specific storage of the fracture zone	1/L
S_{sm}	Specific storage of the matrix	1/L
t	Time since starting the test	T
t_d	Time elapsed from the injection of tracer until the centre of mass of the tracer is recovered	T
t_p	Time elapsed from start of pumping until the centre of mass of the tracer is recovered	T
T	Transmissivity	
u	Defined as $r^2S_{sf} / 4K_ft$	-
v	Natural groundwater velocity	L/T
v_f	Groundwater velocity under forced flow conditions	L/T
W	Volume of fluid contained in the test section	L^3
x_f	Half length of a vertical fracture	L
α	Borehole distortion factor	-
α_L	Longitudinal dispersivity	L
α_T	Transversal dispersivity	L
α_n	Area of a unit sphere in n dimensions	L^2
ε	Kinematic porosity	-
Γ	Gamma function	-
Γ (-N,u)	Incomplete Gamma function	-
Γ (0,u)	W (u) = Theis function	-
ΔM	Injected mass of tracer per unit section = Mass (kg) / Thickness (m)	M/L

INTRODUCTION

Water resources in South Africa are already being stressed and the country is slowly becoming a water-scarce country. This presents a challenge to all water resource managers to ensure that the basic water needs of every South African are met. A good estimation of the aquifer parameters is the basis of managing groundwater resources and understanding groundwater flow and transport processes. Because most of the suitable groundwater resources in Southern Africa occur in fractured rock aquifers, this thesis focuses on aquifer parameter estimation in fractured rock aquifers.

Pictures 1 and 2 give examples of typical fractured rock aquifers from Southern Africa as an illustration of the complexity of flow and transport pathways in secondary aquifers, due to fractures, fissures and porous matrix.

Picture 1 **Natural fracture network in a sandstone outcrop (Table Mountain Group, Hermanus)**

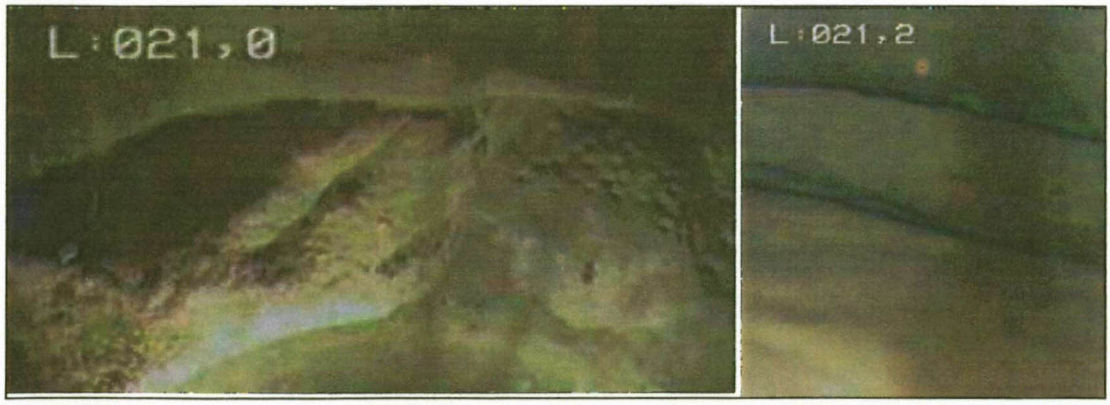

Picture 2 **Natural fracture zone in a sandstone aquifer (Karoo Aquifer, Borehole video of UO23, Campus Test Site Bloemfontein)**

Consider the geological setup and geometry of the fractured rock aquifers in South Africa (e.g. Karoo Aquifer), in general a three-dimensional groundwater flow must be considered when estimating aquifer parameters with pumping test data. However, most pumping test data are evaluated using analytical solutions such as Theis or Cooper-Jacob with assumptions that cannot be applied to fractured rock environments (van Tonder *et al.*, 2001). As the estimated parameters are the basis for further investigation, including sustainable management of groundwater resource and groundwater contamination estimation, a better methodology is required.

The findings in this research are mainly based on the following projects, conducted at the IGS and funded by the WRC:

- Decision Tool for establishing a Strategy for protecting groundwater resources: Data requirements, Assessment and Pollution Risk
- Guidelines for Aquifer Parameter Estimation with Computer Models
- Manual on Pumping Test Analysis in fractured-rock Aquifers

While the task in the first project was to develop methods for estimating transport parameters, the two other projects focused on the estimation of hydraulic parameters.

The purpose of this research is to suggest or develop procedures for aquifer parameter estimation, which are applicable in fractured rock aquifers in southern Africa, meaning working on low costs and without expensive equipment, but with reliable results. This includes field methods as well as analysing methods.

- Methods summarised from other authors are discussed related to their ability according to the above-mentioned criteria.
- New methods for conducting and analysing tracer tests are developed. They mainly account for non-integer flow dimension prevailing during the tests in fractured aquifers.
- A new method for estimating the kinematic porosity from single-well tracer tests is introduced and verified with several field measurements.
- The use of a 3-dimensional numerical model for aquifer parameter estimation is described in detail and discussed related to uncertainties. The results from several field tests are compared with different analytical methods.
- To enable the geohydrologist to conduct effective tracer tests, the software TRACER-PLAN was developed. Depending on the type of test and the geological structure the test set-up, such as discharge rates, amount of tracer and duration of the test, can be optimised.
- To simplify and unify the analysing procedure the software TRACER was developed, which enables the user to choose the correct analysing method depending on the test set-up and the conceptual model of groundwater flow. Most of the analysing procedures mentioned in this thesis are included.
- The ability and effectiveness of the proposed and suggested methods is proved by several field measurements of both hydraulic and tracer tests at different sites and thus different geological structures in southern Africa.

Chapter 1 Theory of Flow in Fractured Aquifers

1.1. Introduction

Characteristic for fractured aquifers is the fact that most of the water flows along fractures. Those fractures are usually embedded in porous matrix blocks (sandstone) or micro fissured blocks (quartzite), which are of low permeability compared to the fracture conductivity, but capable to store water in the uncountable pores or micro fractures. In extreme cases, the blocks between the fractures are of such low permeability (granite) that very little water can be exchanged between the fracture network and matrix, which is then called 'inert'. The following discussion is mainly taken directly from van Tonder *et al.* (2001).

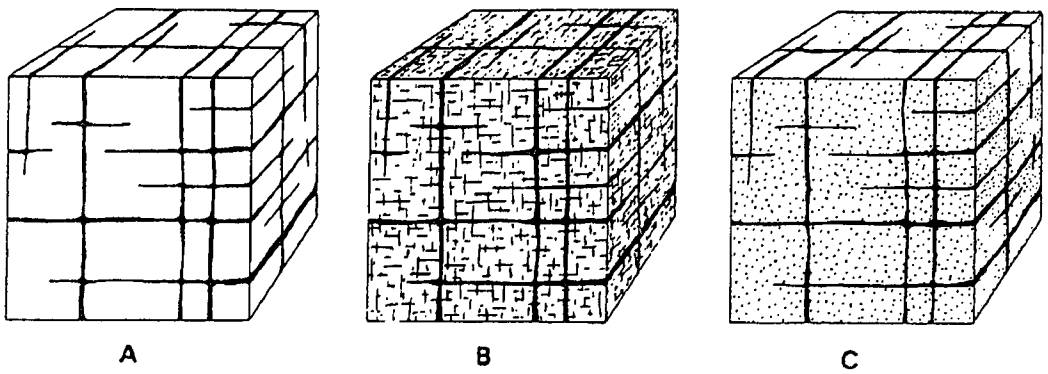

Figure 1-1 Fracture networks embedded in different matrices, (a) impermeable, (b) micro fissured, (c) porous matrix (Krusemann and De Ridder, 1991)

Another characteristic of fracture flow is related to the flow type. While the flow can be generally considered as laminar in porous media, the flow in fractures can vary between laminar and turbulent. The occurrence of turbulent flow depends mainly on the flow velocity and the geometry of the fractures; like roughness, aperture and orientation (see section 1.2).

If fractures are densely interconnected, they conform to a 'fracture network continuum' characterised by a large storage capacity that contributes substantially to the volume extracted by a pumped well. Whether a fracture network can be considered as continuum or not is determined by the following three properties:

- Representative elementary volume (REV).
- Fracture connectivity.
- Conductivity contrast between fracture and matrix.

The representative elementary volume (REV) of a fractured rock is considered hydraulically homogeneous (continuously fractured). A volume of rock larger than the REV would maintain the same hydraulic properties, but not a smaller volume (see Figure 1-2). Despite this physical explanation the REV should be considered a lumped parameter rather than a real geometrical value.

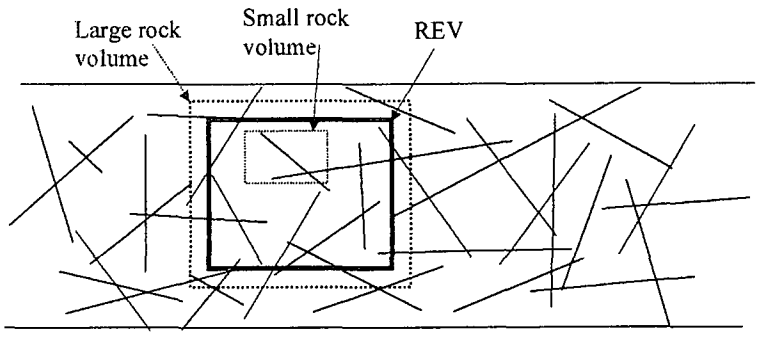

Figure 1-2 The representative elementary volume REV of a fractured rock

Whether the influences of a fracture network can be observed during a pumping test or not depends on the location of the observation point. If the REV is smaller than the drilled radius or the observation well distance is equal or further apart than the REV, the influence of the fracture network cannot be observed and the drawdown curve will follow a Theis curve. Therefore, only an observation point inside the REV can show the influence of the fracture network.

The fracture connectivity describes the interconnection between fractures in a given volume of rock, which is a function of the fracture length and fracture density. Generally, the fracture network continuity of a rock volume increases with increasing fracture length and fracture density (Long and Witherspoon, 1985).

The conductivity contrast between fracture and matrix can diminish or increase the continuous behaviour of a fracture network. Wei *et al.* (1998), by means of numerical modelling, observed linear flow in a well situated in a parallel fracture system, embedded in a matrix with a high conductivity contrast between fracture (K_f) and matrix (K) conductivities ($K_f/K = 10000$). The same fracture distribution with a lower contrast ($K_f/K = 100$) resulted in a long bilinear flow phase followed by a radial flow phase. A similar situation was observed in a perpendicular two-dimensional fracture network with low contrast, whereas using a high contrast, the system behaved a homogeneous media alike.

However, in both extremes the continuum and the single fracture case have very typical flow and drawdown behaviour that can be observed during pumping tests and will be described in the section 4.1.2.1

1.2. Flow Characteristics in Fractured Aquifers

The equations to describe the flow in fractured aquifers depend on the flow characteristic. Louis (1967) and others differentiates five flow characteristics depending on the relative roughness of the fracture walls and the Reynolds number (see Figure 1-3).

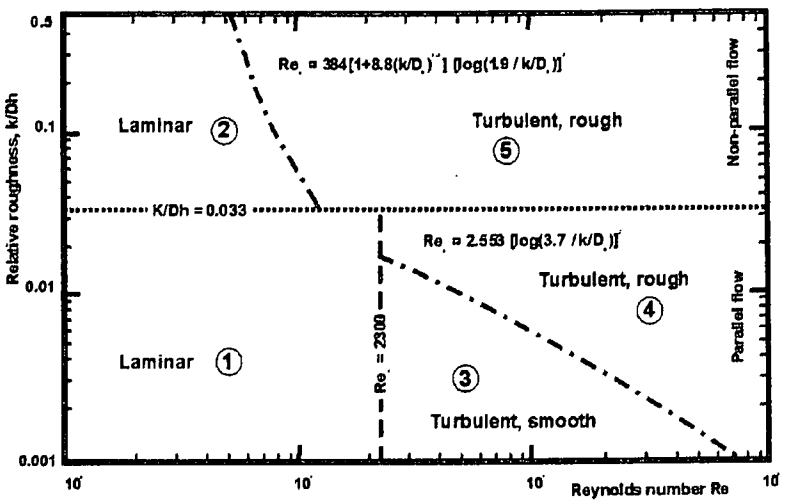

Figure 1-3 Fracture flow domains and corresponding friction factors (after Louis, 1967)

The relative roughness is defined as (Louis, 1967, see Figure 1-4):

$$k_r = k / D_h \qquad \text{(Equation 1-1)}$$

where

k	=	absolute roughness
D_h	=	hydraulic diameter (2 * 2b)
2b	=	fracture aperture

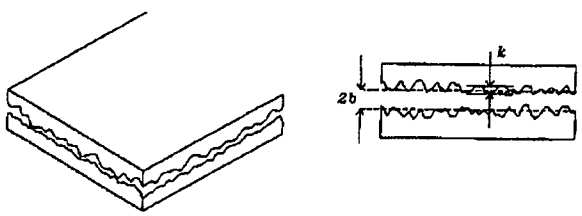

Figure 1-4 Absolute and relative roughness of a parallel plate fracture model

The Reynolds number in fractured flow can be defined as (Louis, 1967):

$$Re = (D_h \, v \, \rho) / \mu \qquad \text{(Equation 1-2)}$$

where

D_h	=	hydraulic diameter (2 * 2b)
v	=	averaged velocity
ρ	=	density of the fluid
μ	=	dynamic viscosity

According to the equations, Louis (1967) gives for the different flow characteristics, laminar flow can be characterised by a linear relation between flow rate and hydraulic gradient. For turbulent flow the flow rate becomes a function of the square root of the gradient. In most fracture networks the flow under natural conditions can be considered as laminar, only in wide-open features as faults and karstic aquifers or under high velocity turbulent flow becomes dominant.

The 'Darcian Law', which is valid for laminar flow, is written as:

$$Q = K \cdot \frac{\Delta h}{\Delta l} \cdot A \qquad \text{(Equation 1-3)}$$

where

Q = flow through the area A [L^3T^{-1}]
A = through-flow area [L^2]
Δh = potential or head difference over the length of interest l [L]
Δl = length of interest [L]
K = hydraulic conductivity [LT^{-1}]

The hydraulic conductivity is defined as

$$K = k\rho g / \mu \qquad \text{(Equation 1-4)}$$

where

ρ = density of the fluid [ML^{-3}]
g = acceleration of the gravity [LT^{-2}]
μ = dynamic viscosity [$ML^{-1}T^{-1}$]
k = permeability [L^2]

In the 'cubic law' (area 1 in Figure 1-3) the hydraulic conductivity is defined as

$$K = (2b)^2 \rho g / 12\mu \qquad \text{(Equation 1-5)}$$

and

$$A = bh \ [L^2] \qquad \text{(Equation 1-6)}$$

Replacing K and A in Equation (1-3) yields:

$$Q = \frac{b^3 \cdot \rho \cdot g \cdot h}{3 \cdot \mu} \cdot \frac{\Delta h}{\Delta l} \qquad \text{(Equation 1-7)}$$

where

b = aperture or width of the fracture [L]
h = height of the fracture [L]

Equation (1-7) represents the Poiseuille equation, which is valid for laminar parallel flow or Reynold numbers smaller than 2300 and a relative roughness smaller than 0.033. It shows that the rate Q is a function of the cube of the fracture aperture, hence the name 'cubic law'.

1.3. Flow Behaviour in Fractured Media

The following flow types can occur during pumping tests in fractured reservoirs (Barker, 1988):

- Linear flow.
- Radial flow.
- Spherical flow.

1.3.1. Linear Flow

The name 'linear flow' derives from the way in which the pressure drops along fractures: linear-proportional to the extraction rate. Linear flow is also described as 'parallel flow' (Kruseman and De Ridder, 1991) because of the parallelism between the streamlines.

The typical geological features where linear flow is observed are subvertical fractures, faults, or dykes. The different flow phases that can be distinguished during pumping tests in those features are listed below (Figure 1-5):

- Linear fracture flow is observed when the feature has a finite conductivity and is either embedded in an inert formation (matrix) or in a low conductive formation.
- If the matrix is permeable enough, the linear flow in the fracture is superposed by a perpendicular linear flow from the formation to the fracture. This flow situation is described as 'bilinear flow'.
- Linear flow from the formation to the fracture in the case of infinite conductive single features with negligible storage.
- A special case of bilinear flow occurs in reservoirs that consist of a continuous fracture network embedded in porous matrix blocks, which is known as double porosity reservoir.

1.3.2. Radial Flow

Radial flow (also known as pseudo-radial flow or radial-acting flow) appears when the cone of depression is approximately circular. It is generally observed in a fully penetrating well (line source) located in homogeneous reservoirs, but also in a well in any fractured reservoir that can be considered as continuum. The start of the radial flow indicates the time at which the fractured reservoir behaves as homogeneous. The distance from the pumped well at which the radial flow starts determines the dimension of the REV, as demonstrated in Figure 1-6.

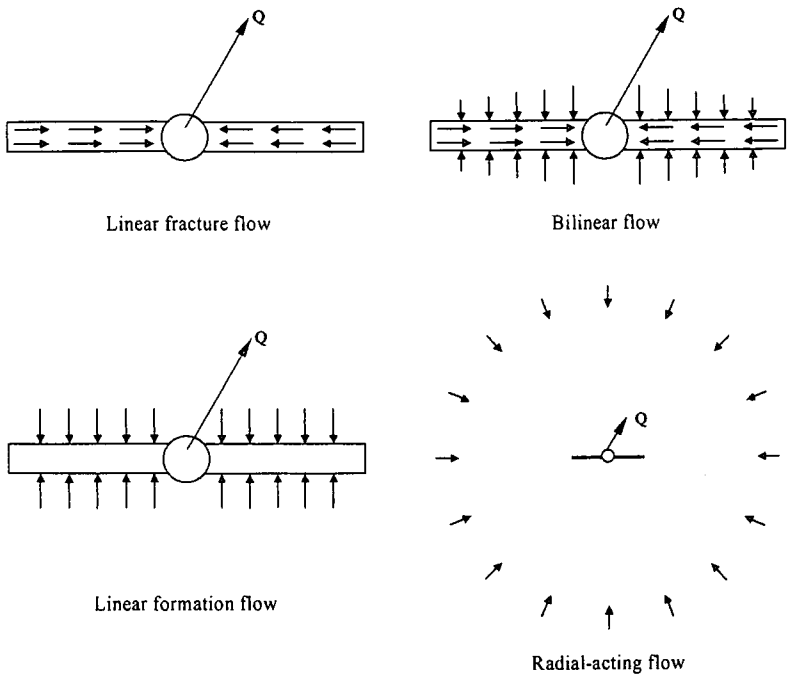

Figure 1-5 Different flow phases observed in a single fracture of finite extension embedded in an infinite formation (adapted from Horne, 1997)

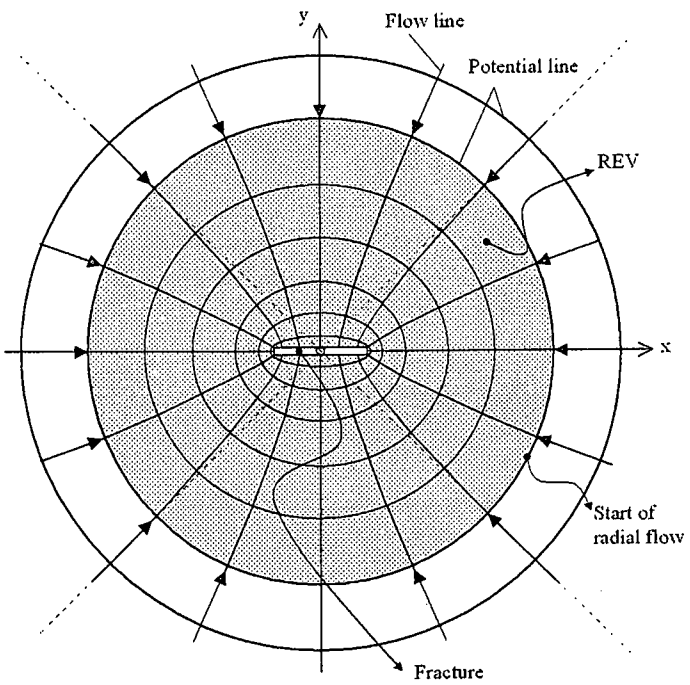

Figure 1-6 REV for a single vertical fracture with infinite conductivity. An observation point beyond the grey area would show only radial-acting flow behaviour (Van Tonder *et al.*, 2001)

The characteristic distance or dimension of the REV for a single fracture embedded in an infinite matrix equals 5 times the fracture's half-length x_f (Figure 1-6). An observation well located outside the REV will show only radial-acting flow as the characteristic flow behaviour. In instances where the REV coincides with the drilled radius r_w, any observation well will show radial-acting flow. Such observation data can then be analysed with methods usually applied to primary aquifers. For observations within the REV, the influence of the fracture network must be considered.

1.3.3. Spherical Flow

In cases where the extraction source is a point in an isotropic medium, the cone of depression becomes a sphere. In the real world, spherical flow will be observed only within small dimensions and over a short time period, because the spherical cone of depression will reach the bottom of the aquifer and the cone will become an ordinary radial flow (Figure 1-7). Furthermore, due to anisotropy effects in the aquifer the sphere will become an ellipsoid. Therefore, the spherical flow can be considered a special case of a partial penetrating well in a formation with isotropic conductivity ($K_x = K_y = K_z$ or $K_r = K_v$).

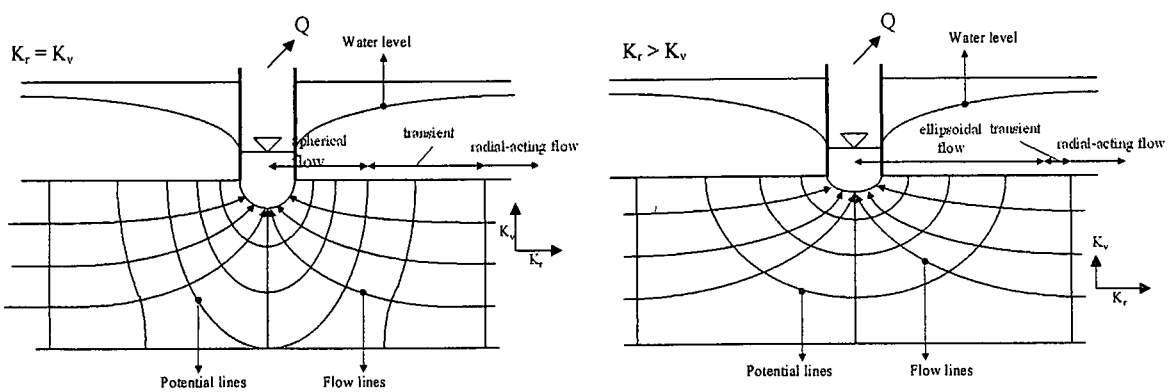

Figure 1-7 Spherical flow behaviour in a bounded aquifer under isotropic (Kr = Kv) and anisotropic (Kr > Kv) conditions (Van Tonder *et al.*, 2001)

1.4. Well and Reservoir Effects

The following well and reservoir effects can affect the drawdown and recovery data within fractured aquifers:

- Well bore storage.
- Well bore skin.
- Partial penetration skin.
- Fracture skin.
- Pseudo-skin.
- Fracture dewatering.
- Reservoir boundaries.

1.4.1. Well Bore Storage

Well bore storage effects occur due to changes in the water level or compressibility of the water well system. These effects are generally important at the beginning of the test but disappear with time. The well bore storage coefficient W_d in its dimensionless form is defined as (Moench, 1984):

$$W_d = \frac{r_c}{2 \cdot r_w^2 \cdot S} \qquad \text{(Equation 1-8)}$$

where

r_c = casing radius [L], where the water-level change occur
r_w = drilled radius [L]
S = specific storage coefficient of the reservoir [-]

Equation (1-8) is valid if the compressibility of the water well system is negligible. Immediately after commencement of extraction, all water is pumped from the storage volume of the well, as the gradient within the reservoir is still small; hence the enormous well bore storage effects at the beginning of the test. With time, the gradient within the reservoir increases gradually until all extracted water is provided by the reservoir and consequently the well bore storage effects disappear (Figure 1-8).

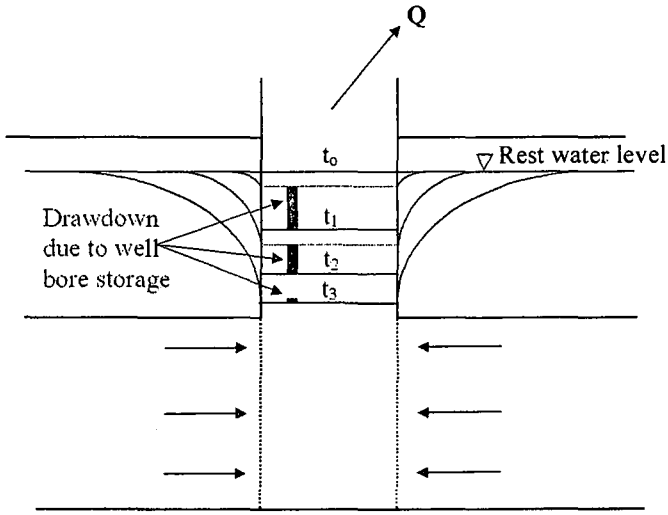

Figure 1-8 Relationship between gradient changes in the reservoir and well bore storage (Van Tonder *et al.*, 2001)

1.4.2. Well Bore Skin

The well bore skin is a thin layer with a very small storage capacity located between the borehole wall and aquifer that restricts the inflow to a pumped well. It averages the effects of various sources as clogged screens, gravel pack, too small open area of the screens and mineral precipitation between the well wall and formation. In the presence of a well bore skin, an additional drawdown is observed within the well (Figure 1-9). This effect is also known as well losses or skin effect.

The drawdown affected by a skin is a curve parallel to that without skin effects, whereas no effects appear during the recovery phase, except during the well bore storage period.

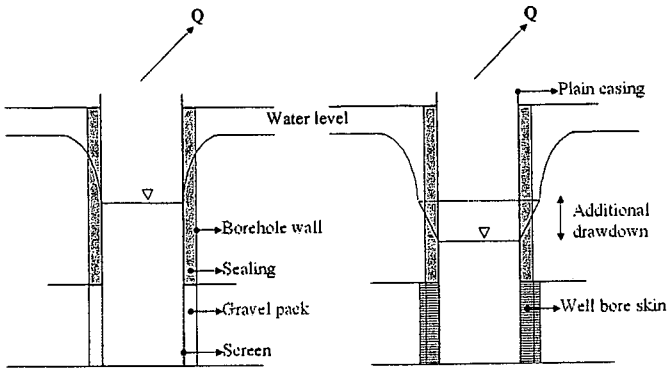

Figure 1-9 Well bore skin and its effect on the drawdown in a pumped well (Van Tonder *et al.*, 2001)

Considering the skin effect, the drawdown s for a fully penetrating well in a homogeneous confined aquifer, pumped at a constant discharge rate and negligible well bore storage writes (Theis, 1935)

$$s = \frac{Q}{4 \cdot \pi \cdot T} \cdot [Ei(u) + 2\xi] \qquad \text{(Equation 1-9)}$$

where

$$u = \frac{S \cdot r_w^2}{4 \cdot T \cdot t}$$

$$F(u) = Ei(u), \quad with \quad Ei = \int_u^{\infty} \frac{e^x}{x} dx$$

Q = discharge rate [L^3T^{-1}]
T = transmissivity [L^2T^{-1}]
t = time [T]
r_w = drilled radius [L]
S = storage coefficient [-]

The dimensionless well skin factor ξ derived from Equation (1-9) reads:

$$\xi = \frac{2 \cdot \pi \cdot T \cdot s}{Q} - 0.5 \cdot Ei(u) \qquad \text{(Equation 1-10)}$$

If $u \leq 0.03$, the exponential integral Ei(u) is satisfied by the Cooper and Jacob (1946) approximation: $Ei(u) \approx -\ln(1/u)-0.5772$ within 1% error. The corresponding additional drawdown s_{add} in metre can be calculated from following relationship (Kruseman and De Ridder, 1991):

$$s_{add} = \frac{\xi \cdot Q}{2 \cdot \pi \cdot T} \qquad \text{(Equation 1-11)}$$

In homogeneous aquifers and an ideal well, ξ is zero. Physically, this would mean that the effective radius r_{eff} is equal to the drilled radius r_w ,because ξ can be related to drilled radius as follows (Sabet, 1991):

$$r_{eff} = r_w \cdot e^{-\xi} \qquad \text{(Equation 1-12)}$$

In case of restricted inflow, ξ becomes positive, which according to Equation (1-12) results in an effective radius smaller than the drilled radius. In cases where the permeability of the formation around the well is improved, for example with well development, a negative ξ will be observed, which results in an enlarged effective radius. An increased effective radius will also be observed in a well situated in a single fracture that acts as a conduit.

1.4.3. Partial Penetration Skin

The reduced entrance area in a partial penetrating well causes an additional drawdown due to high velocity losses at the bottom of the well and anisotropy effects of the aquifer in the area close to the well (Figure 1-10).

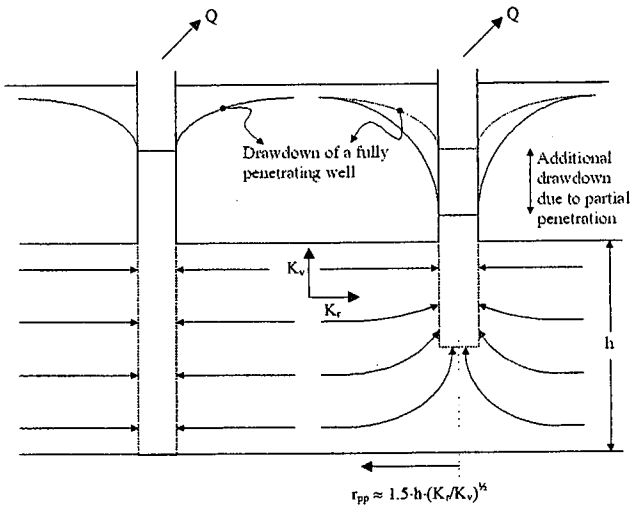

Figure 1-10 Flow to a fully penetrating (left) and a partial penetrating well (right), (Van Tonder *et al.*, 2001)

The slope of the drawdown in the early time data in the pumped and observation wells within the critical distance r_{pp} is increased and not only shifted as in the case of well bore skin. This effect can lead to an underestimation of the reservoir transmissivity, which might not be dangerous in the design of a water-supply scheme, but it certainly is in the design of a dewatering scheme for mining or engineering purposes. For late time data only an additional drawdown, shown as a parallel shift, is observed.

1.4.4. Fracture Skin

The fracture skin is a thin layer between fracture and matrix with reduced conductivity and very small storage capacity. Such a skin can be created by mineral precipitation or by clay minerals as a result of weathering. Fracture skin in a single fracture causes an additional drawdown similar to that of a well bore skin (Figure 1-11), whereas in fractured rock with double porosity behaviour, it results in a pseudo-steady flow exchange between fracture and matrix blocks (Figure 1-12). Cinco-Ley and Samaniego (1977) defined the fracture skin factor ξ_f as follows:

$$\xi_f = \frac{\pi \cdot b_s}{2 \cdot x_f} \cdot \left(\frac{k}{k_s} - 1 \right) \qquad \text{(Equation 1-13)}$$

where
b_s = thickness of the skin [L]
x_f = fracture half-length [L]
k = conductivity of the matrix or formation [LT^{-1}]
k_s = conductivity of the skin [LT^{-1}]

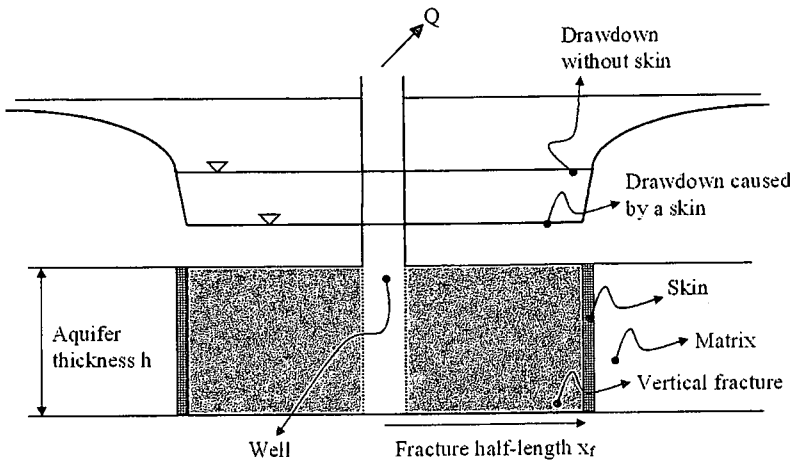

Figure 1-11 Drawdown in a single vertical fracture caused by a skin between fracture and matrix (Van Tonder *et al.*, 2001)

Moench (1984) defined the fracture skin factor for the double porosity solution as:

$$\xi_f = \frac{k \cdot b_s}{k_s \cdot b} \qquad \text{(Equation 1-14)}$$

where
b = average half-aperture of the fracture [L]

(a) No fracture skin (b) Fracture skin

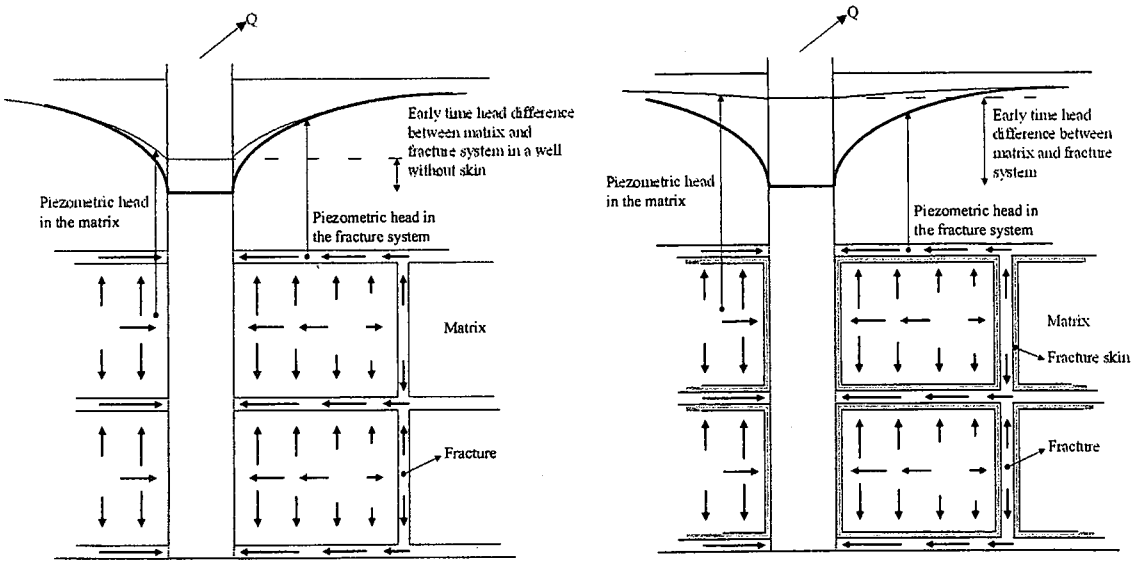

Figure 1-12 Effect of a fracture skin on the drawdown of the matrix and fracture system in a double porosity aquifer (Van Tonder *et al.*, 2001)

1.4.5. Pseudo-Skin

A well located within or in the proximity of a fracture that acts as a conduit shows less drawdown than that expected for wells in a homogeneous formation within the REV. This effect is known as pseudo-skin (Gringarten and Ramey, 1974). The determination of the skin using Equation (1-10) would lead to a negative skin factor ξ [-], which, after Equation (1-12), would result in a larger effective radius.

This effect can be used to determine whether a well is located in a fracture zone, as, in principle, no negative skin factor or enlarged effective radius is observed in a continuous fractured aquifer. If the REV is equal to or smaller than the drilled radius r_w, ξ will be zero. An exception might be a zone of higher permeability due to caving processes during the drilling works.

1.4.6. Fracture Dewatering

If a continuous fracture network (homogenous aquifer) is dewatered, the physical conditions change gradually with time due to the reduction of the down-hole influx area. Under these circumstances, the dewatering phenomenon can be approached, applying the Jacob correction $s' = s - s^2/2h$ to the drawdown data, as in an unconfined aquifer.

If a discontinuous fracture network is dewatered, a flattening followed by a sudden drop of the water level in the borehole is observed when it reaches the fracture (Van Tonder *et al.*, 1998). This effect is characteristic of discrete down-hole water strikes. In these cases the physical conditions in the vertical direction change instantaneously due to following reasons:

- The aquifer above the dewatered fracture becomes a purged aquifer that releases water into the fracture and borehole.
- Unconfined conditions in the dewatered fracture.
- Turbulent flow in the dewatered fracture and along the borehole wall.
- Reduced influx area.

The drawdown scenario can be described as follows:

- As soon the water level in the borehole reaches the water strike, e.g. a bedding plane, the flow conditions in the dewatered fracture change from confined to unconfined.
- If the storage capacity of the fracture is small compared to the discharge rate, the drawdown will drop continuously below the water strike at the cost of the well bore storage (this part of the curve in a log-log plot usually shows a slope of 1), until a new pressure difference between the water level in the borehole and the matrix builds up to cover the discharge rate.
- If radial flow is observed both before and after the dewatering of the fracture, the drawdown curve after the dewatering (e.g. the fracture) in the lin-log plot will show an increased slope compared to the initial one.

Fracture dewatering should be avoided, whenever feasible, because of the danger of mineral precipitation that can cause fracture and well clogging. These effects are directly related to the water chemistry. Precipitation occurs especially when oxygenation of waters with high manganese, iron or bicarbonate content is possible.

1.4.7. Reservoir Boundaries

All groundwater reservoirs are limited. Whether the influence of reservoir boundaries is seen in a pumping test curve is a function of the pumping time, the transmissivity, the storage coefficient and the distance of the boundaries, but not from the discharge rate. This can be demonstrated by the calculation of the distance at which the cone of depression is zero (drawdown s = 0). The Cooper-Jacob equation, which is the solution for the differential flow equation for long time (u < 0.03), gives:

$$s = \frac{0.183 \cdot Q}{T} \cdot \log\left(\frac{2.25 \cdot T \cdot t}{S \cdot r^2}\right) \qquad \text{(Equation 1-15)}$$

The radius at which the drawdown disappears is then given by:

$$r = \sqrt{\frac{2.25 \cdot T \cdot t}{S}} \qquad \text{(Equation 1-16)}$$

This equation is useful to estimate the extension of a cone of depression or, knowing the distance from the well to the boundary, to determine at which time t, the cone of depression will reach the boundary assuming that T/S (Diffusivity) remains constant. Equation (1-16) shows that the larger T and the smaller S, the bigger the cone of depression for a given time. The effects of positive and negative boundaries on the drawdown curve are shown in Figure 1-13. Basically, recharge boundaries show a flattening of the curve, whereas no-flow boundaries show an increase of the drawdown when the cone of depression reaches the boundary.

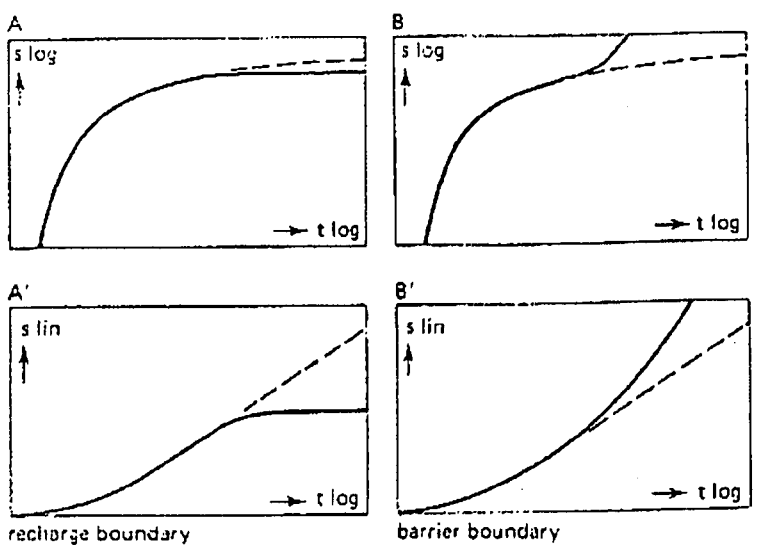

Figure 1-13 Effects of recharge and no-flow boundaries on drawdown curves (after Krusemann and de Ridder, 1991)

Chapter 2 Theory of Transport in Fractured Aquifers

In this chapter the processes involved in mass transport in aquifers will be described briefly with a special focus on processes in fractured aquifers. While in the first section the different factors and their impact on transport and concentration are discussed, followed by a section producing the governing equations, the third section describes the special situation of transport in fractured aquifers.

2.1. Mass Transport in Saturated Media

Mass transport in this document is understood as transport of chemicals or particles, completely in solution with the governing fluid, in this case water. Multi-phase flow is not considered. The following discussion is taken mainly from Fetter (1999).

Solutes in the groundwater generally moves with the groundwater flow, but the velocity and especially the concentration are governed by different phenomena, which are explained in the following sections:

- Advection
- Concentration Gradient
- Dispersion
- Sorption
- Chemical Reaction

2.1.1. Transport by Advection

Dissolved solids are carried along with the flowing groundwater, which is called advective transport or convection. The amount of solute that is being transported is a function of its concentration in the groundwater and the quantity of the groundwater flow. For one-dimensional flow normal to a unit cross-sectional of the porous media, the quantity of water flow is equal to the average linear velocity times the kinematic porosity. The one-dimensional mass flux F_x due to advection is equal to the quantity of water flow times the concentration of dissolved solids and is given by

$$F_x = v_x \varepsilon C \qquad \text{(Equation 2-1)}$$

where

v_x = average linear velocity
ε = kinematic porosity

The solution of the advective transport equation yields a sharp concentration front. On the advancing side of the front the concentration is equal to that of the invading groundwater, whereas on the other side of the front it is unchanged from the background value. This is known as plug flow, with all the pore fluid being replaced by the invading solute front.

Due to the heterogeneity of geologic materials advective transport in different strata can result in solute fronts spreading at different rates in each stratum.

2.1.2. Transport by Concentration Gradients

A solute in water will move from an area of greater concentration toward an area where it is less concentrated, which is known as molecular diffusion. Diffusion will occur as long as a concentration gradient exists, even if the fluid is not moving. The mass of fluid diffusing is then proportional to the concentration gradient which can be expressed as Fick's first law:

$$F = - D_d (dC/dx) \qquad \text{(Equation 2-2)}$$

Where

F	=	mass flux of solute per unit area per unit time
D_d	=	diffusion coefficient
C	=	solute concentration
dC/dx	=	concentration gradient

Fick's first law is valid under the assumption that the solute concentration C is constant over time. For systems where the concentrations change with time Fick's second law applies. In one dimension this is:

$$\partial C/\partial t = D_d \, \partial^2 C/\partial x^2 \qquad \text{(Equation 2-3)}$$

where

$\partial C/\partial t$	=	change in concentration with time

In porous media diffusion cannot proceed as fast as in water because the ions must follow longer pathways as they travel around mineral grains. To account for this an effective diffusion coefficient D* must be used.

$$D^* = \omega D_d \qquad \text{(Equation 2-4)}$$

Where ω is a coefficient that is related to the tortuosity. The value of ω, which is always less than 1, can be found from diffusion experiments in which a solute is allowed to diffuse across a volume of a porous medium. According to Freeze and Cherry (1979), ω ranges from 0.5 to 0.01 for laboratory studies using geologic materials.

Diffusion will cause a solute to spread away from the place where it is introduced into a porous medium, even in the absence of groundwater flow. Figure 2-1 shows the distribution of a solute introduced at concentration C_0 at time t_0. At times t_1 and t_2 the solute has spread out. Diffusion can occur when the concentration of a chemical species is greater in one stratum than in an adjacent stratum.

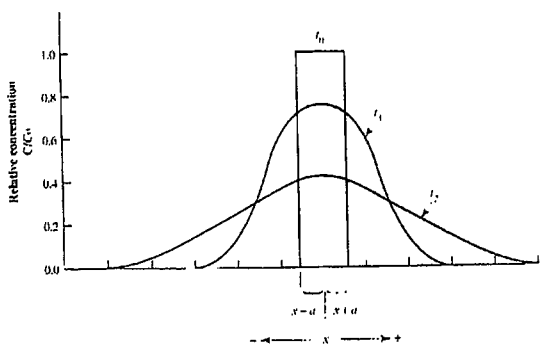

Figure 2-1 Spreading of a solute slug with time due to diffusion (Fetter, 1999)

2.1.3. Influence of Dispersion

Groundwater is moving at rates that both more and less than the average linear velocity. On a macroscopic scale there are three basic causes of this phenomenon (see Figure 2-2):

- As fluid moves through the pores it will move faster in the centre of the pores than along the edges.
- Some of the fluid particles will travel along longer flow paths in the porous media than other particles to go the same linear distance.
- Some pores are larger than others, which allows the fluid to move faster.

Because the invading solute-containing water does not travel at the same velocity, mixing occurs along the flowpath, which is called mechanical dispersion. It results in a dilution of the solute at the advancing edge of flow. The mixing that occurs along the direction of the flow path is called longitudinal dispersion, while mixing in directions normal to the flow path due to diverging flow paths is called transverse dispersion.

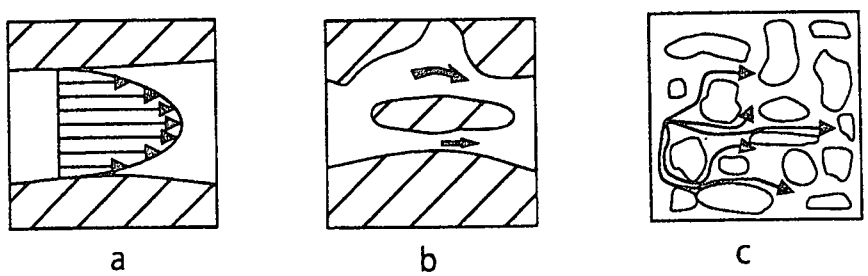

Figure 2-2 Factors causing longitudinal dispersion at the scale of individual pores

Assuming that mechanical dispersion can be described by Fick's law for diffusion and that the amount of mechanical dispersion is a function of the average linear velocity, a coefficient of mechanical dispersion can be introduced which is equal to a property of the medium, called dispersivity α, times the average linear velocity.

$$D_m = \alpha\, v \qquad \text{(Equation 2-5)}$$

Since the effects of molecular diffusion and mechanical dispersion in flowing groundwater cannot be separated, a parameter called hydrodynamic dispersion D is defined that combines both processes. It is represented by

$$D_L = \alpha_L\, v_i + D^* \qquad \text{(Equation 2-6)}$$

And $$D_T = \alpha_T\, v_i + D^* \qquad \text{(Equation 2-7)}$$

where

D_L = longitudinal hydrodynamic dispersion coefficient
D_T = transversal hydrodynamic dispersion coefficient
D^* = effective molecular diffusion coefficient
α_L = dispersivity in direction of flow (longitudinal)
α_T = dispersivity normal to direction of flow (transversal)
vi = averaged linear velocity

However, it is possible to evaluate the relative contribution of mechanical dispersion and diffusion to solute transport by means of calculating the Peclet number, which is a dimensionless number that can relate the effectiveness of mass transport by advection to the effectiveness of mass transport by either dispersion or diffusion. They have the form of

$$Pe = v_x d/D_d \text{ for ratio advection - diffusion} \quad \text{(Equation 2-8)}$$

And $$Pe = v_x L/D_L \text{ for ratio advection - dispersion} \quad \text{(Equation 2-9)}$$

Where

v_x = advective velocity
d = characteristic flow length, e.g. average grain diameter
L = characteristic flow length
D_d = coefficient of molecular diffusion
D_L = longitudinal hydrodynamic dispersion coefficient

At low Peclet numbers (i.e. low flow velocity) the influence of diffusion in solute transport is dominant, while at higher Peclet numbers mechanical dispersion is the predominant cause of mixing of the solute plume and the effects of diffusion can be neglected. Under these conditions D_L and D_T can be replaced with $\alpha_L v$ and $\alpha_T v$, respectively.

Gelhar (1986) showed that dispersion is scale dependent and will vary during the transport process. In the vicinity of the injection the dispersion at macro scale (pore scale) is the dominant factor, while with increasing distance from the injection field scale dispersion due to heterogeneity of the aquifer becomes predominant (see Figure 2-3).

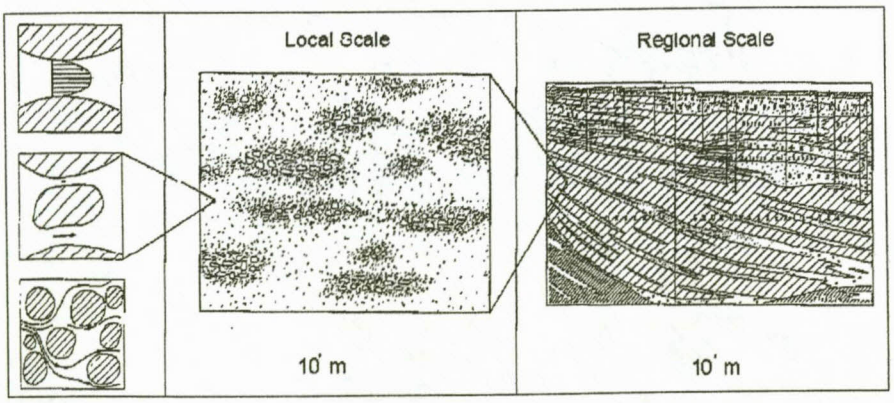

Figure 2-3 Factors for dispersion at different scales (after Kinzelbach, 1992)

2.1.4. Influence of Chemical or Biological Reactions

Solutes dissolved in groundwater, such as non-conservative tracers, can be subject to a number of processes through which they can be removed from groundwater. They can be sorbed onto the surface of the mineral grains of the aquifer, sorbed by organic carbon, undergo chemical precipitation, be subject to abiotic as well as biodegradation and participate in oxidation-reduction reactions. As a result of sorption processes, some solutes will move more slowly through the aquifer than the groundwater that transports them, which decreases the maximum concentration of the plume; this effect is called retardation. Biodegradation, radioactive decay and precipitation will decrease the concentration of solute in the plume but may not necessarily slow the rate of movement.

If the sorptive process is reversible and rapid compared with the flow velocity the solute will reach an equilibrium condition with the sorbed phase, which can be described by an equilibrium sorption isotherm. Introducing a retardation factor r_f the average groundwater velocity v_x and the average velocity of the solution front v_c can be related by:

$$v_c = v_x / r_f \qquad \text{(Equation 2-10)}$$

The definition and calculation of r_f depends on the appropriate sorption isotherm. Most common are the Linear, Freundlich and Langmuir sorption isotherms to describe reversible sorptive processes, which reach equilibrium in short time.

Figure 2-4 shows the general effect of retardation. While the solid curve shows the solute breakthrough with no retardation and no degradation, the dashed line is the breakthrough of a solute that undergoes retardation, which follows a linear sorption isotherm. It can be seen that the retarded substance has a lower peak value and that the peak comes later.

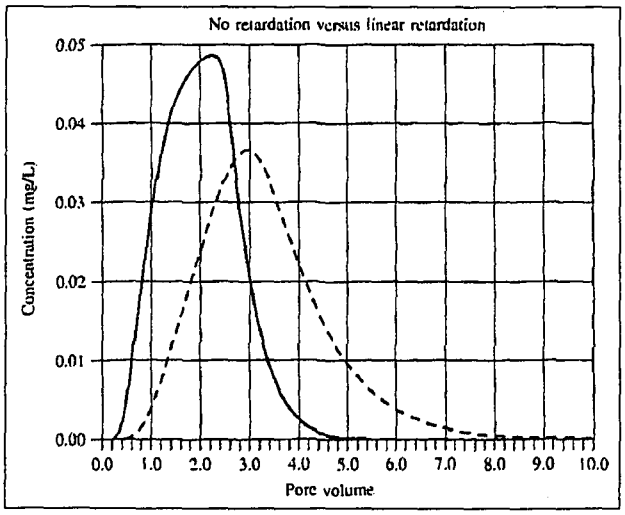

Figure 2-4 Illustration of the effect of retardation by comparing the breakthrough curve of a conservative solute (solid line) with the breakthrough curve of a retarded solute (dashed line); after Fetter (1999)

If the sorptive process is slow compared with the rate of fluid flow and / or irreversible, a kinematic sorption model will be needed to describe the process. Irreversible sorptive processes lead to attenuation of solute and not to retardation, which by definition is reversible.

Processes like biodegradation, radioactive decay and precipitation are irreversible and cause a decrease of concentration during the solute movement. To distinguish between the different effects a solute with multiple tracers should be used, where the different tracers have different physical and chemical properties.

2.2. Governing Equations

The derivation of the advection-dispersion equation is based on the conservation of mass of solute flux into and out of a small representative elementary volume (REV) of the porous media. Working assumptions are that the porous medium is homogeneous, isotropic and saturated with fluid and that flow conditions are such that Darcy's law is valid.

The solute will be transported by advection and hydrodynamic dispersion. The total mass of solute per unit cross-sectional area transported in the i direction per unit time is the sum of advective and dispersive transport and is given by:

$$F_i = v_i \varepsilon C - \varepsilon D_i (\partial C/\partial i) \qquad \text{(Equation 2-11)}$$

The negative sign indicates that the dispersive flux is from areas of greater to areas of lesser concentration.

By the law of mass conservation the rate of mass change in the representative elementary volume must be equal to the difference in the mass of solute entering and the mass leaving:

$$\frac{\partial F_x}{\partial x} + \frac{\partial F_y}{\partial y} + \frac{\partial F_z}{\partial z} = -\varepsilon \frac{\partial C}{\partial t} \qquad \text{(Equation 2-12)}$$

Substituting $F_{x,y,z}$ with Equation (2-11) and cancellation of ε from both sides, the three-dimensional advection-dispersion equation of mass transport for a conservative tracer (i.e. one that does not interact with the porous media or undergo biological or radioactive decay) becomes (Fetter, 1999):

$$\left[\frac{\partial}{\partial x}\left(D_x \frac{\partial C}{\partial x}\right) + \frac{\partial}{\partial y}\left(D_y \frac{\partial C}{\partial y}\right) + \frac{\partial}{\partial z}\left(D_z \frac{\partial C}{\partial z}\right)\right] - \left[\frac{\partial}{\partial x}(v_x C) + \frac{\partial}{\partial y}(v_y C) + \frac{\partial}{\partial z}(v_z C)\right] = \frac{\partial C}{\partial t} \qquad \text{(Equation 2-13)}$$

For one-dimensional uniform flow in a homogeneous, isotropic porous media Equation (2-13) reads as (Fetter, 1999):

$$\frac{\partial C}{\partial t} = D_L \frac{\partial^2 C}{\partial x^2} - v_x \frac{\partial C}{\partial t} \qquad \text{(Equation 2-14)}$$

Including terms for sorption and decay Equation (2-14) becomes (Fetter, 1999):

$$\frac{\partial C}{\partial t} = D_L \frac{\partial^2 C}{\partial x^2} - v_x \frac{\partial C}{\partial t} - \frac{B_d}{\theta} \frac{\partial C^*}{\partial t} + \left(\frac{\partial C}{\partial t}\right)_{rxn} \qquad \text{(Equation 2-15)}$$

(sorption) (decay)

where

C	=	concentration of solute in liquid phase
t	=	time
D_L	=	longitudinal dispersion coefficient
v_x	=	average linear groundwater velocity
B_d	=	bulk density of aquifer
θ	=	volumetric moisture content or porosity for saturated media
C*	=	amount of solute sorbed per unit weight of solid
rxn	=	subscript indicating a biological or chemical reaction of the solute (other than sorption)

The third term is the transfer of solute from the liquid phase to the solid particles by sorption, while the last term simply indicates that there may be a change in concentration of the solute with time due to biological or chemical reactions or radioactive decay.

In most natural cases of solute transport over a wider range of scales the dispersion cannot be expressed fully with Fick's laws. Benson *et al.* (2000) developed a fractional advective-dispersion equation to account for anomalous or non-Fickian dispersion. When the tails of a breakthrough curve are heavy enough, non-Fickian dispersion results for all time scales and space scales. The one-dimensional form of the fractional advection-dispersion equation reads:

$$\frac{\partial C}{\partial t} = -v_x \frac{\partial C}{\partial t} + Dp \frac{\partial^\alpha C}{\partial x^\alpha} + D(1-p) \frac{\partial^\alpha C}{\partial (-x)^\alpha} \qquad \text{(Equation 2-16)}$$

where

D	=	constant dispersion coefficient
p	=	factor, describing the skrewness of the transport ($0 < p < 1$)
α	=	order of fractional differentiation

Solutions of the advective-dispersion equation depends on the kind of tracer test and transport conditions and therefore on the initial and boundary conditions. Mathematical solutions for different types of tracer tests are discussed in Chapter 4.2.

2.3. Transport in Fractured Media

Solute transport in fractured rock media is as important a process as transport in porous media. However, the processes are much more complex and any prediction has to be based on assumptions without knowing the reality in detail.

The rock in which fractures exist is often porous. Hence fluid moves in the fractures as well as in the rock matrix. Solutes in the fractures can diffuse into the fluid contained in the rock matrix and vice versa. The fractures themselves are not smooth channels but contain dead-end passages that hold non-moving water into which solutes can diffuse. Three main effects have to be considered, when analysing solute transport in fractured rock aquifers:

- The geometry of the single fracture
- The geometry of the fracture network, prevailing the flow geometry
- The interactions between fracture flow and matrix

2.3.1. Influence of Fracture Geometry

One of the first considerations in dealing with fracture flow is deciding how to treat flow in a single fracture. Assuming that the fracture can be simulated with a parallel plate model the transport within the fracture is mainly due to advection, which occurs at different rates, depending upon the position between the parallel walls of the fracture. This parabolic velocity profile across the width of the fracture results in an order of dispersion between the fracture walls, called the Taylor dispersion.

Detwiler *et al.* (2000) show the importance of Taylor and macro dispersion for solute transport in a fracture with variable aperture. The relative influence of the two types of dispersion is a non-linear function of the Peclet number *Pe*. At intermediate values of *Pe*, macro dispersion dominates, while at large *Pe* values, Taylor dispersion dominates. The influence of Taylor dispersion can become evident at low Reynolds numbers, indicating laminar flow (see Chapter 1.2) and it is the dominant dispersion mechanism in regions, where 'Darcian Law' is not valid.

At high flow rates advection-dispersion will dominate, while at low velocities diffusion becomes important, since the concentration gradient at the solute front will be high and the distance will be short. Under these conditions diffusion will homogenise the solute across the width of the fracture. Whether or not diffusion inside the fracture can be neglected is a function of the fracture residence time and the fracture aperture.

Raven *et al.* (1988) pointed out that the fractures through which flow occurs are not smooth, parallel plates but have irregular walls that promote the formation of zones along the edge of the fracture where the water is immobile (see Figure 2-5). The fluid moves through the mobile zone, but the solutes can diffuse into the immobile fluid zones. The solute would be stored in the immobile fluid during the early part of solute transport and would be released from storage if the solute concentration in the mobile fluid would decrease sufficiently.

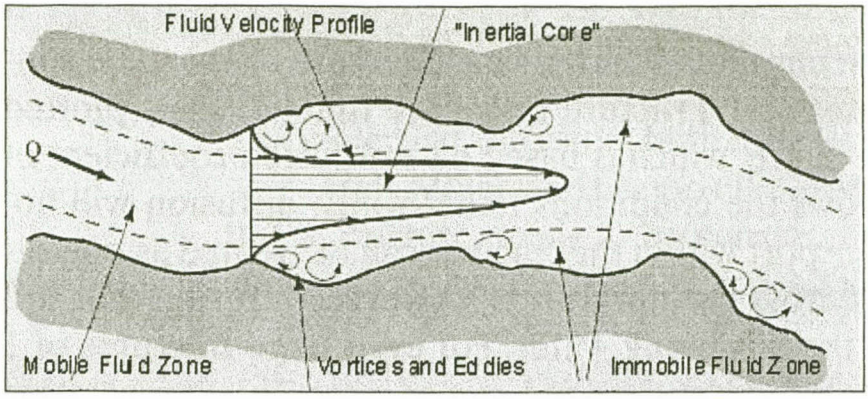

Figure 2-5 Flow and transport in a single fracture, showing zones of mobile and immobile water (Fetter, 1999)

The effect of the immobile fluid zones, caused by variable fracture aperture, on the solute transport is demonstrated by Grenier *et al.* (1998) by means of a numerical model. The stagnant water is a major pathway for the diffusive mass transfer into the rock matrix (see below). By means of Monte-Carlo simulations they illustrate that the surface area of the fracture walls covered by stagnant water is a function of the geometric mean aperture.

2.3.2. Influence of Flow Geometry

At local and regional scales fractured rock aquifers cannot be described sufficiently with a parallel plate model of a single fracture. The flow occurs normally in a fracture zone consisting of several interconnected fractures. Furthermore single fractures have variable apertures, resulting channels of higher velocity and dead-end zones. The geometry of the fracture network as well as single fractures is mostly unknown but influences the flow geometry to a great extent.

Different conceptual and numerical models have been developed to account for the flow geometry. John and Roberts (1991) developed a solute transport model for channelised flow in a fracture, focusing on the large aperture regions in the fracture plane (see Figure 2-6). Nordquist et al. (1996) show by means of a numerical model that channelised flow is caused by high variance of fracture transmissivity or fracture aperture and will result in multi-peak transport breakthrough curves.

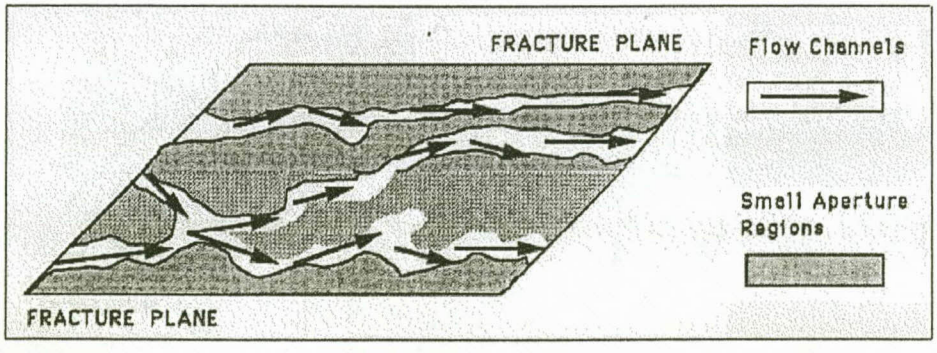

Figure 2-6 Conceptual representation of channeling in the fracture plane (John and Roberts, 1991)

Moench (1995) developed a model for transport in a double porosity aquifer, which accounts for matrix diffusion and retardation effects due to the difference in porosity between fracture network and matrix blocks. In keeping with the double-porosity concept the hydraulic conductivity of the blocks is small in comparison with the hydraulic conductivity of the aquifer as a whole, and advection within the blocks is neglected. The tracer is assumed to diffuse across a layer of low-diffusivity material or fracture skin and throughout the rock matrix in accordance with Fick's law.

The disadvantage of all these models is that they are based on assumptions about the fracture network and geometry, which might be inconsistent with reality, since the flow geometry is still unknown. A generalised model to account for the unknown flow geometry is discussed in Chapter 3, while the applications of the generalised flow model to solute transport are developed and discussed in Chapter 4.2.

2.3.3. Influence of Matrix Diffusion

As discussed above, the solute can diffuse from the flowing fluid into zones of immobile water. Furthermore the solute can diffuse into the fluid, which fills the small pores and micro fissures in the rock matrix (see Figure 2-7). This effect causes a delay in the transport process and a loss of solute and is called matrix diffusion. From field experiments it becomes obvious that the effect of matrix diffusion cannot be neglected in fractured rock aquifers (e.g. Novakowski *et al.*, 1995). In tracer test studies at the Campus Test Site (see section 6.1) the loss of tracer mass due to matrix diffusion was found to be up to 30%.

Shapiro (2001) demonstrates that the effect of matrix diffusion in kilometre-scale transport cannot be distinguished from the retarded solute transport due to fractures with large contrasts in transmissivities. Advective mass exchange from high-permeability fractures to low-permeability fractures results in short migration distances of the solute in low-permeability fractures over an extended period of time. Viewed at kilometre-scale, this process is analogous to the solute diffusing into and out of an immobile fluid phase.

The result of matrix diffusion is similar to sorption processes but should not be confused because the process of matrix diffusion is dominated by the physical properties of the aquifer (i.e. velocity in the fracture, porosity of the matrix, diffusivity of the matrix), rather than the physical properties of the tracer. Van der Voort (2001) examined matrix diffusion coefficients for different rock types of South Africa by means of laboratory experiments. The difference of the coefficient values for different chemicals is small compared with the variety of rock types. The dependency upon the porosity of the rock matrix could be proved for most rock types.

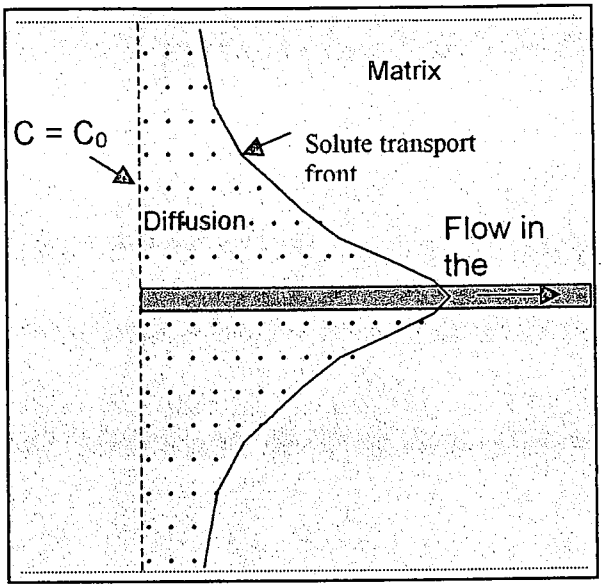

Figure 2-7 Schematic illustration of the effect of matrix diffusion (van der Voort, 2001)

The effect of the porosity on matrix diffusion is also proved by an investigation of Tidwell *et al.* (2000) using X-ray absorption imaging. Significant variations in the diffusion coefficient were calculated, which are related to the heterogeneous porosity characteristic of each rock sample. Specifically, the geometry, position, and orientation of the heterogeneous porosity features appeared to influence the diffusion characteristics.

Diffusion within the matrix is typically modelled as a Fickian process where the concentration gradient controls the mass transfer. However, as a solute is moving between fracture and matrix a sharp gradient is encountered in both porosity and diffusivity, which are both controlling parameters for the mass transfer rate.

Some authors (e.g. Maloszewski and Zuber, 1993) introduce a special retardation factor to account for matrix diffusion. Since sorption processes and matrix diffusion are difficult to distinguish and, if using non-conservative tracers, occur together often, this approach is applicable. The best methods, suitable for conditions in Southern Africa, are discussed in Chapter 4.2.

Chapter 3 Theory of non-integer Flow Dimension

The spatial distribution of flow through the fractures towards the well depends entirely on the properties of the fracture network, such as fracture conductivity, fracture density and connectivity (e.g. Barker, 1988; Black, 1994). The characteristics of the fracture network determine the flow geometry, which is also known as **flow dimension**. Flow towards a pumped well is usually concentrated along a certain fracture zone, while large volumes of hard rock could remain isolated from this zone of relatively high permeability activated by the pumping test. In contrast, the pattern of flow towards a fully penetrating well may be radial (two-dimensional) throughout a hard rock aquifer consisting of a highly connected fracture system with an isotropic distribution. For a correct assessment of the hydraulic parameters of a fractured hard rock aquifer using pumping test data, it is necessary to know how much flow relates to a certain drawdown response of the aquifer, i.e. it is necessary to know the flow geometry or flow dimension (Verweiji and Barker, 1999). Roberts and Beauheim (2001) discussed the concept of a flow dimension and show that it actually represents the rate at which hydraulic conductance (the product of hydraulic conductivity and through-flow area) changes with distance from a test borehole. **No unique estimation of hydraulic parameters is possible from hydraulic tests without knowledge of the flow geometry**. The following discussion is mainly taken from van Tonder *et al.* (2001).

3.1. Introduction

According to Black (1994), the area available to flow in an aquifer is a function of the distance to the pumped well and is given by:

$$A = A_0 r^{(n-1)} \qquad \text{(Equation 3-1)}$$

where,

A	=	through-flow area
A_0	=	through-flow area at the pumped well (r = 0)
n	=	flow dimension
r	=	distance to the pumped well

Flow dimensions range between 1 and 3 (Barker, 1988; Black, 1994) and for a one-dimensional flow geometry (n = 1), the area through which flow occurs will remain constant, regardless of the distance r (Figure 3-1). A period of linear flow through a fracture or dyke during a pumping test, when all the water pumped originates from storage in the dyke or fracture corresponds to a flow dimension of 1. For a flow dimension of 2, corresponding to radial flow to a well, the through-flow area will increase in direct proportion to the distance r from the pumped well. This kind of flow dimension is not an intrinsic property of a fractured hard rock aquifer because it usually changes in time during a pumping test, which is reflected in the time drawdown behaviour at the pumped well and observation wells. The drawdown response at a certain time, as observed at the pumped well and observation wells, might all reflect different flow dimensions. The flow dimension prevailing during a test is thus a function of scale (time).

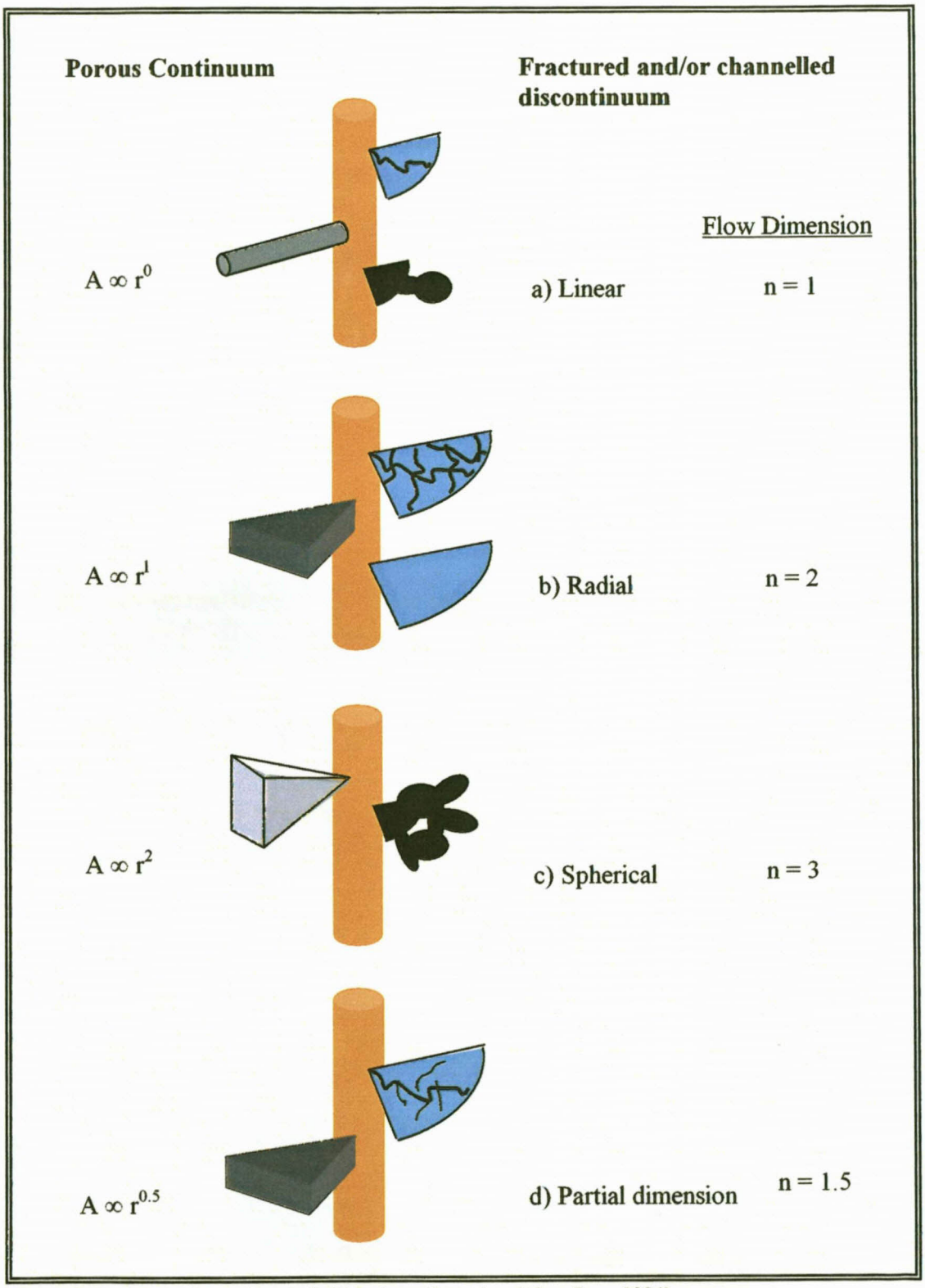

Figure 3-1 Flow dimension definition in well testing (after Doe, 1991)

The time and scale dependence of flow dimension can be illustrated by looking at the flow pattern created when a fractured vertical dyke or fault bisecting an aquifer, the transmissivity of which is several times less than that of the fault, is pumped (see discussion in chapter 1). The concept of flow dimension plays an important role in selecting the appropriate time-drawdown data to be used in a certain method.

Aydin (1997) shows that linear or radial flow to the well can only be considered in the case of a vertical and a horizontal fracture intersected by a vertical well. The geometry of the inner boundary (well–fracture intersection) determines the streamline pattern and subsequently the head distribution. The geometry is, in turn, determined by the angle of intersection between a fracture and the wellbore. For parallel or orthogonal intersections, the inner boundary outlines are linear and circular and the streamlines are parallel and radial, respectively (see Figure 3-2). Acute intersections produce outlet sections that are elliptical in plan view. For a given wellbore radius, as the ratio of the axes of the ellipse varies with the intersection angle, the streamline pattern is not of a fixed form but a general one.

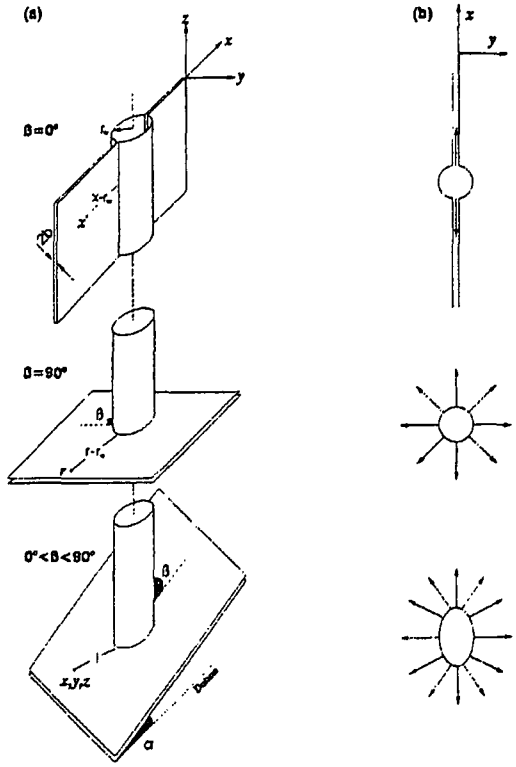

Figure 3-2 (a) parallel, orthogonal and acute fracture-wellbore intersections along a vertical wellbore; (b) corresponding intersection outlines (linear, circular, elliptical) and streamline patterns (parallel, radial, general); (after Aydin, 1997)

The flow to a well in a hard rock aquifer that consists of a fracture system having **fractal properties** may not be adequately characterised by a one-, two- or three-dimensional flow geometry. Instead, non-integer fractional flow dimensions will describe the flow behaviour more accurately (Barker, 1988). The value of the fractional flow dimension depends on the fracture geometry like orientation, connectivity and variability of aperture.

3.2. Fractal Reservoir Model

Presently different models were developed accounting for the flow in fractured rock aquifers to consider for the uncertainty of geometry (Black, 1994). While most of these models simplify the geometry assuming single fractures or dual porosity systems with homogenous distribution of fractures (see Chapter 4), some models account for a fractal geometry or behaviour, which can often be observed in fracture networks (e.g. Acuna and Yortsos, 1995).

3.2.1. Mathematics of Fractals

The word fractal originated from the Latin adjective *fractus*; the corresponding word *frangere* means to fracture or create irregular fragments. A fractal is therefore a geometrical figure in which an identical pattern repeats itself on an ever-diminishing scale. A good example of a fractal is a tree trunk with two branches that separates repeatedly into smaller branches. Each branch, however small, can in turn be regarded as a small trunk that carriers an entire tree. Clouds, mountains, coastlines and turbulent storms are typical physical examples of objects with fractal geometry.

Two very important notions in the mathematics of fractals are those of self-similarity and self-affiness. A set of N scale objects is said to be self-similar if each of the figures has exactly the same form as the original figure, but at a scale r of its predecessor. A self-similar figure is therefore a combination of N copies of itself. A self-affine fractal shares the same properties as a self-similar fractal, except that each point in the set now has its own scaling parameter r_i.

Fractal mathematics hinges on the concept of dimension. Two types of dimensions are used in fractal mathematics: the common topological or Euclidean dimension D_T, and the Haussdorf-Besicovitch or fractal dimension D. A point has a topological dimension of 0, a line a topological dimension of 1, and a plane a topological dimension of 2.

There are many methods to determine the Haussdorf-Besicovitch or fractal dimension. The majority of these methods are based on the relationship

$$N(r) = 1/r^D \qquad \text{(Equation 3-2)}$$

between the number of self-similar part N(r), and a scaling factor r, or

$$D = \frac{\log N(r)}{\log\left(\frac{1}{r}\right)} \qquad \text{(Equation 3-3)}$$

A fractal can now be defined for a set for which the Haussdorf-Besicovitch dimension strictly exceeds the topological dimension *(Mandelbrot, 1983)*. There are at least two philosophies that may be followed, when applying fractals in geohydrology. The first, and the one mainly discussed in literature, is to describe the hydraulic parameters of an aquifer with fractal mathematics. The second philosophy relates to the geometrical representation of an object.

3.2.2. Fractal Reservoir Model

The fractal reservoir model (FR-Model) was proposed by Chang and Yortsos (1990) to account for the fractal character in fracture networks created by natural processes like percolation and fracturing. It is based on the theory of anomalous diffusion in fractals.

A key property of fractals is that their mass or volume density decreases as a power law when an increasingly larger region is considered (see Figure 3-3). Taking the mass or volume M of fractures contained in a circle of radius r and area A, results in a density ρ=M/A. For a fractal of a mass fractal dimension D embedded in dimension d, the density obeys the scaling:

$$\rho(r) \propto r^{D-d} \qquad \text{(Equation 3-4)}$$

since $M \propto r^D$ and $A \propto r^d$. Thus for the homogenous network of Figure 3-3c the mass density is constant, while the fractal network of Figure 3-3b has a mass density decreasing with distance, as described by equation (3) with $1 < D < 2$ and $d = 2$.

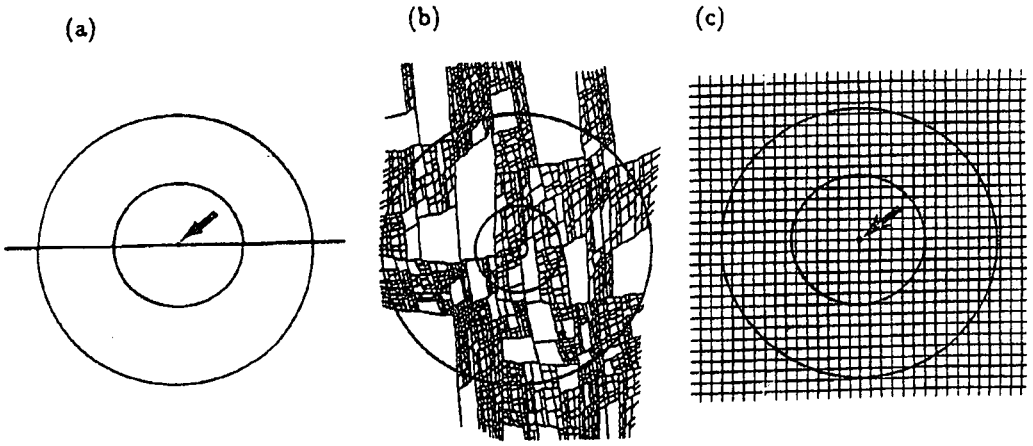

Figure 3-3 Power law properties of fractal networks; a) linear system D = 1, b) fractal network 1 < D < 2, c) radial system D = 2 (Acuna and Yortsos, 1995)

The parameters, which scale with distance *r*, can all be properties of the fracture network, as conductivity, storativity, fracture aperture, fracture density. Consider the steady state permeability in single-phase flow in a fractal object (e.g. the fracture network). If a pressure drop Δp is applied across a region of size r, the overall permeability is not constant, but it scales with the distance *r*:

$$K = K_0(r/r_0)^{D-d-\theta} \qquad \text{(Equation 3-5)}$$

Where

K_0 = permeability at $r=r_0$

r_0 = lower cutoff scale (smallest block size in the fracture network above which a fractal behaviour is obeyed)

θ = transport exponent

The exponent θ is related to the network connectivity and describes the deviation from an ordinary random walk in the fractal network. For the Euclidean networks in Figure 3-3a and c, diffusion is Fickian and θ = 0. For the fractal network of Figure 3-3b, however, the many traps of various scales in the network cause diffusion to slow down. An important consequence of this is that the hydraulic diffusivity η is not constant (but varies with position, $\eta \propto r^{-\theta}$). The different behaviour exhibited by diffusion in fractals compared to Euclidean objects should also be reflected in pressure transients in the fractal networks of fractures. Chang and Yortsos (1990) showed that the response of a well producing at a constant rate is given by:

$$p(r,t) = \frac{r^{(2+\theta)(1-\delta)}}{\Gamma(\delta)(2+\theta)}\Gamma\left(1-\delta, \frac{r^{2+\theta}}{(2+\theta)^2 t}\right) \qquad \text{(Equation 3-6)}$$

Where

p(r,t) = pressure drop at distance r and time t
δ = D / (2+θ)
Γ(x) = Gamma function
Γ (x,y) = incomplete Gamma function

The behaviour of equation (3-6) depends on whether δ < 1 or δ > 1. Since δ = D / (2+θ) the two cases correspond to D < 2+θ (flow behaviour mostly between linear and radial) and D > 2+θ (flow behaviour mostly between radial and spherical). The two types of behaviour in the abstraction borehole are shown graphically in Figure 3-4.

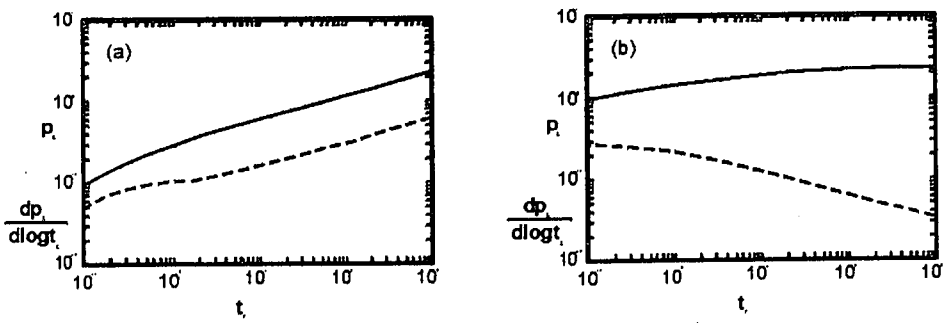

Figure 3-4 Characteristic fractal pressure transient behaviour in the abstraction borehole for a) δ < 1 and b) δ > 1 (Acuna and Yortsos, 1995)

Acuna and Yortsos (1995) give procedures to calculate the parameter δ from the graphs in Figure 3-4. For δ < 1 log-log plots of pressure and pressure derivative versus time will appear as two parallel straight lines of slope 1-δ separated by a distance equal to log(1/(1-δ)). When δ > 1 the pressure derivative will appear in a log-log plot as a straight line with a negative slope equal to 1-δ.

Since δ is a lumped parameter (δ = D/(2+θ)) the procedure will still not yield unique values for the fractal dimension D and the transport exponent θ. To analyse hydraulic test data with the fractal reservoir model, independent information has to be gathered about the fracture network, such as fracture density and fracture connectivity.

3.3. Generalised Radial Flow Model

Barker (1988) introduced an analytical model that describes the drawdown in a fractured aquifer for various flow dimensions including linear, radial and spherical flows. These flow dimensions are seen as dependent on the fracture connectivity rather than as aquifer dimensions and are described by a factor n. Flow dimensions equal aquifer dimensions for integer values of n: for n = 1 the flow is strictly linear, for n = 2 the flow is radial (Theis model) and for n = 3 the flow is spherical. The non-integer values of n describe the excess or lack of fracture connections compared to fracture networks with perfect connections in 1, 2 and 3 dimensions (Leveinen *et al.* 1998).

3.3.1. GRF-Model (Barker, 1988)

Barker (1988) introduced two general equations to describe the head in the source and head in the formation, both related to the abstraction rate (Equations 3-7 and 3-8, respectively). The equations obtained by means of the Laplace transformation read:

$$\frac{\bar{H}(p)}{\bar{Q}(p)} = \frac{\left[1+\xi\Phi_\nu(\mu)\right]}{pS_w + K_f b^{3-n}\alpha_n r_w^{n-2}\Phi_\nu(\mu)} \qquad \text{(Equation 3-7)}$$

$$\frac{\bar{h}(r,p)}{\bar{Q}(p)} = \frac{\rho^\nu K_\nu(\mu\rho)}{K_\nu(\mu)\left[\rho S_w\left(1+\xi\Phi_\nu(\mu)\right)+K_f b^{3-n}\alpha_n r_w^{n-2}\Phi_\nu(\mu)\right]} \qquad \text{(Equation 3-8)}$$

where

$\bar{H}(p)$ = drawdown at the source in the Laplace space [L]
$\bar{h}(p)$ = drawdown in the reservoir in the Laplace space [L]
$\bar{Q}(p)$ = abstraction rate in the Laplace space [L^3T^{-1}]
p = laplace transform variable
n = dimension of the fracture flow system [-]
b = extent of the flow region [L]
r_w = radius of the source [L]
K_f = hydraulic conductivity of the fracture system [LT^{-1}]

$$\alpha_n = \frac{2\pi^{n/2}}{\Gamma(n/2)}$$

S_w = Storage capacity of the source [-]
S_{sf} = Specific storage of the fracture system [L^{-1}]
ξ = skin factor [-]
μ = λr_w
ρ = r/r_w [-]
λ = $(p \cdot S_{sf} / K_f)^{1/2}$
ν = 1-n/2

$$\Phi_\nu(\mu) = \frac{\mu K_{\nu-1}(\mu)}{K_\nu(\mu)}$$

$K_\nu(\mu)$ = modified Bessel function of fractal order
$\Gamma(x)$ = Gamma function

The equivalent system in Barker's GRF-model consists of a homogeneous and isotropic fracture system characterised by a hydraulic conductivity K_f and specific storage S_{sf}, in which the flow to the well is radial and n-dimensional. With this model, Barker presented a way of generalising the conventional models used for pumping test analysis for arbitrary flow dimensions. For instance, after generalising the Theis equation, it will describe the drawdown in a fractured confined aquifer. The generalised Theis equation is written as (Barker, 1988):

$$s(r,t) = \frac{Qr^{2N}}{4\pi^{1-N} K_f b^{3-n}} \Gamma(-N,u) \qquad \text{(Equation 3-9)}$$

where

N = 1-n/2
n = dimension of the fracture flow system [-]
b = extent of the flow region [L]
r = distance from the source [L]
K_f = hydraulic conductivity of the fracture system [LT^{-1}]
Q = discharge rate [L^3T^{-1}]
u = $r^2S_{sf}/4K_ft$
S_{sf} = Specific storage of the fracture system [L^{-1}]

The solution is valid for a homogeneous and isotropic fractured medium and considers 1-, 2-, and 3-dimensional sources with a finite storage capacity. The source dimensions are defined by b^{n-3}, where n = 1 implies a very thin cube source, n = 2 a cylinder source and n = 3 a sphere source. The model also incorporates the possibility of infinitesimal skin located at the source.

The flow area A in Barker's (1988) formulation is given by:

$$A(r) = b^{3-n} \frac{2\pi^{\frac{n}{2}}}{\Gamma\left(\frac{n}{2}\right)} r^{n-1} \qquad \text{(Equation 3-10)}$$

where:

b = extent of the flow zone, L
Γ = gamma function

The flow dimension n is related to the power-law relationship between flow area and radial distance from the borehole. The flow dimension is defined as the power of variation plus one, as follows:

$$n(r) = \frac{d \log A}{d \log r} + 1 \qquad \text{(Equation 3-11)}$$

For example, the relationship between flow area and distance in a standard radial system is given by:

$$A(r) = 2\pi rb \qquad \text{(Equation 3-12)}$$

The flow area is seen to vary linearly with distance (r^1), making the flow dimension, by definition, two.

If n=2 (meaning horizontal radial flow to an abstraction borehole) the parameter b is the thickness of the aquifer; for n=1 (meaning linear flow to an abstraction borehole) the parameter b is the square root of the through-flow area and for non-integer values of n, b has no physical meaning. However, b must always be considered when trying to infer values of K and S_s from hydraulic-test data. Just as a pumping test in a confined aquifer ($n = 2$) actually provides estimates of transmissivity T and storativity S that can only be recast as K and S_s given knowledge of the aquifer thickness b, so does a test in a nonradial system only provide estimates of Kb^{3-n} and $S_s b^{3-n}$ using Barker's (1988) analytical formulation.

Figure 3-5 shows the type drawdown curves for different flow dimensions n. The function F(n, u) is evaluated as:

$$F(n,u)=\frac{1}{\nu}\left[\left(\frac{1}{u}\right)^{\nu}-\frac{\Gamma(1-\nu)}{\nu}\right] \qquad \text{(Equation 3-13)}$$

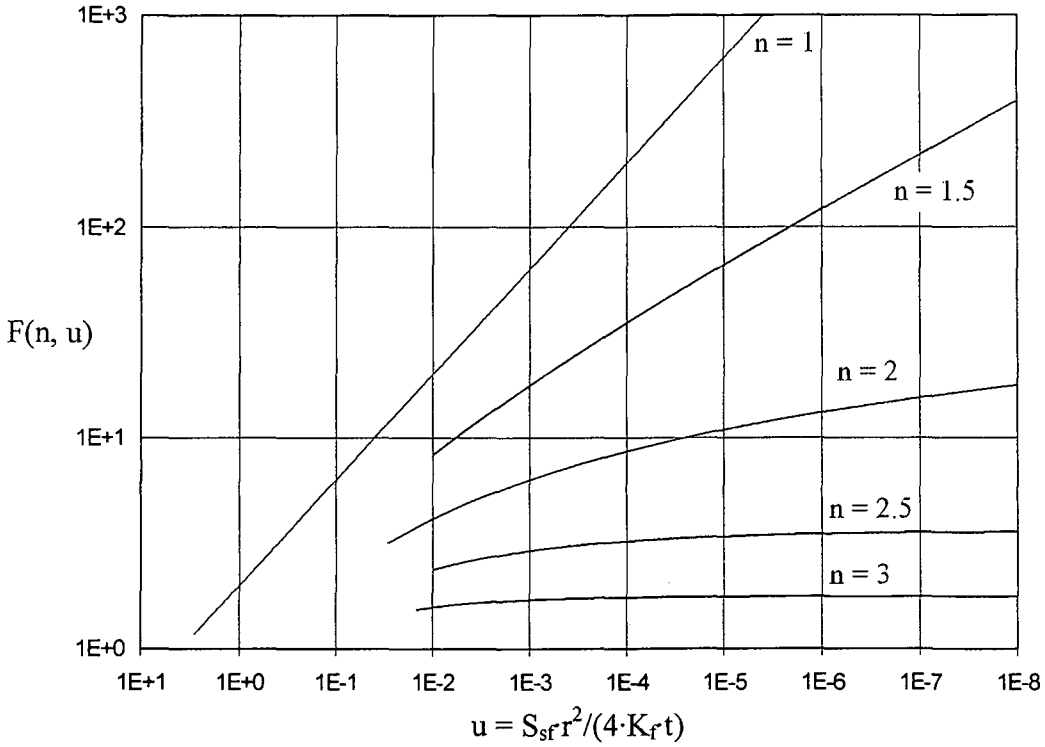

Figure 3-5 Type curves for different flow dimensions (n), (Van Tonder *et al.*, 2001)

3.3.2. Extended GRF-Model (Roberts and Beauheim, 2001)

Roberts and Beauheim (2001) presented a numerical implementation of flow dimensions, derived from hydraulic test data, which differs from the GRF-Model in several respects.

In the GRF-Model the source is an n-dimensional sphere with a given area (see equation 3-10). Thus, the initial flow area and, indeed, source geometry may bear no relation to the cylindrical area and geometry of most borehole test zones. In contrast, in the model of Roberts and Beauheim (2001) the analyst specifies the initial flow area, typically as the surface area of the borehole within the test zone or some smaller part of it. The estimates of the fitting parameters are then understood to be the average values of those parameters over the arbitrarily specified initial flow area.

When the initial flow area $A(r_w)$ is specified along with n, the extent of the flow zone b in Equation (3-10) is seen to be a constant equal to:

$$b = \left[\frac{A(r_w)}{\alpha\, r_w^{n-1}} \right]^{\frac{1}{3-n}} \qquad \text{(Equation 3-14)}$$

where:

r_w = wellbore radius, L

α = $2\pi^{n/2} / \Gamma(n/2)$

At any distance r from the source, Equation (3-10) can, therefore, be reformulated independently of b as:

$$A(r) = \frac{A(r_w)}{r_w^{n-1}}\, r^{n-1} \qquad \text{(Equation 3-15)}$$

Equation (3-15) is valid for any constant-n system, where the flow area at any distance r is determined by the initial specified flow area $A(r_w)$ and the flow dimension, n. If n changes with distance, the same equation can be applied for the following zone of constant n.

Flow-dimension values in systems with constant K and S_s reflect boundaries within the three-dimensional space. For example, radial flow (n = 2) is restricted by two parallel no-flow boundaries, i.e. the upper and lower boundary of the aquifer. Using flow-dimension functions ($n(r)$) to represent all types of no-flow and constant-pressure boundary effects is simply an extension of this logic.

- The flow-dimension function $n(r)$ for a case with a no-flow boundary varies from a value of two to negative one. The negative flow dimension is simply an indication of the rate at which the flow area decreases due to the boundary.
- In the case of a constant-pressure boundary the flow-dimension function is seen in a transition from two to four -- the linear constant-pressure boundary has a flow dimension of four.

While flow dimensions greater than three resulting from constant-pressure boundary effects may initially seem less than intuitive, these constant-pressure boundary effects do have distinct flow-dimension signatures and they can be simulated by manipulating the model geometry (n). This approach allows boundary effects to be incorporated into transient flow-rate simulations (constant-pressure tests), something not possible with the image-well implementation of boundary effects.

Doe (1991) noted that identical hydraulic responses could be produced in both a homogeneous system with varying flow area ($n(r)$) and in a constant flow-area system with varying hydraulic properties ($T(r)$ and $S(r)$). This inherent non-uniqueness combined with the assumption of constant K and S_s means that all real but unknown spatial variations in K, S_s, and n are lumped together in the estimated value of n. The resulting "dimension" described by n can therefore reflect the actual geometry of the flow conduits in three-dimensional space, or it can reflect a combination of factors. Flow dimension is perhaps best viewed as representing the rate of change of hydraulic "conductance" (the product of hydraulic conductivity and flow area) with distance. Thus, Equation (3-11) can be rewritten as:

$$n(r) = \frac{d\log(KA)}{d\log r} + 1 \qquad \text{(Equation 3-16)}$$

Features such as constant-pressure and no-flow boundaries, and processes such as leakage from confining beds, clearly affect conductance and can, therefore, be represented by flow dimensions, resulting in a wide possible range of estimated n values (see Figure 3-6).

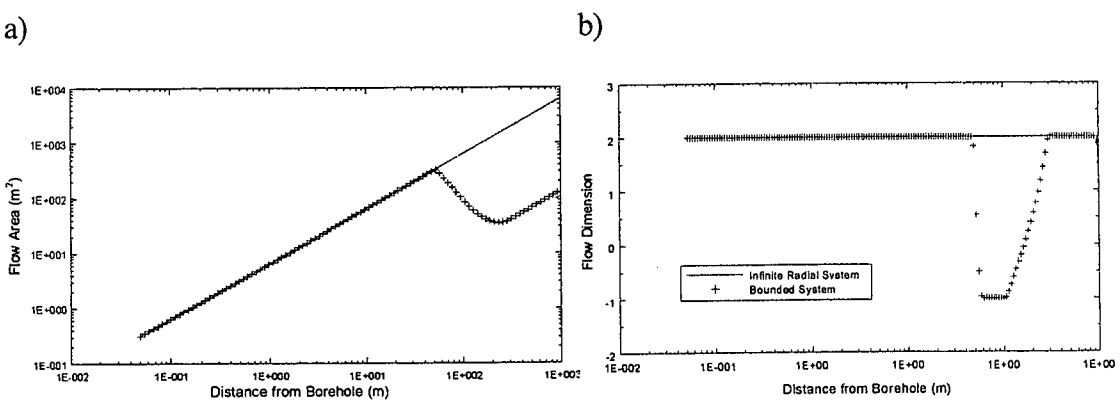

Figure 3-6 Influence of a bounded system (stars) compared to an infinite radial system (solid line) on a) flow area and b) flow dimension (Roberts and Beauheim, 2001)

The use of variable flow dimensions to describe complex flow regimes has several advantages over more traditional approaches. It is not limited by the assumption that all flow is radial until a boundary is encountered at some distance. It is easily applied to complex flow geometries or variable properties or any combination of the two. It can be applied to transient flow-rate (constant-pressure) data as well as transient pressure data. Once a system is described in terms of *n(r)*, a simple transformation can be applied to define multiple combinations of flow geometries and hydraulic properties that would produce the observed response. This makes investigating a wide variety of possible conceptual models easy. Finally, given that the actual combination of flow geometry and properties that produces an observed response is unknown (particularly in a complex geologic setting), describing the combined effects in terms of a single parameter seems appropriate.

3.4. Comparison FR Model – GRF Model

Barker (1988) casually refers to his non-integer or fractional dimension as a fractal dimension. There is however a difference between standard fractal models and Barker's GRF-model (Wei and Chakrabarty, 1996). This difference is best illustrated by means of an example. Consider a fractal reservoir model (FR-model) where scaling laws of diffusion on fractal objects are applied to fluid flow through fractal networks. Diffusion on a fractal is then defined as (Wei and Chakrabarty, 1996):

$$\frac{\partial p}{\partial t} = \frac{\eta_0}{r^{d_f-1}} \frac{\partial}{\partial r}\left[r^{d_f-1-\beta} \frac{\partial p}{\partial r} \right] \qquad \text{(Equation 3-17)}$$

where

η_0 = diffusion constant
p = average pressure at radius r
t = time
d_f = mass fractal dimension
β = fractal exponent

The key geometric property of the network is represented by d_f which controls the fracture mass density scaling. The parameter β depends on both the geometry and the transport properties of an aquifer. This parameter is responsible for the diffusivity scaling of the fractal network. By allowing $\beta = 0$ the FR-model becomes the same as the GFR-model and $n = d_f$. However the physical meanings of the two models still differ. In the FR-model diffusivity is constant but K and S can vary. All three these parameters are assumed to be constant in the GRF-model of Barker (1988), however the geometry varies.

Chapter 4 Parameter Estimation

The most important and maybe most difficult part in groundwater exploration and investigation is the estimation of aquifer parameters. Because they cannot be measured directly, it is necessary to develop procedures to obtain the different parameters from the response in water level or concentration, which is an inverse and often non-unique problem.

The parameters, describing the behaviour of groundwater flow and transport, and therefore important for any kind of prediction, can be subdivided into three groups, the aquifer geometry, hydraulic properties and transport parameters:

- The aquifer geometry describes the general geological set-up and the presence and distribution of water-bearing features, such as fractures. Real geometrical parameters are the aquifer thickness and extent and the fracture properties, like aperture, extent and connectivity, while the flow dimension, which is a lumped parameter accounting for the flow geometry during a specific event, is scale and time dependent.
- The hydraulic properties control the flow behaviour under natural or stressed conditions. They consist of the transmissivity or hydraulic conductivity of the aquifer, or parts of it (matrix, fractures), and the storativity. The hydraulic gradient changes under certain conditions and controls the flow direction and flow velocity.
- The transport parameters are important for any kind of investigation in groundwater contamination. Despite the kinematic porosity, they depend on specific conditions of groundwater flow (velocity) and contaminants (matrix diffusion, dispersion).

To measure and estimate all these different parameters, several techniques, field tests and analysing methods were developed. Table 4-1 shows a selection of field tests and analysing methods to estimate the different parameters. Unfortunately there is no test or method to estimate all parameters:

- Numerical models seem to cover most of the parameters, but different data are required for each group. To perform a transport modelling for parameter estimation the hydraulic properties must be known a priori and a flow model must exist and be calibrated beforehand.
- Hydraulic tests are useful for estimating the parameters of the aquifer geometry and the hydraulic properties, but they fail completely in estimating transport parameters.
- The only way to estimate transport parameters is by means of tracer tests, but it is not possible to obtain all the hydraulic properties from tracer test data.

This chapter will focus on the different field tests and analysing methods, depending on the parameters to be estimated. In Chapter 5 a combination of the field tests (tracer test and hydraulic test) is proposed to simplify the procedure of parameter estimation.

Table 4-1 Methods to estimate the different Flow and Transport Parameter

Aquifer Geometry		Tracer Tests				Hydraulic Tests	
		Multiple Well Tests		Single Well Tests			
		Natural Flow	Radial Convergent	Point Dilution	Injection Withdrawal	Analytical Methods	Numerical Model
Aquifer Thickness	D	Geology / Borehole Logs					
Effective Fracture Zone Thickness			X			X	
Fracture Aperture	2b	X	X			X	
Fracture Extent, Fracture Half Length	x_f					X	
Non-integer Flow Dimension	n		X			X	X
Flow Domain or Flow Extent	b		X			X	
Hydraulic Properties							
Aquifer Transmissivity	T					X	X
Hydraulic Conductivity Horizontal, Matrix	k_{hm}					(X)	X
Hydraulic Conductivity Vertical, Matrix	k_{vm}					(X)	X
Hydraulic Conductivity Fracture	k_f					X	X
Specific Storage Coefficient, Matrix	S_{sm}					(X)	X
Specific Storage Coefficient, Fracture	S_{sf}					(X)	X
Hydraulic Gradient	i		X			X	(X)
Transport Parameter							
Kinematic Porosity	ε	X	X	X			(T)
Flow Velocity	v	X	X		X	X	(T)
Darcy Velocity	q			X			(T)
Matrix Diffusion		X	X				T
Longitudinal Dispersivity	α_L	X	X				T
Transversal Dispersivity	α_T	X					T

T = Transport modelling, requires concentration data of artificial or environmental tracers

4.1. Hydraulic Parameters

In general the flow of groundwater in the aquifer or the spread of the drawdown wave during a pumping test can be significantly affected by several hydrogeological parameters, including:

- the horizontal hydraulic conductivity of the matrix (k_{hm}),
- the vertical hydraulic conductivity of the matrix (k_{vm}),
- the specific storage coefficient of the matrix (S_{sm}),
- the horizontal hydraulic conductivity of the fracture (k_{hf}),
- the vertical hydraulic conductivity of the fracture (k_{vf}),
- the specific storage coefficient of the fracture (S_{sf}),
- the thickness of the aquifer or of the fracture zone,
- the natural or forced hydraulic gradient
- and the flow geometry.

In the following sections the various hydraulic tests and analysing methods will be briefly described. For each parameter the best method or combination of methods is chosen and described in detail as a step-by-step guideline.

4.1.1. Hydraulic Tests

Hydraulic tests are normally conducted to measure the drawdown or pressure response in one or more boreholes, and to relate this response to the hydraulic properties of the aquifer. Several test set-ups were developed to account for different purposes and geological structures. The most commonly used tests are described below.

4.1.1.1. Slug Tests

Slug tests are conducted by introducing a sudden pulse to increase the pressure in the borehole and to measure the drop of pressure back to the steady state level, which then can be related to the transmissivity of the aquifer. These methods were primarily developed for hydraulic tests in low permeable aquifers. They are cost-effective in both equipment and time. The disadvantage is the very small radius of influence during the test, which can result in wrong estimations, when the measured data do not reflect the aquifer but rather the borehole construction.

However the test is useful as a first approximation of the yield of the borehole, as discussed in Van Tonder *et al.* (2001). For the issue of parameter estimation the test will not be considered further.

4.1.1.2. Multirate Tests

Multirate tests were developed to determine the borehole efficiency. Water is abstracted from the borehole at different discharge rates. After each rate the recovery of the water level is awaited. The measured drawdown during the pumping and the recovery can be related to the hydraulic properties of the aquifer as transmissivity and storativity. From the different responses at different discharge rates the efficiency of the borehole can be calculated. A special case of the multirate test is the step drawdown test, where no recovery will occur between the different steps. The advantage of both tests lies in the possibility to increase the discharge rate until a water strike is reached. Therefore the test is useful to determine the depth of water-bearing fractures and to estimate the sustainable yield of the borehole, as discussed in Van Tonder *et al.* (2001). If the duration of one step is long enough, the methods for parameter estimation, developed for constant discharge tests, can be applied to the test data.

4.1.1.3. Constant Head Tests

Constant head tests are conducted by injecting or abstracting water in a way to keep the water level in the borehole constant. The flow rate will be measured and related to the hydraulic properties of the aquifer. This test is very accurate because small changes in the flow rate can be measured. The disadvantage lies in the complicated set-up and expensive equipment. Only few analysing methods were developed for this kind of test. Because this test is cost-intensive and not common it will not be considered further.

4.1.1.4. Constant Discharge Tests

The most common hydraulic test is the constant discharge test or constant rate test, where water is abstracted from a borehole at a constant discharge rate. The change in pressure or drawdown in the borehole or observation boreholes will be measured and can be related to the aquifer properties. The test is a very powerful tool and opens a lot of possibilities for analysing data.

Even with a small budget the results can be reliable, because the test does not require expensive equipment or long-term measurements in general. Depending on the purpose of the test, few hours of abstracting can be sufficient (Van Tonder *et al.*, 2001).

A suggestion for using the constant rate test, especially in combination with tracer tests, for aquifer parameter estimation is given in Chapter 5.

4.1.2. Analysing Methods

There are different analysing methods for different hydraulic tests. According to the discussion in the section above, the most common test for aquifer parameter estimation is the constant discharge test. Therefore the following section will focus on the various analysing methods for constant discharge tests. In the first part the analytical methods are briefly described and discussed, while the second part emphasises the use of numerical models.

4.1.2.1. Diagnostic Tools

The first step in analysing hydraulic test data should always be identifying the flow characteristics to choose an applicable conceptual model and apply the correct analysing method.

The flow phases that appear during a pumping test in a fractured aquifer show characteristic patterns like straight lines, either in a double logarithm (log-log) or in a linear-logarithm (lin-log) plot (see Figure 4-1). Using the concept of derivatives, additional information about the flow regimes can be gathered.

(a) Straight Lines

A log-log plot will provide information at early time as follows:

- Well bore storage shows a slope of 1.
- Linear flow shows a slope of 0.5.
- Bilinear flow shows a slope of 0.25 (= flow from fracture and formation).
- Fracture storage shows a slope between 0.5 and 1 in the linear flow case and between 0.25 and 1 in the bilinear flow case.

At late time, the log-log plot will provide information as follows:

- Two parallel no-flow boundaries show a slope of 0.5.
- Three equidistant no-flow boundaries show a slope of 0.5.
- Limited reservoir (four closed boundaries) shows a slope of 1.

In cases of a single vertical or horizontal fracture, the log-log plot can also be used to determine linear formation flow (slope 0.5 at intermediate time) and limited extent of the fracture (slope 1 at intermediate time).

A lin-log plot provides the following information:

- Radial-acting flow appears as a straight line.
- One no-flow boundary doubles the slope of the radial-acting flow straight line.
- Two perpendicular no-flow boundaries quadruple the slope of the radial-acting flow straight line.

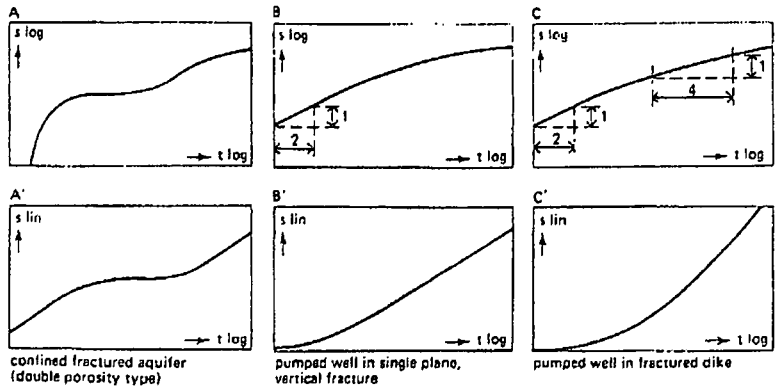

Figure 4-1 Log-log and semi-log plots of theoretical time-drawdown relationships of consolidated fractured aquifers; (A) double-porosity aquifer; (B) single vertical fracture; (C) permeable dyke in a low permeable aquifer (after Kruseman and deRidder, 1991)

(b) Special Plots

Besides the lin-log and log-log plots, the following three additional plots are very useful for the diagnosis of pumping test data in fractured aquifers:

- Linear drawdown versus square root of time.
- Linear drawdown versus fourth square root of time.
- Linear drawdown versus one divided by square root of time.

The first plot is useful for the determination of linear flow behaviour, as the drawdown data will plot on a straight line that starts at the origin of the diagram. In the second plot, the drawdown data of the bilinear flow phase plot on a straight line starting at the origin.

The drawdown data of a spherical flow plot on a straight line that starts at the origin of the third plot.

The first two diagrams are very useful to determine skin effects in drawdown data of wells in single fractures with either linear or bilinear drawdown behaviours. Such skin effects cause an additional drawdown.

(c) Recovery

The same plots can be applied to recovery data after correction of the measured time. In most practical cases, the quality of the recovery data is better than that of the drawdown, as they are not influenced by fluctuations in the pumping rate. This holds true especially for the application of derivatives that are commonly used as diagnosis tools of drawdown phases. On the recovery t/t' plot, a limited closed reservoir will result in a horizontal flattening at late time.

(d) Curve Derivatives

The use of derivatives is of great advantage due to their sensitive reaction to small changes in the drawdown or recovery, while they are independent of skin effects. Usually, the first derivative is plotted as ($\Delta s/\Delta t$ vs. t), which provides the following advantages:

- All characteristics of the straight-line slopes remain the same.
- Well bore storage shows a line with slope 1 at early times.
- The radial-acting flow phase is plotted as a horizontal line, which eases identification with the human eye.
- A closed boundary shows a line with slope 1 at late times.
- A dip in the first derivative after the well bore storage is an indicator of a double porosity aquifer.
- At the position of a fracture, the derivative shows a decrease and after the fracture is dewatered, the derivative will go up again.
- A recharge boundary or fixed head boundary is seen on the derivative graph as a strong downward trend at late times.
- While reaching a no-flow boundary, the horizontal line of a radial-flow period will shift to a doubled value.

Using the second derivative, the following information will be provided:

- A second derivative of 1 shows a closed boundary.
- During radial flow, the second derivative is equal to zero and is therefore not visible in a log-log plot.

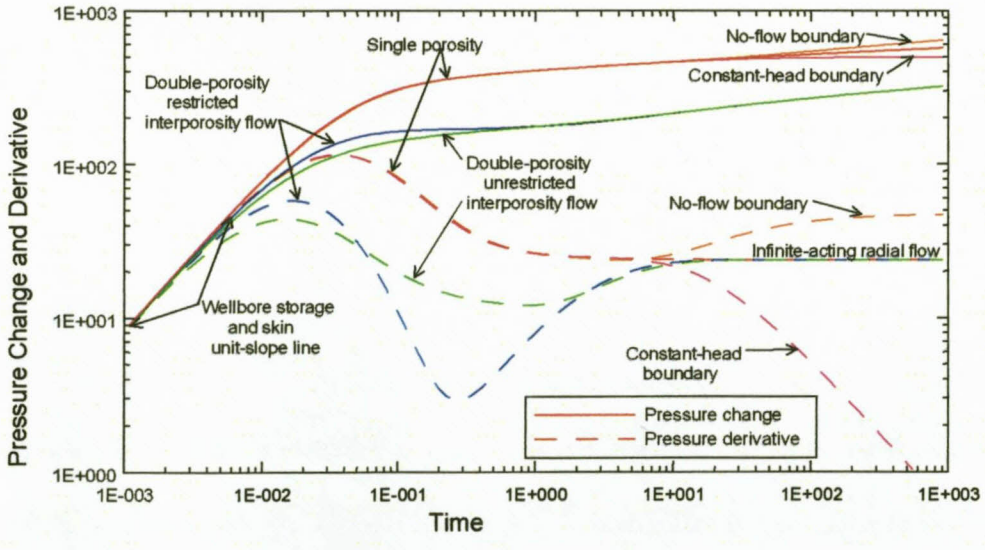

Figure 4-2 Effects of different conditions on drawdown and drawdown-derivative log-log plots (Roberts and Beauheim, 2001)

Unfortunately, derivatives applied to real data often show noisy results. Smoothing of the derivatives would overcome this problem, but it cannot be ensured that the applied mathematical algorithm would not produce misleading artefacts.

4.1.2.2. Analytical Methods

Currently usually two kinds of models are applied in fractured-rock aquifers, namely the single fracture model and the double porosity model as described below, while the methods for porous media (i.e. Theis and Cooper-Jacob) are still applied for parameter estimation in fractured aquifers. If the geometry of the fracture network is not known, it is impossible to use a correct conceptual model. Here the generalised radial flow model or the fractal reservoir model can be applied. Some of these models have inherent problems, as the following short discussion indicates.

(a) Porous Media Model

The most commonly used methods to analyse hydraulic test data are derived for porous media under different aquifer and flow conditions. There are methods for confined, unconfined and leaky aquifers as well as for steady-state and transient flow conditions. In the following the porous media methods for transient flow in confined aquifers are described, because fractured aquifers often show similar behaviour, when they can be considered as continuum.

Theis Method

Theis (1935) was first to develop a formula for unsteady-state flow that introduces the time factor and storativity. The rate of decline of head, multiplied by the storativity and summed over the area of influence, equals the discharge. The Theis equation is written as:

$$s = \frac{Q}{4\pi KD} W(u) \qquad \text{(Equation 4-1)}$$

where

s = drawdown in m, measured in a piezometer at a distance r from the well
Q = constant well discharge in m^3/d
KD = transmissivity of the aquifer in m^2/d
u = $\frac{r^2 S}{4KDt}$
S = dimensionless storativity of the aquifer
t = time in days since pumping started
W(u) = Theis well function

Cooper-Jacob Methods

The Cooper-Jacob methods (Cooper and Jacob, 1946) are based on the Theis equation (Equation 4-1). For late time the drawdown plots as a straight line on a lin-log graph. The Cooper-Jacob equation is written as

$$s = \frac{2.30Q}{4\pi KD} \log \frac{2.25KDt}{r^2 S} \qquad \text{(Equation 4-2)}$$

The slope of the straight line and its interception at s=0 can be used to determine the hydraulic parameters transmissivity and storativity. Using the measured drawdown at a specific time, but at different piezometers, the plot drawdown versus distance (Cooper-Jacob II) shows a straight line in the case of a homogeneous aquifer. The slope of the straight line and the interception at s=0 yield values for the transmissivity and storativity.

In a fractured aquifer we are dealing with two systems, i.e. fracture and matrix. During a pumping test groundwater is released from matrix, flows vertically to the fracture and then along the fractured zone towards the abstraction borehole (Van Tonder *et.al.*, 2001). However, neither the Theis nor Cooper-Jacob methods consider this situation. When applying these methods, only the portion of groundwater, which is released outside of the radius of the observation borehole, is considered by the analytical solution. And this portion decreases with the increasing distance of the observation borehole. This explains the decrease of the S-values with distance. As a result of applying Theis or Cooper-Jacob methods, the estimated T- and S-values represent a mixture of the matrix and fracture properties.

(b) Double Porosity Model

The concept of double porosity was introduced by Barenblatt *et al.* (1960), considering homogenously distributed conductive fractures embedded in a homogenously distributed matrix. For both fracture and matrix, different conductivity and storage coefficients can be adopted. Two matrix types are generally discussed; the spherical block matrix (Warren and Root, 1964) used to represent aquifers like quartzite and the layered matrix (Kazemi, 1969) adopted, for example, for sandstones with bedding planes (Figure 4-3).

Warren and Root (1964) introduced a pseudo-steady state block-to-fracture flow solution, which seems to adequately represent field data, but Kazemi (1969) and Wei *et al.* (1998), using numerical models, found that the flow is of transient block-to-fracture nature. However, Moench (1984) shows that the pseudo-steady flow case is, in fact, a special case of the transient flow restricted by a skin between fracture and matrix caused by mineral precipitation on the matrix blocks' surfaces.

Initially, mainly the fracture network of a double porosity aquifer releases water when pumping from a well starts and the drawdown is characterised by a straight line in a lin-log plot that is proportional to the transmissivity of the fracture system. The flattening of the curve is originated by the ever-increasing additional contribution from the matrix storage. The later drawdown is the response of both the matrix and the fracture storage, and is also proportional to the transmissivity of the fracture system and plots as by a straight line parallel to the initial one in the lin-log plot. In a log-log plot, both the initial and the late drawdown are characterised by Theis curves shifted horizontally from each other. The distance between the two parallels or two Theis curves depends on the fracture/matrix storage coefficient ratio.

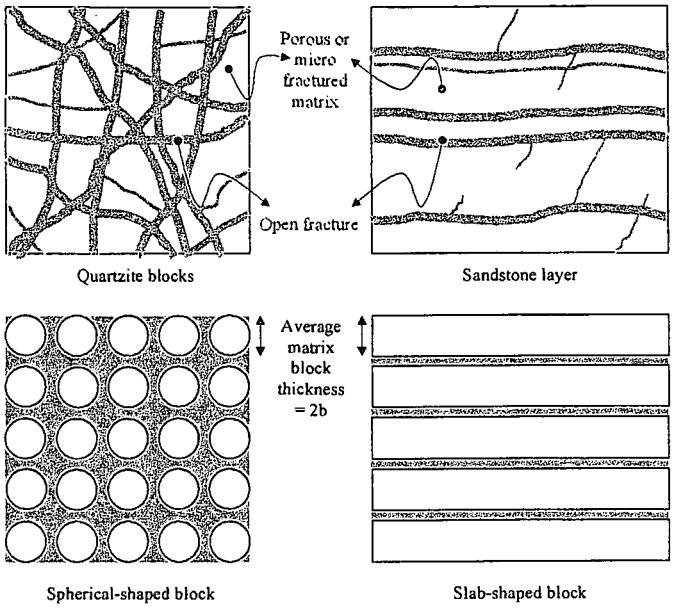

Figure 4-3 Natural fracture systems and their simplification into spherical-shaped blocks and slab-shaped blocks (van Tonder *et al.*, 2001)

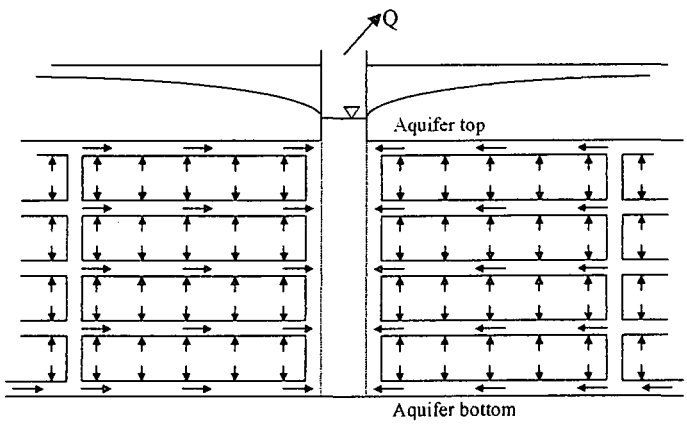

Figure 4-4 Groundwater flow in an idealised double porosity aquifer (van Tonder *et al.*, 2001)

Moench (1984) proposed a type curve approach for the analysis of double porosity data, which includes well bore storage, well skin and fracture skin and is therefore more advanced than the simple straight line approach proposed by Warren and Root (1963) and Kazemi (1969). However, due to the tremendous increase of computer calculation power, a combined approach of straight line and forward modelling is nowadays possible. The advantage of this proposed method lies in the ability to calculate different drawdown scenarios after model calibration to find the optimal abstraction rate for a particular well.

Once a double porosity case is diagnosed and it has been determined that the influence of the well bore storage is negligible, the Warren and Root straight line method can be applied to the pumped well data to determine the transmissivity T of the fracture system and the storage coefficients S_f and S for the fracture system and the matrix, respectively. The steps to follow in the application of the Warren and Root method for the pumped well data using a lin-log plot are:

- One straight line must be fitted to the early time data (first branch) of the curve.
- A second straight line must be fitted to the late time data (second branch).

Both straight lines must have the same slope, as they reflect the transmissivity of the fracture system. In the presence of skin at the well, the Warren and Root method gives incorrect results for the two storage coefficients. The Kazemi straight-line method should be applied to observation data. Both methods are in fact similar to the Cooper-Jacob straight-line method.

The Moench model (1984) is usually applied for double porosity aquifers, but it was found from practical applications of the method that the estimated S-values still show the same distance dependency that is experienced when the Theis method (using the real observation distances) is applied to pumping tests in fractured aquifers (see Kirchner and Van Tonder, 1995). Six parameters also have to be fitted, which makes the solution non-unique.

(c) Single Fracture Models

If a pumped well intersects a major fracture, fault or dyke, embedded in a very hydraulic conductivity matrix, it may significantly influence the part of the time drawdown behaviour of the fractured hard rock aquifer. Single fracture models deal with such a situation. The main types of single fracture models are: infinite conductivity fracture, uniform flux fracture, finite conductivity fracture, and dykes. The first three models have been developed for artificially fractured wells in petroleum reservoirs (Verweiji and Barker, 1999). Only the dyke model has been developed for groundwater purposes. The equivalent system in a single fracture model is a homogeneously confined aquifer of large areal extent, which is dissected from top to bottom by a vertical fracture of relatively short length or by a dyke of infinite length. The pumped well fully penetrates the fracture or dyke.

Vertical Fracture with Infinite Conductivity

A pumped well tapping an assumed plane fracture of infinite conductivity will initially receive water from the aquifer by linear flow towards the fracture (and the well) and after continued pumping, the water will flow towards the well by radial flow (e.g. Gringarten *et al.*, 1974). The assumption of an infinite conductivity in the fracture, however, cannot be considered realistic for highly conductive fractures in hard rock aquifers with low permeable rock matrices (Verweiji and Barker, 1999).

Gringarten *et al.* (1974) presented solutions for two different boundaries along the fracture surface:

- Uniform flux, where the flux distribution is homogeneous along the fracture and constant in time. In reality, the flux distribution along a fracture may approach uniformity only if there is a skin, and a low permeability layer between the fracture and the aquifer matrix (Cinco and Samaniego, 1981b).
- Infinite flux, where the flux distribution is uniform along the fracture during the linear flow phase, but not in the transient and radial-acting flow phases. Simultaneously, it varies with time until the radial-acting flow phase is reached.

Although the drawdown for both cases does not differ much, measured data can usually be described by only one of them. The drawdown s in a fracture at early times is given by Gringarten *et al.* (1974) for both the uniform and infinite flux cases and reads:

$$s = \frac{Q}{2 \cdot \pi \cdot T} \cdot \sqrt{\pi \cdot t_d} \qquad \text{(Equation 4-3)}$$

with
$t_d < 10^{-2}$ for uniform flux
$t_d < 2 \cdot 10^{-1}$ for infinite flux

Equation (4-3) describes the drawdown during the linear flow phase, which implies uniformity of flux along the fracture for both cases. Due to the fact that the fracture has infinite conductivity, there is an infinite small pressure gradient along the fracture that can be neglected ($\Delta p/\Delta x_f = 0$). Therefore, at early time the same drawdown is observed along the entire length of the fracture, and an observation well located in the fracture will show the same curve as the pumped well.

The long-term solution describes the radial-acting flow phase ($t_d > 5$) on the fracture as:

$$s = \frac{Q}{2 \cdot \pi \cdot T} \cdot \left[\frac{1}{2} \ln(t_d) + 1.1 \right] \qquad \text{(Equation 4-4)}$$

Equation (4-4) plots as a straight line in a lin-log plot. Analogous to a homogeneous aquifer, the transmissivity value for the formation can be obtained from the Cooper-Jacob approach.

Horizontal Fracture with Infinite Conductivity

Gringarten and Ramey (1974) introduced an analytical model that describes the drawdown in a penny-shape bedding plane fracture with infinite conductivity and finite extension with uniform flux. The fracture is embedded in an infinite, homogeneous, horizontal matrix that has anisotropic radial and vertical conductivities and is limited by upper and lower impermeable boundaries. The model considers linear flow followed by radial-acting flow after a transition period.

The equation presented by Gringarten and Ramey (1974) assumes that the flux is constant and uniform along the fracture. Basically, two methods of analysis can be used to determine the formation or matrix transmissivity T from the drawdown data: a straight-line method using a lin-log plot and a type curve method using a log-log plot.

Finite Conductivity Fracture

Cinco-Ley *et al.* (1978) introduced a semi-analytical model that describes the drawdown in a single vertical fracture with finite conductivity and length, which is embedded in an infinite, isotropic, homogeneous, horizontal matrix limited by upper and lower impermeable boundaries. It considers bilinear flow in the system and is therefore a generalised solution for this type of aquifer's geometry. The Gringarten *et al.* (1974) infinite flux solution is a special case of this model.

The gradient along the fracture cannot be neglected due to its finite conductivity and the solution requires the knowledge of the flux distribution along the fracture in time. However, the flux distribution stabilises after a certain period of time that coincides with the start of the radial-acting flow phase. This stable distribution is known as stabilised flux distribution.

The solution uses the concept of relative conductivity Cr to relate the conductivities of fracture and matrix as follows:

$$Cr = \frac{T_f \cdot w}{\pi \cdot T \cdot x_f} \qquad \text{(Equation 4-5)}$$

where

T_f = fracture transmissivity [L^2T^{-1}]
w = fracture width or aperture [L]
T = matrix transmissivity [L^2T^{-1}]
x_f = fracture half-length [L]

Cinco-Ley *et al.* (1978) presented a series of type curves for the pumped well for Cr values in the range of 0.1 to 100 and dimensionless time t_d between 10^{-3} and 10^3. The curve that corresponds to $Cr \geq 100$ practically coincides with the infinite flux solution from Gringarten *et al.* (1974).

Basically, two methods of analysis for the drawdown data are used to determine these parameters: a straight-line method using a lin-log plot and a type curve method using a log-log plot. The following parameters can be determined:

- Reservoir transmissivity.
- Reservoir storage coefficient.
- Fracture half-length.
- Fracture transmissivity.
- Fracture storage coefficient.

1159 528 73

(d) Generalised Radial Flow Model for Fractured Reservoirs

Barker (1988) introduced an analytical model that describes the drawdown in a fractured aquifer for various flow dimensions including linear, radial and spherical flows. These flow dimensions are seen as dependent on the fracture connectivity rather than as aquifer dimensions and are described by a factor n. Flow dimensions equal aquifer dimensions for integer values of n: for n = 1 the flow is strictly linear, for n = 2 the flow is radial (Theis model) and for n = 3 the flow is spherical. The non-integer values of n describe the excess or lack of fracture connections compared to fracture networks with perfect connections in 1, 2 and 3 dimensions (Leveinen *et al.* 1998).

The solution is valid for a homogeneous and isotropic fractured medium and considers 1-, 2-, and 3-dimensional sources with a finite storage capacity. The source dimensions are defined by b^{n-3}, where n = 1 implies a very thin cube source, n = 2 a cylinder source and n = 3 a sphere source. The model also incorporates the possibility of infinitesimal skin located at the source.

The methods can be applied if the following conditions are true:

- Matrix is infinite
- Aquifer (fracture and matrix) is confined
- Darcian flow prevails in fracture and matrix
- Negligible fracture skin
- Straight line can be applied for n = 2 if u < 0.01.

Type Curve Method by Barker (1988)

The handling of the Barker type curve method is similar to that of the Theis type curve method. Data from the pumped well can be used only if the well bore storage and the well bore skin are negligible, but data from observation boreholes can always be analysed using this method.

After matching the data curve of the pumping well with one of the type curves, the product $K_f \cdot b^{3-n}$ (that equals the transmissivity of the fracture system for n = 2) and the inverse of diffusivity of the fracture system S_{sf} / K_f can be calculated by substituting the values for the match point co-ordinates in Equations (4-6) and (4-7), respectively.

$$K_f \cdot b^{3-n} = \frac{Q}{4\pi^{1-\nu} h(r,t)\nu}\left[\left(\frac{4K_f t}{S_{sf}}\right)^{\nu} - \Gamma(1-\nu) r^{2\nu}\right] \qquad \text{(Equation 4-6)}$$

$$\frac{S_{sf}}{K_f} = \frac{4ut}{r^2} \qquad \text{(Equation 4-7)}$$

Barker (1988) suggests that any two of these three parameters (K_f, S_{sf}, or b) can be determined if the third is estimated or known.

Straight Line Method by Bangoy *et al.* (1992)

The method requires timedrawdown data from the pumped well **and** at least two observation wells. The drawdown-response for a constant rate test in an arbitrary fractured confined aquifer (n<2) is given by Barker (1988).

For $t = t_0$, the equation can be expressed by

$$s(r, t_0) = A(r) = A_0 - Br^{2N} \qquad \text{(Equation 4-8)}$$

with

$$A_0 = \frac{Q}{4\Pi^{1-N} K_f b^{3-n} N} (t_0 / E)^N$$

$$B = A_0 (E / t_0)^N \Gamma(1 - N)$$

$$E = S_{sf} / 4K_f$$

On a graph of A versus r^{2N} Equation (4-8) yields a straight line of slope –B and intercepts A_0. A straight line can be fitted to the values of A derived from drawdown analysis at the abstraction borehole and at several observation boreholes. The values of A_0 and B obtained by the fit are used to determine the ratio K_f/S_{sf} and the product $K_f b^{3-n}$.

$$K_f/S_{sf} = 1/4\ t_0\ [(A_0/B)\ \Gamma(1 - N)]^{1/N} \qquad \text{(Equation 4-9)}$$

$$K_f b^{3-n} = (Q\ \Gamma(1 - N))/(4\pi^{1-N} BN) \qquad \text{(Equation 4-10)}$$

The following procedure is proposed by Bangoy *et al.* (1992):

- On a log-log paper, plot s versus t for the pumped well and for observation wells;
- Draw a straight line through the late time data for each observation point and determine the slope N of each straight line;
- Choose a suitable value of t_0, and extrapolate the straight line to t_0;
- Read for $t = t_0$, the corresponding value of drawdown A for each extrapolated straight line
- Plot A versus r^{2N} on a linear plot, and draw a straight line through the plotted points;
- Extend the straight line; read for $r^{2N} = 0$, the value of A_0; determine the slope, -B, of the straight line;
- From t_0, A_0, B and N, calculate K_f/S_{sf};
- From Q, N and B calculate $K_f b^{3-n}$

A linear plot of A versus r^{2N} will only yield a straight line for parts of the aquifer in which K_f/S_{sf} is constant, e.g. for observation wells placed along a major fracture zone. If an aquifer is heterogeneous with respect to K_f/S_{sf}, a linear plot of A versus r^{2N} will not result in a single straight line. Provided the number and distribution of observation wells are adequate, the method allows different zones in the fractured aquifer to be identified and characterised by its diffusivity K_f/S_{sf} and the quantity $K_f b^{3-n}$.

Straight Line Method by Roberts and Beauheim (2001)

The pressure derivative (p') displays late-time straight lines with slopes related to the flow geometry/dimension as shown in Figure 4-5. The relationship between the slope and the flow geometry/dimension is given by Barker (1988) as:

$$m = 1 - \frac{n}{2} \qquad \text{(Equation 4-11)}$$

By defining a scaled second derivative as:

$$p'' = -2\frac{d\log(p')}{d\log(t)} + 2 \qquad \text{(Equation 4-12)}$$

the late-time data will plot on a semilog plot of the scaled second derivative versus log time as a constant value equal to n. Figure 4-6 shows an example flow-dimension diagnostic plot for a constant-rate test with data from simulated tests in systems of various flow dimensions.

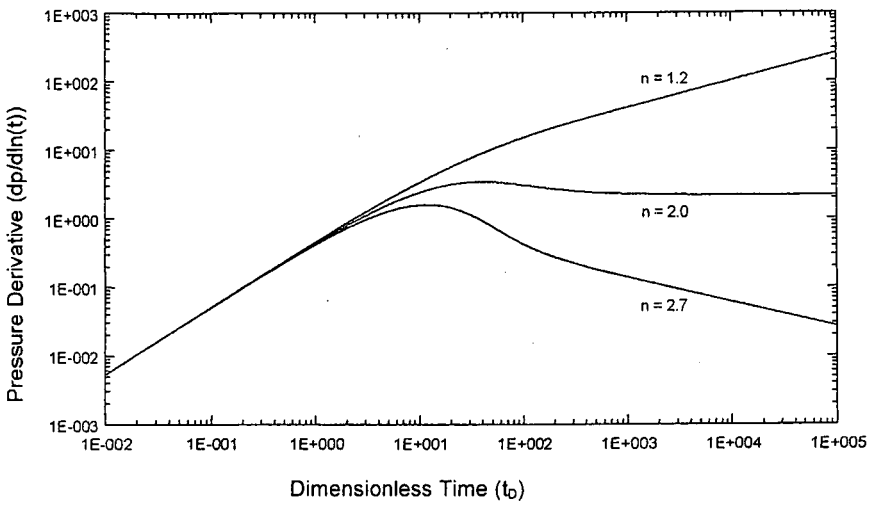

Figure 4-5 Example log-log plot of pressure change derivative showing the late-time straight line for flow dimension of n = 1.2, 2.0 and 2.7 (Roberts and Beauheim, 2001)

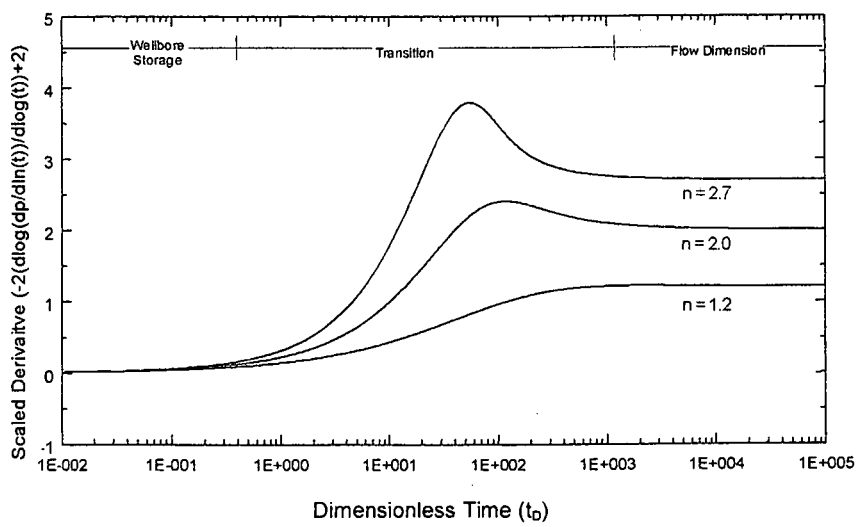

Figure 4-6 Semilog plot of the scaled second derivative of pressure change for constant rate tests with different flow dimension (Roberts and Beauheim, 2001)

Note that the scaled second derivative cannot be used to diagnose flow dimension visually during the periods in which the pressure response is dominated by well bore storage and transitioning to the final infinite-acting behavior, i.e. before the first derivative takes on a constant slope. However, just as the first derivative shows shapes and patterns indicative of such things as well bore storage, skin, double-porosity, and boundaries, so too does the scaled second derivative show recognisable patterns diagnostic of specific factors. For example, well bore storage, which appears as a unit slope on a log-log plot of the first derivative, is shown as a horizontal segment with a value of zero on the diagnostic plot of the second derivative. A positive skin, which appears as a maximum in the first derivative immediately after the wellbore storage unit slope, also appears as a maximum in the second derivative. Double-porosity, which appears as a minimum in the first derivative, appears as a maximum in the second derivative. If the effects of skin and double-porosity are not well separated in time, distinguishing between the two factors may be difficult.

The transforms described above can also be applied to the observation-well data from a constant-rate test to create flow-dimension diagnostic plots.

If the flow dimension n is estimated with the straight-line method of Roberts and Beauheim (2001), the aquifer parameters K_f, S_{sf} and b can be estimated applying the approach of Barker (1988) or Bangoy *et al.* (1992).

4.1.2.3. Numerical Models

It is obvious that in order to analyse pumping test data correctly, either with an analytical method or a numerical model, the following points need to be considered:

- A correct conceptual model for the hydrogeological system
- The geometry of the aquifer
- Inner boundary conditions such as well bore storage effects
- Outer boundary conditions, for example no-flow boundaries.
- Characteristics of the flow conditions

The geometry of the aquifer system and the fracture system is often unknown. This can result in an incorrect conceptual model and therefore an incorrect parameter estimation, when performing and analysing a pumping test with both analytical methods and numerical models.

In the following sections different software, which was especially developed for analysing hydraulic tests with numerical models, are briefly described. Then the use of a three-dimensional numerical model like MODFLOW is discussed in more detail.

(a) TPA

The TPA program (Test Pumping Analysis for fractured and non-fractured aquifers) is designed by Bardenhagen (1999) for analysing step test data, multi-rate test data and constant discharge test data for primary aquifers and especially for fractured aquifers. TPA provides 14 analysis methods for the drawdown data and recovery data. In addition to the conventional curve fitting or straight-line methods, it provides the specially designed TPA simulator, which contains 18 different solutions for forward modelling of hydraulic test data.

The complex nature of fractured aquifers requires an appropriate data diagnosis before the evaluation of drawdown and recovery data. For this purpose TPA provides a special diagnosis window, which contains several diagnosis plots, first and second derivative, and a straight-line analysis that can be applied to the test data.

Using the appropriate Type curve fitting method and/or Straight line fitting method in the curve-fitting window, the aquifer parameters and well parameters can be calculated.

The final step of any test evaluation should be the simulation of the drawdown and recovery curve by using the TPA simulator, a forward modelling. This tool enables the user to evaluate effects like well bore storage, up to four reservoir boundaries, leakage coefficient, other pumping wells that could interfere with the test, etc. The simulator is designed to study those effects on theoretical analytical models. Furthermore, simple predictions for the drawdown in a well or well field can be made.

The analysing methods and solutions, implemented in the TPA simulator, include:

Primary aquifer solution

- Unconfined aquifer
- Delayed responding aquifer or delayed yield
- Leaky aquifer
- Water table aquitard
- Two aquifers
- Confined aquifer
- Confined aquifer with boundaries

Single Vertical Fracture/Fault/Dyke solution

- Finite conductivity fracture
- Dyke/Formation aquifer
- Infinite conductivity fracture and uniform flux
- Infinite conductivity fracture and infinite flux
- Infinite conductivity fracture and uniform flux and boundaries
- Infinite conductivity fracture and infinite flux and boundaries

Single Horizontal Fracture solution

- Infinite conductivity fracture and uniform flux

Double Porosity or Natural Fractured Aquifer solution

- Fissured aquifer
- Double porosity
- Double porosity with boundaries

General Radial Flow solution

- Generalised radial flow

(b) RPTSOLV

RPTSOLV is a two-dimensional numerical model, developed by Verwey *et al.* (1995) for aquifer parameter estimation from hydraulic test data. It considers the distance dependence of the storativity values, estimated with analytical methods, and is able to avoid this effect.

In the absence of regional base flow, groundwater flow is towards the borehole during a pumping test. Therefore, flow directions are (1) radially, towards the borehole and (2) in the vertical direction. A section through the aquifer in the form of a wedge-shaped slice takes advantage of this restricted flow, as shown in Figure 4-7, with θ in the direction of no-flow. A slice of angular size θ has, at a distance r, an angular width of $r\theta$. The product of the three-dimensional parameters, that is either the specific storativity S_0 or hydraulic conductivity K, with $r\theta$ should not be confused with the horizontal two-dimensional parameters of storativity and transmissivity. These angular parameters, $r\theta \cdot S_0$ and $r\theta \cdot K$ serve the same purpose of reducing the dimensions of the flow equation, but they are distance-related and only of use in this radial numerical model. The user must, if needed, calculate S and T from a predefined thickness of the whole aquifer, or a specific layer of interest. However, when using this model, the thickness of the aquifer, or different layers, must always be known, because this information is necessary for the development of the numerical model. The advantage of this presentation is that vertical variations in the aquifer can be taken into account, but with a two-dimensional flow model.

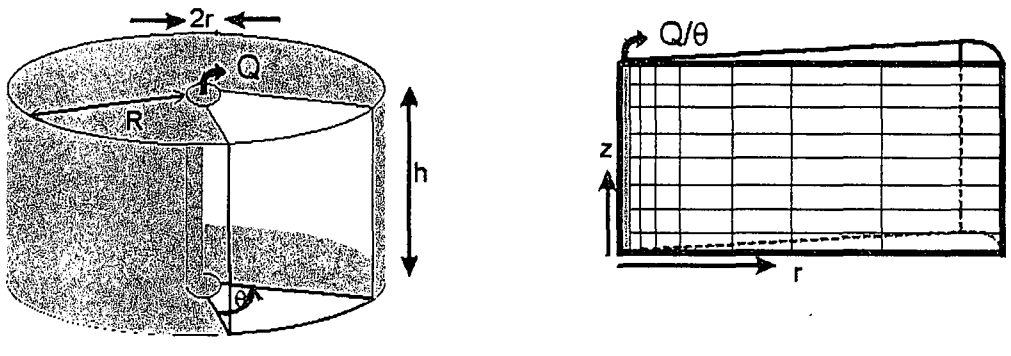

Figure 4-7 The wedge-shaped slice taken from a full three-dimensional aquifer. Groundwater in this slice is assumed to be two-dimensional (after Verwey *et al.*, 1995)

The two-dimensional slice in Figure 4-7 is discretised into 20 horizontal layers, with $\Delta z = 2$ m. A logarithmic scale is used in the radial direction, with 16 nodes placed on r = {0; 0,05; 0,2; 1,1; 2,3; 4,7; 9,5; 19,1; 18,3; 38,9; 76,7; 153,5; 307,1; 614,3; 1228,7; 1638,3}. This spacing ensures a detailed solution near the borehole, but still allows the simulation of a large diameter area. However, as with any numerical model, the exact grid and time spacing can suit the requirements of the user.

(c) nSIGHTS

The software nSIGHTS (n-dimensional Statistical Inverse Graphical Hydraulic Test Simulator) is developed by Roberts *et al.* (2001) for hydraulic test interpretation in low permeable aquifers. The program is based on the GRF-model of Roberts and Beauheim (2001) and written in the code GTFM 6.2, which is an enhanced version of the original graph theoretic field model (GTFM). Currently the software exists as a beta-trial version and will be released during 2002.

The code GTFM (graph theoretic field model) 6.2 simulates the hydraulic response of a single-phase flow regime in one-dimensional geometry to boundary conditions applied at a borehole located at the origin of the modelled flow system. In this instance, "one-dimensional" refers only to the fact that pressure is calculated at specific radial distances from the borehole, and that flow within the formation is either towards or away from the borehole. The problem domain is discretised by dividing the flow system into a series of concentric rings centered on the borehole, with each ring represented by a node. A constant multiplicative factor is used to increase the spacing between nodes with increasing distance from the origin (borehole, see Figure 4-8). The dimensionality of the flow system is defined using the flow-dimension parameter (n), which defines how the cross-sectional area of nodes changes with distance from the borehole. Thus, linear flow can be simulated by maintaining a constant nodal cross-sectional area (n = 1), radial flow can be simulated by changing nodal cross-sectional areas linearly with distance from the borehole (n = 2), etc. Using n, the model can simulate transient flow and pressure responses in a formation that has varying thickness but assumes vertically homogeneous hydraulic properties. In cases where boundary effects are indicated by the test data, those effects are also simulated by varying the cross-sectional areas of the nodes at various distances.

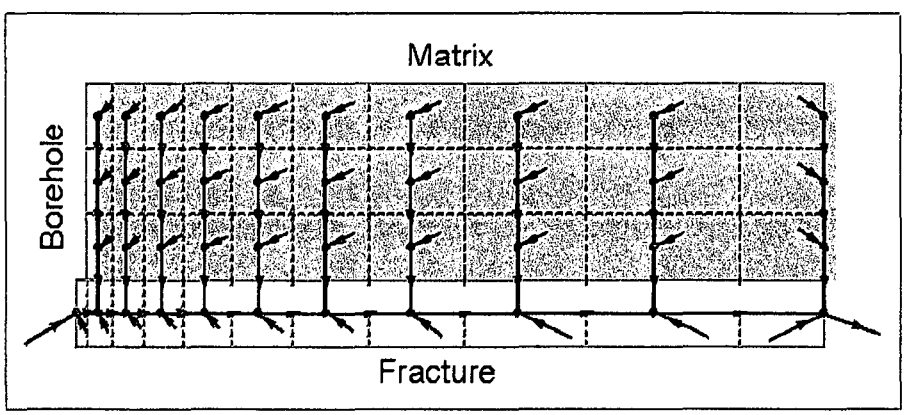

Figure 4-8 System graph for dual-porosity system with 11 radial nodes and 3 matrix nodes (Roberts *et al.*, 2001)

- Fracture networks, which can be considered as continuum, are simulated in a single-porosity mode, meaning that a differentiation between fracture and matrix parameter is not possible.
- Fracture networks showing double porosity characteristics are simulated with the dual-porosity mode, differentiating the fracture and matrix parameter.

- The case of a single horizontal fracture or a horizontal fracture zone can be simulated as a leaky aquifer, where the aquifer is represented by the fracture zone and the leakage is contributed from the matrix above and / or below the fracture.
- Features like single vertical fractures or faults cannot be simulated with this approach, because they are not homogenous in the area extent (radially centered).

Formations may include radially centered heterogeneities (hydraulic conductivity (K) and/or specific storage (S_s) varying with radial distance) to simulate the presence of a "skin" zone adjacent to the borehole or more complex composite systems. K and S_s may also vary as a function of the calculated pressure at each node to simulate the effect of fractures opening/closing as a function of pressure.

The external boundary conditions of the model may be either fixed pressure or zero flow. The model has wellbore (inner) boundary conditions that can be used to simulate pulse-injection/withdrawal tests, specified borehole-pressure conditions, specified flow rates into or out of the formation, and slug-injection/withdrawal tests. The cumulative effects of consecutive tests are incorporated in the simulations. The model can also incorporate test-zone pressure changes resulting from temperature variations in the test zone as well as from test-equipment- and/or formation-induced changes in the test-zone volume. The model output consists of simulated pressure responses in the borehole and at selected radial distances from the borehole. The model can also calculate formation flow rates and cumulative production based on the formation's estimated hydraulic properties.

The primary input parameters to nSIGHTS include the formation's hydraulic properties (hydraulic conductivity, pore pressure, and specific storage or its constituent parameters), fluid properties (density, compressibility, and thermal-expansion coefficient), test-zone parameters (radius, length, contained fluid volume, and compressibility), flow dimension (geometry), and, if used, skin properties (radial thickness, hydraulic conductivity, and specific storage). If run in double-porosity mode, the formation hydraulic properties become fracture hydraulic properties, and matrix properties (volume factor, hydraulic conductivity, specific storage, and geometry factor) are also specified. Fitting parameters typically include the formation's hydraulic properties, and can also include (as determined by the conceptual model and available constraints) matrix properties, skin properties, flow dimension, and test-zone compressibility. All other parameters (non-fitting) are initially fixed at the best estimates of their true (but imperfectly known) values. The non-fitting parameters are sampled at a later stage of the analysis process to perform uncertainty analysis.

For interpretations performed with nSIGHTS, individual testing periods are subdivided into discrete time intervals, called sequences. Sequences may be of different types, which are differentiated by the well bore boundary conditions in effect during those time periods.

- Sequences during which borehole pressures are prescribed in the model are referred to as *history* sequences.

- Sequences during which a test zone is shut in and pressures in the test zone and the surrounding formation are equilibrating are referred to as *pulse* sequences.
- *Flow* sequences are used to represent periods during which water is pumped from or injected into a well. A rate history is typically used with a single flow sequence if the rates are highly variable. Multiple flow sequences can be used when the rates are stepped. A flow sequence with a zero rate is used to represent the recovery period following a pumping or injection test. Model output during flow sequences consists of transient pressures in both the test zone and formation.

The well-test analysis code nSIGHTS consists of two modules: *nPre* and *nPost*. The *nPre* module is the simulator and *nPost* is used for post processing the simulation results.

The simulator operates in several different modes, referred to as *Simulation Type* and *Simulation Sub-Type* in the *nPre* menu. The two primary modes (*Simulation Type*) are "Forward" and "Optimization". In "Forward" mode, *nPre* simply simulates a hydraulic test response based on the user input. In "Optimization" mode, the code uses non-linear regression algorithms to adjust the values of user-specified fitting parameters to obtain an optimal fit to the field data. There are three *Simulation Sub-Types* for both the "Forward" and "Optimization" modes: 1) "Normal," 2) "Range", and 3) "Sampling." The possibilities are briefly described below.

- Normal – Simulation based on input parameter values in Forward-mode and Fitting-parameter values are optimised using non-linear regression algorithms to obtain an optimal fit to the specified constraints (field data) in Optimization-mode
- Range – A range is assigned to two or three variables and forward simulations are performed for each combination of the range variables (user chooses the number of intervals for each range). Each forward simulation is compared to a user-defined constraint and a corresponding error is calculated. Maps of the error surfaces (typically called parameter-space maps or fit surfaces) are created to find the optimal fitting-parameter combinations. In Optimization-mode the specified variables are optimised for each combination of "range" variables, allowing investigation of more complex fit surfaces.
- Sampling – Uncertainty ranges and distributions are assigned to parameters of interest. These distributions are sampled and a forward simulation is produced for each sample set. Can be used to investigate the correlation between fitting and non-fitting parameters.

nPre has statistical routines that allow uncertainty in the estimates of fitting parameters to be quantified. These uncertainties are inherent in well-test analysis (or any inverse problem), but they are typically not quantified. For a given conceptual model, uncertainty in the estimated values of the fitting parameters can result from

- correlations among fitting parameters,
- noise in the measured field data, and
- correlations among fitting and non-fitting variables within the model.

(d) 3D-Model

To analyse a hydraulic test with a numerical model the hydrogeological structure of the aquifer should be represented by the model. E.g. in case of an aquifer, consisting of a horizontal, bedding-plane fracture in a matrix of sandstone or mudstone, the model should consist of one layer, representing the fracture zone, and above and below this layer some layers, representing the matrix. The whole aquifer should be treated as homogeneous and confined. Therefore smaller horizontal fractures and vertical fractures are neglected. The parameters used in the model that have to be calibrated by inverse modelling, are the T matrix, T fracture, S matrix, S fracture and Leakage in the matrix.

The steps to build a numerical model correctly and to use it for the purpose of parameter estimation are explained in detail in the "Guidelines for aquifer parameter estimation with computer models" (Chiang and Riemann, 2001).

- Step 1 Conceptualisation
- Step 2 Create a new model
- Step 3 Assign the model data and parameters
- Step 4 Assign the observation data
- Step 5 Perform the flow simulation
- Step 6 Assign data and parameters for inverse modelling

A conceptual model is used to denote the parameters (such as hydraulic conductivity) and conditions (such as boundary conditions) needed to solve the governing equations in a mathematical model. As base for the numerical model the conceptualisation must be able to represent the aquifer system. This will be demonstrated by means of an example, the analysing of the so-called UO5-test at the Campus Test Site, University of the Free State in Bloemfontein (see Chapter 6, Case Studies).

The conceptual model for the Campus Test Site is based on the geology and hydrogeology of the site as described in Botha *et al.* (1998). The main aquifer is situated in a horizontal layer of sandstone with a bedding-plane fracture zone at a depth of approximately 21 m. The thickness of the sandstone layer is between 15m and 20m. The extent of the fracture zone is unknown, but at least some hundred meters.

Comparing to the high hydraulic conductivity of the fracture, the hydraulic conductivity of the matrix is small. But the storage of the matrix is much higher than that of the fracture. During the pumping in the fracture, groundwater is released from the matrix, and flows vertically to the fracture and then horizontally to the pump.

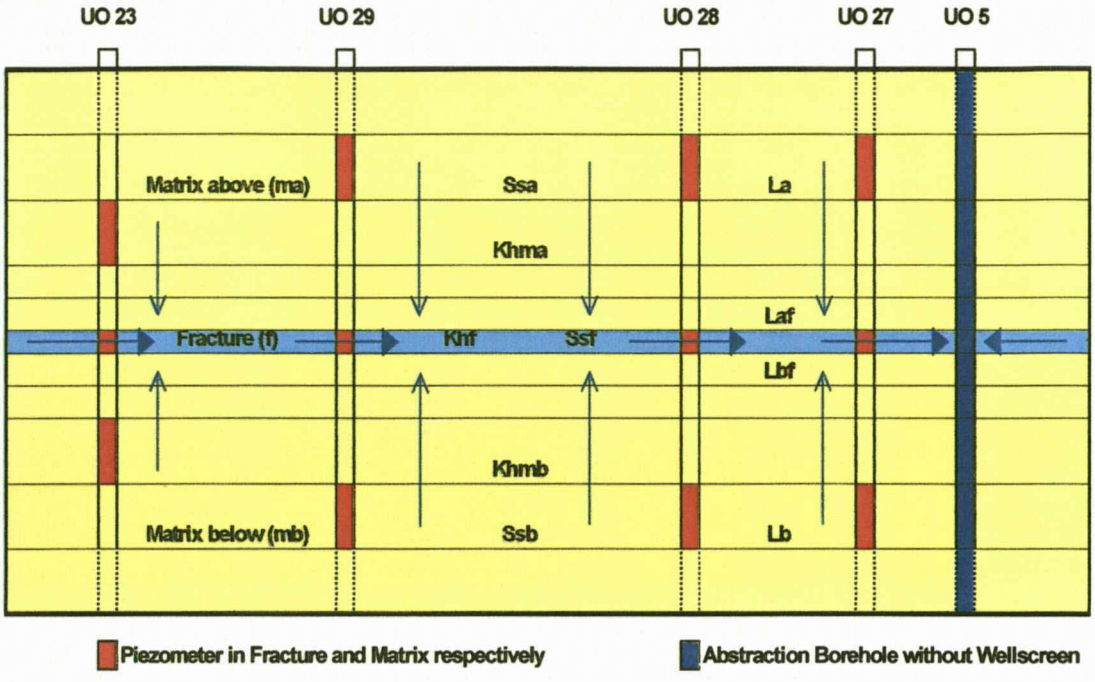

Figure 4-9 Conceptual model of the flow in the sandstone aquifer of the Campus Test Site with the relevant parameters (explanation of the abbreviations in Table 4-2)

Table 4-2 Complete list of parameters for PEST-calibration

Aquifer / Layer	Parameter Description	Abbreviation
Matrix above (ma)	Leakage of the matrix above	La
	Leakage from the matrix above to the fracture	Laf
	Hydraulic Conductivity of the matrix above	Khma
	Specific Storage of the matrix above	Ssa
Fracture (f)	Hydraulic Conductivity of the fracture	Khf
	Specific Storage of the fracture	Ssf
Matrix below (mb)	Leakage of the matrix below	Lb
	Leakage from the matrix below to the fracture	Lbf
	Hydraulic Conductivity of the matrix below	Khmb
	Specific Storage of the matrix below	Ssb

The first step in analysing the groundwater flow in an aquifer with a numerical model is to develop a suitable mesh or grid for the aquifer. The finite difference mesh used in the present model consists of 88 rows, 115 columns and 23 layers of nodes. The horizontal extent of the model chosen was large enough to avoid boundary effects (6200m x 6200m). The grid size varies from 400m at the outer part to 2m surrounding the abstraction borehole UO5.

The 12th layer of the model represents the fracture. The other layers represent the sandstone matrix above and below the fracture. The two layers directly above and below the fracture are each assigned a thickness of 0.5 m, and the other layers a thickness of 1 m (see also Figure 4-9 and Figure 4-10). This fine vertical discretisation is necessary to account for the vertical flow in the rock matrix.

As mentioned in chapter 6.1.1, the fracture zone has an aperture of 0.2 m, while its horizontal extent was estimated as 150 m x 200 m, based on the geological profiles of the boreholes. The abstraction borehole UO5 and the observation boreholes (UO27, UO28, UO29 and UO23) were also placed in the mesh within the fracture and the matrix respectively.

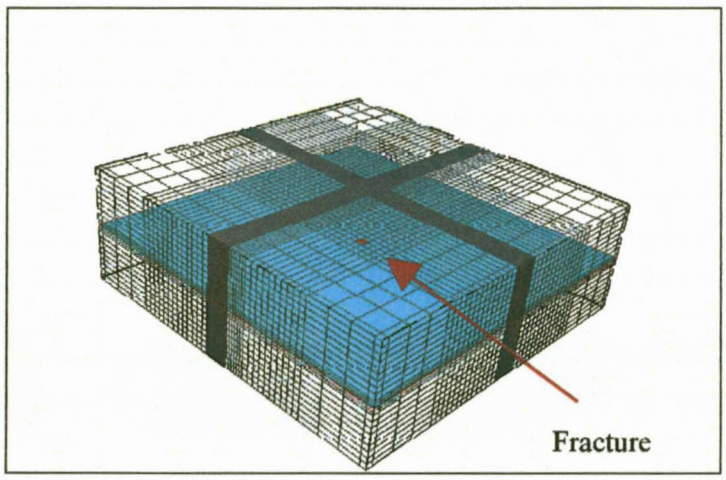

Figure 4-10 Model discretisation in three dimensions

To calibrate the model with the pumping test data, the inverse model PEST (Doherty, 2000) is used. The criterion for the automatic parameter estimation with inverse modelling technique is the sum of squared residuals (called phi), where residuals are the differences between the measured and calculated data (e.g. hydraulic head or drawdown).

The parameters to estimate were assigned different parameter numbers. For each parameter initial values, upper and lower bounds were defined. For the first calibration runs the estimated parameters from analytical methods should be used as initial values, while the bounds are chosen as big as reasonable while avoiding any effects.

To estimate the unknown parameters with the inverse modelling technique PEST it is essential to get at first a good guess of the initial values (see steps 1 to 3 in the following procedure). Using initial values which are not suitable for the aquifer system, will lead to an incorrect estimation of the parameters. The following procedure should be used to estimate unknown parameters:

1. Assume initial values and run the model forward – to make sure that the initial values are in a reasonable range.

2. Estimate initial values for all parameters by running PEST with the assumed initial values (step 1) and bounds, and using only the observation data in the fracture – to update the initial parameter values.
3. Fix the parameter values for the fracture, which are obtained from step 2, and run PEST using the observation data in the matrix piezometers to update the initial values for the matrix parameters.
4. Estimate all parameters by running PEST with the fracture and matrix parameter values obtained from steps 2 and 3 as initial values and using all observation data.
5. Eventually improve the fit by changing parameters individually (change one parameter at a time) and running the model forward.
6. Use the parameter values from step 5 as initial values and run PEST to get a final estimate of parameter values.
7. Use the parameter values from step 5 as initial values and run the inverse model with a different geometry (extent of the fracture, thickness of the matrix), to estimate the impact (parameter sensitivity) due to the unknown geometry.

4.1.2.4. Uncertainties of Numerical Models

The parameter estimation with numerical models show uncertainties in the estimation process, which can lead to incorrect estimates, as long as the user is not able to recognise and quantify this phenomenon. Possible reasons are given below. In most cases, these reasons also apply to analytical methods.

- The geometry of the aquifer is not well known and is simplified in the model (e.g. constant thickness over the whole model) and the real extent of the fracture is unknown.
- The drawdown behaviour in the abstraction borehole cannot be simulated correctly with the numerical model due to effects like well bore storage and well bore skin. The radius of the borehole and the cell size in the model are often different, therefore it is only possible to get the same trend of the curve, but not the same values.
- Secondary horizontal and vertical fractures which intersect the main fracture, and the resultant semi-confined or unconfined conditions are not considered.
- Heterogeneity in both matrix and fracture systems is unknown and not considered. The unknown heterogeneity could even affect the hydraulic test data.
- Inverse modelling technique is often non-unique and can therefore provide an infinite number of parameter sets, which result in a good fit.
- In fractured aquifers a non-linear relationship between drawdown and discharge rate can be observed (Van Tonder and Riemann, 2001).

(a) Uncertainty due to Non-Uniqueness of Inverse Modelling

The influence of the different parameters on the drawdown curves can be summarised as follows:

- The drawdowns in two different fracture piezometers become closer together, when the T-fracture increases or the leakage to the fracture decreases. The influence of the transmissivity is stronger.
- The shape of the drawdown curve in fracture piezometer is controlled by the T-matrix and the leakage to the fracture, while an increase of the transmissivity of the matrix and the leakage to the fracture results in a decrease of the drawdown in fracture piezometers at late time. An increase of the S-matrix or a decrease of the S-fracture shows a similar result.
- The delay in the drawdown behaviour of the matrix is mainly controlled by a high S-matrix, but even a decrease of the T-matrix or the vertical K-matrix can result in a longer delay.
- The absolute drawdown in the matrix piezometers increases when the T-matrix or the S-matrix decreases or the vertical K-matrix increases.

If for instance the T-matrix increases, the influence will be seen in the drawdown curves of both the fracture piezometer (i.e. drawdown decreases at late time and the shape of the curve is changed) and the matrix piezometer (i.e. drawdown increases and delay becomes less). An increase of the S-matrix results in a decrease of the drawdown in the fracture at late time, a decrease of the drawdown in the matrix, and in a longer delay of the drawdown in the matrix piezometer.

It is apparent that there is no unique solution in a mathematical, numerical way. It is possible to get a good fit with a parameter combination, which is not reasonable (e.g. in Figure 4-11 the vertical K-matrix is higher than the horizontal K-matrix).

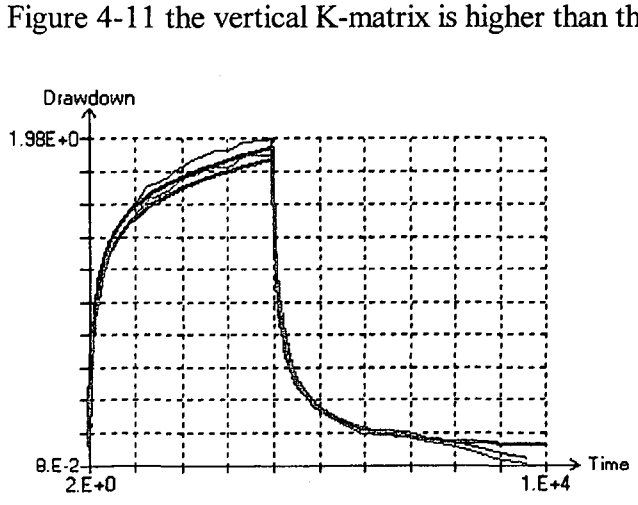

Thin lines – measured data of two observation boreholes

Bold lines – calibrated data of two observation boreholes

Figure 4-11 Result of inverse modelling with vertical K-matrix higher than horizontal K-matrix

(b) Uncertainty due to Unknown Geometry

The influence of the chosen geometry was estimated with several inverse models using PEST and the same initial conditions as for the best fit. The runs are called run 31, 32 and 33. In run 31 the thickness of the aquifer was reduced, while in run 32 and 33 the extent of the fracture was changed (halved and doubled respectively). The results are listed in Table 4-3.

One reason for the higher drawdown, observed in the matrix piezometers below the fracture, can be a smaller thickness of this part of the aquifer. To evaluate this the parameters of the layers 19 to 23 were changed to simulate an aquiclude. The change of the parameter values, obtained from the inverse model (i.e. T matrix for 1m thickness, S matrix for 1m thickness, leakage between layers of 1m thickness), between the best fit and this calibration run is not evident, but a calculation of the aquifer parameter shows a decrease of the S matrix for the whole aquifer from 1.25E-2 to 6.84E-3 (see Table 4-3) due to the change of the aquifer thickness.

Because the real extent of the fracture is unknown, it is important to know the impact of the fracture's extent on the estimated parameters. As described above the area of the fracture was chosen at 150m x 200m. For the first run this area was halved to 100m x 150m and for the second run the area was doubled to 200m x 300m. The estimated parameters for the matrix differ from the values of the best fit (see Table 4-3) and the relationship can be described clearly:

- When the area of the fracture is **halved**, the S matrix **doubles** and the K vertical matrix increases.
- When the area of the fracture is **doubled**, the S matrix **halves** and the K vertical matrix decreases.

Table 4-3 Influence of the geometry of the model (a: best fit, b: Thickness below fracture is halved, c: Area of the fracture is halved, d: Area of the fracture is doubled)

Parameter	Unit	Best Fit	Thickness	Area x 0.5	Area x 2
T matrix (aquifer)	m^2/day	9.0	9.1	10.6	6.1
T fracture	m^2/day	616	778	519	526.3
K horizontal matrix	m/day	0.45	0.61	0.53	0.31
K vertical matrix above	m/day	1.54E-4	1.64E-4	2.61E-4	9.27E-5
K vertical matrix below	m/day	1.19E-3	1.10E-3	1.83E-3	1.15E-3
K horizontal fracture	m/day	3080	3890	2596	2632
S matrix (aquifer)		1.25E-2	6.84E-3	2.41E-2	7.63E-3
S fracture		1.71E-5	2.11E-5	1.11E-5	2.37E-5

(c) Uncertainty due to Non-Linear Relationship between Drawdown and Discharge Rate

The UO5 test with 0.5 l/s was repeated with an abstracting rate of 2 l/s (see section 6.1.2). Using the parameter values, obtained from the inverse modelling of the UO5 test (0.5 l/s), the observation data in both the fracture and matrix piezometers don't fit well (see Figure 4-12).

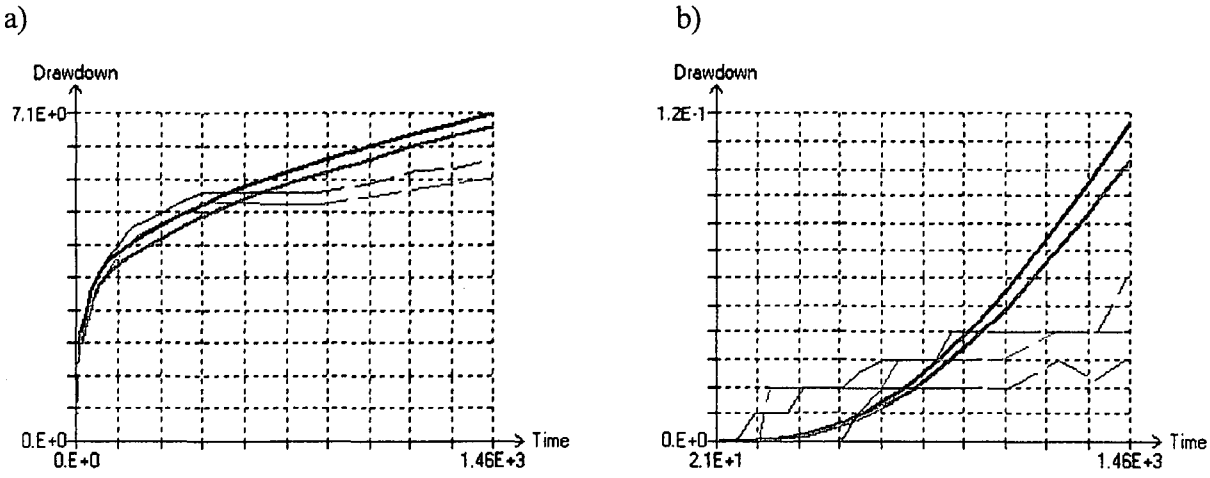

Figure 4-12 Comparison observed and calculated data for the UO5 test (2 l/s). Forward run with estimated values from UO5 test (0.5 l/s); a) Fracture piezometers, b) matrix piezometers above (bold = calibrated, fine = observed)

After calibrating the data with inverse modelling the fit of the observation data in the matrix piezometers is better, and the estimated parameter values differ from the values obtained as the best fit from the UO5 test in July 2000, but they are still between the minimum and maximum values from the UO5 test.

Table 4-4 Comparison of the estimated parameter values for the UO5 tests, July and September 2000, obtained from the best fit of inverse modelling (July 2000) and the geometric mean of reasonable runs of inverse modelling (September 2000)

Parameter	Unit	UO5 Test July 2000 Best Fit	UO5 Test Sept. 2000 Geometric Mean
Discharge Rate	l/s	0.5	2.0
T matrix (aquifer)	m^2/day	9.0	28
T fracture	m^2/day	616	530
K horizontal matrix	m/day	0.45	1.4
K vertical matrix	m/day	1.54E-4	1.8E-4
K horizontal fracture	m/day	3080	2650
S matrix (aquifer)		1.25E-2	8E-3
S fracture		1.71E-5	1.6E-5

4.1.2.5. Analytical vs. Numerical Models

A comparison between the results of analytical methods and numerical models is used for different cases to determine the validity of analytical methods. In most case studies the applied analytical methods and numerical models yield different values for the aquifer parameter. This phenomenon is caused by the underlying assumptions of analytical methods, which are not always satisfied in reality, and different conceptual models. In general the results can be described as follows:

- Porous media methods, such as Theis or Cooper-Jacob, are only applicable in specific geological set-ups, as described below.
- Methods considering the flow behaviour in single fractures or fracture networks, such as the double porosity model or vertical fracture model, are applicable in specific cases and yield values similar to the estimation obtained from a three-dimensional numerical model. The inherent problem of these methods is that they are limited to few specific cases, which do not often occur in Southern Africa. The estimation of the storativity shows still scale-dependency.
- The GRF-model of Barker (1988) is applicable to most cases of hydraulic tests in fractured rock aquifers, because it accounts for the unknown flow geometry by introducing the flow dimension. The estimated values for the fracture hydraulic conductivity and fracture storage coefficient are mostly lower than the estimation obtained from a three-dimensional numerical model.
- Applying the one- and two-dimensional numerical models nSIGHTS (Roberts *et al.*, 2001) and RPTSOLV (Verwey *et al.*, 1995) yield better estimates than the analytical methods, if the correct conceptual model is chosen. RPTSOLV is only applicable in the case of a horizontal fracture and yields the storage coefficient of the matrix and the vertical hydraulic conductivity. nSIGHTS yields values for the aquifer parameters similar to the GRF-Model of Barker (1988).

In the case of a horizontal, bedding-plane fracture zone, a comparison between the results of analytical models and the numerical model reveals the possibility of simplifying the procedure of parameter estimation from a hydraulic test. The results of the methods used are listed in Table 4-5, where

- *T aquifer min/max* are the minimum and maximum transmissivity values of the entire aquifer, obtained by using different observation boreholes in analytical methods.
- *T matrix* and *T fracture* are transmissivity values of the matrix (sandstone) and fracture, respectively.
- The arrows in the table indicate the way to obtain to bold-type faced values, which are comparable to values from a numerical model.
- The same rule applies to S aquifer min/max, S matrix and S fracture.
- *K v matrix* is the vertical hydraulic conductivity of the matrix.

Table 4-5 Comparison of the results from analytical and numerical models for a aquifer with single, horizontal fracture zone in a sandstone matrix

Parameter	Unit	Numerical Model	CJ / Theis Fracture [1]	CJ / Theis Matrix [2]	Cooper-Jacob II	Gringarten
T aquifer min	m^2/day	n.a.	9	4.2	50 [4]	10
T aquifer max	m^2/day	n.a.	11	88.5	743 [3]	15
T matrix [5]	m^2/day	9.0	10	n.a.	n.a.	12.5
T fracture [5]	m^2/day	616	n.a.	n.a.	743	n.a.
K v matrix	m/day	1.54E-4 to 1.19E-3	n.a.	n.a.	n.a.	3.0E-3
S aquifer min		n.a.	1.3E-5	5.4E-3	2.0E-15 [3]	2.0E-5
S aquifer max		n.a.	8.0E-3	3.3E-1	2.3E-2 [4]	3.0E-3
S matrix		1.25E-2	8.0E-3	n.a.	2.3E-2	n.a.
S fracture		1.71E-5	1.3E-5	n.a.	n.a.	2.0E-5

[1] Cooper-Jacob I / Theis method using observed values in fracture, [2] Cooper-Jacob I / Theis method using observed values in matrix, [3] Using observation data from fracture piezometer, [4] Using observation data from matrix piezometer, [5] Estimated T-values are effected by chosen thickness

From the above-mentioned comparison the following suggestions are recommended to estimate the aquifer parameters with analytical models:

- To estimate the **transmissivity of the matrix**, the Cooper-Jacob or Theis method can be used, when the assumptions for applying these methods are valid. That means the drawdown curve must show radial acting flow and there are no boundary effects.
- To estimate the **transmissivity of the fracture**, the drawdown-distance method (known as Cooper-Jacob II) can be used. At least two observation boreholes are required in addition to the abstraction borehole.
- To estimate the **storage coefficient of the fracture**, the Cooper-Jacob or Theis method can be used. It requires an observation borehole which intersects the fracture far away from the abstraction borehole. The problem is that the definition of 'far away' is unclear.
- To estimate the storage coefficient of the matrix:
  1 The Cooper-Jacob or Theis method: Both methods require an observation borehole which intersects the fracture close to the abstraction borehole. The problem is that the definition of 'close' is unclear. These methods can also be applied by using the effective borehole radius of the abstraction borehole itself.
  2 The Cooper-Jacob II method: Observation data of at least two matrix piezometers are required.
- For the parameters of the matrix (**T, K_v and S**), the Gringarten method can be used, but it is non-unique and it is difficult to fit the data without prior information. If the parameters T-matrix, S-matrix and half-length of the fracture are estimated with other analytical methods, it is possible to get a unique fit of the drawdown data.

To use analytical methods for parameter estimation for aquifers with a vertical fracture is more complicated than for aquifers with a horizontal fracture, because more aquifer systems are involved in the former.

As shown in Table 4-6 the use of analytical solutions will yield a geometric mean value of transmissivity of the involved aquifer systems:

- The abstraction borehole (M1) represents the whole aquifer and therefore applying the analytical method to the drawdown curve will yield a geometric mean of the transmissivity of all aquifer systems.
- The observation borehole M2 intersects all aquifer systems and including the fracture. Analytical methods yield values close to the fracture transmissivity, as the groundwater movement occurs dominantly in the fracture.
- The observation boreholes M3, M5 and M6 intersect the mudstone and the dolerite. Analytical methods yield values close to the dolerite transmissivity, as it is higher than the mudstone transmissivity and groundwater movement occurs dominantly in the dolerite.

An analytical method for estimating the storage coefficient of the matrix could not be determined for this case.

Table 4-6 Comparison of estimated transmissivities and their geometric mean values, obtained from the numerical model application and the analytical methods

		Geometric Mean Values					
Run 10	T-value	Fracture	Dolerite	Mudstone	Fr.+ Dyke	Dol.+ Mud	all
Fracture	121.00	121.00				23.98	4.85
Dolerite	380.00	214.43	380.00		12.25		
Mudstone	0.30	6.02	10.68	0.30	1.13		
Dyke	0.04	2.20	3.90	0.11		1.66	
Analytical Methods (Cooper-Jacob I / Theis)							
M1		23.8		represents parameter of all aquifer systems			
M2		82.1		represents mainly fracture parameter			
M3		167.5		represents mainly dolerite parameter			
M5		294.4		represents mainly dolerite parameter			
M6		273.7		represents mainly dolerite parameter			
all (CJ II)		34.75		represents parameter of all aquifer systems			

T-value: Estimated transmissivity values using PEST

Geometric Mean Value: Geometric mean of transmissivity values of involved aquifers, e.g. 214.43 is the geometric mean of the transmissivity values of Fracture and Dolerite.

4.1.3. Parameter Estimation

In the following sections the optimal procedure for parameter estimation, as a step-by-step guideline, will be discussed for each relevant parameter, based on the measurements during a constant discharge test or a tracer test, if applicable. Different geological set-ups and fractured systems will be considered in this procedure. Therefore the first group of parameters are needed to define the geometry, while the following group consists the hydraulic properties of the aquifer.

4.1.3.1. Thickness

The thickness of the aquifer, or the thickness of the part of the aquifer which contributes to the flow in the aquifer, is an important parameter of the aquifer geometry. The estimation of hydraulic properties like hydraulic conductivity or transport parameters requires the knowledge of the thickness. Depending on the geological system and the parameter to estimate, the required value can differ (see Figure 4-13).

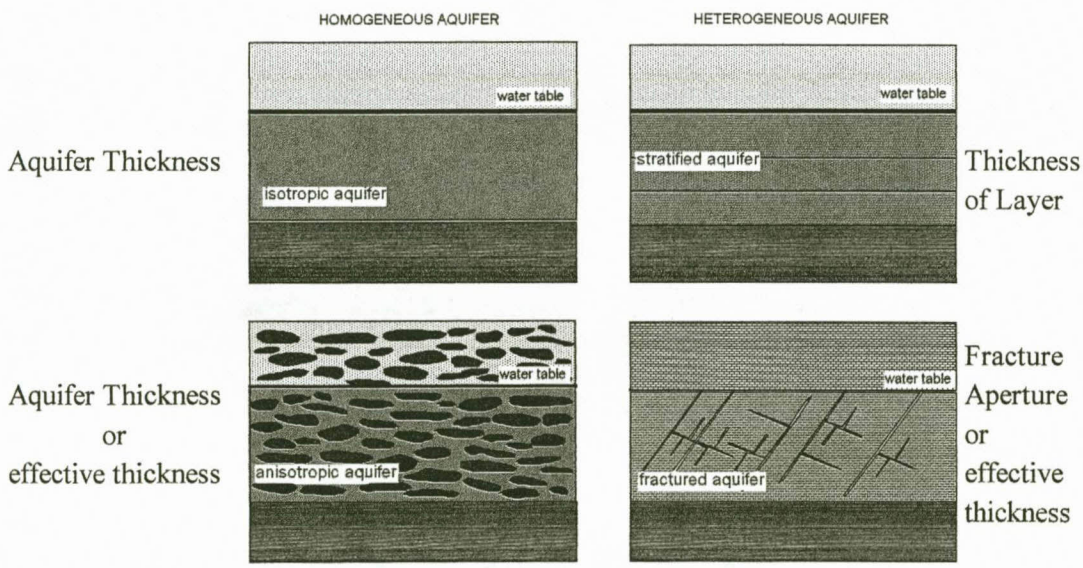

Figure 4-13 Required thickness for parameter estimation depending on geological set-up and aquifer test

(a) Aquifer Thickness

Because most analytical methods for interpreting hydraulic tests will yield estimations of the Transmissivity and the Storativity, knowledge of the aquifer thickness is necessary to calculate hydraulic conductivity and specific storage.

An estimation of the aquifer thickness by means of hydraulic test data is not possible. Therefore geological information from the area and borehole logs from the relevant wells should be used to determine aquifer thickness.

(b) Thickness of Fracture Zone

Several analysing methods of hydraulic and tracer tests require the knowledge of the thickness of the fracture zone or of the through-flow area, which can be defined as

$$A = D_f * L \qquad \text{(Equation 4-13)}$$

with

A = through-flow area
D_f = thickness of the fracture zone
L = length of the fracture, intersected in the borehole

or $$A = 2r_w * D_w \qquad \text{(Equation 4-14)}$$

with

A = through-flow area
$2r_w$ = borehole diameter (in some cases half the circumference of the borehole [πr_w] is used, e.g. see section 4.2.2.1)
D_w = vertical width of the fracture, intersected in the borehole

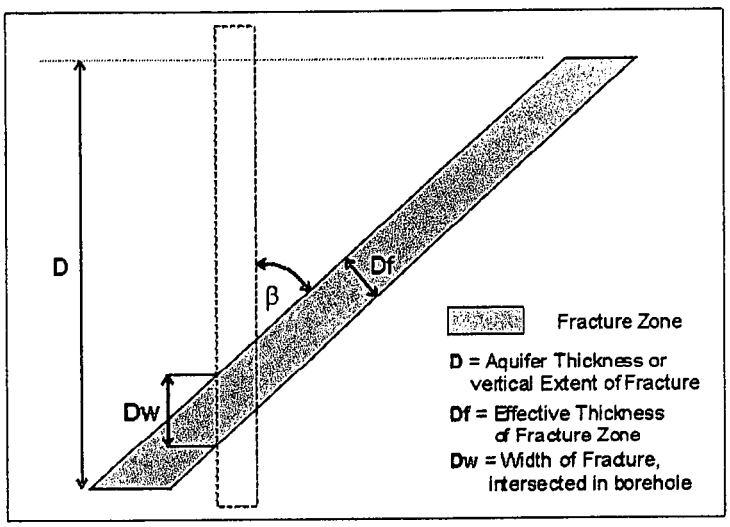

Figure 4-14 Definition of the vertical width of a fracture, intersected in a borehole

The parameters D_w and L depend on the intersection angle β. If the dip of the fracture is known, the angle can be determined and used to calculate D_w and L.

$$D_w = D_f / \sin(\beta) \qquad \text{(Equation 4-15)}$$

$$L = 2r / \sin(\beta) \qquad \text{(Equation 4-16)}$$

With

β = intersection angle

The effective thickness of the facture zone, which contributes to the flow in the aquifer, can be distinguished by means of several methods. The position or depth of the fractures in the borehole must be known beforehand or detected. If the fracture zone is large enough, borehole logs during drilling will give a first approximation. Otherwise direct measurements with borehole geophysics or interpretation of hydraulic or tracer tests should be conducted.

Borehole Geophysics

Several downhole geophysical methods are able to detect fracture zones. In an investigation of Karoo-Aquifers (Botha *et al.*, 1998) it was found that the acoustic scan yield a very good estimation. Additionally, the borehole video log is suggested to verify the results from other borehole geophysical methods.

Hydraulic Test

Because the drawdown response during a hydraulic test shows a flattening at the position of a fracture and an increase in the slope, when dropping deeper, a multirate or step drawdown test can be conducted to distinguish the position of fractures. Furthermore hydraulic tests offer two possibilities to estimate the effective thickness of the fracture zone:

1. Using early drawdown data

De Lange (1999) proposed as an approximation for the thickness of the facture zone the following equation (obtained from experience from tracer tests):

$$D_f = (0.2*Q/s)*0.14 \qquad \text{(Equation 4-17)}$$

With

s = drawdown (m) in abstraction borehole after 1 minute
Q = abstraction rate (l/s)

Because the drawdown response depends on the available through-flow area, the estimated value actually represents the vertical width of the fracture D_w rather than the thickness of the fracture zone D_f.

2. Applying the GRF-Model

If applying the GRF-Model (Barker, 1988) to the data of a hydraulic test, the parameter b (flow domain) in the generalised equations will give an estimate of the thickness of the fracture zone. The GRF-Model is described in section 4.1.2.2(d), while the procedure to estimate the parameters will be discussed in section 4.1.3.3

- In cases where the flow dimension n is close to 2 (i.e. between 1.8 and 2.1), the flow domain will approximately represent the thickness of the through-flow area and therefore the thickness of the fracture zone.
- When the flow dimension n is close to 1 (i.e. between 1 and 1.2), the parameter b is the square root of the through-flow area. If the length of the fracture zone inside the borehole is known, the thickness can be calculated by

$$D_f = b^2/L \qquad \text{(Equation 4-18)}$$

  Where
  L = length of the fracture zone inside the borehole
- If the flow dimension shows bi-linear flow (i.e. around 1.5), there is no unique solution to calculate the thickness of the fracture zone from the flow domain b.

Tracer Test

If using a directly detectable tracer (e.g. salt) the position of fractures can be detected using a down hole logging with an adequate measurement tool (e.g. EC meter). This method was successfully conducted at the Campus Test Site to detect the fracture positions before installing the piezometers (see section 6.1.1.2, Figure 6-4)

Conducting a multiple-well tracer test also offers the possibility to estimate the thickness of the fracture zone, as the thickness of the through-flow area is one important parameter in the analysing procedure.

If conducting a Radial Convergent Test (see section 4.2.2.4(a)), the thickness will be one of three fitting parameters. The governing equation for tracer transport in a radial flow field towards an abstraction borehole requires a value for the injected mass of tracer per unit section. Because the total mass of injected tracer is known, the thickness can be estimated by fitting the parameter to the measured breakthrough curve. Assuming a flow perpendicular to the dip of the fracture, the estimated value represents the vertical width of the fracture W rather than the real thickness of the fracture. This procedure is implemented in the software TRACER, which is explained in section 5.4.2.

For a natural flow multiple-well tracer test the thickness of the through-flow area should be known a priori. But the same procedure as for the Radial Convergent Test can be applied in this case, even if it is not yet implemented in the software TRACER in the same way.

(c) Fracture Aperture

Researchers in the field of fracture flow used to consider a rock fracture as a pair of parallel plates separated by a constant distance, b, the aperture of the fracture. Since the fractures consist of rough walls, channelling and closings, it cannot be correctly represented by a unique fracture aperture. Therefore the term "equivalent aperture" was introduced to describe the effective aperture contributing to flow or transport in the fractured rock. There are commonly three definitions and estimations of the "equivalent aperture" with respect to different measurements. According to Tsang (1992) they are called mass balance aperture, frictional loss aperture and cubic law aperture. The frictional loss aperture requires data from both hydraulic tests and tracer tests, while the others only require data from one kind of test. Furthermore the values for the frictional loss aperture were found to be between the mass balance aperture and the cubic law aperture. Therefore it will not be considered further.

Tracer Test

The mass balance aperture, b_m, is derived from the mean residence time of a tracer transport and the volumetric flow rate. It can be calculated by the following equations, depending on the flow field (Tsang, 1992):

For linear flow: $$b_m = \frac{Qt_w}{LW} \qquad \text{(Equation 4-19)}$$

For radial flow: $$b_m = \frac{Qt_w}{\pi\left(r_1^2 - r_0^2\right)} \qquad \text{(Equation 4-20)}$$

where
t_w = mean residence time of tracer transport
Q = volumetric flow rate
L = flow path length
W = fracture width
r_0 = radius of the pumping well
r_1 = distance between injection and pumping.

Hydraulic Test

The cubic law aperture is the equivalent aperture of a parallel plate which would permit a certain flow rate at a given pressure drop. Depending on the flow field it can be calculated by (Tsang, 1992):

For linear flow: $$b_c = \left(\frac{12 \mu Q L}{\gamma W |\Delta H|} \right)^{1/3} \quad \text{(Equation 4-21)}$$

For radial flow: $$b_c = \left(\frac{6 \mu Q}{\gamma \pi |\Delta H|} \ln\left(\frac{r_1}{r_0} \right) \right)^{1/3} \quad \text{(Equation 4-22)}$$

where
γ = weight density of the fluid
μ = viscosity of the fluid
ΔH = hydraulic head difference

Since the cubic law aperture relates to the transmissivity of the fracture, it can be estimated from the result of a hydraulic test by (Novakowski, 1996):

$$b_c = \left(\frac{12 \mu T}{9804} \right)^{1/3} \quad \text{(Equation 4-23)}$$

where
T = transmissivity of the fracture in m^2/sec.

As it will be demonstrated below, the application of the theory of equivalent fracture aperture in tracer tests is questionable (see section 4.2.3.1). Nonetheless the procedures for both mass balance and cubic law aperture are implemented in the software TRACER, which is explained in section 5.4.2.

4.1.3.2. *Fracture Extent*

While most analytical methods assume an infinite aquifer extent, the extent of the fracture is mostly assumed to be finite. Knowledge of the fracture extent is required by several analytical methods (see section 4.1.2.2) and will also increase the accuracy of a numerical model (see section 4.1.2.4). The half-length of the fracture (x_f in the case of vertical fractures) or the radius of the fracture extent (r_f for horizontal fractures) can be estimated by applying the following equations, depending on the geological set-up:

Vertical fracture (Gringarten and Ramey, 1974)

$$x_f = \frac{Q\sqrt{t}}{2s_w\sqrt{\pi T_f S_f}} \qquad \text{(Equation 4-24)}$$

with

x_f = half-length of the fracture(m)
Q = abstraction rate in m^3/d
s_w = drawdown in m after time t (minutes)
T_f = T-value of fracture
S_f = S-value of fracture

Horizontal fracture: early storage (Gringarten and Ramey, 1974)

$$r_f = \sqrt{\frac{Qt}{\pi s_w S_f}} \qquad \text{(Equation 4-25)}$$

Vertical or horizontal fracture - assuming bi-linear flow at early time in fracture (de Lange, 1999).

$$r_f = \frac{Q(t)^{0.25}}{4s_w(T_f S_f)^{0.25}} \qquad \text{(Equation 4-26)}$$

Vertical or horizontal fracture - assuming bi-linear flow at early time in fracture (de Lange, 1999).

$$r_f = \frac{Q(t)^{0.333}}{4s_w(T_f S_f)^{0.333}} \qquad \text{(Equation 4-27)}$$

Adapted Bohmer equation (bi-linear flow in vertical dyke/fault)

$$x_f = \frac{Q(t)^{0.25}}{2.74s_w(T_f S_f)^{0.25}} \qquad \text{(Equation 4-28)}$$

4.1.3.3. Flow Dimension

As mentioned in Chapter 3, the concept of non-integer flow dimension plays an important role in describing the flow geometry and flow system of fractured aquifers. Because the flow geometry is mostly unknown a priori, knowledge of the flow dimension indicates the behaviour of the fracture network. All real but unknown spatial variations in K, S_s, and $2b$ are lumped together in the estimated value of n. The resulting "dimension" described by n can, therefore, reflect the actual geometry of the flow conduits in three-dimensional space or it can reflect a combination of factors. Flow dimension is perhaps best viewed as representing the rate of change of hydraulic "conductance" (the product of hydraulic conductivity and flow area) with distance. According to Barker (1988) two parameters are used, the flow dimension n and the extent of the flow region b. The concept of fractal dimension will not be considered further due to the wider range of applicability of the GRF-Model.

(a) Flow Dimension n

As discussed in Chapter 3 and section 4.1.2.2(d), there are various methods to estimate the flow dimension n from hydraulic tests. The most suitable methods are proposed and the requirements are discussed. Besides these methods the flow dimension n can also be estimated from tracer test data under specific conditions, as described below.

Analytical Method

The proposed analytical method to estimate the flow dimension n is the approach by Robert and Beauheim (2001), which is described in section 4.1.2.2(d). The first derivative of the time-drawdown data on a log-log plot shows at late time a straight line with slope related to the flow dimension. Using a scaled second derivative the late time data directly yield the flow dimension n.

To ensure a correct estimation the following procedure is suggested:

- The first derivative on a semilog plot must show a horizontal straight line.
- Using this part of constant flow dimension, the scaled second derivative on a log-log plot yields the corresponding flow dimension n.

This procedure is implemented and partly automated in the software TRACER, which is explained in section 5.4.2. The software offers the possibility to choose between the Barker-Bangoy method and the approach of Roberts and Beauheim for estimating the flow dimension n.

Numerical Model

A standard numerical model like MODFLOW is not able to account for a non-integer flow dimension. Using the software nSIGHTS (see section 4.1.2.3(c)) offers the possibility to estimate the flow dimension n by means of inverse modelling. The software uses the same approach, as described above for the analytical method. It can also account for the scale-dependent varying of the flow dimension.

Multiple-well Tracer Test

If a point dilution test is used as the source in the injection borehole for a radial convergent test, the Darcy velocity q can be estimated with unknown values for n and b (see section 4.2.2.1(a) for more details):

$$q = \frac{W}{\alpha\ At}\ln(\frac{C_0}{C}) \qquad \text{(see Equation 4-55)}$$

with $$A = \frac{r_w^{n-1}\pi^{\frac{n}{2}}b^{3-n}}{\Gamma(\frac{n}{2})} \qquad \text{(see Equation4-59)}$$

The flow velocity v is obtained by fitting the equation of Sauty (1980) to the data from the breakthrough curve (see section 4.2.2.4(a)). The kinematic porosity can be estimated directly from the radial convergent test by (see section 4.2.3.4for more details):

$$v = \frac{Q}{\varepsilon\ A} \qquad \text{(see Equation 4-89)}$$

with $$A = \frac{2\pi^{\frac{n}{2}}r^{n-1}b^{3-n}}{\Gamma(\frac{n}{2})} \qquad \text{(see Equation 4-90)}$$

Assuming a homogeneous aquifer system between the injection and the abstraction borehole the kinematic porosity estimated from the relation v = Q/εA should be the same as the one obtained from the relation v = q/ε. Therefore:

$$\varepsilon = q/v = Q/vA \qquad \text{(Equation 4-29)}$$

Substituting q with Equation 4-55 and 4-59 and A with Equation 4-90 yields:

$$-\frac{W}{\alpha t} * \frac{\Gamma(n/2)}{r_w^{n-1}\pi^{n/2}b^{3-n}} * \log(\frac{C}{C_0}) = Q * \frac{\Gamma(n/2)}{2r^{n-1}\pi^{n/2}b^{3-n}} \qquad \text{(Equation 4-30)}$$

or after rewriting

$$-\frac{W}{\alpha t} * \frac{1}{r_w^{n-1}} * \log(\frac{C}{C_0}) = Q * \frac{1}{2r^{n-1}} \qquad \text{(Equation 4-31)}$$

Rearranging of Equation 4-31 and solving n gives:

$$n = 1 + \frac{\log[2 * 2.3W\log(C/C_0)]/(\alpha Qt)}{\log(\frac{r_w}{r})} \qquad \text{(Equation 4-32)}$$

where

n = flow dimension, according to the generalised radial flow model of Barker (1988).

The procedures are implemented in the software TRACER, which is explained in section 5.4.2. The software offers the possibility to choose between the analytical method and the tracer test approach for estimating the flow dimension n.

However, if hydraulic test data are available, the analytical method or the numerical model nSIGHTS should be used due to its wider application and range of validity.

(b) Flow Domain b

The second parameter in the approach of non-integer flow dimension is the flow domain or extent of the flow region b.

Analytical Method

The proposed analytical method to estimate the flow domain b is a combination of the Barker method and the approach by Robert and Beauheim (2001), which are both described in section 4.1.2.2(d).

- To estimate the flow dimension n the approach of Roberts and Beauheim (2001) should be used, as described above.
- The estimated value should then be used as a fixed parameter in the Barker (1988) method. A non-linear least square method applied to the hydraulic test data will then yield estimations for the flow domain b, the hydraulic conductivity of the fracture k_f and the storativity of the fracture S_f.
- If information about the thickness of the fracture zone is available, lower and upper levels should be set for parameter b in the range of the thickness.

This procedure is implemented and partly automated in the software TRACER, which is explained in section 5.4.2. The software offers the possibility to choose between the Barker-Bangoy method and the approach of Roberts and Beauheim for estimating the flow dimension n.

Multiple-well Tracer Test

When the flow dimension n is estimated from tracer test data, as described above, the parameter b (extent of the flow region or flow domain) is set equal to the effective flow thickness, which is obtained from fitting the equation of Sauty (1980) to the breakthrough curve of the radial convergent test (see section 4.2.2.4(a)).

As discussed in section 4.1.3.1(b) this procedure is only valid for n-values between 1.8 and 2.2. For smaller n-values it is not possible to relate the flow domain b to the effective thickness of the fracture zone.

The procedures are implemented in the software TRACER, which is explained in section 5.4.2. The software offers the possibility to choose between the analytical method and the tracer test approach for estimating the flow dimension n and the flow domain b.

However, if hydraulic test data are available, the analytical method should be used due to its wider application and range of validity.

4.1.3.4. Transmissivity

The transmissivity T is the product of the average hydraulic conductivity K and the saturated thickness of the aquifer D. Consequently, transmissivity is the rate of flow under a unit hydraulic gradient through a cross-section of unit width over the whole saturated thickness of the aquifer. The effective transmissivity of a fractured aquifer then becomes a function of the transmissivity of the matrix and the fractures, where the transmissivity of the matrix is a function of the horizontal hydraulic conductivity, the vertical hydraulic conductivity and the thickness.

(a) Aquifer

When dealing with water management on a regional scale, the transmissivity of the entire aquifer is an appropriate choice, because the influence of the fracture transmissivity becomes small and can be neglected. Van Tonder (pers. comm.) and Chiang and Riemann (2001) show by means of a numerical model that the transmissivity of the entire aquifer is equal the geometric mean of the involved aquifer systems as fracture network and matrix. The same applies to a heterogeneous system consisting of areas with different transmissivity values.

Analytical Methods

Most analytical methods yield a value for the transmissivity of the entire aquifer without distinguishing between the matrix and the fracture system. Depending on the geological set-up, the conceptual model and the available drawdown data, an appropriate method should be chosen.

If the fractured network can be considered as a continuum, porous media methods like Theis or Cooper-Jacob can be applied to the hydraulic test data of the radial acting flow phase. Applying the straight-line method of Cooper-Jacob the slope of the straight line and its interception at s=0 can be used to determine the transmissivity as:

$$T = 2.3Q / 4\pi \Delta s \qquad \text{(Equation 4-33)}$$

with

Δs = drawdown difference per log cycle of time

In the case of horizontal bedding-plane fractures the transmissivity of the aquifer can be estimated using the Cooper-Jacob or Theis method, as discussed in section 4.1.2.5

For vertical fractures the methods of Cinco-Ley and Samaniego (1978) yield values for the aquifer transmissivity. If the drawdown data show radial acting flow phase, porous media methods like Cooper-Jacob or Theis are also applicable. They yield the geometric mean value of the involved aquifer systems (fracture, matrix, eventually dyke), which gives the transmissivity of the entire aquifer (see above).

The GRF-model from Barker (1988) does not account for the transmissivity of the matrix or the entire aquifer and therefore cannot be applied here.

In the case of a double-porosity aquifer the drawdown response depends only on the transmissivity of the fracture network and the ratio of storativity. Therefore the transmissivity of the entire aquifer cannot be determined directly.

Numerical Model

The purpose of using a numerical model for aquifer parameter estimation is normally to differentiate between the aquifer systems and to account for boundary effects. Therefore a two- or three-dimensional homogenous model is proposed, when estimating the transmissivity of the entire aquifer. Such a model would not account for fractures or areas of different transmissivity. The drawdown response can then only be simulated, when the fracture network can be considered as continuum.

It is not suggested to use a numerical model for estimating the transmissivity of the entire aquifer due to the high requirement of initial data. Analytical methods are mostly suitable and result in the same values.

(b) Fracture

While for water management purposes the transmissivity of the entire aquifer is of importance, when dealing with contamination in both investigation and protection the knowledge of the transmissivity (or hydraulic conductivity) of the fracture is necessary to predict velocities or length of contamination plumes.

Approximation

Using the early data from a hydraulic test the following equation (Logan equation, adapted by de Lange, 1999) will give an estimate of the transmissivity of the fracture:

$$T = 10^{(Log\frac{104Q}{s} + Log15Q)/2} \qquad \text{(Equation 4-34)}$$

with

T = transmissivity in m^2/d
Q = abstraction rate in L/s
S = drawdown in abstraction borehole in m after 1 minute

Analytical Methods

Only few analytical methods can distinguish between the transmissivity of the aquifer and of the fracture network. Applying porous media methods will always yield the transmissivity of the entire aquifer.

In the case of a double-porosity aquifer the approach of Moench (1984) can be used (see section 4.1.2.2(b)). The method can be applied with data from an abstraction or observation borehole. Using the straight-line method of Kazemi (1969) or Warren and Root (1964) the transmissivity of the fracture system is calculated as:

$$T_f = \frac{0.183 \cdot Q}{d} \qquad \text{(Equation 4-35)}$$

where
d = drawdown of the straight lines over one log cycle [-]

In the case of horizontal bedding-plane fractures with finite conductivity the transmissivity of the fracture can be estimated using the drawdown-distance method of Cooper-Jacob. It requires a minimum of two observation boreholes, which intersect the fracture at different distances from the abstraction borehole. Using the measured drawdown at a specific time, but at different piezometers, the plot drawdown versus distance (Cooper-Jacob II) shows a straight line in the case of a homogeneous aquifer. The slope of the straight line and the interception at s=0 yield the transmissivity as:

$$T_f = 2.3Q / 2\pi \Delta s \qquad \text{(Equation 4-36)}$$

where
Δs = drawdown difference per log cycle of distance

Most methods for single fractures assume an infinite conductivity in the fracture. The method of Cinco-Ley and Samaniego (1978) for a vertical fracture with finite conductivity can be applied to estimate the transmissivity of the fracture. Porous media methods like Cooper-Jacob or Theis are not applicable because of the non-uniqueness of the results, as shown in section 4.1.2.5

The transmissivity of any kind of fractured network (with non-integer or integer flow dimension) can be estimated applying the GRF-model (Barker, 1988). The method actually yields a value for $k_f * b^{(3-n)}$, which can be seen as equal to the transmissivity of the fracture.

Numerical Model

As discussed above, analytical methods are often not suitable to estimate the transmissivity of the fracture, due to the underlying assumptions. Therefore a numerical model should be used to distinguish between the hydraulic properties of the matrix and the fracture network.

A step-by-step guideline for constructing and running a numerical model for aquifer parameter estimation is proposed by Chiang and Riemann (2001) and summarised in section 4.1.2.3(d).

4.1.3.5. Hydraulic Conductivity

The hydraulic conductivity is the constant of proportionality in the 'Darcian Law'. It is defined as the volume of water that will move through a porous medium in unit time under a unit hydraulic gradient through a unit area measured at right angles to the direction of flow. Related to the transmissivity it is given by (Krusemann and de Ridder, 1991):

$$K = T / D \qquad \text{(Equation 4-37)}$$

The hydraulic conductivity of fractured rocks depends largely on the density of the fractures and the width of their apertures. Fractures can increase the hydraulic conductivity of solid rocks by several orders of magnitude. Because fractured aquifers consist of fractures embedded in a permeable matrix, any response of water levels to stressed conditions shows a mix of the influence from the matrix and the fracture conductivity.

While in homogeneous, porous media the flow can be considered as mainly horizontal, this might not be the case in fractured rocks. Consider a horizontal fracture. The flow in the matrix would be vertical towards the fracture or upwards from the fracture under stressed conditions. Whether the flow in the matrix can be considered as horizontal, vertical or sub-vertical depends on the kind of fracture network, the distribution of main fractures and micro fissures, and the anisotropy of the matrix.

(a) Horizontal Hydraulic Conductivity – Matrix

Since analytical methods yield values for the transmissivity, the hydraulic conductivity can be calculated from the transmissivity by dividing it with the thickness of the aquifer. But analytical methods cannot distinguish, whether the flow is horizontal or vertical, and therefore cannot differentiate between horizontal and vertical hydraulic conductivity.

Analytical Methods

Assuming a vertical fracture, the flow towards the fracture in the matrix under stressed conditions can be considered horizontal. In this case the estimated transmissivity using the methods described above reflect the horizontal flow in the matrix towards the fracture. Then the horizontal hydraulic conductivity of the matrix can be expressed as:

$$K_{hm} = T / D \qquad \text{(Equation 4-38)}$$

In cases other than vertical fractures the flow in the matrix is a mix of horizontal, vertical and subvertical flow and the above-mentioned relation between transmissivity of the aquifer and horizontal hydraulic conductivity is not necessarily applicable.

Numerical Model

The only way to estimate the horizontal hydraulic conductivity accurately is by means of a numerical model. Because a two-dimensional model cannot distinguish between horizontal and vertical hydraulic conductivity, a three-dimensional numerical model should be used, as described in section 4.1.2.3(d).

(b) Vertical Hydraulic Conductivity - Matrix

The vertical hydraulic conductivity of the matrix can be estimated by means of analytical methods only in very specific cases, as shown below.

Analytical Methods

Assuming a horizontal fracture, the flow in the matrix towards the fracture under stressed conditions can be considered vertical. Using the approach of Gringarten *et al.* (1974) for a horizontal fracture with infinite conductivity, the vertical hydraulic conductivity can be estimated as one of several fitting parameters. The method is applicable, if the other parameters are known a priori or estimated by means of other methods beforehand.

There are no analytical methods to estimate the vertical hydraulic conductivity in cases other than horizontal fractures. The only way to obtain accurate estimates of the vertical hydraulic conductivity is by means of a three-dimensional numerical model.

Numerical Model

A three-dimensional numerical model should consist of several layers of equal thickness to account for a vertical flow and to estimate the vertical hydraulic conductivity. The way the programs deal with the vertical hydraulic conductivity is quite different. For instance MODFLOW uses the term of vertical leakance (VCONT) between layers instead of real values for the vertical hydraulic conductivity. The vertical leakance is defined as:

$$VCONT = 2 \Big/ \left(\frac{\Delta Vk}{Kz|i,j,k|} + \frac{\Delta Vk+1}{Kz|i,j,k+1|} \right) \qquad \text{(Equation 4-39)}$$

with

ΔVk	=	Thickness of Layer k
ΔVk+1	=	Thickness of Layer k+1
Kz|i,j,k|	=	Vertical hydraulic conductivity of layer k
Kz|i,j,k+1|	=	Vertical hydraulic conductivity of layer k

Most pre-processors for MODFLOW, like PMWIN (Chiang and Kinzelbach, 2001), offer the possibility to enter values directly for the vertical hydraulic conductivity, while the program calculates VCONT. Unfortunately when using inverse modelling the assigned and estimated parameter is VCONT so that the vertical hydraulic conductivity must be recalculated using Equation (4-39). Due to the definition of the vertical leakance the value changes, if the thickness of a layer changes. Therefore the thickness of layers should be kept constant, if applicable.

For estimating vertical hydraulic conductivity accurately with a numerical model, drawdown data at different depths in the matrix should be available. Therefore piezometers with short wellscreen should be installed in different depths for water level measurement. These are also useful to estimate the storativity of the matrix, which can be seen clearly in a delay of the drawdown response.

The influence of the vertical hydraulic conductivity on the drawdown response in fully penetrating wells or in fracture piezometers depends on the relative conductivity Cr (see section 4.1.2.2(c)), but in general the same drawdown response can be produced with a change in storativity or hydraulic conductivity of the fracture, which makes inverse modelling non-unique. A change of the vertical hydraulic conductivity in the matrix will then be seen in all drawdown curves (fracture and matrix piezometers), as long as the leakance in the matrix and the leakance to the fracture are linked, which is applicable in a case of high vertical hydraulic conductivity in the fracture and the absence of fracture skin.

A step-by-step guideline for constructing and running a numerical model for aquifer parameter estimation is proposed by Chiang and Riemann (2001) and summarised in section 4.1.2.3(d).

The software RPTSOLV as a two-dimensional vertical model can also account for vertical flow in the case of a horizontal fracture. More complicated fracture networks cannot be simulated with this approach.

(c) Fracture

If the transmissivity of the fracture could be estimated, as described in section 4.1.3.4(b), the vertical width of the fracture, intersected by the borehole, must be known or estimated to calculate the hydraulic conductivity of the fracture by the following relation (see Figure 4-14):

$$K_f = T_f / W \qquad \text{(Equation 4-40)}$$

If not measured directly with borehole geophysics, the vertical width can be calculated from the thickness of the fracture zone D_f and the intersection angle β (see above).

Approximation

For a horizontal fracture the vertical width of the fracture is equal to the thickness or aperture:

$$K_f = T_f / D_f \qquad \text{(Equation 4-41)}$$

or $$K_f = T_f / (2b) \qquad \text{(Equation 4-42)}$$

For a vertical fracture the vertical width is equal to the depth of the fracture, or the thickness of the aquifer:

$$K_f = T_f / D \qquad \text{(Equation 4-43)}$$

Analytical Methods

Most analytical methods yield values for the transmissivity, which must be recalculated with the abovementioned Equations (4-40) to (4-43) to obtain an estimate for the hydraulic conductivity of the fracture.

The only method directly yielding the hydraulic conductivity of the fracture is the GRF-model (Barker, 1988), which can be applied for fracture networks with fractal patterns or non-integer flow dimensions. Because the method yields a value for $k_f \cdot b^{(3-n)}$ the hydraulic conductivity cannot be calculated without knowledge of the flow geometry, i.e. the parameters flow dimension n and flow domain b (see section 4.1.3.3).

Numerical Model

The one-dimensional vertical model nSIGHTS (see section 4.1.2.3(c)) can be applied to fracture networks, considered as continuum or showing double-porosity behaviour, or can be applied to a single horizontal fracture for estimating the hydraulic conductivity of the fractures. It is not applicable for vertical or subvertical fractures. The program requires or yields values for the hydraulic conductivity rather than for the transmissivity.

For more complicated fracture networks or vertical fractures a three-dimensional numerical model is required to differentiate between the hydraulic conductivity of the matrix and of the fracture. The general procedure is discussed in section 4.1.2.3(d).

Because in any case other than a double-porosity aquifer the shape of the drawdown response is mainly influenced by the matrix properties, the sensitivity of the fracture properties is very low. Therefore for an accurate estimation a minimum of two observation boreholes is suggested. Then the influence of the hydraulic conductivity of the fracture is seen in the absolute shift of drawdown in the observation data, similar to the drawdown-distance method of Cooper-Jacob.

A fracture skin would neither change the shape of each drawdown curve nor the shift of drawdown, but it would result a similar shift of all drawdown curves. The procedure to prove the influence of a fracture skin in a numerical model is linked to the procedure for estimating the vertical hydraulic conductivity of the matrix (see above).

4.1.3.6. Storativity

The storativity of a saturated confined aquifer of thickness D is the volume of water released from storage per unit surface area of the aquifer per unit decline in the component of hydraulic head normal to that surface. In a vertical column of unit area extending through the confined aquifer, the storativity S equals the volume of water released from the aquifer when the piezometric surface drops over a unit distance. Storativity is defined as (Kruseman and de Ridder, 1991):

$$S = S_s D = \rho g(\alpha + n\beta) D \qquad \text{(Equation 4-44)}$$

With

S_s = Specific storage [$S_s = \rho g(\alpha + n\beta)$]
ρ = mass density of water
g = acceleration due to gravity
α = compressibility of the rock
n = porosity
β = compressibility of water

While the knowledge of the storativity is essential for water management and the calculation of the sustainable yield of boreholes, the estimation procedure is complicated and most methods are non-unique and less accurate regarding storativity.

(a) Rock-Matrix

In a fractured aquifer the water is normally stored in the rock-matrix, while fractures can be considered as conduits or extensions of boreholes. Therefore effective methods should be chosen to estimate the storativity of the matrix.

Analytical Methods

In general analytical methods to estimate the storativity of the matrix are mostly not suitable due to the distance dependency which can be observed in fractured aquifers. Only in few cases can analytical methods be used, which limits their applications in fractured aquifers.

If the fractured network can be considered as a continuum, porous media methods like Theis or Cooper-Jacob can be applied to the hydraulic test data of the radial acting flow phase. Applying the straight-line method of Cooper-Jacob, the storativity of the aquifer is then calculated as:

$$S = 2.25\ KD\ t_0 / r^2 \qquad \text{(Equation 4-45)}$$

where

t_0 = value for t at interception point (s=0)

In the case of a double-porosity aquifer the approach of Moench (1984) in combination with the straight line method of Warren and Root or Kazemi can be used, when accounting for distance dependency, as described below. The method can be applied with data from an abstraction or observation borehole. The storativity of the matrix is then calculated as:

$$S = \left[\frac{2.25 \cdot t_{02} \cdot T_f}{r^2} - S_f \right] \cdot \beta \qquad \text{(Equation 4-46)}$$

where

r = effective well radius (Warren and Root method) or distance to the pumped well (Kazemi method) [L]
T_f = transmissivity of the fracture system [L2T-1]
S_f = storage coefficient of the fracture system [-]
S = storage coefficient of the matrix [-]
β = shape factor: 1/3 for spherical blocks; 1 for slab blocks [-]. This parameter implies that the conceptual model of the geological situation is known
t_{02} = time at which the second straight line intercepts the time axis [T]

In the case of horizontal bedding-plane fractures the storage coefficient of the matrix can be estimated using the Cooper-Jacob or Theis method, as discussed in section 4.1.2.5 It requires an observation borehole which intersects the fracture close to the abstraction borehole. The problem is that the definition of 'close to' is unclear.

Using the drawdown-distance method of Cooper-Jacob would require observation data from piezometers installed in the matrix, which are often not available. The storativity is then calculated as:

$$S = 2.25\ KD\ t / r_0^2 \qquad \text{(Equation 4-47)}$$

where

r_0 = value for r at interception point (s=0)

For vertical fractures the methods of Cinco-Ley and Samaniego (1981) yield values for the matrix storativity with the same distance dependency. Porous media methods like Cooper-Jacob or Theis are not applicable in this case.

The GRF-model from Barker (1988) does not account for the storativity of the matrix and therefore cannot be applied here.

To avoid the distance dependency in the estimation procedure the parameter r, which accounts for the distance between source and observation, should be substituted independently of the real distance. For the calculation of the parameter r, which should be used in the methods instead of the real distance, a value in the range of the effective borehole radius as discussed below is suggested.

As discussed in section 1.4.5 drawdown data in fractured aquifers often show less drawdown than expected due to the so-called pseudo-skin effect. The determination of the skin leads to a negative skin factor, which results in a larger effective radius. Using the definition of the skin-factor ξ, as mentioned in section 1.4.2, the effective borehole radius r_{eff} can be calculated by Equation (1-12).

To calculate the skin factor the early-time data of the hydraulic test are used as shown in the FC-program of Van Tonder *et al.* (2001). A problem related to the use of this approach is that it requires early measurement. Depending on the chosen time of the "early" data, the estimation can be different. The longer the time interval, the bigger the estimated values, which results in an under-estimation of the storage coefficient.

In any case it must be kept in mind that the estimation of the matrix storativity using analytical methods is actually a guess. It can be a good guess, if the conceptual model is correct, but it remains a guess. For an accurate estimation a numerical model must be used.

Numerical Model

Flow of groundwater is essentially a three-dimensional phenomenon, especially in fractured-rock aquifers, so that a three-dimensional numerical model should be chosen. The use of such a model for parameter estimation is described in section 4.1.2.3(d). The chosen conceptual model must reflect the geological set-up and the considered flow geometry.

Unfortunately the influence of the storativity of the matrix on the drawdown data in boreholes, intersecting the fracture, is non-unique, so that applying inverse modelling can easily yield incorrect estimations. The best results are obtained when drawdown data of piezometers in the matrix are available. Because this is often not the case it is suggested that the sensitivity of the estimated value be controlled using statistic procedures or a stochastic modelling approach. The result should be mentioned together with its confidence limits.

Since three-dimensional models require vast quantities of data and sophisticated computer equipment they are often not very suitable for use in practice. This leaves one with the two-dimensional vertical model (RPTSOLV) or a one-dimensional vertical model (nSIGHTS), if this approach is applicable in the specific geological set-up (conceptual model). In a case of a vertical fracture or of a fracture network considered as continuum, only a three-dimensional numerical model can distinguish between the storativity of the fracture network and the storativity of the matrix.

(b) Fracture

The storage of a single fracture or a fracture cluster is very limited, which can be demonstrated by the following calculation:

$$V_f = l_f \cdot h_f \cdot b = 2000m \cdot 200m \cdot 0.002m = 800m^3$$

where

V_f = fracture volume [L^3]
l_f = fracture length [L]
h = fracture height [L]
b = fracture aperture [L]

A well located in a fracture that pumps at a rate of 10 m^3/h would empty it within 80 hours. Under real-world conditions, this is usually not the case because the matrix, where the fracture is embedded, is drained by the fracture, which in this instance acts as a conduit.

Compared to the storage capacity of the matrix, the storage of the fracture is normally very small and can often be neglected in cases of water management. A correct estimation is even more complicated than for the matrix storativity, as shown below.

Approximation

For a first approximation of the fracture storativity, two other parameters must first be determined as the storativity is defined as the product of specific storage and thickness:

According to Kruseman and De Ridder (1991) the theoretical specific storage S_s is calculated by

$$S_s = \rho g\,(\alpha + n\beta) \qquad \text{(Equation 4-48)}$$

With

ρg = specific weight of water (= 9804)
n = porosity
α = compressibility of the rock
β = compressibility of water (= 4.74×10^{-10})

De Lange (1999) gives the following values for n and α as a suggestion for aquifers in South Africa (obtained from inverse modelling and tracer tests):

n = 0.13 (=porosity)
α = 5.56×10^{-9} (= compressibility of the rock)

Therefore the proposed value for S_s would be **5.6×10^{-5} / m**

Own measurements in aquifers in Southern Africa show that the porosity of the fracture zone can vary between 5% and 49%. Even the compressibility of the rock can differ depending on material and density of fracturing. Therefore the proposed value for the specific storage varies between **2.5×10^{-5} / m** and **8.5×10^{-5} /m**

Using the estimated thickness of the fractured zone (D_f) as described in section 4.1.3.1the storativity of the fracture is then given by applying Equation (4-44). It is important to use the thickness of the fracture zone and not the fracture aperture for this approach.

Analytical Methods

In general analytical methods to estimate the storativity of the fracture are not suitable due to the distance dependency. Only in few cases can analytical methods be used, which limits their applications in fractured aquifers.

In the case of a double-porosity aquifer the approach of Moench (1984) can be used, when accounting for distance dependency, as described below. The method can only be applied with data from an observation borehole, meaning that the straight-line method of Kazemi (1969) should be applied. The storativity of the fracture system is then calculated as:

$$S_f = \frac{2.25 \cdot t_{01} \cdot T_f}{r^2} \qquad \text{(Equation 4-49)}$$

where

r = effective well radius (Warren and Root method) or distance to the pumped well (Kazemi method) [L]
T_f = transmissivity of the fracture system [L2T-1]
S_f = storage coefficient of the fracture system [-]
t_{01} = time at which the first straight line intercepts the time axis [T]

In the case of horizontal bedding-plane fractures the storage coefficient of the fracture can be estimated using the Cooper-Jacob or Theis method, as discussed in section 4.1.2.5It requires an observation borehole which intersects the fracture far away from the abstraction borehole. The problem is that the definition of 'far away' is unclear. With the straight-line method of Cooper-Jacob the storativity of the fracture is then calculated as:

$$S_f = 2.25\ T_f\ t_0 / r^2 \qquad \text{(Equation 4-50)}$$

where

t_0 = value for t at interception point (s=0)

Using the drawdown-distance method of Cooper-Jacob will result an underestimation of the storativity of the fracture, when the flow towards the fracture is dominated by uniform flux (see Gringarten, 1984, section 4.1.2.2(c)).

For vertical fractures the methods of Cinco-Ley and Samaniego (1981) yield values for the fracture storativity with the same distance dependency. Porous media like Cooper-Jacob or Theis are not applicable in this case.

The storativity of a fractured network with fractal patterns or a non-integer flow dimension can be estimated applying the GRF-model (Barker, 1988). Because the method yields a value for the reciprocal diffusivity S_{sf}/K_f the storativity cannot be calculated independently of the hydraulic conductivity and therefore without knowledge of the flow geometry, especially the parameters flow dimension *n* and flow domain *b* (see section 4.1.3.3).

To avoid the distance dependency in the estimation procedure the parameter *r*, which accounts for the distance between source and observation, should be substituted independently of the real distance. For the calculation of the parameter r, which should be used in the methods instead of the real distance, it is suggested to use a value in the range of the half-length of the fracture or radius of the fracture extent (see section 4.1.3.2).

Numerical Model

The only way to estimate the storativity of the fracture or fracture network in an accurate way is by means of a numerical model. Flow of groundwater is essentially a three-dimensional phenomenon, especially in fractured-rock aquifers, so that a three-dimensional numerical model should be chosen. The use of such a model for parameter estimation is described in section 4.1.2.3(d). Unfortunately the influence of the storativity of the fracture on the drawdown data is mostly not dominant, so that applying inverse modelling can easily yield incorrect estimations. Therefore it is suggested that the sensitivity of the estimated value be controlled using statistic procedures or a stochastic modelling approach.

Since three-dimensional models require vast quantities of data and sophisticated computer equipment they are often not very suitable for use in practice. This leaves one with the two-dimensional vertical model (RPTSOLV) or a one-dimensional vertical model (nSIGHTS), if this approach is applicable in the specific geological set-up (conceptual model). In the case of a vertical fracture or of a fracture network considered as continuum, only a three-dimensional numerical model can distinguish between the storativity of the fracture network and the storativity of the matrix.

4.1.3.7. Hydraulic Gradient

The hydraulic gradient determines the velocity of the groundwater, when the hydraulic conductivity and the porosity are assumed as constant. The 'Darcian Law' can be rewritten as:

$$v = \frac{ki}{\varepsilon} \qquad \text{(Equation 4-51)}$$

with

v = flow velocity
k = hydraulic conductivity
i = hydraulic gradient
ε = kinematic porosity

If the hydraulic conductivity, the hydraulic gradient and the porosity were known, the flow velocity could be calculated, without conducting special field measurements like tracer tests. Otherwise the hydraulic gradient can be calculated, if the hydraulic conductivity, the velocity and the kinematic porosity are known or estimated beforehand. All three parameters must represent the same aquifer system, i.e. the fracture zone or the matrix of prefixed thickness.

Field Measurement

The standard method to determine the hydraulic gradient is to measure the water level or hydraulic heads in several boreholes or piezometers and to construct a map with lines of equal hydraulic head. The hydraulic gradient is always directed perpendicular to the lines of equal piezometeric level, and the distance between the lines yields the value of the hydraulic gradient.

The measured piezometric level mainly depends on the vertical position of the piezometer. If the water levels of piezometers are compared, which do not represent the same fracture or fracture network, an interpretation of the data can yield an incorrect estimation of the resulting hydraulic gradient. Water-level measurements in fully penetrating wells and piezometers can differ considerably. Therefore field measurements to estimate the hydraulic gradient should be interpreted with caution.

Hydraulic Test

The hydraulic gradient prevailing during a hydraulic test is easy to determine from the measured water levels or pressure heads in the abstraction and observation boreholes.

During a constant discharge test the flow field is assumed to be radial towards the abstraction borehole. Then the hydraulic gradient at any point in this flow field is directed towards the abstraction borehole, which has the lowest hydraulic head. Then the averaged hydraulic gradient can be calculated by

$$i = \frac{(h_1 - h_0)}{r} = \frac{(z_1 - s_1) - (z_0 - s_0)}{r} \qquad \text{(Equation 4-52)}$$

with

i = hydraulic gradient
h_1 = hydraulic head at observation borehole
h_0 = hydraulic head at abstraction borehole
r = distance between abstraction and observation borehole
z_1 = elevation of the measurement point at observation borehole
z_0 = elevation of the measurement point at abstraction borehole
s_1 = drawdown in observation borehole at time t
s_0 = drawdown in abstraction borehole at time t

Note that this calculation yields an averaged hydraulic gradient over the distance r, which differs from the real value at distance r due to the actual shape of the cone of depression (see Figure 4-15).

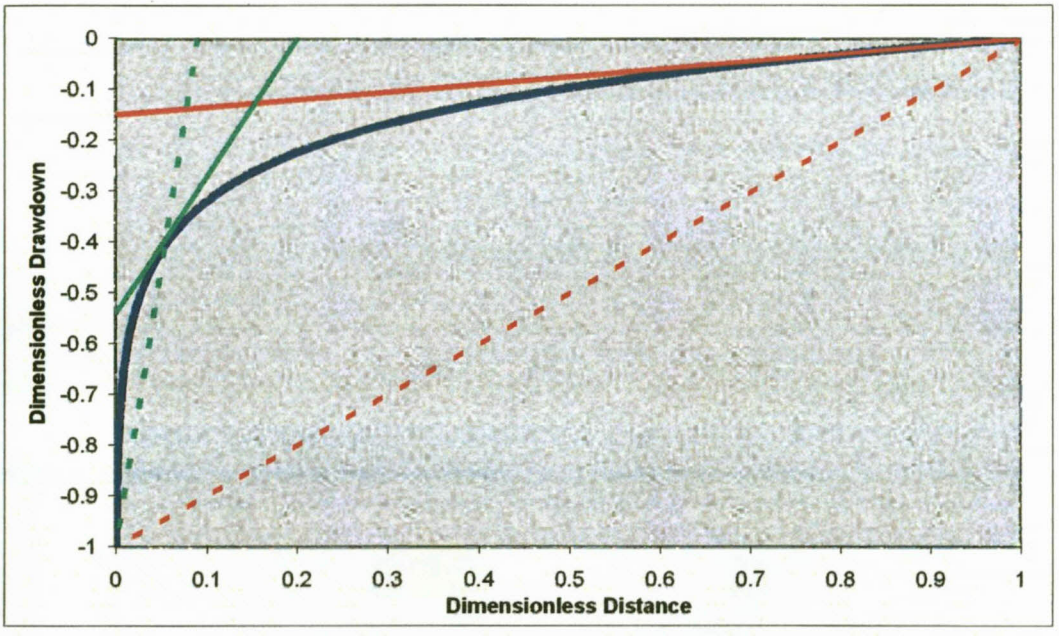

Figure 4-15 Cone of depression during constant discharge test with the real hydraulic gradient (solid line) and averaged hydraulic gradient (dashed line) at observation points

To reduce the difference between real gradient and averaged gradient, which yields to an overestimation of the hydraulic gradient, the averaged hydraulic gradient can be recalculated depending on the relation of the distance r to the radius of influence R. The dimensionless distance is defined as real distance related to the radius of influence [r/R]. In most cases of short-duration tests in fractured media it can be assumed that the observation borehole is situated in a dimensionless distance to the abstraction borehole of less than 0.1. Then the error using the abovementioned approximation is less than 4:1 (i.e. the real gradient is up to four times smaller than estimated).

In the software TRACER-PLAN a calculation of the theoretical hydraulic gradient at any time t and distance r is implemented, and estimated with the approach for porous media from Cooper-Jacob (see section 5.4.1).

Tracer Tests

Using the approach discussed above offers the possibility to estimate the hydraulic gradient under natural conditions, when two tracer tests are performed at the same observation borehole. A point-dilution test, performed at the observation borehole during the constant discharge test, yields a value for the Darcy velocity under the specific forced gradient (q_f), while a point-dilution at the same borehole under natural conditions yield the Darcy velocity und natural gradient (q). For the estimation procedure see section 4.2.2.1(a).

According to the 'Darcian Law' (see Equation 1-3) the Darcy velocity can be expressed as a linear function of the hydraulic gradient by

$$q = k\,i \qquad \text{(Equation 4-53)}$$

with

k = hydraulic conductivity

Since the hydraulic conductivity is a constant, the Darcy velocities and hydraulic gradients under the two conditions can be related by:

$$q_f / i_f = q / i \qquad \text{(Equation 4-54)}$$

With

q_f = Darcy velocity under forced gradient i_f
q = Darcy velocity under natural gradient i

The two Darcy velocities are obtained from the independent Point dilution tests, while the hydraulic gradient i_f is estimated with the above-mentioned approach. Both procedures are implemented in the software TRACER, which is explained in section 5.4.2.

4.1.4. Discussion

At first glance the different approaches for the parameter estimation are confusing and it clearly shows the difficulties when dealing with groundwater flow in fractured aquifers. Therefore any analysing procedure should involve several steps:

- Build up a conceptual model for the hydrogeological situation
- Verify the conceptual model applying the tools of diagnostic plots (e.g. derivatives, see section 4.1.2.1)
- Apply analytical methods, according to the conceptual model, as a preliminary estimation
- Verify results with a numerical model, if comprehensive estimation is necessary

In general the approach of non-integer flow dimension should be applied (methods of Barker, 1988 and Roberts and Beauheim, 2001) to account for the mostly unknown geometry of the fracture network.

4.2. Transport Parameters

For the investigation, risk assessment and remediation of groundwater contamination it is important to estimate transport parameters such as groundwater velocity, kinematic porosity and dispersion. These parameters normally have to be analysed from field tests, known as tracer tests. In the first part of this chapter the different tests and analysing methods are described, while the second part focuses on the estimation procedure for the different parameters.

4.2.1. Tracers

Tracers are identifiable substances, which may be used to infer the general behaviour of a flowing medium. They may be broadly categorised by their origin. Substances normally present in the medium are generally termed environmental tracers, while those deliberately introduced into the medium for the purpose of the study are termed artificial tracers. An ideal groundwater tracer has the following characteristics:

- It is conservative and will follow the movement of the water without loss from flow due to physical or chemical processes, like adsorption on sediment or equipment.
- It is non-toxic and can be applied without administrative or legislative requirements.
- It is detectable with a high sensitivity and can be measured accurately *in situ*.
- It does not contaminate the terrain of investigation and does not affect results of further tests.
- It is inexpensive and analysis costs are low.

Since no ideal tracer exists, the selection of the tracer should be based on the most important considerations, which will depend on the nature of the investigation. For instance, if the advective properties of a medium are investigated, care should be taken that the tracer is physically compatible with the fluid, while a study of the diffusive flow through a porous medium will require attention to the diffusion constants and molecular size of the tracer. A detailed discussion about the choice of the tracer and a recommendation of mostly usable tracers will follow in section 5.2.1.2

Studies with environmental tracers are normally carried out for water budget analysis on regional scale. If a site is already contaminated and concentration measurements of the contaminant exist for different time steps, the contaminant can be used as an environmental tracer for transport predictions. The use of artificial tracers for parameter estimation requires special equipment for introducing, mixing and sampling, but the tests can be carried out on a local scale with low time consumption and costs. In most cases conducting tracer tests with artificial tracers is sufficient for the purpose of the study. Therefore the following part, as taken from Van Wyk *et al.* (2000), will focus on the description of artificial tracers.

Artificial tracers can be categorised by their method of analysis, as follows:

- Radioactive tracers: These elements are detected by means of their radioactive emissions.
- Activatable tracers: These elements are stable during use, but activated to emit radioactivity for analysis.
- Chemical tracers: Detection is based on mass (mass spectrometry), orbital electron arrangements (chemical reactions) or shell binding energies (energy adsorption or emission properties).
- Particulate tracers: Tracers detected by collection, weighing or counting of individual particles

A brief discussion on the different types of tracers categorised above will follow to illustrate the properties of each type.

(a) Radioactive Tracers

Although some chemical tracers are more toxic than radioactive tracers, and their concentrations do not decrease due to radioactive decay, all radioactive tracers are subjected to legislation in most countries, and the disadvantage of a negative general public reaction to the use of radioactivity limits their applicability. Other associated disadvantages are the need to transport the tracer in special containers and the use of specialised personnel.

In spite of this, radioactive tracers have some special advantages:

- A high sensitivity and precision of detection,
- for γ- emitting tracers, the possibility of accurate *in-situ* measurements, and
- small volumes of tracer are needed for injection in the aquifer which minimises disturbance to the flow system.

Tritium (^3H) is commonly used as an environmental and artificial tracer, and since it forms part of the water molecule it will faithfully follow the movement of water. Since the vapour pressure of HTO is lower than H_2O, it is extensively used in evaporation and recharge studies. For analyses, samples have to be taken and returned to a laboratory for measurement by liquid scintillation counting or gas counting.

(b) Activatable Tracers

These are stable elements, which are capable of neutron irradiation over a short term during activation to produce a radioactive isotope, and they are generally used as anionic complexes. During irradiation measurements are made with a high resolution Ge(Li) detector. These tracers present no radioactive hazard to natural waters, and no authorisation is required for use. High levels of sensitivity are reached but the costs of analyses are very high. Elements applied as activatable tracers, are indium, bromide and iodine.

(c) Chemical Tracers

They have the advantage that they can be used without authorisation, and that field detection equipment is readily available (especially for the dyes). For some tracers, like many salt tracers for instance, analysis requires sample treatment and has to be carried out in the laboratory.

Inorganic salt tracers, such as the anions Cl^- (NaCl) and Br^- (NaBr, KBr), are commonly used to trace groundwater movement, while the cations are often lost by ion-exchange. Iodide is not as conservative as the bromides or chlorides, but the background concentration is usually less than 10 µg/l compared to the 100 µg/l for bromide and 30 mg/l for chloride. $NaNO_3$ is easy to dissolve and to detect with ion-selective electrodes, but background concentrations of NO_3 may be a problem. NaF and KF are detectable in small concentrations, but losses due to precipitation with calcium to form CaF_2 could occur. Na_2SO_4 too, could precipitate with calcium to form $CaSO_4$ while LiCl is expensive and also takes part in ion exchange reactions with the earth alkalis. The most commonly used salt tracers are NaCl and NaBr.

Organic dyes are frequently used as groundwater tracers, since the sensitivity of a fluorometric analysis is very high, and dye tracers are detectable in very low concentrations compared to salt tracers. The main advantage is that field measurements can be performed with filter fluorometers.

The sensitivity of the analysis depends on the efficiency of the dye to convert the excitation energy into fluorescene and the transmission of the filter combination in the fluorometer. The detectability depends on the background fluorescene value. Rhodamine B and Rhodamine WT have the lowest level of sensitivity and detectability, while the sensitivity of Fluorescein is about ten-times higher.

Some of the dyes, however, are not conservative, and are influenced by water quality. Temperature variations may affect the measured concentration of the dye tracer. During the measurement process non-adsorptive dye loss can happen due to chemical reactions and decay under light. Adsorption onto sediment surfaces is another disadvantage of some tracers such as Rhodamine B and Rhodamine WT, for instance. Rhodamine B is toxic to aquatic organisms and therefore should not be used as a water tracer. The toxicity of Fluorescein, Eosin and Photine is relatively low.

Taking all this information into account and comparing the properties of the different dye tracers, it is recommended to use Fluorescein as a tracer in groundwater studies.

(d) Particulate Tracers

Particulate tracers have been used in a number of groundwater tracing experiments. The particles may be of biological, botanical, geological or man-made origin, and could be detected by means of counting, fluorimetry, etc. Micro-organisms such as *Serratia marceescens*, bacteriophages, spores of Lycopodium (club moss) have been used in groundwater tracing studies.

4.2.2. Tracer Tests and Analysing Methods

Tracer tests aim to relate the concentration of chemical, biological or solid substances measured in observation boreholes to the flow velocity. The range of usable tracers is substantial and can be divided into environmental tracers and artificial tracers, as described above. Because this thesis focuses on tests which are applicable in the circumstances of Southern Africa, it will describe only tests with artificial tracers.

Because tracer tests under natural conditions with several observation boreholes are time- and cost-expensive, different single-well and dual-well tracer tests were explored. Both single-well and multiple-well tracer tests are described together with their analysing methods in the following sections.

4.2.2.1. Single-well Tracer Tests, Natural Gradient

As the name indicates, single-well tracer tests are conducted in one borehole only, meaning that injection of the tracer and measurement of the concentration take place in the same borehole. Conducting and measuring types vary for the different test types.

(a) Point Dilution Test

The single-well point dilution test method aims to relate the observed rate of tracer dilution in a borehole (Freeze and Cherry, 1979), or in a segment isolated in a borehole, to the average groundwater velocity in the aquifer. The groundwater through flow gradually removes a tracer introduced to the well from the well bore to produce a time-concentration relationship (see Figure 4-16), from which the Darcy velocity is computed. The tracer is not recovered by pumping. Under conditions of steady flow and thorough mixing of the tracer in the borehole, the Darcy velocity is computed from a dilution test as (Drost and Neumaier, 1974):

$$q = \frac{W}{\alpha\, At}\ln\left(\frac{C_0}{C}\right) \qquad \text{(Equation 4-55)}$$

With:

W	=	volume of fluid contained in the test section
A	=	cross sectional area normal to the direction of flow
C_0	=	Tracer concentration at t = 0
C	=	Tracer concentration at time = t
α	=	Borehole distortion factor (between 0.5 and 4; =2 for an open well) (note that $q\alpha=v^*$, where v^* = apparent velocity inside well)
t	=	Time when concentration is equal to C

In practice either the radial flow solution (porous media) or the parallel plate model (single fracture) is used to estimate the cross sectional area A (Novakowski, 1992):

$$A = \pi r_w d \quad \text{(for the radial flow model)} \qquad \text{(Equation 4-56)}$$

With:

r_w	=	well radius
d	=	the length of the tested section in the borehole

And $A = \pi r_w(2b)$ for the parallel plate model (Equation 4-57)

Where
2b = equivalent aperture of the fracture.

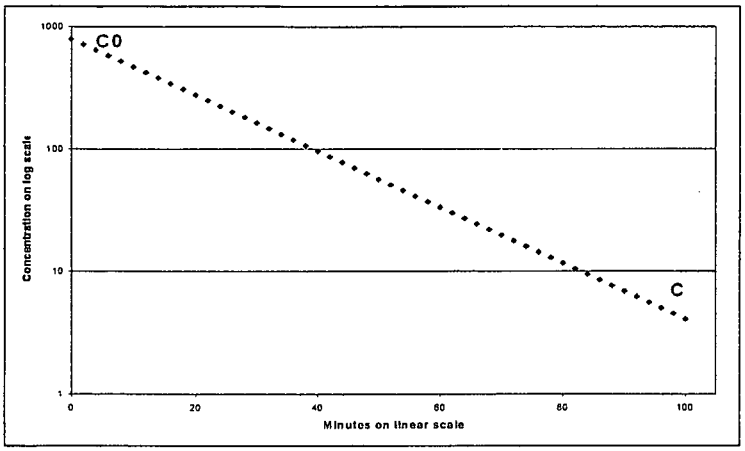

Figure 4-16 Typical Time-Concentration relationship during a Point-Dilution Test

The theory of equivalent aperture applied to tracer test data seems unreliable, as discussed below. But as it is possible to account for the flow geometry in generalising the flow in fractured aquifers, it is also possible to estimate the cross-sectional area *A* in a more general way by using fractional flow dimensions (see Chapter 3).

Consider the region bounded by two equipotential surfaces, which have radii r and r+Δr. These surfaces are the projection of n-dimensional spheres through three-dimensional space by an amount of $b^{(3-n)}$. For example, when n is equal to two, the surfaces are finite cylinders of length b. A sphere of radius r has an area $\alpha_n r^{(n-1)}$ where α_n is the area of a unit sphere in n dimensions:

$$\alpha_n = \frac{2\pi^{\frac{n}{2}}}{\Gamma(\frac{n}{2})} \qquad \text{(Equation 4-58)}$$

where
Γ = Gamma function

In the case of the dilution test, the cross sectional area for n-dimensional flow is thus given by (half the borehole circumference is used):

$$A = \frac{r_w^{n-1}\pi^{\frac{n}{2}}b^{3-n}}{\Gamma(\frac{n}{2})} \qquad \text{(Equation 4-59)}$$

If n=2, Equation (4-59) reduces to Equation (4-56) (b = d) and for n=1, the equation describes linear flow (analogue to the parallel plate model described in Equation (4-57)). For non-integer values of *n*, the flow dimension becomes a fractional dimension.

(b) Injection-Withdrawal Test

The single well injection-withdrawal test (also known as the drift and pumpback test) was described by Borowczyk *et al.* (1966) and Leap and Kaplan (1988) for a homogeneous, isotropic and confined aquifer. To conduct a single well injection-withdrawal test a tracer is introduced to the standing water column of the test well and allowed to drift, under natural gradient, away from the well bore. After a period of time pumping the test well retrieves the tracer plume. Groundwater flow velocity is then calculated, based on the amount of pumping needed to recover the tracer, by the following equation (Leap and Kaplan, 1988):

$$v = \frac{\sqrt{Qt_p / \pi \varepsilon D}}{t_d} \qquad \text{(Equation 4-60)}$$

where:

v = seepage velocity (m/d)
Q = Pumping rate during recovery of tracer (m^3/d)
t_p = Time elapsed from start of pumping until the centre of mass of the tracer is recovered (d)
ε = Kinematic porosity
D = Aquifer thickness (m)
t_d = Time elapsed from the injection of tracer until the centre of mass of the tracer is recovered (d)

The inconsistency of this method is in the assumptions. The method should "account for regional velocities that are too high to be neglected during pumpback", but one of the assumptions is that "the aquifer is homogeneous and isotropic and possesses no regional hydraulic gradient" (Leap and Kaplan, 1988).

The geometric principle of this method is shown in Figure 4-17. Leap and Kaplan state clearly that the distance r_2 shows the position of the plume at time t_a (arrival time at borehole), if no pumping would occur. But they use the distance r_2 for calculating the whole travel distance of the tracer plume during the test:

$r = r_1 + r_2 + r_3;$ (eq. 7, Leap and Kaplan, 1988)

This is contradictory to the scheme in Figure 4-17, where $r_1 = r_3$.

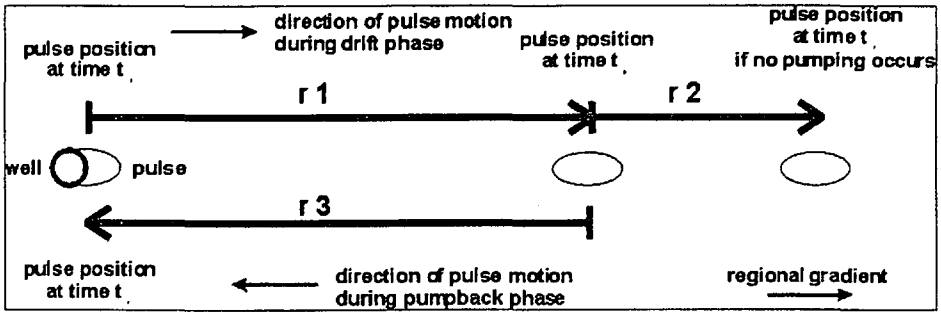

Figure 4-17 Movement of a tracer pulse during drift phase and pumpback phase (after Leap and Kaplan, 1988)

Neglecting the distance r_2 in the final equation of Leap and Kaplan (1988) and therefore neglecting the natural hydraulic gradient during the pumpback phase will yield the equation of Borowczyk *et al* (1966):

$$v = \frac{(Q/\Pi\varepsilon\, b)^{1/2} t_p^{\,1/2}}{t_*} \qquad \text{(Equation 4-61)}$$

where

t_p = Time elapsed from start of pumping until the centre of mass of the tracer is recovered (d)

t_* = drift time of tracer ($t_p - t_i$).

Despite the mathematical inconsistency in the theory of Leap and Kaplan (1988) the method seems to be valid only in a small range of the relation of drift time to pumpback time. If the pumpback time t_p becomes close to the drift time t_*, the estimated value for the velocity reaches a maximum and when t_p further increases the estimated velocity decreases (Figure 4-18). The velocity is a linear function of [$t_p^{1/2}$ / T], which is equal to [$t_p^{1/2}/(t_* + t_p)$]. If $t_p = t_*$ the term reaches a maximum, for $t_p > t_*$ the value of the term decreases slowly. In the version of Borowczyk *et al.* (1966) the velocity is a linear function of [$t_p^{1/2}$ / t_*], which does not show the above-mentioned behaviour (Figure 4-18).

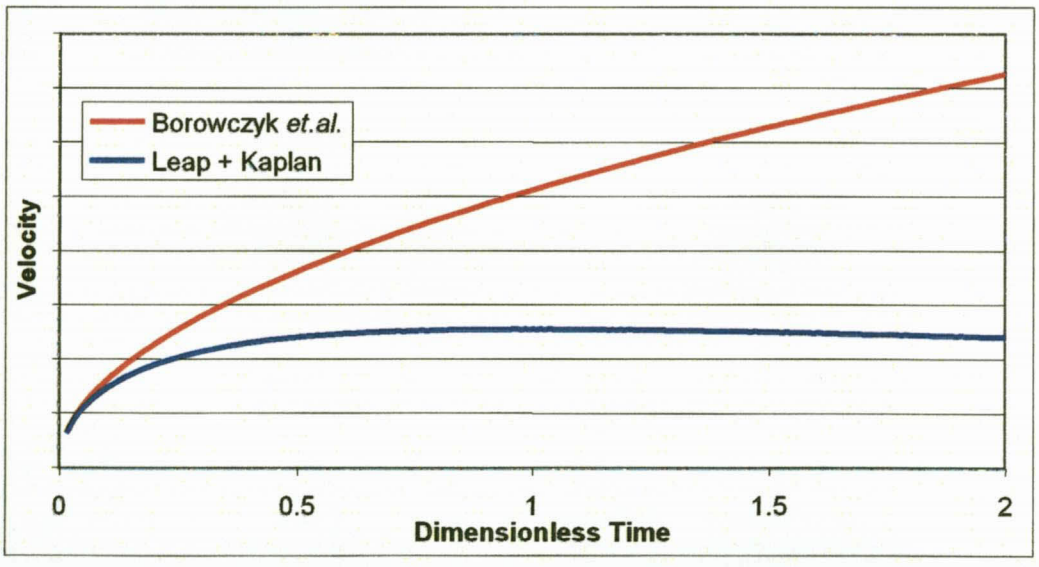

Figure 4-18 Velocity as a function of dimensionless time (t / t_*), applying Leap and Kaplan (1988) and Borowczyk *et al.* (1966)

Especially in cases with a high velocity (i.e. the regional velocity cannot be neglected) this relation will yield to practical problems, because the used pump for the pumpback phase is then often not sufficient to get the plume back to the borehole in a short time. In the experimental verification Leap and Kaplan (1988) use a relation of pumpback time to drift time of 0.1 to 0.3, which is far smaller than most practical situations as described above. Further practical problems and how they can be solved when conducting the test will be discussed in Chapter 5.2.

The equations of Leap and Kaplan (1988) and Borowczyk *et al.* (1966) are applicable in the case where a flow dimension *n* of 2 exists, i.e. steady state horizontal flow during drift phase and radial flow during the pumping phase. It is also possible to estimate the seepage velocity in a more general way by using fractional flow dimensions (Barker, 1988).

The volume of water pumped during a time *t* into a sphere is given by:

$$V=Qt \qquad \text{(Equation 4-62)}$$

where

Q = constant volumetric flow rate.

The volume out of an n-dimensional sphere with radius r is given by:

$$V = \varepsilon b^{(3-n)}\beta_n r^n \qquad \text{(Equation 4-63)}$$

with

$$\beta_n = \frac{\pi^{\frac{n}{2}}}{\frac{n}{2}\Gamma(\frac{n}{2})} \qquad \text{(Equation 4-64)}$$

If a tracer travels a distance r in time t, the averaged velocity is estimated by:

$$v = r/t \qquad \text{(Equation 4-65)}$$

Evaluating Equations (4-62), (4-63) and (4-65) yields:

$$v = \frac{(Qt_p / \varepsilon b^{3-n} \beta_n)^{\frac{1}{n}}}{t_d} \qquad \text{(Equation 4-66)}$$

If n=2 (meaning radial flow field), Equation (4-66) reduces to Equation (4-60). Using the drift time t_* instead of t_d generalises the equation of Borowczyk *et al.* (1966), which then reads:

$$v = \frac{(Qt_p / \varepsilon b^{3-n} \beta_n)^{\frac{1}{n}}}{t_*} \qquad \text{(Equation 4-67)}$$

Hall *et al.* (1991) uses a combination of the Leap and Kaplan equation and Darcy's Law ($v = Ki/\varepsilon$) to estimate the groundwater velocity and kinematic porosity with the same assumptions like Leap and Kaplan (1988):

$$v = \frac{Qt_p}{\pi D t_d^{\,2} Ki} \qquad \text{(Equation 4-68)}$$

and

$$\varepsilon = \frac{\pi D K^2 i^2 t_d^{\,2}}{Qt_p} \qquad \text{(Equation 4-69)}$$

Where:

V = seepage velocity
Q = Pumping rate during recovery of tracer
t_p = Time elapsed from start of pumping until the centre of mass of the tracer is recovered
D = Aquifer thickness
t_d = Time elapsed from the injection of tracer until the centre of mass of the tracer is recovered
K = Horizontal hydraulic conductivity
i = Horizontal hydraulic gradient
ε = Kinematic porosity

For the case of a non-integer flow dimension of n, the Hall equations generalise to (for n>1):

$$v = [\frac{Qt_p}{\beta_n b^{3-n} t_d{}^n Ki}]^{\frac{1}{n-1}} \quad \text{(Equation 4-70)}$$

and

$$\varepsilon = [\frac{\beta_n b^{3-n} (Kit_d)^n}{Qt_p}]^{\frac{1}{n-1}} \quad \text{(Equation 4-71)}$$

(c) Combination of Injection-Withdrawal and Point Dilution Test

If the injection part of the Injection-Withdrawal Test is used as a Point-Dilution Test, both tests will independently yield values for the Darcy velocity and flow velocity, respectively. The analysing procedure stays the same for each part of the test. This opens new possibilities of parameter estimation as described in section 4.2.3.

4.2.2.2. Single-well Tracer Tests, Forced Gradient

This method is also known as the Injection-Withdrawal test. The main difference to the above-mentioned Injection-Withdrawal test is the injection part. The first step is to create a radial flow field by recharging water constantly for a period of time into the borehole and then injecting the tracer in the recharging borehole. The tracer will be pushed into the surroundings of the borehole and will drift with the forced gradient. The withdrawal part is then equal to the above-mentioned test.

Sutton *et al.* (2000) recently developed a dipole-flow test with tracer as a single-well tracer test. The DFTT device isolates an injection and an extraction chamber in a well and utilises a small pump to create a dipole-flow pattern in which a tracer is introduced.

Because these methods require specific equipment, which is cost-intensive and difficult to handle accurately, the methods are normally not used in Southern Africa and therefore not discussed further.

4.2.2.3. *Multiple-well Tracer Tests, Natural Gradient*

Multiple-well tracer tests under natural gradient are usually conducted with one injection borehole and one or more observation boreholes.

(a) Natural Flow Tracer Test

When conducting a natural flow tracer test, one borehole is used for the injection of the tracer, while several boreholes downstream of the source borehole are used for observing the concentration of the tracer at different times. The analysing methods for this type of tracer test can also be applied to natural conditions with environmental tracers, such as pollutants at contaminated sites, if measurements of the concentration at different times are available.

The transport and spread of the tracer plume is controlled by advection (i.e. flow velocity) and longitudinal and transversal dispersion, while the certain concentration at time t and position (x,y) is also a function of matrix diffusion, retardation due to non-ideal tracing behaviour, and decay. A typical plume movement is shown in Figure 4-19.

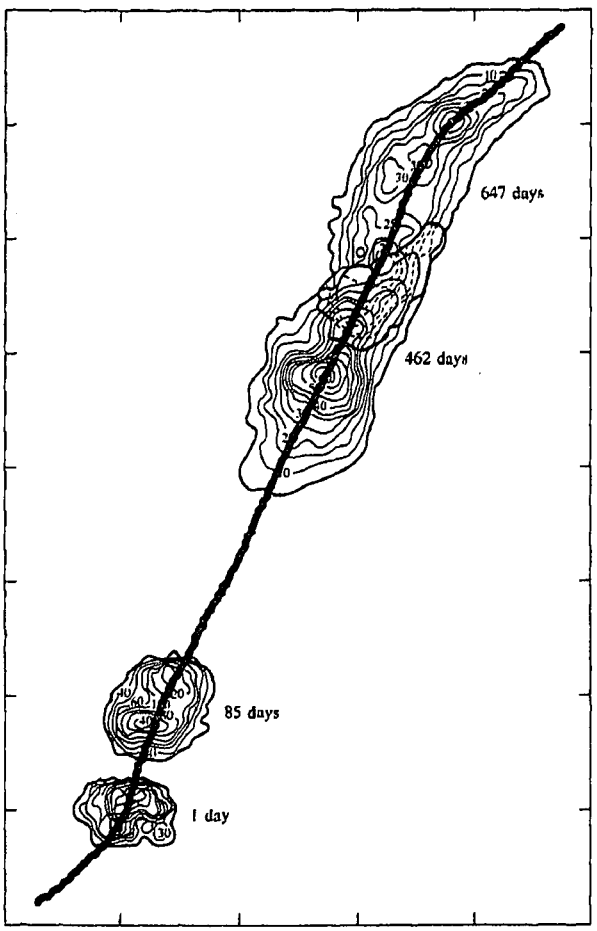

Figure 4-19 Tracer plume movement in a natural flow field with influence of longitudinal and transversal dispersion and changing flow direction (after Fetter, 1999)

1-dimensional Solution

If the observation borehole is located direct downstream the source borehole and the transversal dispersivity can be neglected, a one-dimensional parallel flow can be considered. Assuming an ideal, non-reactive tracer and neglecting the influence of matrix diffusion, the concentration of the tracer at the observation borehole at certain time is then given by (Sauty, cited in: Kinzelbach, 1992):

$$c(x,t) = \frac{M}{2A\varepsilon\sqrt{\pi\, tD_L}} \exp\left[-\frac{(x-vt)^2}{4D_L t}\right] \qquad \text{(Equation 4-72)}$$

with:

M = injected mass of tracer (kg)
A = through-flow area
D_L = longitudinal dispersion coefficient (m^2/s); $D_L = \alpha_L\, v$
v = groundwater velocity under natural gradient (m/s)
ε = kinematic porosity
x = distance (m) between the injection and observation borehole in x-direction (= direction of groundwater flow)

2-dimensional Solution

In most natural situations the flow direction is not known exactly a priori, meaning that the exact downstream location of the observation borehole cannot be assumed. Additionally the transversal dispersivity cannot be neglected in general. Therefore a two-dimensional parallel flow should be considered. Using the same assumptions as above the solution is given by (Sauty, cited in: Kinzelbach, 1992):

$$c(x,y,t) = \frac{M}{4\pi D\varepsilon\sqrt{D_L D_T}\, t} \exp\left[-\frac{(x-vt)^2}{4D_L t} - \frac{y^2}{4D_T t}\right] \qquad \text{(Equation 4-73)}$$

with:

D_T = transversal dispersion coefficient (m^2/s); $D_T = \alpha_T\, v$
y = distance of the observation borehole perpendicular to the flow direction

The disadvantages of this test are the time, which is necessary to carry out the test, and the difficulties in measuring the tracer concentration in the observation boreholes. The measurement tool should not disturb the natural flow field. On the other hand the real concentration in the flow path (i.e. the fracture zone) is required, which cannot be realised properly in open boreholes.

Another practical problem related to this test is the position of the boreholes, which are often not located exactly in the flow direction. And the flow direction is often not known exactly, or can change along the flow path (see Figure 4-19).

4.2.2.4. *Multiple-well Tracer Tests, Forced Gradient*

The most common methods in conducting tracer tests are multiple-well tracer tests, where a specific flow field is created by recharging and / or abstracting water at different boreholes. Injection and observation of the tracer will then take part at specific places in the created flow field. The tests and the analysing methods differ according to the created flow field.

(a) Radial Convergent Test

Pumping a well until steady state conditions are reached creates a radial convergent flow field (like a constant discharge hydraulic test, see section 4.1.1.4). A tracer is then quickly introduced in an injection well located in the vicinity of the pumping well in such a way that a minimum disturbance of the flow field is caused, while the tracer breakthrough curve is monitored at the pumping well. Analyses of the resulting breakthrough curves yield estimates of the kinematic porosity, aquifer dispersivity and groundwater velocity. The convergent test is attractive because it is theoretically possible to recover the tracer from the aquifer completely. Furthermore, it most closely represents reality as groundwater pollution often occurs in the vicinity of pumping wells where radial flow fields are present. The convergent tracer test, in combination with the borehole dilution test, has proved to be a powerful hydrogeological tool for measuring groundwater velocity and kinematic porosity.

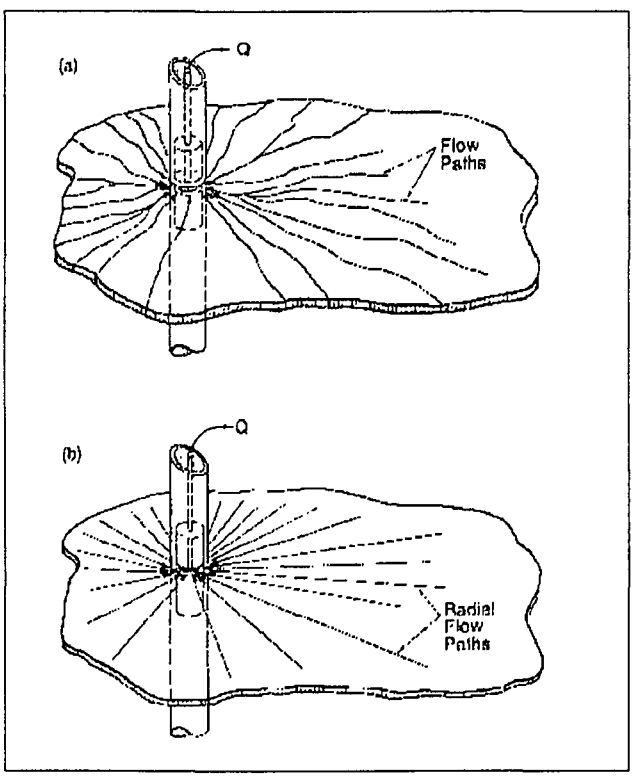

Figure 4-20 Radial flow field in a single fracture; a) possible flow paths due to heterogeneity, b) idealised flow paths in homogeneous medium (Shapiro and Nicholas, 1989).

Solutions without Matrix Diffusion

When the tracer test is conducted in a homogeneous and isotropic aquifer, where the transport is dominated by advection and dispersion and where molecular diffusion can be neglected, the approximate solution for a converging radial flow with a pulse injection is given by (Sauty, 1980):

$$c(r,t) = \frac{\Delta M}{2Q\sqrt{\pi D_L t^3}} \exp\left[-\frac{(r-vt)^2}{4D_L t}\right] \qquad \text{(Equation 4-74)}$$

with:

ΔM = injected mass of tracer per unit section (Mass (kg)/ Thickness (m))
D_L = longitudinal dispersion coefficient (m^2/s); $D_L = \alpha_L v$
α_L = longitudinal dispersivity (m)
v = v_f; groundwater velocity under forced gradient (m/s)
Q = pumping rate of the well (m^3/s)
r = radial distance (m) between the two boreholes

Welty and Gelhar (1994) show that the above-mentioned solution of Sauty is characterised by the problem of mass conservation and underprediction of dispersion, since the analytical solution is based on the one-dimensional uniform flow solution. But during a radial convergent test a non-uniform flow field is established with variable velocity values along the travel distance.

Another drawback of this test is that in some geologic settings the slug input may not leave the borehole as a true pulse, but rather as a gradually decreasing concentration input, generating a breakthrough curve with a very long tail. The solutions, given by Welty and Gelhar (1994) for non-uniform convergent flow with accounting for borehole flushing, indicate that the borehole flushing effect will be most significant in fractured media, where the kinematic porosity is of the order of 10^{-2} to 10^{-4}.

Zlotnik and Logan (1996) derived boundary conditions for radial convergent tracer tests to account for the effect of well bore mixing. Their study indicates the importance of correct injection regarding the sufficient mixing of the tracer in the borehole. Furthermore they discovered a main advection dominated zone of transport from the injection to the abstraction borehole, surrounded by a zone with both advection and dispersion (see Figure 4-21)

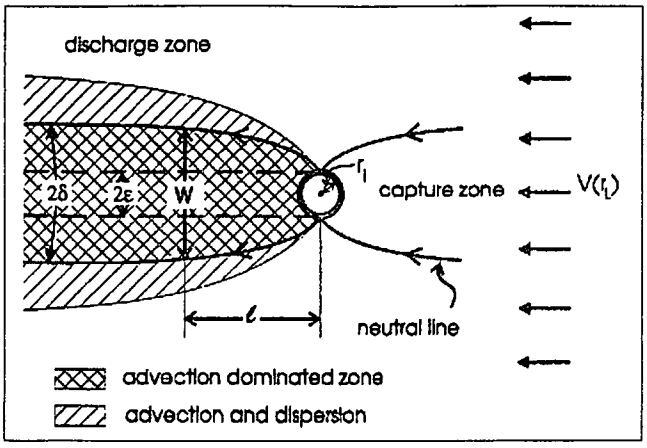

Figure 4-21 Schematic view of capture and discharge zones in the vicinity of the injection well (Zlotnik and Logan, 1996)

Solutions with Matrix Diffusion

Since matrix diffusion cannot be neglected in most cases of solute transport in fractured media, the analysing method for tracer tests should account for this effect. Maloszewski and Zuber (1985, 1993) developed a model and analytical solutions to estimate velocity, dispersivity and matrix diffusion from radial convergent tracer tests:

$$c_f(t) = \frac{Ma}{2\pi Q}(Pet_0)^{1/2}\int_0 \exp\left[-\frac{Pe(t_0-u)^2}{4ut_0}-\frac{a^2u^2}{t-u}\right]\frac{du}{\left[u(t-u)^3\right]^{1/2}} \qquad \text{(Equation 4-75)}$$

where t_0, a and Pe are the fitting parameters, as defined below.

t_0 = x_0/v, mean travel time of mobile water in the fracture
x_0 = distance along the direction of flow in the fracture between the entrance to the system and the observation point
u = $(Pe\ t_0)/(4\xi^2)$
ξ = integration variable
Pe = $v\ x_0 / D = x_0 / \alpha$, Peclet number
D = coefficient of intrinsic dispersion
α = intrinsic dispersivity
a = $n_p\ (D_p\ R_{ap})^{1/2} / (2b)$, diffusion parameter
n_p = matrix porosity
D_p = molecular diffusion coefficient in the matrix
2b = fracture aperture
R_{ap} = Retardation factor caused by exchange in the matrix

(b) Combination of Radial Convergent and Point Dilution Test

If a point dilution test is used as the source in the injection borehole, the Darcy velocity q_f can be estimated. The radial convergent test yields independently a value for the flow velocity. The analysing procedure stays the same for each part of the test. This opens new possibilities of parameter estimation, especially for

- the flow dimension n and flow domain b, as described in section 4.1.3.3
- the kinematic porosity, as described in section 4.2.3.4

(c) Radial Divergent Test

The Radial Divergent Test is similar to the Radial Convergent Test, but deals with an injection borehole in the center and an observation borehole in the surrounding area. The first step is to create a radial flow field by recharging water constantly for a period of time into the borehole and then injecting the tracer in the recharging borehole. The tracer will be pushed into the surroundings of the borehole and will drift with the forced gradient. The breakthrough curve will be measured in an observation borehole located in the surroundings of the injection borehole.

Because this method requires specific equipment, which is cost-intensive and difficult to handle accurately, this method is normally not used in Southern Africa and therefore not discussed further.

(d) Injection-Withdrawal Test

This multiple-well test is also known as Injection-Withdrawal test. The main difference to the other Injection-Withdrawal tests is the created flow field. The first step is to create a specific flow field by recharging water constantly for a period of time into the injection borehole and abstracting the same amount of water from an abstraction borehole. Then the tracer will be injected in the recharging borehole, pushed into the surrounding area of the borehole and will drift with the forced gradient. A part of the injected tracer will flow to the abstraction borehole, while another part will disappear in the aquifer. The breakthrough curve of the tracer will then be measured in the abstraction borehole.

Because this method requires specific equipment, which is cost-intensive and difficult to handle accurately, it is normally not used in Southern Africa and therefore not discussed further.

4.2.3. Parameter Estimation

In the following sections the procedure for estimating the different transport parameters from tracer test data are described and discussed. As discussed in the section above the tracer tests, normally conducted in Southern Africa and therefore considered in this discussion, are the combination of the point-dilution and injection-withdrawal test as a single-well test, the combination of the point-dilution and radial-convergent test as multiple-well test and the natural flow test.

4.2.3.1. Flow Velocity

The most important parameter for transport prediction is the flow velocity of the groundwater, as it describes only advective transport. Depending on the purpose of the study and the conducted test the natural flow velocity or the flow velocity under the forced gradient of the specific test can be determined. From some tests the Darcy velocity can be obtained, which is actually a flux and can be related to the flow velocity.

(a) Darcy Velocity

The Darcy velocity of an aquifer is defined as the volume of water flowing per unit time through a unit cross sectional area normal to the direction of flow. The Darcy velocity, however, is a flux and not a velocity, although its physical dimensions are those of velocity (Length/Time; e.g. m/day).

The Darcy velocity can be estimated by means of single-well or multiple-well tracer tests, as described in detail below.

Single-well Tracer Test

As mentioned in section 4.2.2.1(a) the dilution of a tracer in the injection borehole can be related to the Darcy velocity by applying the equation of Drost and Neumaier (1974). It is important to conduct the test in an accurate manner, as it is described in section 5.2.2. The analysing procedure is then as follows:

- Subtract the background concentration of the tracer
- Calculate the volume of the tested section
- Choose the correct conceptual model to calculate the through-flow area
- Choose the correct conceptual model to predict the distortion factor
- Fit a straight line on the graph on a semi-log plot
- Calculate the Darcy velocity from the slope of the straight line

Since the tracer dilution is an exponential process and the natural tracer background value in the groundwater is constant, the background value should be subtracted prior to interpretation. This is especially of importance where the background concentration is high compared to the measured values. The significance is illustrated in Figure 4-22.

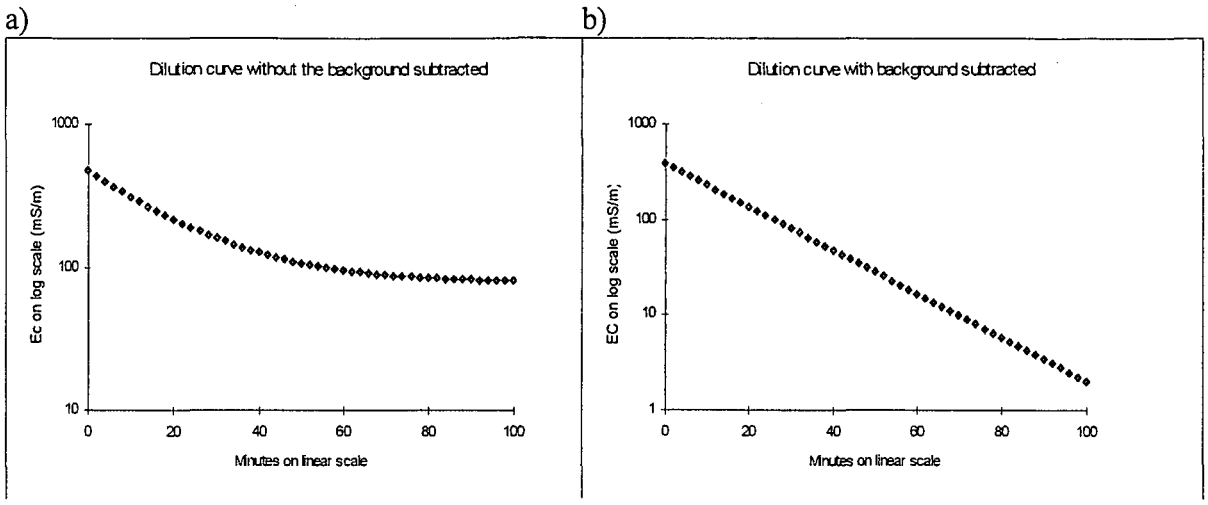

Figure 4-22 Typical Dilution curve of a tracer test, (a) without subtracted background and (b) with subtracted background (Van Wyk, 1998)

The calculation of the through-flow area depends on the purpose of the test and the conceptual model for the flow behaviour in the tested system. If the purpose is the estimation of averaged values for the whole aquifer, the through-flow area should be calculated using the length of the tested section. But if real values of the velocity field have to be estimated, the choice of the correct conceptual model to calculate the through-flow area becomes more complicated. Considering that the flow prevails only in open fractures, the equivalent aperture could be used to calculate the through-flow area. But in most natural systems the flow occurs in a zone of interconnected fractures. Using the approach of non-integer flow dimension, as described in Chapter 3, the through-flow area can be calculated in a more general way (see section 4.2.2.1(a)). The equations to calculate the through-flow area with the different approaches are listed below.

$A = \pi r_w d$ (for the radial flow model) (see Equation 4-56)

With:

r_w = well radius

d = the length of the tested section in the borehole

$A = \pi r_w(2b)$ (for the parallel plate model) (see Equation 4-57)

Where

2b = equivalent aperture of the fracture.

$$A = \frac{r_w^{n-1}\pi^{\frac{n}{2}}b^{3-n}}{\Gamma(\frac{n}{2})}$$ (for the flow dimension model) (see Equation 4-59)

with

n = non-integer flow dimension

b = flow domain or extent of the flow region

Γ = Gamma-function

As mentioned in the discussion about the effective thickness of the fracture zone (section 4.1.3.1(b)), the actual needed parameter is the vertical width of the fracture zone, intersected in the borehole.

The borehole distortion factor, α, takes the distortion of the flow field by the well into account (see Figure 4-23). It is a function of the Reynolds number (Re).

$$\alpha = \alpha_0[1 - f(\mathrm{Re})] \qquad \text{(Equation 4-76)}$$

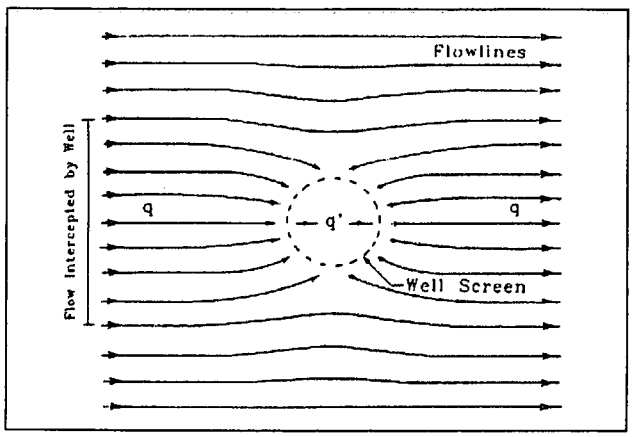

Figure 4-23 Distortion of the flow field causes increased flux through the well (after Freeze and Cherry, 1970)

The distortion of the groundwater flow field by the well was analytically derived from a model developed by Drost *et al.* (1968) for tests in sand or gravel aquifers. The distortion factor was empirically ascertained for these aquifers and α ranges from 0.5 to 4. For boreholes with a single filter zone (gravel pack and well screen) the distortion factor is computed as:

$$\alpha_0 = \frac{4}{1 + \left(\frac{r_1}{r_2}\right)^2 + \frac{k_2}{k_1}\left[1 - \left(\frac{r_1}{r_2}\right)^2\right]} \qquad \text{(Equation 4-77)}$$

Where

k_1 = Permeability of the gravel pack
r_1 = Radius of the well screen
k_2 = Permeability of the formation
r_2 = Radius of the borehole

If this model is adapted for hard-rock aquifers, where normally no gravel pack or well screen is present, then the distortion factor α is 2.

In a case study the three approaches were used independently to analyse point dilution tracer tests, conducted in the vicinity of an abstraction borehole, which was then used for radial convergent tests to compare and eventually to verify the results. The tests were conducted on the Campus Test Site of the University of the Free State in Bloemfontein, South Africa (see section 6.1.3 for details).

Hydraulic and tracer tests were conducted on several boreholes, including boreholes UO5 and UO26, intersecting the main fracture zone. Applying the method of Barker (1988) to the hydraulic test data, the flow dimension n was estimated at 1.75 and 1.85 respectively (i.e. between bi-linear and radial flow), while the flow extent b was estimated to 0.15 and 0.16 respectively. The transmissivity of the fracture obtained from analytical and numerical models is estimated at 700 and 750 m^2/day respectively (Chiang and Riemann, 2001).

To estimate groundwater velocity, effective thickness of the fracture zone and the kinematic porosity, radial convergent tests were conducted between boreholes UO5 and UO20, which are 15 m apart (called the UO5-tracer test), and between boreholes UO26 and UO28, which are 14 m apart (called the UO26-tracer test), whereby the injection of the tracer was used as a point-dilution test. These point-dilution tests in boreholes UO20 and UO28 were analysed with the approaches mentioned above. The results are shown in Table 4-7 and Table 4-8.

Table 4-7 Parameter values obtained from the UO20 point dilution test (injection for the UO5 radial convergent test) with different approaches.

Parameter	Radial flow model	Fractional flow dimension	Mass balance aperture	Cubic law aperture
Transmissivity (m2/d)				700
Mean residence time (min)			424	
Flow dimension	2.0	1.75	2.0	2.0
Fracture zone or aperture (m)	1.0 (tested section)	0.15 (from RCT)	0.036	0.0024
Darcy velocity (m/d)	3.48	24.9	96.8	1455

Table 4-8 Parameter values obtained from the UO28 point dilution test (injection for the UO26 radial convergent test) with different approaches.

Parameter	Radial flow model	Fractional flow dimension	Mass balance aperture	Cubic law aperture
Transmissivity (m2/d)				750
Mean residence time (min)			395	
Flow dimension	2.0	1.85	2.0	2.0
Fracture zone or aperture (m)	2.0 (tested section)	0.15 (from RCT)	0.027	0.0024
Darcy velocity (m/d)	0.73	9.44	54.2	596.5

The data of the radial convergent tests were analysed by fitting the parameters flow velocity, dispersivity and thickness of through flow to the breakthrough curve of the tracer in the abstraction borehole. Both tests yielded a flow velocity of 51 m/day, which is then compared to the estimation of the Darcy velocity (see Table 4-7 and Table 4-8) and to the estimation of the flow velocity from hydraulic test data. The results are shown in Table 4-9.

Table 4-9 Estimated flow velocities obtained from both the UO5 and UO26 tracer test, using different approaches.

Parameter	Hydraulic test	Radial flow model	Fractional flow dimension	Mass balance aperture	Cubic law aperture
UO5 Test					
Darcy velocity (m/d)		3.48	24.9	96.8	1455
Kinematic Porosity		0.07 [1)]	0.49 [1)]	1.0 [2)]	1.0 [2)]
Flow velocity (m/d)	57.35	51.0	51.0	96.8	1455
UO26 Test					
Darcy velocity (m/d)		0.73	9.44	54.2	596.5
Kinematic Porosity		0.01 [1)]	0.19 [1)]	1.0 [2)]	1.0 [2)]
Flow velocity (m/d)	60.8	51.0	51.0	54.2	596.5

1) Porosity is calculated from the relation between Darcy velocity and flow velocity
2) Porosity is set equal to 1 due to the chosen model

The comparison of the results from the two tests (see Table 4-9) indicates that the parallel plate model, using the equivalent aperture of the fracture, will yield values that are too high for the groundwater velocity. There is also evidence that the estimated cubic law aperture is far too small and therefore will yield velocity values which are ten to twenty times higher than those obtained from the radial convergent test. The estimation of the flow velocity using the hydraulic test data and Darcy's law compares well to the results from the radial convergent tests.

The analysing procedure, as described here, is implemented completely in the software TRACER, which offers the possibility to choose between the different approaches to calculate the through-flow area. However, using the flow dimension model for calculating the through-flow area is recommended for the reasons described above.

Multiple-well Tracer Test

Flow velocity is normally obtained from multiple-well tracer tests the, but nonetheless they offer two possibilities of estimating the Darcy velocity:

- If the injection of the tracer is conducted as a point-dilution test, the Darcy velocity can be estimated using the same analysing procedure as described above.
- If the flow velocity is estimated from a multiple-well test, as described below, and the kinematic porosity is known, the Darcy velocity can be computed by $q=v/\varepsilon$.

Both possibilities are implemented in the software TRACER, which is explained in detail in section 5.4.2.

(b) Natural Groundwater Velocity

The groundwater flow velocity (in some publications referred to as pore velocity or seepage velocity) describing the advective transport, is defined as the length the water flows per time unit [L/T, e.g. m/day]. Because the velocity is related to the hydraulic gradient by the 'Darcian' law, the measured velocity depends on test conditions. Therefore the natural flow velocity and forced flow velocity are distinguished.

The natural flow velocity can be estimated or calculated from the results of different field tests, e.g. hydraulic test, tracer test.

Hydraulic Test

The flow velocity can be expressed as a function of the hydraulic properties of the aquifer by the following equation:

$$v = \frac{ki}{\varepsilon} \qquad \text{(see Equation 4-51)}$$

with

k = hydraulic conductivity
i = natural hydraulic gradient
ε = kinematic porosity

If the hydraulic conductivity is estimated from hydraulic test data, as described above, and the natural hydraulic gradient and kinematic porosity are known or can be assumed in a certain range, the flow velocity can be calculated from Equation (4-51). Unfortunately both the hydraulic gradient and the kinematic porosity vary over a great range and are difficult to measure properly. Approximations for the estimation of the hydraulic gradient are given in section 4.1.3.7

Due to the fact that fractured aquifers often consist of several reacting systems (i.e. fractures and matrix) it is important to use parameters which were measured for the same system. E.g. using the estimated hydraulic conductivity of the fracture system and the averaged kinematic porosity of the entire aquifer yields a flow velocity value, which is not representative of any system.

Multiple-well Tracer Test

The most common way to estimate the flow velocity is by means of a multiple-well tracer test. Conducting a natural flow tracer test will yield directly the natural flow velocity, as the name of the test implicates.

Using one of the analytical solutions for natural flow, a theoretical breakthrough curve is compared to the measured data and fitted by changing mainly the parameters flow velocity and dispersion. The choice of the correct analysing method depends on the conceptual model.

- If a uniform, parallel flow along the fracture system can be considered (e.g. horizontal fracture), the one-dimensional solution can be used as a first approximation.
- In most cases, the flow in the fracture system cannot be assumed as parallel and the transversal dispersion cannot be neglected. Then the two-dimensional solution should be used, which requires a minimum of three observation boreholes for correct analysis.

If the positions of the observation boreholes, relative to the abstraction borehole and the flow direction are known, the two-dimensional solution can be applied directly after computing the values for x and y as

$$x = (x_1-x_0)\cos\alpha + (y_1-y_0)\sin\alpha \qquad \text{(Equation 4-78)}$$

and

$$y = (y_1-y_0)\cos\alpha - (x_1-x_0)\sin\alpha \qquad \text{(Equation 4-79)}$$

with

x_1, y_1 = real coordinates of observation borehole
x_0, y_0 = real coordinates of injection borehole (source)
α = flow direction, as an angle relative to North

In most real cases of natural flow tracer tests the exact flow direction is not known. Then the following procedure is recommended to estimate the transport parameters:

- Assuming a flow direction close to the real one, the breakthrough curve of an observation borehole directly in the assumed flow direction can be used to apply the one-dimensional solution. This will yield a first approximation of the flow velocity, thickness and longitudinal dispersion.
- In a second step the concentration data from boreholes situated outside the flow direction are used to apply the two-dimensional solution. This will yield mainly estimates for the transversal dispersion and the flow direction. When the assumed value for the flow direction has to be changed, the flow velocity, thickness and longitudinal dispersion have to be adjusted.

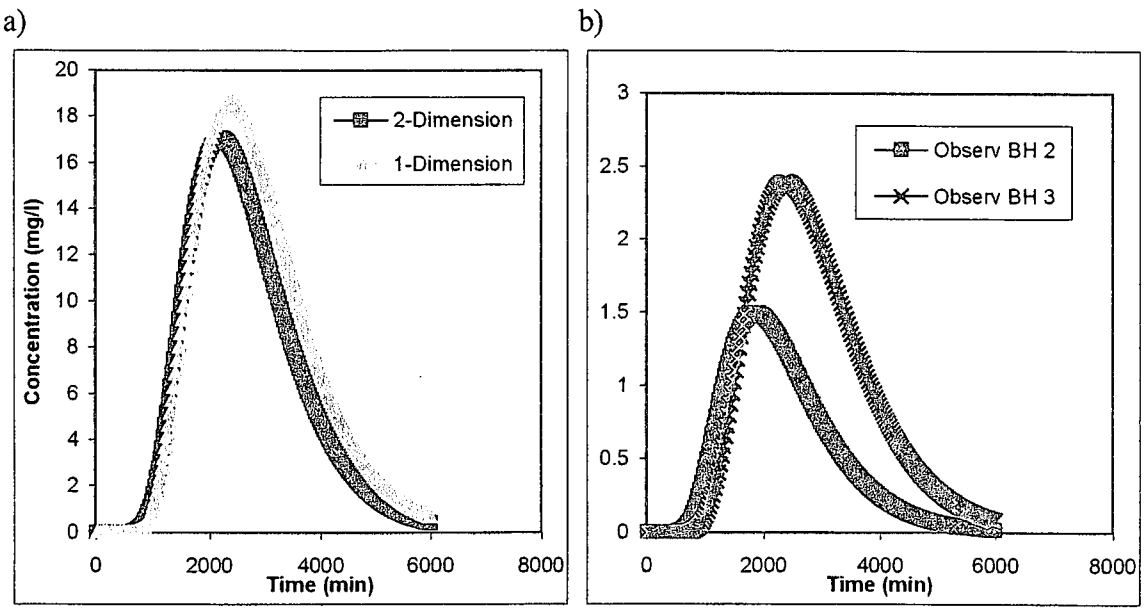

Figure 4-24 Applying one-dimensional and two-dimensional solutions to observation boreholes of natural flow tracer test; a) in the flow direction, b) normal to flow direction

Analysis of a natural flow tracer test is implemented in the software TRACER.

However, the flow velocity can be estimated with fewer observation boreholes, when calculating the mean residence time t_m (i.e. time, where half of the tracer passed the borehole). Assuming a straight flow path between injection and observation borehole, the flow velocity is then calculated as

$$v = r / t_m \qquad \text{(Equation 4-80)}$$

with

r = distance between injection and observation borehole
t_m = mean residence time of the tracer

Conducting a radial convergent tracer test will yield the forced flow velocity, which can be used to calculate the natural flow velocity, if the hydraulic gradient during the test and the natural hydraulic gradient are known. The difficulties and possible solutions in measuring and estimating the hydraulic gradient are described in section 4.1.3.7

If the injection of the tracer was used for a point-dilution test, a second point-dilution test could be conducted under natural flow conditions. The relation of the two obtained Darcy velocities can be used to calculate the natural flow velocity as

$$v = (v_f / q_f) * q \qquad \text{(Equation 4-81)}$$

where

vf = forced flow velocity
qf = Darcy velocity under forced gradient
q = Darcy velocity

Single-well Tracer Test

Actually single-well tracer tests yield only an estimate of the Darcy velocity, unless the kinematic porosity is known. Then the point-dilution test or the injection-withdrawal with the approach of Leap and Kaplan (1988) can be used to estimate the natural flow velocity. If the hydraulic conductivity and the hydraulic gradient are known, the approach of Hall *et al.* (1991) will yield the flow velocity.

The more efficient way in estimating the natural flow velocity is by means of a single-well tracer test, conducted as a combination of a point-dilution and injection-withdrawal test. As discussed later, the kinematic porosity can be obtained from such a combination (see section 4.2.3.4). The natural flow velocity is then computed using the approach of Leap and Kaplan (1988) or Borowczyk *et al.* (1966) for the injection-withdrawal test.

The main assumption is a properly conducted test with reliable data, as described in detail in section 5.2.2. The analysing procedure for both the point-dilution test and the injection-withdrawal test are described above.

As the kinematic porosity and therefore the flow velocity will be computed from a combination of two tests, it is important to use the same values of parameters in both tests in the analysing procedure (e.g. thickness of fracture zone, kinematic porosity). In the software program TRACER this procedure is implemented with the possibility to link both analyses to ensure that the correct values are used.

(c) Groundwater Flow Velocity under Forced Gradient

The groundwater flow velocity under forced gradient is defined here as the flow velocity, which occurs under the specific conditions of a hydraulic test or a permanent pumping schedule (e.g. water supply production, groundwater remediation).

Hydraulic Test

The approach for the natural flow velocity discussed above can be directly applied in the same way to calculate the forced flow velocity. The hydraulic conductivity should be estimated from the hydraulic test data and the hydraulic gradient should be measured during the steady state part of the test. If the kinematic porosity is known or can be assumed properly, the forced flow velocity can be estimated with Equation (4-51).

Multiple-well Tracer Test

The most common and certain way to estimate the forced flow velocity is by means of a radial convergent test. Injecting a tracer into a borehole in the vicinity of a pumping borehole and measuring the tracer concentration in the abstracted water result in a breakthrough curve of the tracer concentration. As with the point-dilution test the background concentration of the tracer must be subtracted from the measured data due to the fact that the analytical solutions do not account for a normal concentration of the tracer in the groundwater.

The measured data are then compared to the theoretical breakthrough curve, calculated with the equation of Sauty (1980), and fitted by changing the values for forced flow velocity, dispersion and thickness of the fracture zone. To obtain a more accurate fit, the recovery of the tracer is also computed for both the theoretical and the measured data and compared. In fractured aquifers the breakthrough curve often shows a long tailing above the background concentration, which results from matrix diffusion rather than dispersion. In such a case, the fit should focus on the upgradient part of the breakthrough curve, as shown in Figure 4-25.

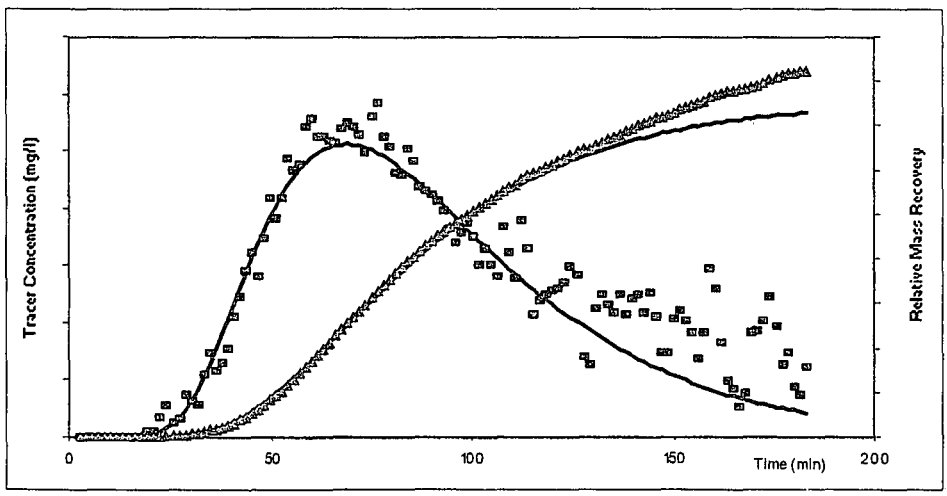

Figure 4-25 Breakthrough curve from a radial convergent tracer test (dots) and relative recovery (triangle) with best fit (lines)

4.2.3.2. Dispersion

The assessment of aquifer dispersivity is essential for predicting contaminant plume migration in groundwater. Dispersivity is one of the key input parameters to the governing transport equation used to mathematically estimate the distribution of a solute in the subsurface environment over time and space. As discussed in Chapter 2 dispersivity is a function of the heterogeneity of a geologic formation and exhibits scale dependence. The effect of heterogeneity on the spread of the plume is normally expressed in terms of two values, namely the longitudinal dispersivity and the transversal dispersivity.

(a) Longitudinal Dispersivity

The longitudinal aquifer dispersivity, α_L, causes velocity variations in the medium, which disperses the tracer solutes, so that the coefficient of longitudinal hydrodynamic dispersion takes the form:

$$D_L = \alpha_L |v| \qquad \text{(Equation 4-82)}$$

where v is the pore velocity of the aquifer.

The influence of α_L on theoretical, simulated, breakthrough curves, with groundwater advection taken as a constant value, is illustrated in Figure 4-26. The simulations were done with an analytical model for advection-dispersion interpretation in radial flow field with a pulse tracer input. The peak of the tracer breakthrough curve (radial flow) at α_L = 0,1 is regarded to represent the advective velocity of the aquifer since dispersivity is small. The diagram clearly illustrates that the simulated peak arrival times decrease with increasing values of longitudinal dispersivity, suggesting that the peak of a tracer breakthrough curve does not represent the mean advective velocity of the aquifer, which was kept constant during the simulations.

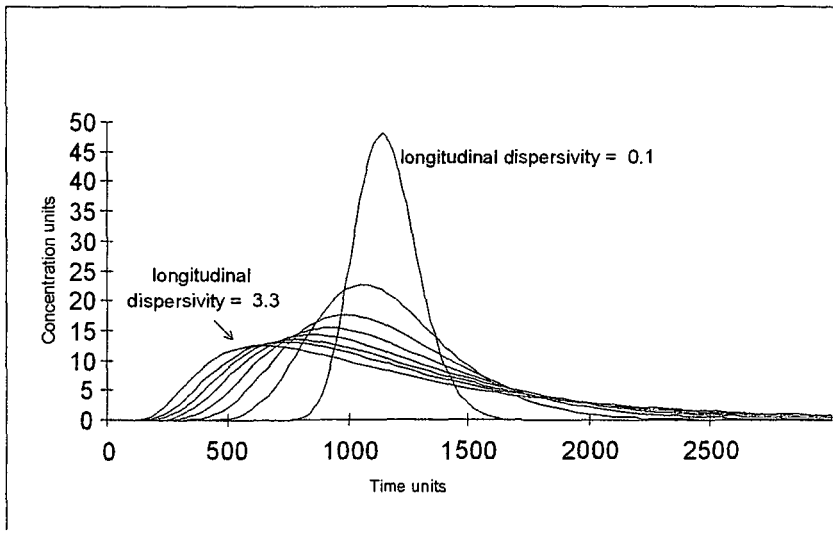

Figure 4-26 Theoretically simulated breakthrough curves showing the influence of dispersivity (Van Wyk *et al.*, 2001)

Natural Flow Tracer Test

The procedure for estimating the fitting parameters flow velocity and dispersion from a natural flow tracer test is described in detail above. A minimum of three observation boreholes in flow direction is required to distinguish between longitudinal and transversal dispersion. Since the dispersion controls the shape of the breakthrough curve, as seen above, the fitting of the breakthrough curve with simulated data must focus on the shape of the breakthrough curve.

The following procedure is recommended to estimate the longitudinal dispersivity, as discussed above:

- Assuming a flow direction close to the real one, the breakthrough curve of an observation borehole directly in the assumed flow direction can be used to apply the one-dimensional solution. For comparison the two-dimensional solution is also applied to the same data. This will yield a first approximation of the natural flow velocity, thickness and longitudinal dispersivity.
- To verify the estimations the concentration data from boreholes situated outside the flow direction are used to apply the 2-dimensional solution. This will mainly yield estimates for the transversal dispersion and the flow direction. When the assumed value for the flow direction has to be changed, the flow velocity, thickness and longitudinal dispersion have to be adjusted.

Radial Convergent Test

The concentration data obtained from a radial convergent tracer test can be used to estimate the dispersion coefficient. The analysing procedure is described above for the estimation of the flow velocity. Since the dispersivity controls the shape of the breakthrough curve, as seen above, the fitting of the breakthrough curve with simulated data must focus on the shape of the breakthrough curve.

To control the accuracy of the estimated value, the calculated and simulated mass recovery are plotted on the same graph and compared. This method is also used to distinguish between dispersivity and matrix diffusion. The estimated value for the longitudinal dispersivity should be about one order smaller than the distance between injection and abstraction. Otherwise the test data and or the chosen analysing procedure (i.e. conceptual model) are not trustworthy and the result is not reliable.

Chao *et al.* (2000) demonstrate by means of intermediate-scale experiments and numerical simulations that the dispersivity varies over a wide range in a heterogeneous porous medium, indicating the limitations of type-curve matching techniques for the analysing procedure.

Since the dispersivity is scale-dependent (see Chapter 2), it has to be considered and noted in analysing reports, that the estimated value is valid for the conditions of the tracer test, especially regarding the scale of the test.

(b) Transversal Dispersivity

Transversal dispersivity causes the tracer plume to spread perpendicular to the direction of flow. As illustrated in Figure 4-27, the spread of the plume depends on the relationship of longitudinal to transversal dispersivity.

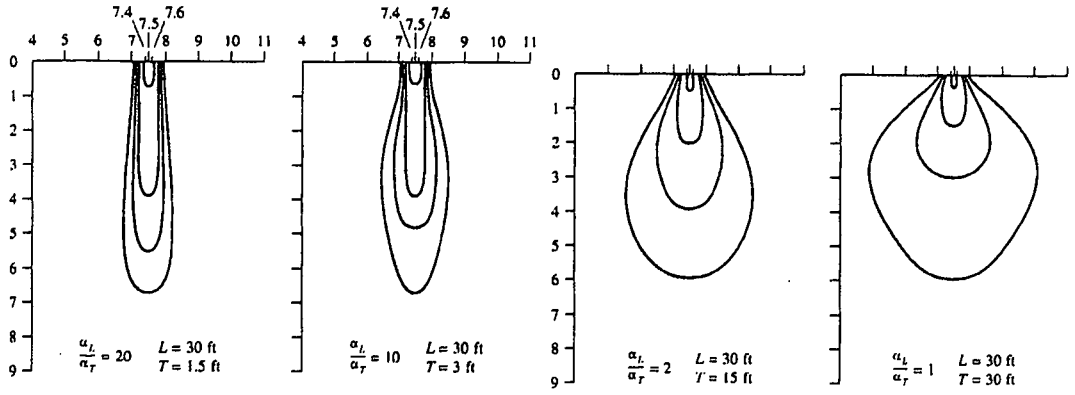

Figure 4-27 Influence of transversal dispersivity on shape of contamination plume (Fetter, 1999)

Natural Flow Tracer Test

The transversal dispersivity can only be estimated properly by means of a natural flow tracer test. The analysing procedure is described above. For estimating the transversal dispersivity the second step, applying the two-dimensional solution to the boreholes outside the direct flow direction, is the important part, because the transversal dispersivity controls the spread of the plume normal to the direction of flow. Since natural systems do not always follow the underlying assumption of homogeneity, the spread of the plume can be influenced by heterogeneity rather than dispersion, as illustrated in Figure 4-28.

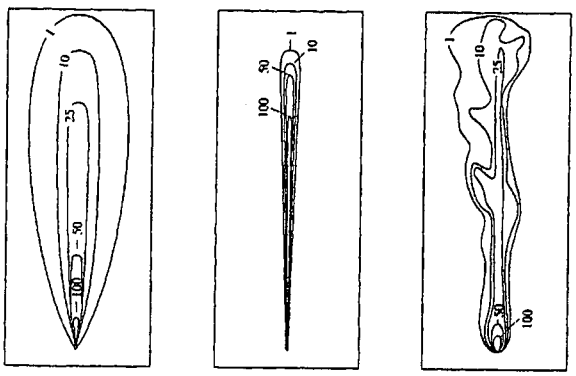

a) homogeneous aquifer, high transversal dispersivity
b) homogeneous aquifer, small transversal dispersivity
c) heterogeneous aquifer, small transversal dispersivity (equal to b))

Figure 4-28 Influence of transversal dispersivity and heterogeneity on a tracer plume (after Fetter, 1999)

Chen *et al.* (1999) developed a method to evaluate transversal dispersivity for tracer tests in a radially convergent flow field, using two wells. A curve-fitting procedure allows estimating simultaneously the longitudinal and transversal dispersivity, as long as the breakthrough curves at the pumping well and an observation well are known. Because this procedure requires an additional observation borehole, it is not recommended for application in Southern Africa.

4.2.3.3. Matrix Diffusion

In fractured rock aquifers the effect of matrix diffusion is often an essential factor in the transport process. The diffusion of the tracer from the fracture into the matrix results in a retardation of the tracer plume and in a loss of tracer (see section 2.3.3). There are different approaches to quantify the effect of matrix diffusion. Since matrix diffusion is a combination of diffusion, retardation and attenuation, it can be best expressed with a partly irreversible kinetic sorption model. The current approaches do not account for the irreversible part of the process.

Van der Voort (2001) examined matrix diffusion coefficients for different rock types of South Africa by means of laboratory experiments. The difference of the coefficient values for different chemicals is small compared with the variety for different rock types. The dependency upon the porosity of the rock matrix could be proven for most rock types.

Multiple-well tracer tests will show the effect of matrix diffusion in the shape of the breakthrough curves. A long tailing without reaching the background value, which cannot be fitted with an analytical model, indicates the presence of matrix diffusion. Although, Becker and Shapiro (2000) show by means of a case study that a long breakthrough tailing can also be caused by advective, nondiffusive transport processes. Calculating the relative mass recovery for both the measured field data and the simulated concentrations verifies the effect of matrix diffusion (see Figure 4-25). The relative mass recovery is computed as (Maloszewski and Zuber, 1993):

$$RR(t) = Q \int_0^t c(t')\,dt' / M \qquad \text{(Equation 4-83)}$$

In a system without other outflows and sinks, for $t \Rightarrow \infty$, RR(t) should yield 1. Any normalisation of the concentration data leads to a loss of information on the mass recovery. If the calculated relative mass recovery for the end of the test is less than 1, it indicates the loss of tracer due to matrix diffusion, which is given by:

$$L_{MD} = 1 - RR(t) \qquad \text{(Equation 4-84)}$$

If the tracer test data show the dominance of matrix diffusion in the transport process, the approach of Maloszewski and Zuber (1993) should be used to calculate a retardation factor for the effect of matrix diffusion, after a first estimate of the flow velocity is obtained with the approach of Sauty (1980), as described above.

Since the effect of matrix diffusion cannot be quantified with one parameter value only, the results of a tracer test should indicate the presence of matrix diffusion and, if applicable, the values for the loss of tracer due to matrix diffusion, L_{MD}, the retardation factor due to matrix diffusion and the matrix diffusion coefficient should be calculated. To distinguish between retardation due to matrix diffusion and retardation due to adsorption the double tracing method should be used for conducting the tracer test, as described in Chapter 5.

4.2.3.4. Porosity

The porosity of a rock is its property of containing pores or voids. Dividing the total unit volume V_t of an unconsolidated material into the volume of its solid portion V_s and the volume of its voids V_v, porosity can be defined as

$$n = V_v / V_t \qquad \text{(Equation 4-85)}$$

With consolidated and hard rocks a distinction is usually made between primary porosity, which is present when the rock is formed, and secondary porosity, which develops later as a result of solution or fracturing.

It is obvious that water can only move through pores that are interconnected. Hard rocks may contain numerous unconnected pores in which the water is stagnant. The important parameter to describe the groundwater flow is therefore the kinematic porosity ε (some authors refer to it as effective porosity) rather than the total porosity. The kinematic porosity is then the volume of the aquifer which is able to contribute to the groundwater flow. In fractured aquifers this volume is mainly influenced by the volume of fractures. Nonetheless the porosity of the rock-matrix should not be neglected.

While the total porosity can be determined in the laboratory, the kinematic porosity should be estimated by means of field measurements, as proposed below.

Single-well Tracer Test

A combination of the single-well Point Dilution and the Injection-Withdrawal test (see section 4.2.2.1) will independently yield values for the Darcy velocity q and the flow velocity v. These two parameters are related to the kinematic porosity by:

$$v = q / \varepsilon \qquad \text{(Equation 4-86)}$$

where

ε = kinematic porosity

From the dilution of the tracer during the point dilution test, the Darcy velocity is computed by Equation (4-55), while the flow velocity is determined from an injection-withdrawal test by:

$$v = \frac{\sqrt{Qt_p / \pi \varepsilon D}}{t_d} \qquad \text{(see Equation 4-60)}$$

The combination of Equation (4-86) and (4-60) will yield the kinematic porosity of the tested section.

$$\varepsilon = \frac{\pi \cdot b \cdot q^2 \cdot t_d^{\,2}}{Q \cdot t_p} \qquad \text{(Equation 4-87)}$$

Multiple-well Tracer Test

A radial convergent test is conducted between two boreholes, where one borehole is used as the source for the tracer while the other borehole is used for abstracting. From the tracer concentration in the abstraction borehole the flow velocity can be obtained (see section 4.2.2.4(a)). If a point dilution test is used as the source in the injection borehole, the Darcy velocity q can be estimated (see section 4.2.2.1(a)). The kinematic porosity is then given by

$$\varepsilon = q_f / v_f \qquad \text{(Equation 4-88)}$$

where

q_f = Darcy velocity, obtained from Point Dilution test in the injection borehole
v_f = Flow velocity, obtained from Radial Convergent test

The Darcy velocity q is defined as flow rate divided by the through-flow area. Substituting q with Q/A will yield another approach to estimate the porosity from a multiple-well tracer test:

$$v = \frac{Q}{\varepsilon A} \qquad \text{(Equation 4-89)}$$

where

A = through-flow area.

For a non-integer flow dimension n the area A is given as:

$$A = \frac{2\pi^{\frac{n}{2}} r^{n-1} b^{3-n}}{\Gamma(\frac{n}{2})} \qquad \text{(Equation 4-90)}$$

If n=2, Equation (4-90) reduces to $A = 2\pi rb$ (through-flow area of a cylinder in which case b= thickness of cylinder).

The value of the kinematic porosity, estimated with the approaches discussed above, represents the averaged kinematic porosity over the tested volume. Because the changes vary more perpendicular to the flow path than in the direction of the flow, the chosen thickness is the important parameter in the analysing procedure. E.g. using the length of the tested section in a single-well tracer test will yield the kinematic porosity of the rock matrix rather than of the fracture. Using the fracture aperture the porosity is equal to 1 per definition. Which thickness should be used in the analysing procedure, depends on the task of the tracer test.

Applying the multiple-well tracer test procedure for calculating the kinematic porosity the estimated effective thickness of the fracture zone must be used for calculating the Darcy velocity from the point-dilution test porosity, because the estimated flow velocity is computed for this thickness.

4.2.4. Discussion

Tracer tests are a powerful tool for estimating transport parameters, which are required for environmental investigations and well field management purposes. In fractured aquifers the analysing procedure becomes more complicated, because the common solutions of the advection-dispersion-equation are derived for homogeneous, porous media and do not consider the different flow geometry and the matrix-fracture interactions (see Chapter 2.3).

However, even porous media solutions can be applied to tracer tests in fractured aquifers, when the correct conceptual model for flow and transport behaviour is chosen. There are mainly three effects influencing the estimated values for the transport parameters:

- Flow geometry
- Effective thickness of flow
- Matrix-fracture interactions

Since these effects are mostly unknown and difficult to quantify, the approach of non-integer flow dimension should be applied to tracer test data, as described above. Introducing the concept of non-integer flow dimension, as derived by Barker (1988), into the equations for solute transport accounts for the unknown geometry of the fracture network. Flow and transport processes are sensitive to spatial variability and to the complex, high variable nature of subsurface formations. Incomplete knowledge of subsurface heterogeneity will create a high uncertainty in predicting the movement of contaminant plumes (Painter and Mahinthakumar, 1999).

The concept of fractal geometry is widely used in interpretation of hydraulic test data (see Chapter 3). While some authors (e.g. Wheatcraft and Tyler, 1988; Cushman and Ginn, 1993) explained the scale-dependency of dispersion with fractal geometry, the influence of fractal flow geometry on the solute transport is not restricted to dispersion, but also involves advective and diffusive transport.

While it is in the moment not possible to use the fractional flow dimension, obtained from hydraulic or tracer tests, directly in a numerical flow model or mass transport prediction model, the knowledge of the flow dimension is important for the calculation of flow and transport in fractured aquifers. There are several possibilities to account for non-integer flow dimension in numerical models. E.g. a porous media model can be used with a spatial variability of hydraulic parameters, stochastically produced and showing the same flow dimension (van der Voort and van Tonder, 2000).

However, if the flow dimension that prevails in an aquifer is less than two and porous mass transport models are used to predict contaminant movement, it could easily result in an estimated travel distance that is too small (i.e. the hydraulic conductivity of the fracture zone is underestimated, which will result in an underestimation of the travel distance of the pollutant).

Chapter 5 Proposed Procedure for Conducting Hydraulic and Tracer Tests

This chapter proposes procedures to conduct hydraulic and tracer tests in the field in such a way that the data are useful for the analysing process and the results reliable. While the two following sections describe the steps involved when conducting the tests, the third section will suggest a meaningful combination of hydraulic and tracer tests to reduce the costs for the fieldwork without losing important information for the analysing process. To simplify the planning, conducting and analysing of this combined hydraulic-tracer test, the software programs TRACER-PLAN and TRACER were developed, which will be described in detail in the last section.

5.1. Procedure for Hydraulic Tests

The procedure for planning and conducting hydraulic tests in fractured aquifers is described in detail in the "Manual on Pumping Test Analysis in fractured-rock Aquifers" (Van Tonder *et al.*, 2001). In the following section the main issues are discussed related to the intention of this research and in relation to the combination of hydraulic and tracer tests, as described in Chapter 5.3.

5.1.1. Planning of Hydraulic Test

The purpose of the hydraulic test should be identified in the beginning of the planning stage because this will influence the execution of the test. The objectives can either be to estimate aquifer parameters for a management model or it can be to estimate the long-term sustainable yield for the borehole. This research focuses on parameter estimation.

The first and most important step in the planning phase is to determine the kind of hydraulic test (calibration test, slug test, step-drawdown test, multirate test, constant discharge test) and to choose the abstraction and observation boreholes. The geohydrologist should visit the site and check the chosen boreholes to make sure that the test can be performed in the suggested way. For parameter estimation a constant discharge test is recommended. This test can be combined easily with a tracer test as discussed below. The duration of the test, the chosen discharge rate and the conditions of the measurements (manually, electronically) depend on the kind and the goal of the test. More details will be discussed below.

The second step is to gather all available information about the different boreholes and the aquifer, to ensure the correct planning of the depth and abstraction rate for the pump.

Step three in the planning phase is to gather the necessary equipment for the pumping test and to check their ability to ensure the successful and accurate performing of the pumping test.

5.1.2. Conducting Hydraulic Tests in the Field

The performing phase can be divided into three parts:

- Installing equipment and preparing the test.
- Conducting the test and measurement.
- Removing equipment and checking field data.

Observation boreholes, used for the hydraulic test, should never intersect more than one reacting aquifer system to avoid a mix of observation. If a borehole intersects more than one reacting aquifer system, the drawdown data show a mix of drawdown resulting from different systems and it is difficult to use those data in a numerical or analytical model. Prior to installing the equipment for the pumping test, the abstraction borehole should be checked for damages (e.g. incorrect depth, damaged casing, damaged column).

The best type of pump to be used is a positive displacement pump like the Mono-type pump. The yield of this type of pump remains constant and will not change if the water level drops. The main drawback of a positive displacement pump is that it is not easy to specify a pre-selected abstraction rate. Submersible (negative displacement) pumps can be used, but the abstraction rate will decrease with an increase in drawdown. It is, however, a simple task to set an exact initial pumping rate. The pump should have a built-in valve on the bottom to avoid back flow of water into the borehole after switching off the pump.

The discharge rate should be kept constant over the whole period of abstraction. Otherwise no analytical method should be used to estimate the parameter values unless the drawdown is corrected. When using a numerical model, every change in the discharge rate must be considered (in another stress period).

The maximum yield of the pump must be chosen so that the drawdown, which is necessary to achieve the goal of the pumping test, will be reached in time. As discussed above, the dewatering of fractures should be avoided when the purpose of the hydraulic test is parameter estimation. On the other hand, the duration of the test should be sufficient to reach the radial acting flow phase.

To ensure reliable test data the discharge pipe should transport the abstracted water far enough from both the abstraction and observation boreholes. The best choice is to discharge into a sewage system or onto a tar road.

After finishing the test, the equipment should be removed from the borehole, cleaned or decontaminated (if necessary) and the site should be left in the same condition as before the test. The field data and all gathered information should be checked directly after the test and before beginning the analysis. Any question of uncertainty in the data should be solved between the pumping test contractor and the geohydrologist as soon as possible.

5.1.3. Data Measurement and Interpretation

During the test, measurements of the water levels in the chosen boreholes and the discharge rate must be taken in fixed time intervals prescribed by the geohydrologist in the planning phase and discussed in detail below.

Every measurement and observation on site should be recorded on the pump test form. Especially changes in the condition of the test, like change of discharge rate, heavy rainfall or interruptions of the test due to technical problems, must be recorded to ensure that the geohydrologist can analyse this test correctly.

The following points for data measuring and interpreting hydraulic test data in fractured aquifers are recommendations:

- The measurement of the drawdown must have an accuracy of at least 1cm.
- It is strongly recommended that electronic device, such as a pressure transducer and data logger be used.
- The time intervals of measurement in the beginning of the test should be small, at least less than 1 minute (recommended 10 seconds) in the abstraction borehole. The time interval can be changed during the test exponentially, but not more than 1hour.
- The measurement of the discharge rate must have an accuracy of at least 0.1 L/s or 5% of proposed discharge rate.
- The discharge rate should be measured at least every hour. When a short-term hydraulic test is conducted, the time interval should be less than half an hour.

To analyse a hydraulic test correctly, the geohydrologist should be able to identify the following important characteristics as primary part of the interpretation procedure:

- The correct geological conceptual model (for use of the correct analytical model).
- Inner boundary conditions (i.e. well bore storage effects, well bore skin, fracture skin and the lateral extent of the fracture or fracture zone).
- Outer boundary conditions (i.e. especially no-flow boundaries but also fixed head boundaries).
- Characteristic flow regimes (the choice of the correct part of the curve to be fitted by looking at the flow dimension that prevails during that specific part of the test).

5.2. Procedure for Tracer Tests

The procedure to conduct and analyse tracer tests is more complicated than for hydraulic tests and needs detailed planning and proper conducting of the test as well as accurate measurements.

5.2.1. Planning of Tracer Test

The planning phase is the most important and most difficult part of conducting tracer tests. A tracer test, which is not planned in detail, results in data that are not usable for the analysing procedure. The following parameters should be considered a priori due to their impact on the accuracy and success of tracer tests, as it is implemented in the software TRACER-PLAN (see below):

- Type and purpose of tracer test
- Type of tracer
- Flow rate during circulation and abstraction
- Duration of test

5.2.1.1. Type of Test

Depending on the purpose of the investigation and the local situation, the type of tracer test can vary.

(a) Single-well Tracer Test

Single-well tracer tests should be conducted, if only one borehole is available or for a first approximation of specific transport parameters. To estimate the vertical distribution of matrix and fracture porosity, single-well tracer tests must be conducted in different depths of the borehole. But the results should be verified with a radial convergent test.

(b) Radial Convergent Test

In general a radial convergent tracer test is suggested, if a minimum of two boreholes close to each other are available. For most of the transport parameters this kind of test, eventually in combination with a point-dilution test, yields reliable results. The disadvantage of the test is that two pump-rigs are required, one for the injection borehole and one for the abstraction borehole.

(c) Natural Flow Test

If a wellfield with several evenly distributed boreholes exists, a natural flow tracer test can be a good choice to estimate the natural flow velocity. However, the required measurement tools in the observation boreholes are complicated and to complete the test is time-consuming. On the other hand the natural flow tracer test offers the only practical possibility for estimating the transversal dispersivity.

5.2.1.2. Tracer

Because of the different physical and chemical behaviour of tracer substances (see section 4.2.1), it is important to choose an applicable tracer in a certain range of concentration under the circumstances of the test, so that the tracer can be detected accurately at the observation point.

(a) Kind of Tracer

The kind of tracer depends on the kind and purpose of the test. If only the dilution in the injection borehole is of interest, a tracer like salt, which is easily detectable, would be suitable. If the tracer is mixed thoroughly with fresh water, i.e. in the abstraction borehole, the tracer must be detectable over a wide range of concentrations (e.g. bromide, Fluorescein). To avoid sampling and chemical analysis in the laboratory, the tracer should be detectable in the field. The following tracers are suggested for application:

Table 5-1 Suggested tracers and their possible application

Tracer	Measurement	Range of Concentration	Application
NaCl	EC-Meter	2 orders of magnitude	Single-well test Natural flow test Point-Dilution test
NaBr	EC-Meter Ion-sensitive Sensor	4 orders of magnitude	Single-well test Multiple-well test
Fluorescein	Fluorometer	5 orders of magnitude	Single-well test Multiple-well test

(b) Amount of Tracer

The optimal amount of tracer injected into the source borehole depends on the mixing in the injection borehole, the degree of dilution, the decay due to dispersion and diffusion, the mixing in the abstraction borehole and the detection limit. To conduct a successful test, the amount should be calculated a priori, as discussed below.

Mixing in the Injection Borehole

At first the concentration of the injected tracer decreases due to mixing with the volume of water in the tested section. In the case of the proposed set-up for the tracer injection (see below), the volume of water can be computed as:

$$V_c = \pi r_w^2(h_p-h_i) + \pi r_p^2 h_i + \pi r_i^2 h_i \qquad \text{(Equation 5-1)}$$

With

r_w = Borehole radius
r_p = Radius of the discharge pipe
r_i = Radius of the injection pipe
h_p = Depth of the pump inlet
h_i = Depth of the injection pipe outlet

The maximal tracer concentration in the injection borehole is then computed as:

$$C_0 = M / (V_t + V_c) \qquad \text{(Equation 5-2)}$$

With

M = injected mass of tracer
V_t = Volume of injected water
V_c = Volume of circulating water

Degree of Dilution

During the dilution process in the injection borehole the tracer concentration of the tracer plume will decrease further, depending on the degree of dilution which is a function of the Darcy velocity and the through-flow area. Since the velocity shall be estimated from the tracer test data, the Darcy velocity is not normally known beforehand. A first approximation can be derived from existing or assumed hydraulic data of the aquifer. From the 'Darcian Law' the Darcy velocity can be expressed as a function of the hydraulic conductivity k and the hydraulic gradient i.

The choice of the through-flow area depends on whether the hydraulic conductivity value represents the formation or the fracture system. If the hydraulic conductivity k in the equation above represents the formation, the through-flow area is computed with the length of the tested section. Otherwise an approximation of the fracture aperture or fracture zone thickness is required to estimate the through-flow area. Then the degree of dilution and the tracer concentration in the plume is computed using the approach of Drost *et al.* (1968) for the point dilution test.

Decrease due to Dispersion and Diffusion

When the tracer plume moves according to the groundwater velocity, the concentration will decrease further due to the influence of dispersion and diffusion. While dispersion causes the plume to spread out, diffusion causes a loss of tracer due to movement from the fracture system into the matrix. Both factors are difficult to predict a priori. Based on experience and field experiments, values for both parameters are assumed according to the test set-up, the geological situation and groundwater regime.

Table 5-2 Assumed values for dispersion and diffusion for different geological structures

Geological Situation	Assumed Dispersion [1)]	Assumed Diffusion [2)]
Single fracture in permeable matrix	5%	10%
Single fracture in impermeable matrix	5%	5%
Fracture zone in sandstone matrix	10%	20%
Fracture zone in mudstone matrix	10%	20%
Fracture zone in quartzite	10%	10%
Fracture network	30%	20%
Double porosity aquifer	30%	30%

1) expressed as percentage of test length
2) expressed as percentage tracer mass loss

Mixing in the Abstraction Borehole

When the tracer plume reaches the abstraction borehole, the concentration decreases further. In the abstraction borehole the tracer plume is mixed with "fresh water" (not influenced by the tracer). The relation between the amount of traced water and total water entering the borehole determines the decrease in tracer concentration. For a radial flow field, as created during both a radial convergent test and an injection-withdrawal test, this relation depends on the distance injection to abstraction borehole (or distance tracer plume to abstraction borehole in the case of the single-well Injection-Withdrawal test) and the occurrence and yield of fracture zones in the abstraction borehole.

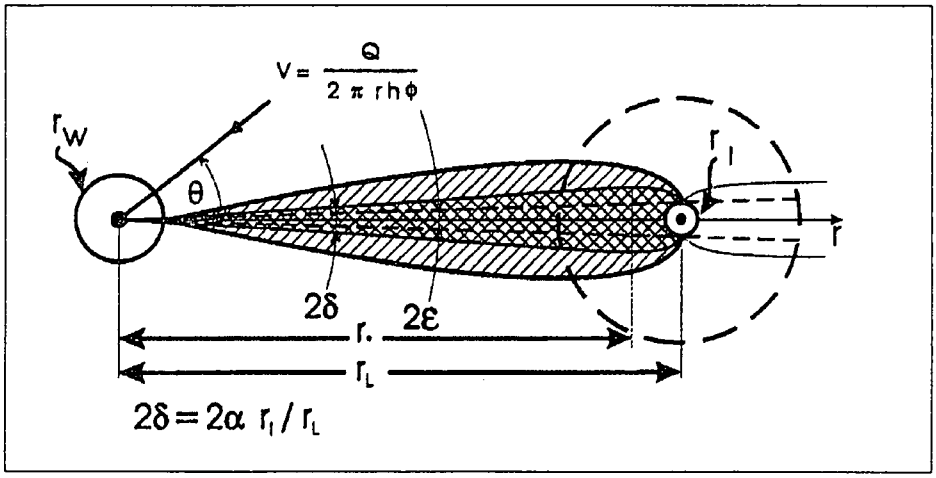

Figure 5-1 Tracer Movement in radial flow field (Zlotnik & Logan)

The above-mentioned procedures are described as a simulation of the test. However, in the program TRACER-PLAN the forward simulation and the inverse calculation are implemented. If the optimal amount of tracer cannot be calculated a priori due to lack of information, a small amount should be chosen for a short test. This ensures that the dilution in the injection borehole is reached in short time, so that the test can be repeated shortly, if necessary.

(c) Combination of Tracers

To optimise the procedure for conducting and analysing tracer tests it is mostly suitable to use a combination of tracers. Depending on the purpose of the test the combination can vary:

- Tracers with different detection limits can be combined to simplify the measurement, e.g. salt for the dilution part and Fluorescein for the observation in the abstracted water. Both tracers have to be injected simultaneously in the source borehole.
- Tracers with different molecular diffusion coefficients can be combined to analyse the influence of matrix diffusion and retardation, e.g. Bromide and Fluorescein.

5.2.1.3. Flow Rate

The flow rate of the pump has a significant influence on test data and results and must be determined a priori. During the test the flow rate cannot be changed. For instance, if the flow rate is too high, the tracer might reach the observation point too quickly to be detected properly.

Point Dilution Test

The flow rate of the pump in the injection borehole for the point-dilution test determines the time in which the volume of water in the tested section is circulated completely once. The circulating time should be minimised for accurate injection and measurements. On the other hand, to avoid turbulence in the borehole, the flow rate should be minimised. The circulating time t_c is computed as

$$t_c = V_c / Q_c \qquad \text{(Equation 5-3)}$$

with

V_c = Volume of water in tested section

Q_c = Flow rate of circulating pump

Decreasing the flow rate will increase the circulating time. From practical experience the following conditions are suggested:

$$t_c << 5 \text{ min} \qquad \text{(Equation 5-4)}$$

$$0.2 \text{ L/s} < Q_c < 3 \text{ L/s} \qquad \text{(Equation 5-5)}$$

Using the above-mentioned conditions and the equations for the circulating time and the circulating volume, the program TRACER-PLAN optimises the flow rate, based on the set-up of the test.

Injection Withdrawal Test

The correct choice of the flow rate for the withdrawal part of the Injection-Withdrawal test is crucial and essential for the tracer test data and analysing results. The chosen flow rate depends mainly on the flow velocity, which should be estimated from the Point-Dilution test. In general it can be concluded that when the flow velocity is higher the flow rate should be higher as well. If the flow rate is too high, the tracer breakthrough is too quick and might be covered by other factors as a still high concentration in the tested section. A too low flow rate will result in a long time for the tracer recovery (i.e. the approach of Leap and Kaplan (1988) is not valid) or even no tracer recovery, when the plume is already moved out of the radius influence (i.e. the hydraulic gradient cannot be turned back).

The optimal flow rate for the withdrawal part is calculated in the software program TRACER-PLAN based on the available information about the groundwater regime. Before starting the withdrawal part, the Point-Dilution test as first part of the Injection-Withdrawal test should be analysed in the field to give a first estimate of the Darcy velocity, which should be used to optimise the estimation of the flow rate as implemented in the software program.

Radial Convergent Test

The optimal flow rate of a Radial Convergent test should be chosen in a way to ensure a sufficient drawdown in the abstraction borehole and the establishment of a radial flow field. The established flow field must force the tracer, injected in the source borehole, to move towards the abstraction borehole in a sufficient time. On the other hand if the flow rate is too high, it takes a long time to establish the radial flow field and probably the drawdown in the abstraction boreholes reaches discrete fractures or the pump inlet.

Based on the geological structure, the groundwater regime and known or assumed values for the hydraulic properties the software program TRACER-PLAN gives a suggestion for the optimal flow rate.

5.2.1.4. Duration of Test

The optimal duration of the test depends on the kind and the purpose of the test. Due to the impact of many parameters on the duration, it is difficult to predict the time a priori. For the different tests the following rules are recommended:

- The Point-Dilution test should be carried out until the dilution in the source borehole is complete and the background concentration of the tracer is reached. Minimum time of measurements should be 1 hour.
- When using the PDT as source for a Radial Convergent test, the circulating in the injection borehole should continue until the Radial Convergent test is completed.
- The withdrawal part of an Injection-Withdrawal test should start only after a minimum of 50% of dilution is reached. If the dilution is sufficient, it is better to wait with the pumpback until dilution is complete.
- The duration of the withdrawal part should last at least until the tracer is abstracted (i.e. breakthrough curve is observed) and the background concentration is reached.
- The injection of the tracer for a Radial Convergent test should start only, when a steady state flow field is established, which is indicated either by a constant hydraulic gradient between the injection and abstraction borehole or by a constant drawdown in both the abstraction and observation borehole.
- The duration of the Radial Convergent test depends on the occurrence of the breakthrough curve and should last at least until the background concentration of the tracer is reached.

The approximated duration of the tests is calculated with the software program TRACER-PLAN, based on assumed or known values for the hydraulic properties of the tested aquifer system and by means of forward simulation.

5.2.2. Conducting Tracer Tests in the Field

After completing the planning phase the tracer test can be conducted, which is divided into three parts:

- Installing the equipment
- Conducting the tracer test
- Data measurement and interpretation

All three parts have to be carried out accurately as this can have a significant influence on data quality and results.

5.2.2.1. Installing the Equipment

The equipment required for a tracer test goes beyond that for a hydraulic test. Depending on the depth of the injection section in the boreholes and the chosen flow rate for the test the required equipment can be small submersible pumps (see Figure 5-2a) or complete pump rigs with high-yielding mono pumps (see Figure 5-2b)

Figure 5-2 Equipment installing at injection and abstraction borehole; a) submersible pumps with a flow rate of 0.3 to 1 L/s, b) mono pump rigs, discharging up to 20 L/s

Injection Borehole

The equipment installed in the injection borehole must fulfil several tasks:

- Mixing and circulating the water in the tested section sufficiently
- Injecting the tracer into the depth of the tested section
- Allowing for continuous measurements of tracer concentration in tested section

In the literature, double packer systems are mostly suggested (e.g. Novakowski *et.al.*, 1995), where a mixer and the measurement tool is installed in the chamber between the packers. Van Wyk (1998) used this type of injection device in a case study on the Campus Test Site (see section 6.1), but found it too susceptible and cost-intensive, so he did not recommend it for application in South Africa.

The recommended system creates the barrier function of packers with a hydraulic system of pumping and injecting the water at different depth. The water in the tested section is circulated with a submersible pump, installed at the bottom of the tested section, a rising pipe to the surface and an injection pipe with the outlet at the top of the tested section. Measurements of tracer concentration or other parameters, sampling and the injection of tracer occur directly in the circulating water. The principle is shown in Figure 5-3.

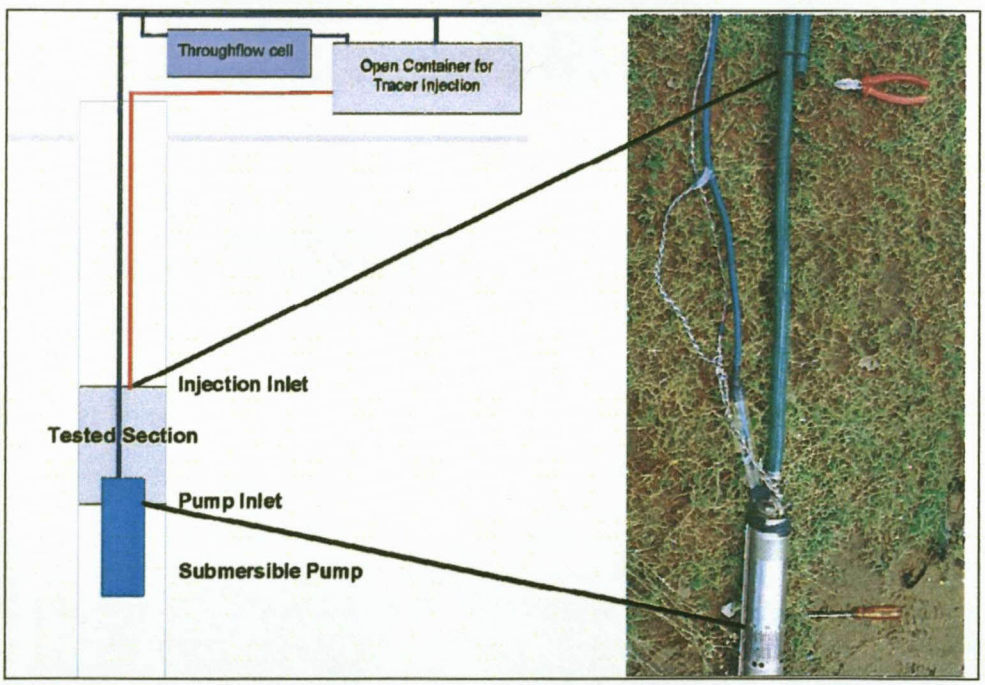

Figure 5-3 Required equipment and borehole installation for the injection borehole

As shown in the figure above, the tracer will be injected into the circulating water by means of an open container. This system accounts for an easy and sufficient way of injection as well as for the need to open the circulating system for pressure equalisation. A closed circulating system creates a vacuum or low pressure in the injection pipe due to the suction caused by the difference in hydraulic head.

Any open container with sufficient volume related to the flow rate can be used. A proposed design is explained in Figure 5-4

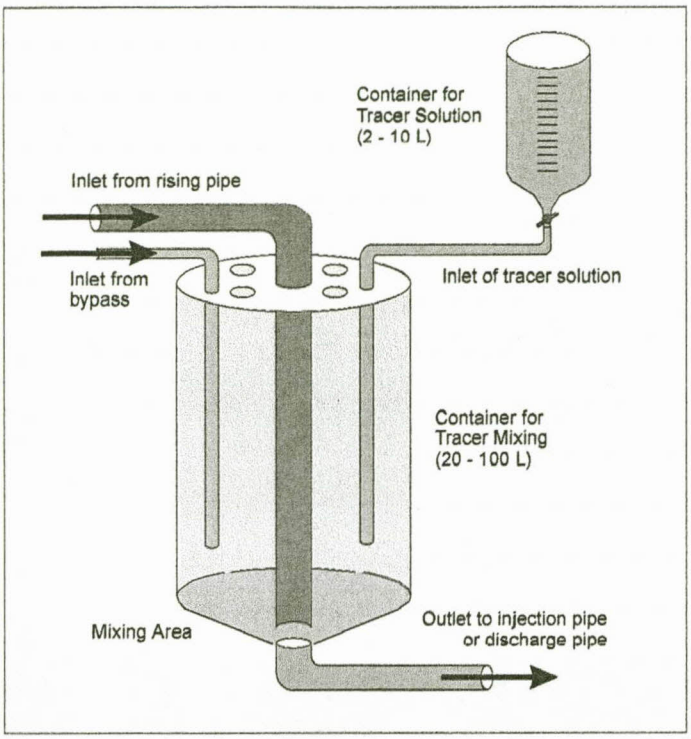

Figure 5-4 Proposed design of an open container for tracer injection

At the rising pipe, between the borehole head and open container, a tap with valve should be installed to allow for sampling or connecting a bypass in smaller diameter for field measurements. The bypass must be connected directly to the open container. Behind the outlet of the open container a Y-connection in the injection pipe is required with valves on both outlet ways to connect the injection pipe and a discharge pipe for the pumpback phase of the test.

Abstraction Borehole

If a single-well test is conducted, the equipment for the abstraction part of the test remains the same as for injection (see above).

For a radial convergent test the equipment in abstraction borehole is similar to the required equipment of a hydraulic test (see section 5.1.2), except the additional need for the measurement of tracer concentration in the abstracted water. Therefore a tap with valve is required at the rising pipe close to the borehole head. On the tap a bypass is fixed for installing the measurement tools like through-flow cell and / or fluorometer (see below). For the accurate measurement of the discharge rate the main discharge pipe and bypass should be connected before the measurement point for the discharge. A possible scheme is shown in Figure 5-5.

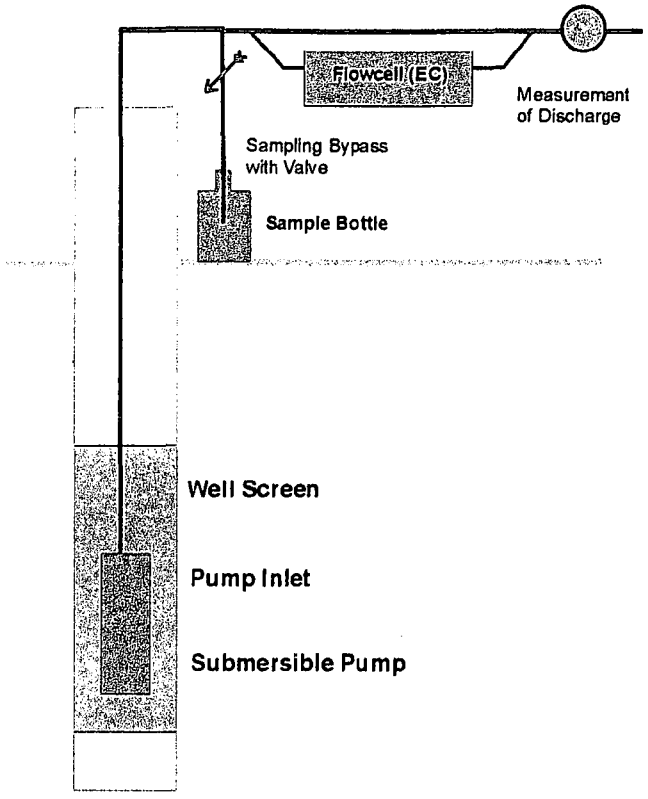

Figure 5-5 Equipment and borehole installation for abstraction borehole

Observation Borehole

When conducting a natural flow tracer test, special conditions are required for the measurement of the tracer concentration in the observation boreholes:

- No change of flow field due to abstracting water
- No mixing of tracer solute in the fracture system with borehole water

Several authors recommend the application of a straddle packer with a special sampling port. Besides the general consideration of packer systems, as discussed above, the sampling procedure is problematic due to loss of tracer in the system (see detailed discussion below). Therefore a direct measurement without sampling is suggested.

If mixing between the traced flowing water and the standing water in the borehole can be neglected, a measurement with downhole logging can be used. The measurement probe is placed at the position of the fracture, or if this is not known exactly, moved up and down slowly.

Because mixing effects cannot be neglected in general, a low-rate sampling pump should be installed, which circulates the water from the position of the fracture at a very low rate (similar to the groundwater flow rate) to the surface and back to the borehole. The system is similar to the one used at the injection borehole, except for the lower flow rate.

5.2.2.2. Conducting the Test

The proposed way to conduct the tracer test in the field is described for each test or part of test separately.

Point-Dilution Test

The Point-Dilution test, either carried out as a single-well test or as the source for a multiple-well test, starts with the injection of the tracer after the circulating system is established. Therefore the water levels in the injection borehole and, if applicable, in an observation borehole, should be monitored. The required equipment for the injection borehole is described above.

The tracer must be dissolved in a certain amount of water (2 to 20 L), which depends on the calculated circulation time. To avoid oscillation in the measured concentration the injection time, time to inject the tracer solute into the open container, should be at least twice the circulating time. When dealing with a big circulating volume the injection time can go up to 10 minutes, but should not exceed this time. From the beginning of injection measurements of tracer concentration in the circulating water should be taken to control and eventually revise the calculated circulating time. The measurements have to be continued in certain intervals as given in the field forms until the background concentration is reached again.

Before injecting the tracer the circulation of water must be established without any disturbance of the flow field. The open system, as proposed above, normally works due to the gravitational difference of water levels and due to the induced suction of water in the injection pipe. To create suction the system must be closed for a short time. When the suction in the injection pipe starts, the system must be opened to allow the water flowing freely through the injection pipe. If the system remains closed, a low pressure or vacuum will be created in the pipes, which decreases the flow rate and can cause damage.

Injection-Withdrawal Test

The Injection-Withdrawal test starts as a Point-Dilution test in the way described above. When the tracer concentration in the circulating water reaches a certain value, which should be less than 50% of the starting concentration and defined beforehand, the withdrawal phase of the test starts. The valves at the Y-connection behind the open container are used to close the injection and open the discharge pipe.

If the proposed discharge rates for the circulation and abstraction are not equal, the discharge rate for the withdrawal part must be adjusted either by changing the discharge of the pump, if applicable, or by adjusting a valve at the rising pipe. In cases where the proposed discharge rate for the withdrawal part is less than the one for circulation, the valves at the Y-connection can be used to adjust the discharge rate. Then a part of the abstracted water is circulated while another part is discharged.

Especially in cases of low flow velocity in the tested section this procedure is recommended to avoid both a too quick recovery of the tracer and a too quick dilution due to emptying the tested section, which will cover the tracer recovery (see Figure 5-6).

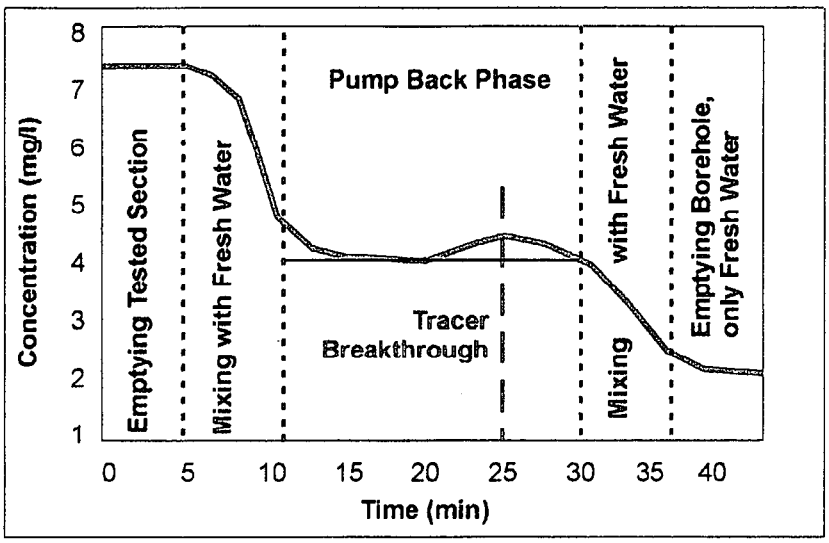

Figure 5-6 Different steps during the withdrawal part of the Injection-Withdrawal tracer test (values for concentration and time are examples)

From the beginning of the withdrawal part, measurements of the tracer concentration in the abstracted water should be taken until the breakthrough curve is observed and the background value of the tracer is reached.

Radial Convergent Test

The first step of a radial convergent tracer test is creating the radial flow field. Water is abstracted from the abstraction borehole with a specific constant discharge rate. Water level measurements in both the abstraction and observation borehole should be taken to control the developing of the flow field. After a steady state situation is established, the tracer test can start with the injection of the tracer in an injection borehole, situated in the vicinity of the abstraction borehole. The procedure of injection is equal to the point-dilution test and described above.

From the beginning of injection, measurements of tracer concentration in the abstracted water should be taken until the breakthrough curve is observed and the background value of the tracer is reached again.

5.2.2.3. Measurement Tools

The tools used for tracer concentration measurement depend on the tracer and its chemical and physical properties (see Table 5-3). However, the place of measurement and the kind of maintenance are important factors for the quality and accuracy of the data.

Table 5-3 Measurement tools for proposed tracer substances

Tracer	Measurement tool
NaCl Salt	EC-Meter
NaBr	EC-Meter and or Ion sensitive Sensor
Fluorescein	Fluorometer

(a) Through-Flow Cell

The measurement tool should be installed in a closed through-flow cell (see Figure 5-7), which is situated at a bypass on the main pipe. The closed through-flow cell is important to avoid chemical or physical changes in the measured tracer concentration due to contact between the groundwater and atmosphere.

Figure 5-7 Through-flow cell for measurement tracer concentration and physico-chemical properties of the water using electrodes (e.g. EC, pH, Ion sensitive Sensor)

The correct location of the flow cell related to the part of test must be considered and prefixed:

- For the measurement during the injection and dilution part the flow cell should be installed at a bypass on the rising discharge pipe before entering the container for tracer injection.
- For measurement during the withdrawal part, the flow cell should remain at the same place on the rising discharge pipe.
- For the measurement in the abstracted water during a radial convergent test the flow cell should be installed at a bypass on the rising discharge pipe, close to the abstraction borehole.

(b) Calibration

Each measurement tool must be calibrated according to the conditions of the tool before using in the field. When a direct calibration of the tool is not possible (e.g. most EC-meters), the measured concentrations must be recalculated from calibration graphs and functions produced in the laboratory. The influence of recalculating can be significant, as demonstrated in Figure 5-8, where the estimated Darcy velocity is about three times higher with the calibrated data than with the field data.

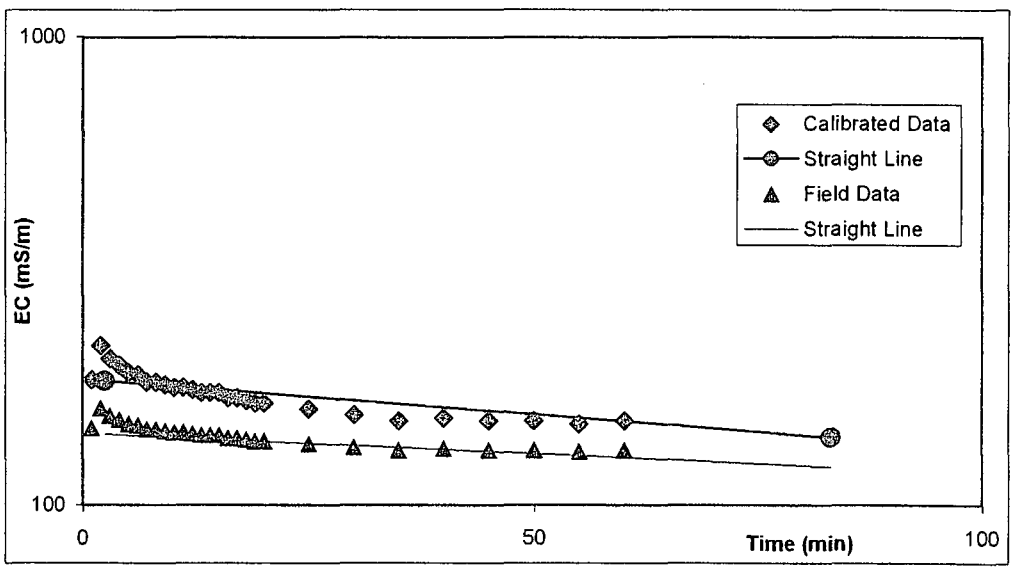

Figure 5-8 Influence of calibration and recalculating on Darcy velocity, obtained from a Point-Dilution test; a) field data, b) calibrated and recalculated data

The calibration and recalculation procedure for EC-meter readings is implemented in the software programme TRACER.

5.2.3. Data Measurement and Interpretation

During the test measurements of the tracer concentration at specified places and the discharge rate must be taken at fixed time intervals, which are prescribed by the geohydrologist in the planning phase and discussed in detail below. Every measurement and observation on site should be recorded on the tracer test form (see Appendix). Especially changes in the condition of the test, like change of discharge rate, heavy rainfall or interruptions of the test due to technical problems, must be recorded to ensure that the geohydrologist can analyse this test correctly.

(a) Direct Measurement

The best choice of measurement is the measurement in the field using a closed through-flow cell at a bypass, as proposed above. The following time intervals and levels of accuracy are given as recommendation:

- The measurement of the discharge rate must have an accuracy of at least 0.1 L/s or 5% of the proposed discharge rate.
- The measurement of the tracer concentration using an EC-meter must have an accuracy of at least 5% of the maximum value.
- The measurement of tracer concentration using Ion sensitive Sensor or Fluorometer must have an accuracy of at least 1ppm, or better 1ppb, if possible.
- It is strongly recommended to make use of electronic device, such as data logger.
- The time intervals of measurement in the beginning of the test should be small, at least less than 1 minute (recommended 10 seconds) in the injection borehole. The time interval can be changed exponentially during the test, but not more than 10 minutes. The suggested time intervals are given in the tracer test forms (see Appendix B).

(b) Sampling

If a direct measurement in the field is not possible, for whatever reason, samples of the water must be taken at a bypass of the rising discharge pipe and analysed in a laboratory. If this procedure is applied during a Point-Dilution test, the exact sample volume and the concentration in each sample must be recorded for the following recalculating procedure.

Each time a sample is taken out of the circulating water, a certain amount of tracer is removed artificially and not due to tracer dilution. Not considering this effect in the analysing process results in an overestimation of the Darcy velocity, as demonstrated by means of an example in Figure 5-9. At each measurement time a sample of 200ml was taken from the circulating water. Using field data yielded a Darcy velocity of 0.35 m/day. After recalculating, the correct Darcy velocity was 0.02 m/day.

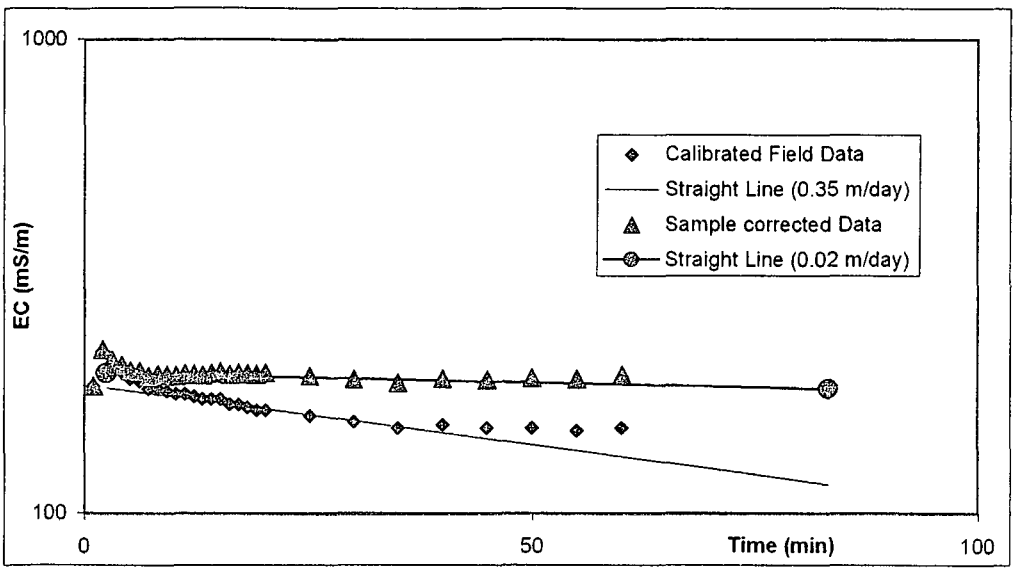

Figure 5-9 Influence of sampling on Darcy velocity, obtained from Point-Dilution test

The removed amount of tracer is calculated as

$$M_r = C_s * V_s \qquad \text{(Equation 5-6)}$$

with

C_s = Concentration of tracer in the sample
V_s = Volume of the sample

Adding this amount of tracer to the measured concentration results in the recalculated concentration, which is then given by

$$C_{c,i} = \frac{\left(C_{s,i} V_w + \sum_{0}^{i-1} M_{r,i-1} \right)}{\left(V_w + V_{s,i-1} \right)} \qquad \text{(Equation 5-7)}$$

with

C_c = recalculated concentration
C_s = measured concentration
V_w = volume of circulating water
M_r = removed amount of tracer
i = index for number of measurements

Since the volume of sample is small compared to the volume of circulating water and can be assumed as constant for all measurements, the term $[V_w+V_{s,i-1}]$ reduces to $[V_w]$, which is a constant over the period of the test.

Although sampling during a Point-Dilution test should be avoided due to the loss of accuracy, the recalculating procedure is implemented in the software programme TRACER as a matter of quality assurance.

5.3. Combination of Hydraulic and Tracer Test

Since both hydraulic and common tracer tests require abstracting groundwater, it seems practical to conduct both kinds of test in one step. Depending on the tracer test which should be carried out there are two possibilities for combining the tests:

- For a radial convergent tracer test the abstraction to create the specific flow field can be used as a hydraulic test.
- If conducting a single-well tracer test, the pumpback phase in the withdrawal part can be extended to collect data for a hydraulic test.

5.3.1. Radial Convergent Tracer Test – Hydraulic Test

When two boreholes close to each other are available for abstracting water and injecting a tracer solution, a combination of a Radial Convergent tracer test and a Constant Discharge hydraulic test should be carried out.

- The hydraulic test starts with abstracting water at a constant discharge rate from the abstraction borehole. Water level measurements must be taken at specific time intervals, as prescribed above, in both the abstraction and the observation borehole, which becomes the source borehole for the tracer injection.
- When a radial flow field is established and a steady state situation is reached, the tracer test starts with injecting the tracer into the source borehole. Tracer concentration measurements have to be carried out in the injection borehole to measure the dilution and in the abstraction borehole to measure the tracer breakthrough curve.
- During the tracer test part of the combined test, water level measurements in both boreholes should be continued.

5.3.2. Single-Well Tracer Test – Hydraulic Test

If only one borehole is available, a combination of a single-well Injection-Withdrawal tracer test and a short-term Constant Discharge hydraulic test should be carried out.

- In this case the combined test starts with the tracer test. When a sufficient circulation in the injection borehole is established, the tracer can be introduced into the circulating water. Measuring the tracer concentration in the circulating water will estimate the dilution of the tracer. During this phase water level measurements should be taken several times.
- When the dilution is sufficient, the withdrawal phase can start. At the moment all or a part of the circulating water is abstracted (i.e. not re-injected into the borehole) the tracer concentration in the abstracted water and the water level in the borehole must be recorded.
- Even when the withdrawal part of the tracer test is completed, abstraction and measurement of the water level should be continued to gather enough data for analysing the hydraulic test. A minimum of 2 hours' abstracting is suggested.

5.4. Developed Software for Tracer Test Analysis

During this research two software programmes were developed for conducting and analysing tracer tests in fractured aquifers. Both are prepared as easy to handle spreadsheets in MS EXCEL, written in Visual Basic. While the programme TRACER-PLAN can be seen as an expert system supporting the user in planning the tracer test, the programme TRACER consists of several tools for analysing the tracer test, applying either the standard methods or the approach of non-integer flow dimension.

5.4.1. TRACER-PLAN

As discussed above the planning of a tracer test is the most important and most difficult part of conducting a tracer test. The programme TRACER-PLAN consists of different tools to support the user in choosing the correct equipment and planning the best way of conducting the test. The different parts and spreadsheets of the programme are briefly described below.

(a) Basic Information

The basic information, needed for the program to calculate and recommend the parameters for the test set-up, have to be inserted in this screen. The following information is required, either as known or assumed values:

- Purpose of testing (i.e. which parameters are to be estimated)
- Geological structure
- Depth of fracture zone, or zone of interest
- Thickness of fracture zone
- Hydraulic parameters of formation and / or fracture
- Available boreholes on test site, including distance from each other

The suggestions based on this information are given at the bottom of the screen and transferred to the following screens, 'Test Set-Up' and 'Simulation'.

(b) Test Set-Up

Based on the information on the first screen, the test set-up and the necessary equipment are suggested. However, the suggestions can be changed and adapted to the situation on the test site. After fixing the equipment, the program calculates and / or recommends the following parameters for conducting the test:

- Flow rate for circulating
- Circulating time
- Injection time for injecting tracer into the borehole
- Kind of tracer
- Amount of tracer
- Flow rate for abstraction, if applicable

The two latter parameters are calculated from both the test set-up and the forward simulation, as described in the next section.

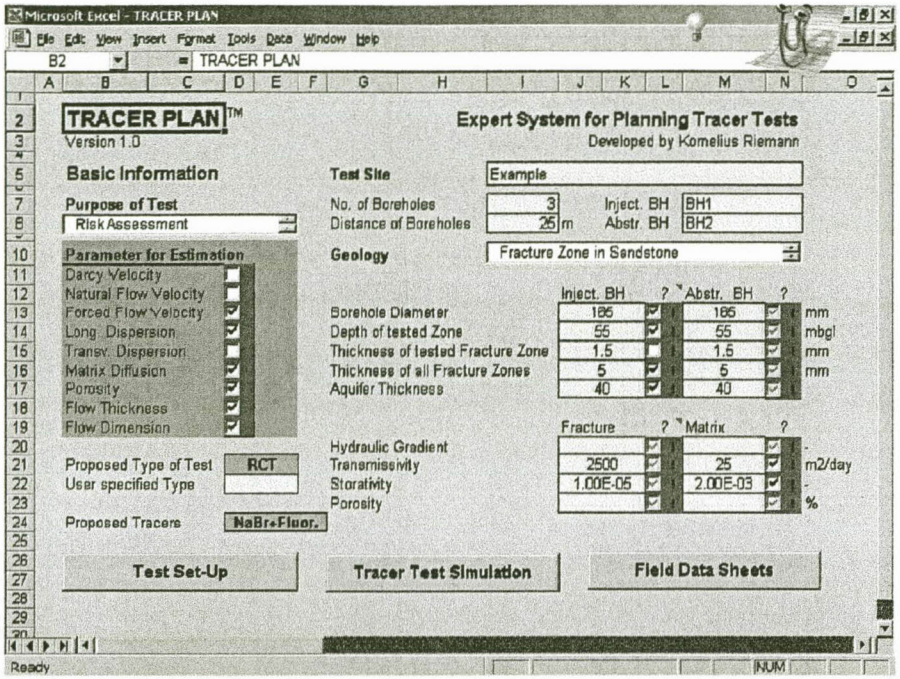

Figure 5-10 Input Screen 'Basic Information' of software TRACER-PLAN

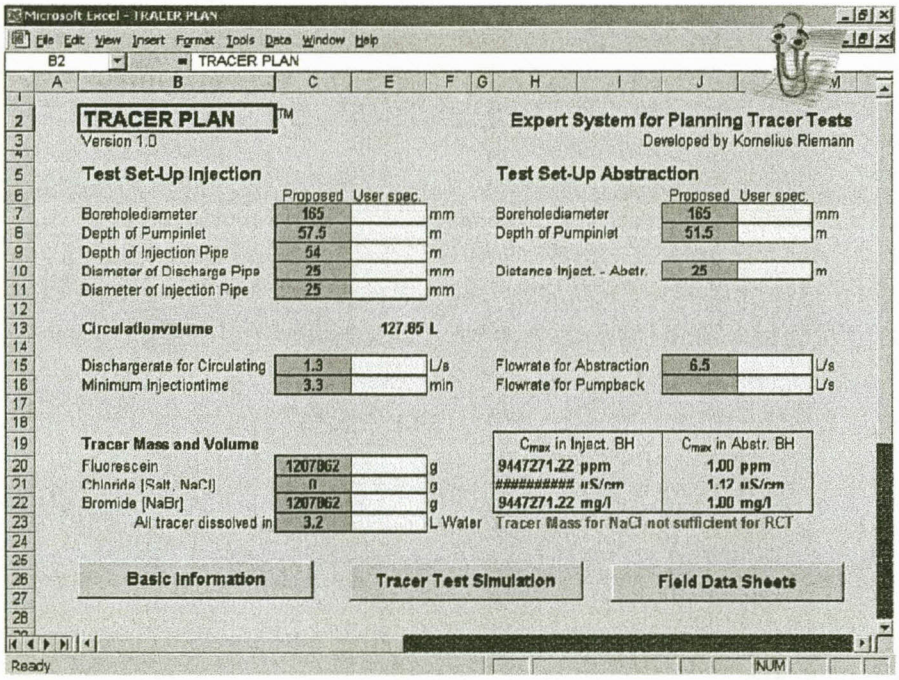

Figure 5-11 Input and output screen 'Test Set-Up' of software TRACER-PLAN

(c) Simulation

Using the available data about the flow system and the test set-up a forward simulation of the tracer test is produced before conducting the test to estimate the parameters, needed for conducting the test. The result of the simulation will feed back automatically to the above-mentioned parameters and gives new recommendations for their range of suitable values. For example, if the simulation shows that the amount of tracer is too small to be detected in the abstracted water, a backward calculation yields a recommended value for the amount of tracer for injection.

During the test the simulation can be used to optimise the test set-up and the initial parameters. For instance after the dilution part is completed a rapid analysing of the test data will yield a first approximation of the Darcy velocity, which will result in a better simulation of the withdrawal part, if inserted in the program as a known value.

The simulation accounts for the uncertainty of the input data by means of applying the upper or lower value of the possible range. If a parameter value is known a priori, the uncertainty is set as small, while assumed parameter values will get an uncertainty range of up to one order of magnitude (lognormal distribution) or 50% (normal distribution).

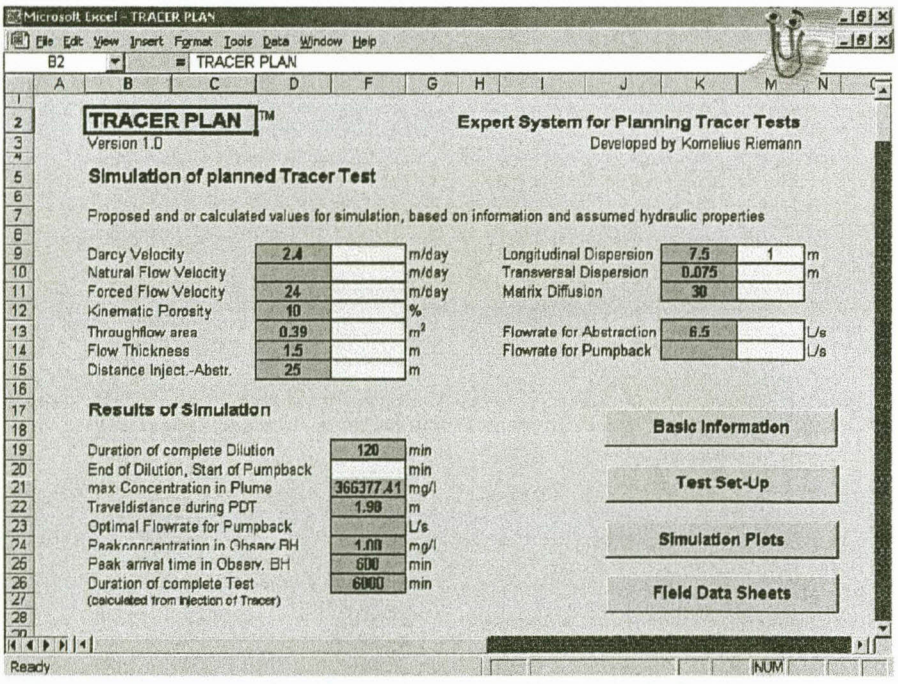

Figure 5-12 Output screen 'Simulation' of software TRACER-PLAN

(d) Forms for Field Measurements

Forms for the field measurements are implemented in the program in such a way that the suggestions or the user-specified values for the test set-up are printed onto the forms. Furthermore time intervals for measurements and assumed duration of the test are shown on the forms. A general example is given in Appendix B.

5.4.2. TRACER

In Chapter 4.1 and 4.2 different methods for estimating hydraulic and transport parameters are discussed and an approach of non-integer flow dimension is proposed to analyse hydraulic and tracer test data. Since the method of non-integer flow dimension, applied to tracer test data, is a new development, no existing software programme can handle this approach. Therefore the programme TRACER was developed, mainly to account for the non-integer flow dimension when analysing tracer tests. The different parts and spreadsheets of the programme are briefly described below.

In general the structure is equal in all parts of the program and further information is given in comments related to the input cells.

- Input cells are marked yellow
- Linked cells are marked light blue (i.e. information required on other screen)
- Calculated cells are marked grey (i.e. never overwrite!)
- Results are marked in different colours

(a) Main

The main screen (see Figure 5-13) serves as an entering platform for the program. All relevant parts of the program can be opened from this screen. Furthermore the basic information about the conducted test or tests is required in this screen. The three options are:

- Forced Gradient test between 2 boreholes (RCT)
- Natural Gradient with Dilution and Withdrawal
- Natural Gradient just Dilution

Additional information is required, whether pumping test data from the same boreholes are available, which method for estimating the parameter flow dimension and porosity should be applied and about the names of abstraction, injection and observation boreholes, because this information will be used in the following parts of the program.

(b) Hydraulic Test Data

The part of the program for the hydraulic test data is taken from the FC-program (van Tonder *et al.*, 2001) and can be divided in the input of the field data, the diagnostic and the analysis. Because the focus of the program is analysing tracer tests, the analysing procedure of the hydraulic test data is reduced to the necessary part of estimating the flow dimension and flow domain, applying the methods of Barker (1988) and Roberts and Beauheim (2001).

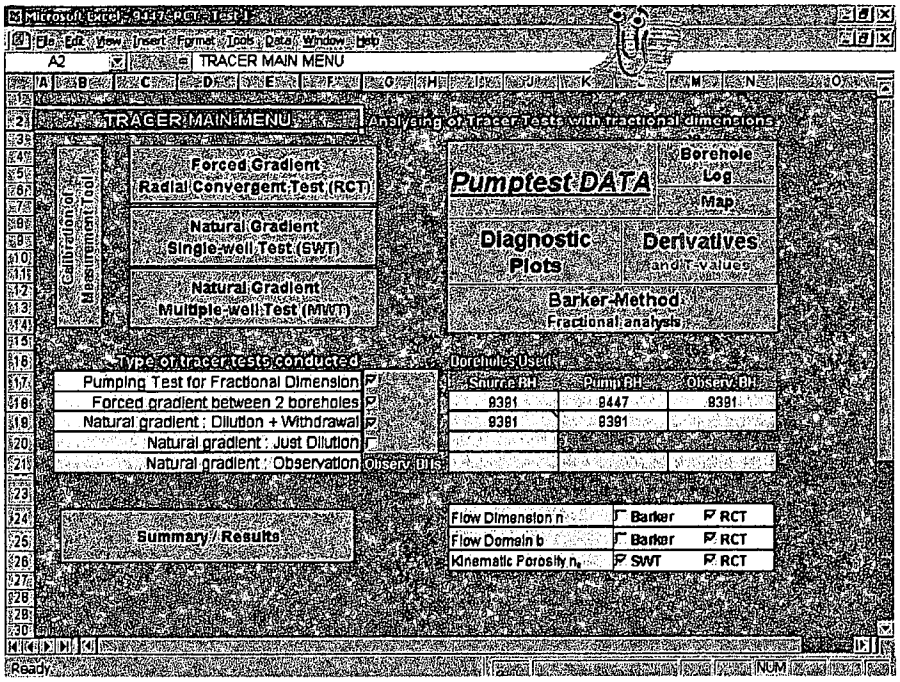

Figure 5-13 Input screen 'Main' of software TRACER

Field Data (Pumptest Data, Borehole Logs, Map)

The required data from the hydraulic test are the discharge rate Q in L/s, the time, elapsed since starting abstraction in minutes, the static water level and the measured water level in meter below ground level [mbgl] during the drawdown and recovery phase. The data sets for both the abstraction and observation borehole should be completed on this sheet.

For a preliminary estimation of the transmissivity and storativity the effective borehole radius of the abstraction borehole is required. The geographic data of the boreholes, such as x- and y-values and elevation are required in the screen 'map', where additionally there is the possibility to insert a bitmap with the borehole locations. The borehole logs can be inserted onto the screen 'Borehole Log' for the convenience of the user.

Diagnostic Plots

Several diagnostic plots, as discussed in section 4.1.2.1, are provided to enable the user distinguishing the different flow phases occurring during the test.

Derivatives and T-Values

The diagnostic tool of derivatives is separated due to their importance. The preliminary estimation of the transmissivity, based on the order of the first derivative, is included. Unlike the FC-program the tools are provided for both the abstraction and observation borehole.

Barker – Method, Fractional Analysis

The estimation of the flow dimension and flow domain, as obtained from hydraulic test data, is the crucial part of the analysing procedure. A non-linear least square method is implemented, which can be used manually or automatically, using the EXCEL-tool Solver. Due to the non-uniqueness of the method, additional information can be used as upper or lower bounds for the range of a single parameter. On the graph the field data and the simulated drawdown curve, applying the chosen parameter values, are plotted together for comparison.

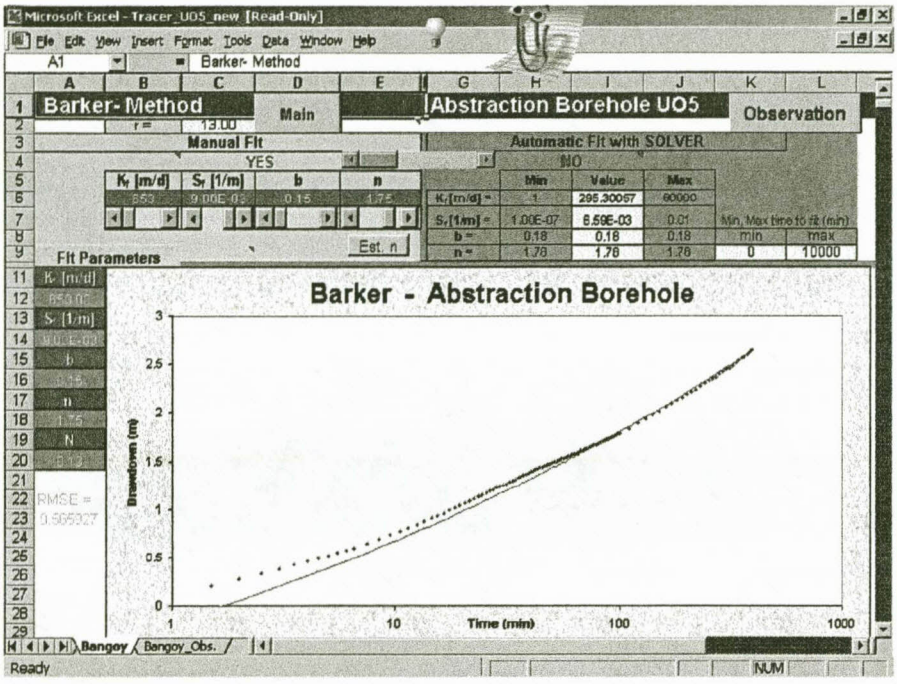

Figure 5-14 Input and output screen 'Barker' of software TRACER

(c) Tracer Test Data

The tracer test data and analysing procedures are separated for each type of test. In the first step virtual calibration of the measurement tool is required, if the used tool cannot be calibrated in the field.

Calibration of Measurement Tool

The calibration screen provides the input of calibration data from laboratory comparison. Therefore the used measurement tool should be measured against fixed concentrations of different solutes at different scales, and the readings should be entered into the table. The result of the comparison is shown on the plot 'measured values vs. fixed values'.

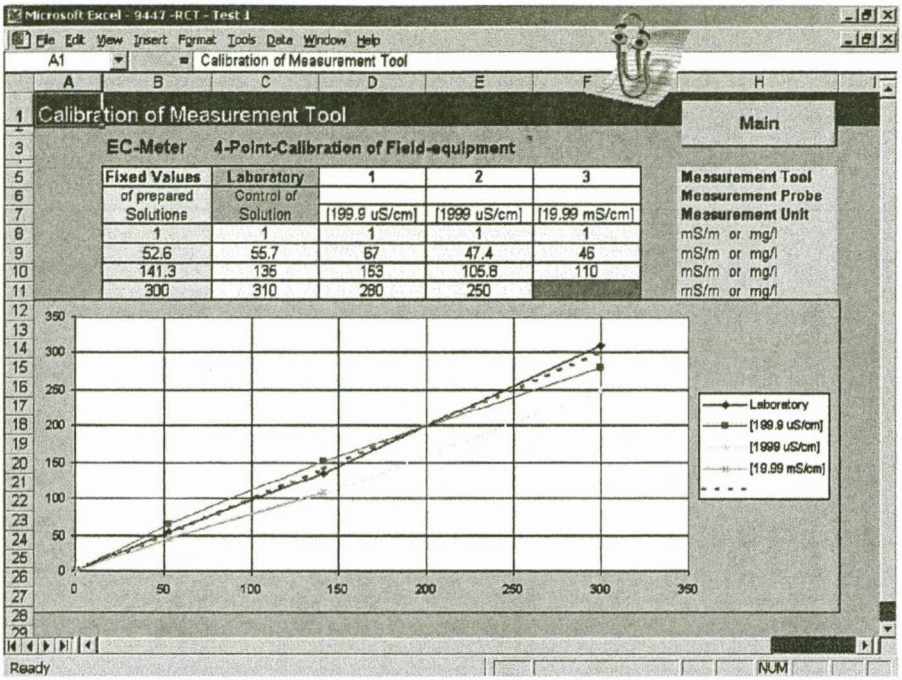

Figure 5-15 Inputscreen 'Calibration' of software TRACER

Forced Gradient, Radial Convergent Test (RCT)

The tracer test data and analysing procedure for a radial convergent test is divided into two parts, namely the injection (i.e. Point-Dilution test), and the abstraction (i.e. Radial Convergent test).

For analysing the injection part as a Point-Dilution test the field data and the test set-up are required. In detail:

- Radius of borehole,
- Interval length (i.e. distance from pump inlet to injection pipe outlet)
- Distortion factor (equal to 2 in open boreholes)
- Measurement unit (choose from selection)
- Measurement tool (choose from selection)
- Background value
- Time elapsed since start of injection
- Concentration in circulating water at time t

Depending on the chosen approach for the analysing procedure (see 'Main' screen), the flow dimension, the flow thickness or the fracture aperture and the kinematic porosity will be calculated. However, the calculated values can be changed manually for comparison purposes.

The field data are plotted in a semilog plot (concentration vs. time) and should show a straight line. Fitting the straight line will yield the Darcy velocity. The value for the forced flow velocity depends on the kinematic porosity and should be equal to the estimation from the radial convergent test.

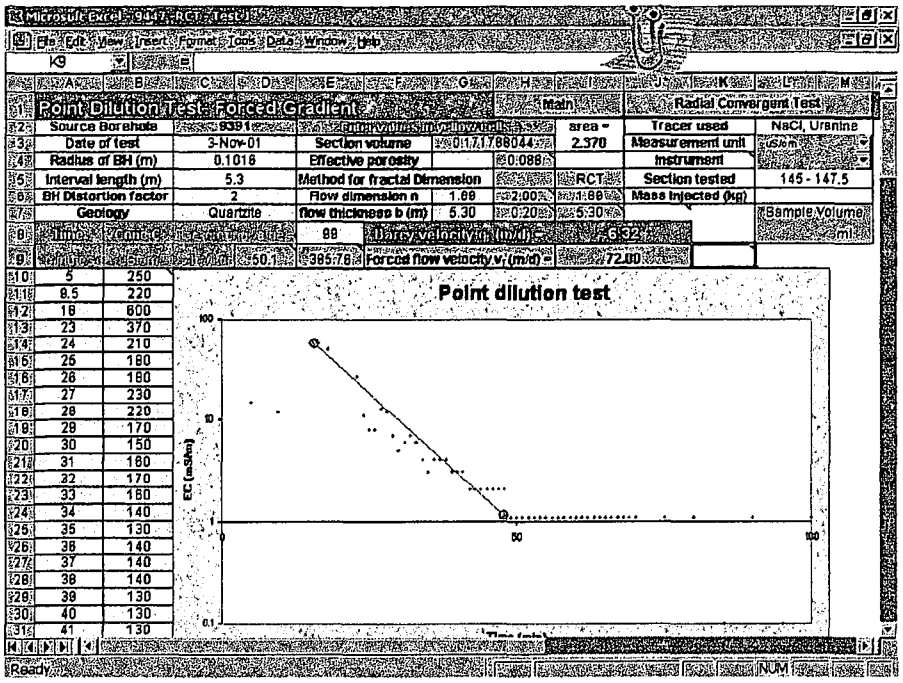

Figure 5-16 Input and output screen 'Point Dilution' of software TRACER

The analysing procedure for the breakthrough curve in the abstraction borehole requires additional data about the established flow field:

- Abstraction rate (value is taken from 'Pumptest Data' sheet)
- Distance between injection and abstraction (value is taken from 'Map' sheet)
- Injected mass of tracer in kg
- Measurement units (chosen from selection)
- Time elapsed since injection of tracer in minutes
- Concentration of tracer in abstracted water at time t

On the graph the measured concentration is plotted against the elapsed time. Furthermore the relative mass recovery is calculated and plotted vs. time. Changing manually the values for the flow thickness, dispersion and velocity until the measured data and the simulated data show a good fit, will yield the estimation of the fitting parameters. The accuracy of the fit can be controlled by checking the calculated RMSE, which should be as small as possible.

With the combination of the Point-Dilution test and Radial Convergent test the kinematic porosity on the flow path and the flow dimension is calculated. These parameter values and the estimated flow thickness should be used when analysing the Point-Dilution test, as it is set as default in the program.

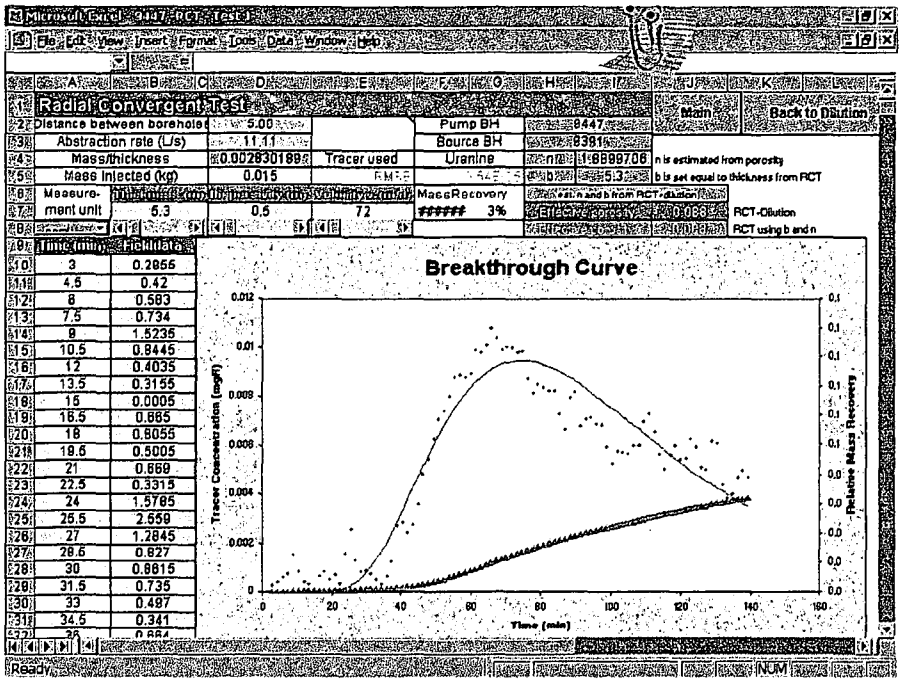

Figure 5-17 Input and output screen 'Radial Convergent' of software TRACER

Natural Gradient, Single-well Test (SWT)

The tracer test data and analysing procedure for a single-well test is divided into two parts, namely the injection (i.e. Point-Dilution test), and the abstraction (i.e. Injection-Withdrawal test). The injection part is equal to the injection part of a radial convergent test and described above.

For analysing the withdrawal part of a single-well tracer test the following information and data are required:

- Abstraction rate during withdrawal part
- Time of the drift phase (i.e. between injection and pumping)
- Time elapsed since start of pumping in minutes
- Concentration of tracer in abstracted water at time t

Depending on the chosen approach for the analysing procedure (see 'Main' screen), the flow dimension, the flow thickness and the kinematic porosity will be calculated. However, the calculated values can be changed manually for comparison purposes.

The measured concentration is plotted against the elapsed time and should show a breakthrough curve. Moving the purple dot to the centre of recovered mass, which is shown by the minimum value of 'delMass', yield the flow velocity. For comparison both the approach of Leap and Kaplan (1988) and the method of Borowczyk *et al.* (1966) are included.

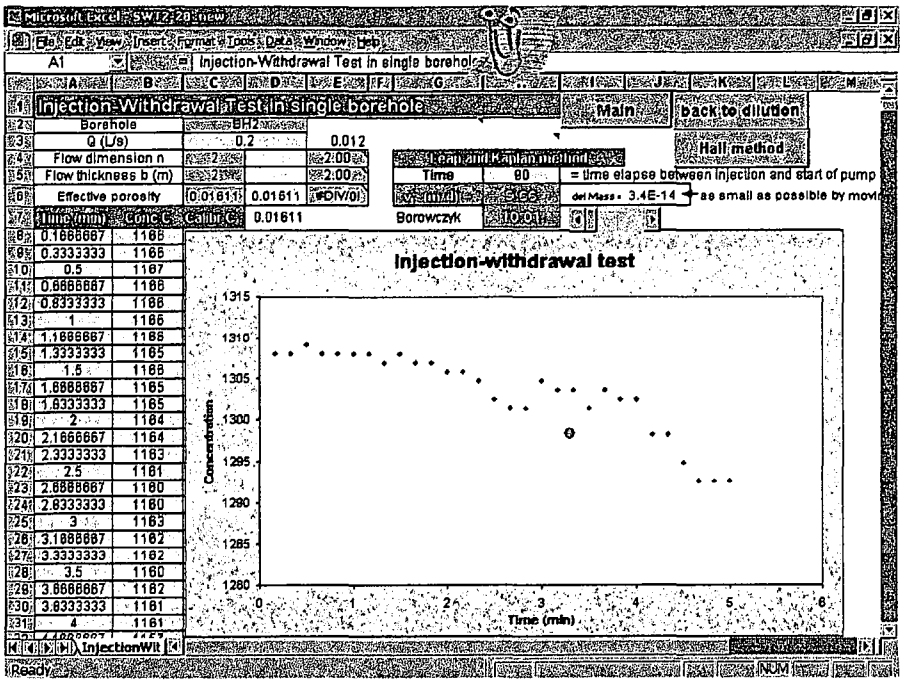

Figure 5-18 Input and output screen 'Injection Withdrawal' of software TRACER

Natural Gradient, Multiple-well Test (NFT)

The tracer test data and analysing procedure for a natural flow test is divided into two parts, namely injection (i.e. Point-Dilution test) and observation. The injection part is equal to the injection part of a radial convergent test as described above.

The analysing procedure for the breakthrough curves in the observation boreholes requires additional data:

- Approximated direction of flow in degree
- Relative position of observation boreholes (values are calculated from 'Map' sheet)
- Injected mass of tracer in kg
- Measurement units (chosen from selection)
- Time of injection (date and time)
- Time of measurements (date and time)
- Concentration of tracer in observation borehole at time t

The concentration in observation borehole 1, situated in the assumed flow direction, is plotted against time and compared with simulated curves, using one-dimensional and two-dimensional approaches. The concentrations in the other two boreholes are plotted against time and compared with simulated curves using a two-dimensional approach. Changing the values of the flow velocity, longitudinal dispersion, transversal dispersion and eventually flow direction manually until best fits of all breakthrough curves is reached, will yield estimations of the fitting parameters.

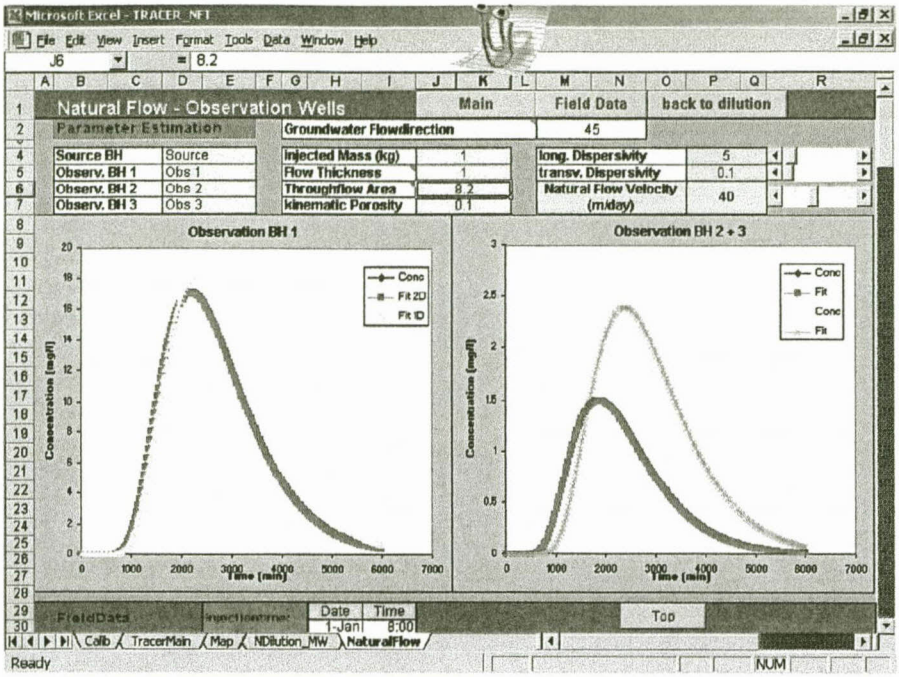

Figure 5-19 Input and output screen 'Natural Flow' of software TRACER

(d) Results

The results of all analysing procedures and tests are summarised in the 'Result' screen. Additionally the following parameters are calculated, which are not implemented explicitly in the analysing sheets:

- Transmissivity of the formation, using the FC approach (i.e. T_{late})
- Hydraulic gradient during hydraulic and / or radial convergent tests
- Natural hydraulic gradient

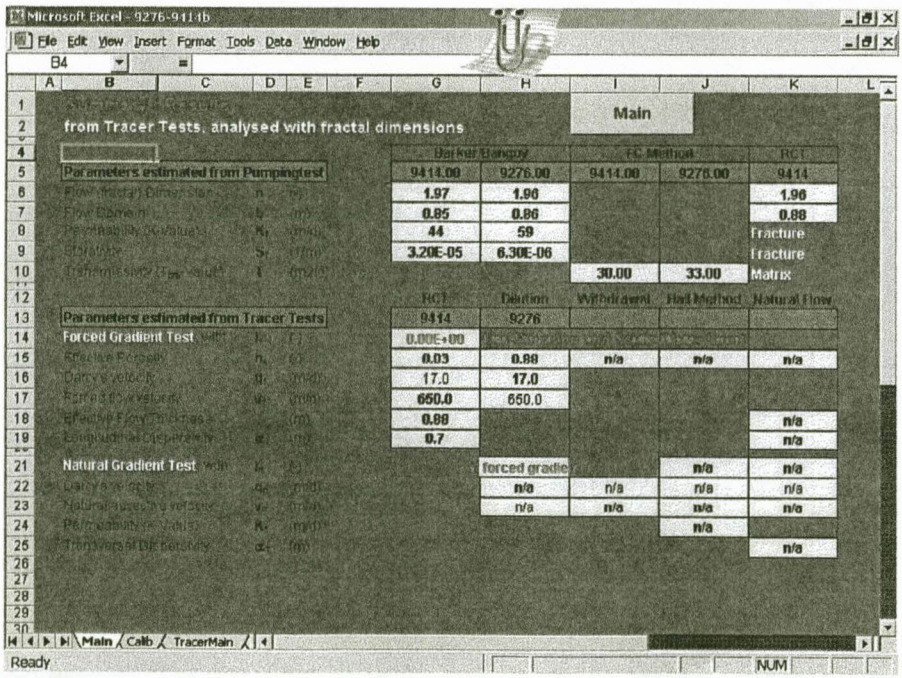

Figure 5-20 Output screen 'Results' of software TRACER

Chapter 6 Case Studies

To verify the different approaches proposed in Chapter 4 a number of field tests were conducted and analysed, applying different approaches. The following test sites are chosen to account for different geological set-ups and hydrogeological flow regimes:

Table 6-1 Test Sites for the case studies and their hydrogeological flow regime

Test Site Name and Location	Geological set-up and Hydrogeological flow regimes	Hydraulic Tests	Tracer Tests
Campus Test Site, Bloemfontein	Horizontal, bedding-plane fracture in sandstone aquifer, Karoo	X	X
Meadhurst Test Site, outside Bloemfontein	Vertical fracture system parallel to a dyke, in sand- and mudstone, Karoo	X	X
Farm Griesel, Free State	Horizontal fracture in weathered Dolerite, underlain by mudstone, Karoo		X
Tsabong, Botswana	Highly fractured Quartzite and Phyllite, Olifantshoek-sequence	X	X

6.1. Campus Test Site

The Campus Test Site is located on the campus of the University of the Free State in Bloemfontein.

6.1.1. Geology

6.1.1.1. General

The Campus Test Site was originally intended as a test site for postgraduate students and covers an area of approximately 180x192m. To date thirty percussion and seven core-boreholes were drilled (see Figure 6-1). Several projects sponsored by the Water Research Commission of South Africa also used this site for research on (a) Karoo Aquifers (Botha *et al.*, 1998), (b) tracer tests in fractured aquifers (Van Wyk *et al.*, 2000) and (c) parameter estimation with computer models (Chiang and Riemann, 2001). The Campus Test Site is underlain by a series of mudstones and sandstones from the Adelaide Subgroup of the Beaufort Group of formations in the Karoo Sequence. Mapping of geological outcrops around the Campus Site reveals the existence of extensional fractures (Mode I) and shearing fractures (Mode II). The dominant type of fractures recognised in the sediments includes sub-horizontal bedding-parallel fractures and orthogonal and diagonal fractures with dominant north-west, north-east and east-west trends.

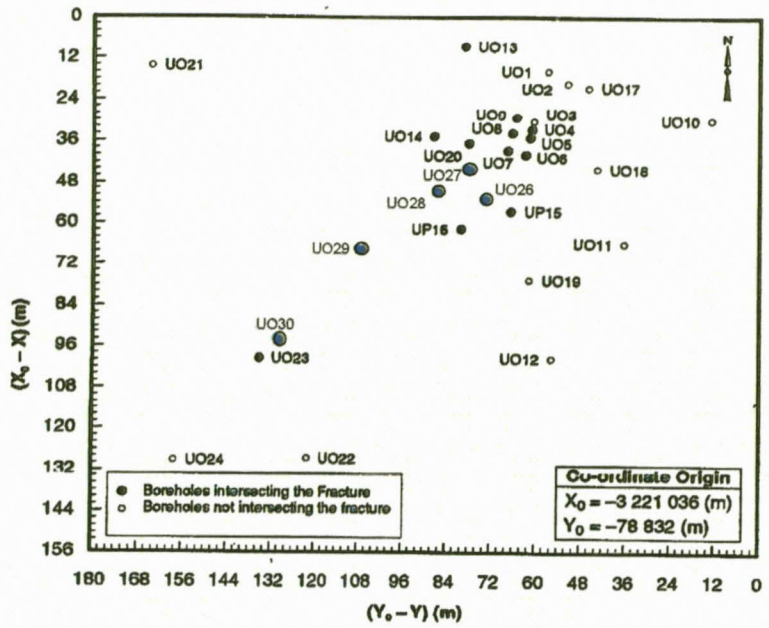

Figure 6-1 Locations of the boreholes at Campus Test Site

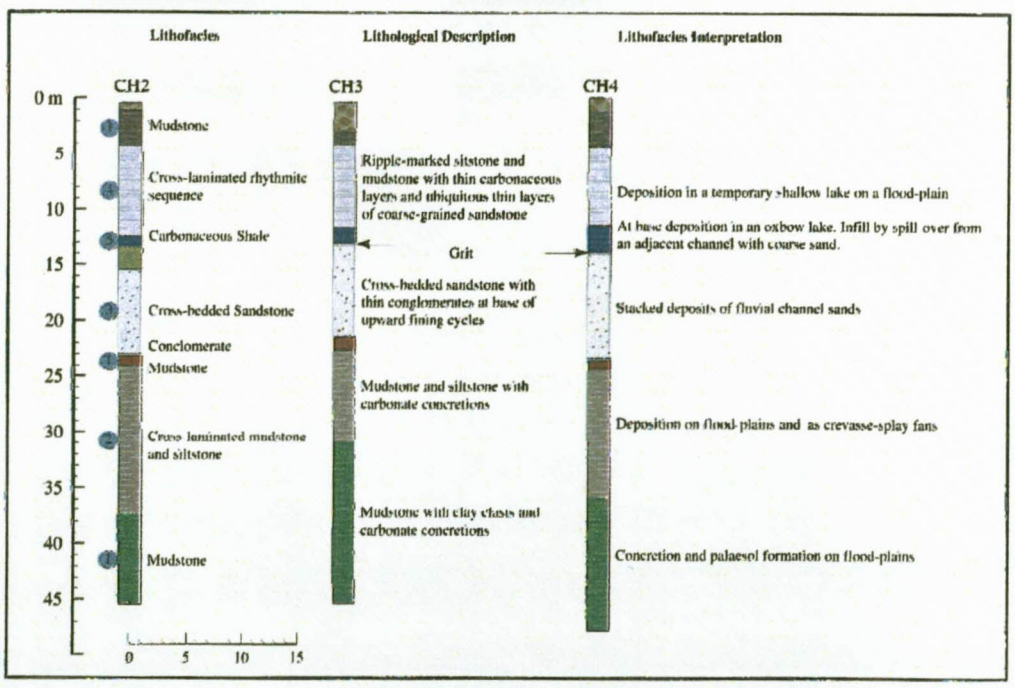

Figure 6-2 Lithology of boreholes on the Campus Test Site (after Botha *et al.*, 1998)

Five of the seven core-boreholes were drilled vertically and two at an angle of 45 degrees. The two north-easterly fractures detected in core-boreholes CH6 and CH7 are the only subvertical structures intersected during the core drilling and both were calcified. The geological column of the Campus Site (see Figure 6-2) can be subdivided into five different easily recognisable rock units, each characterised by a unique assemblage of rock types and structures. These lithological units may be subdivided into different lithofacies. The vertical lithofacies represent vertical accretion of deposits in flood-plains (mudstone and siltstone facies), shallow lakes (rhythmite facies) and channels (sandstone facies). A major feature of the core samples is the large number of bedding-parallel fractures whose frequency decreases downward from the upper, more weathered zone, as thicker and more competent units are encountered. The bedding plane fractures in the upper, more weathered part are often transected by a large number of orthogonal, oblique and diagonal fractures. These fractures clearly represent secondary fracturing of the rock mass caused by the post-lithification process.

The Mode I fracture is the most significant fracture on the Campus Site and all boreholes with high yields (11 has yields in excess of 3 l/s) intersected this bedding-plane fracture. The yields of the other 19 percussion boreholes are less than 0.6 l/s because the Mode I fracture was not intersected during drilling. It is clear from both the acoustic scan and borehole video of borehole UO23 (see Figure 6-3), that the Mode I fracture, which is situated at about 21 m below surface, consists of a fracture zone with a thickness that varies between 100 and 200 mm (i.e. the fracture zone has developed as consequence of the weathering of the rock between two bedding-plane fractures which were close together).

Figure 6-3 Borehole video of the fracture zone in borehole UO5 at a depth of between 20.9 – 21.1 m below surface, showing a fracture zone thickness of about 200 mm

A very dominant black shale layer at about 13 meters below surface forms an aquitard between the top mudstone and the bottom sandstone layer (which could thus be viewed as semi-confined). There are three aquifers present on the Site. The top, a phreatic aquifer, occurs within the upper mudstone layers on the Site. This aquifer is separated from the middle and main aquifer, which occurs in a sandstone layer between 8 and 10 m thick, by a layer of carbonaceous shale with a thickness of 0.5 – 4 m. The bottom aquifer occurs in the mudstone layers (more than 100 m thick) that underlies the sandstone unit (Botha *et al.*, 1998).

6.1.1.2. Borehole Construction

To estimate the specific yield of the boreholes and to allocate the correct positions of the fracture zone in each borehole, different tests (e.g. constant rate tests, tracer tests, borehole fluid logs) were conducted.

- A constant rate test, conducted at UO26 with a discharge of about 0.8 l/s, shows good hydraulic contact between boreholes UO26, UO27, UO28 and UO29. The drawdowns in all observation boreholes were very similar and in the same range (see section 6.1.2(a)).
- A constant rate test, conducted at UP16 with a discharge of about 3 l/s, shows a similar behaviour of the observed boreholes in the beginning of the test. When the water level in the abstraction borehole reached the position of the fracture (about 21 m below surface) the water levels in UO29 and UO30 reached the same position (20.84 m and 20.67 m below surface respectively), which is estimated as the position of the fracture zone. The water levels in the other observed boreholes stabilised between 18.54 m and 19.24 m below surface, which lies above the fracture.
- Radial convergent tracer tests, conducted between UO28 and UO26 give an estimate for the flow thickness (i.e. hydraulic effective thickness of the fracture zone) and the porosity of the fracture zone, which are needed for the computer model.
- Borehole conductivity logs, measured with an EC-meter under natural conditions, give a good estimation of the depth of the fracture zone. By using salt as a tracer the estimated position of the fracture can be verified. Figure 6-4 shows the EC-profile in UO28 with two fracture zones at 20.5 m and 22 m respectively as seen from the jump in the EC-concentration.

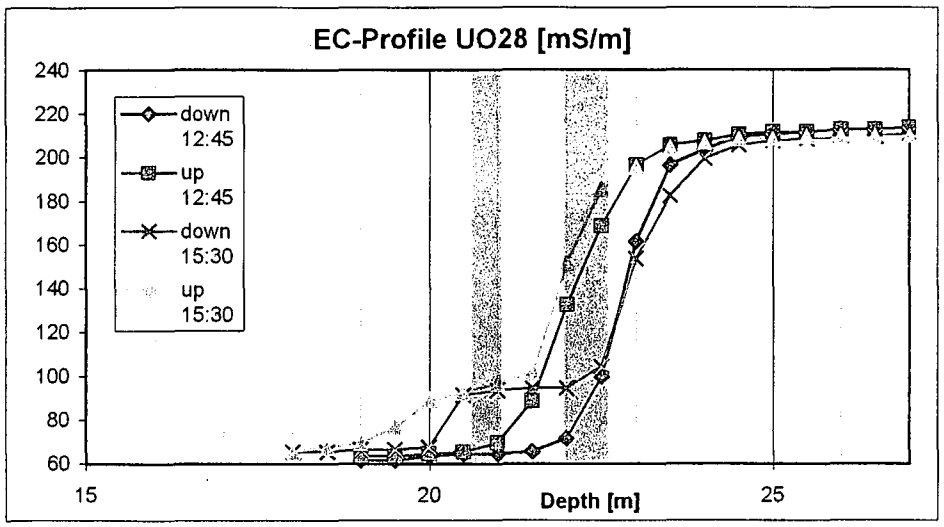

Figure 6-4 Borehole Conductivity Log of UO28, showing the position of the fractures at 20.5m and 22m

The results from the tests, which are important for the following steps of this project, are listed in table 2.2.1. For complete results see the appendix.

Table 6-2 Depth of the fracture zone in the new boreholes (m under surface)

Borehole	Depth of fracture	Method of estimation
UO23	21 m	Borehole video
UO26	24 m	Tracer test, borehole conductivity log
UO27	21 m	Tracer test, borehole conductivity log
UO28	20.5 m and 22 m	Tracer test, borehole conductivity log
UO29	21 m	Tracer test, borehole conductivity log
UO30	21 m	Tracer test, borehole conductivity log

After drilling and testing the boreholes with the above-mentioned tests the piezometers were installed in boreholes UO23, UO29, UO28 and UO27, lying exactly on line with borehole UO5, to be used for abstraction during the hydraulic tests. In each the borehole three piezometers were installed in the following way:

- one piezometer in DN 32 about 1.5m (UO23) or 2.5m above the fracture,
- one piezometer in DN 50 in the fracture zone with a wellscreen length of 1m (UO23), 2m (UO27 and UO29) and 3m (UO28),
- one piezometer in DN 32 about 1,5m (UO23) or 2.5 m below the fracture.

Between the piezometers a sealing of bentonite was put to avoid flux or pressure contact between the three zones (Figure 6-5). At the bottom of the bentonite sealing a thin layer of cement was installed to avoid contact between the bentonite and the piezometer.

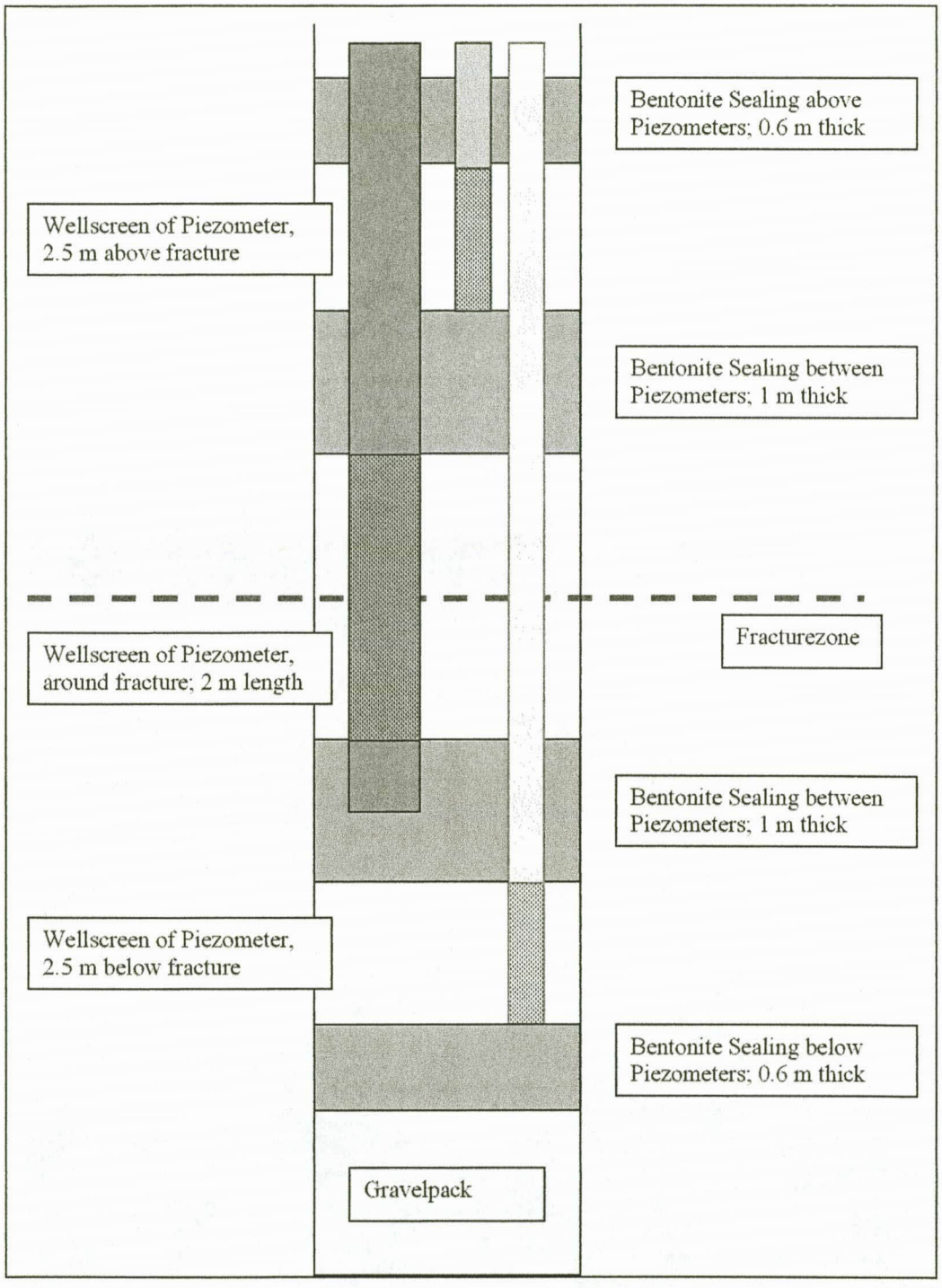

Figure 6-5 Scheme of installing the piezometers into the boreholes

6.1.2. Hydraulic Tests

On the Campus Test Site several hydraulic tests were conducted in the past years, including constant rate tests with and without the installed piezometers. The tests described and analysed here were conducted at boreholes UO5 and UO26. For the test before installing the piezometers, as described above, borehole UO26 was used for abstracting water and the boreholes UO27, UO28 and UO29 were observed permanently. The test was conducted in March 2000.

The hydraulic tests, using the boreholes with installed piezometers, were conducted in July 2000, September 2000 and February 2001. For the abstraction of water borehole UO5 was used and permanent observations were taken from the piezometers of boreholes UO27, UO28, UO29 and UO23. The water levels in other boreholes were also measured over the period of the tests. These tests are compared to a constant rate test, which were conducted at borehole UO5 in March 1994.

(a) UO26 – Test, March 2000

As shown in Table 6-3, the constant discharge test on the Campus Test Site was conducted at borehole UO26 for the abstraction with a discharge rate of 0.71 l/s for period of 13 hours. The open boreholes UO27, UO28 and UO29 were used to observe the water level in the aquifer permanently with a pressure transducer and automatically data logger.

Table 6-3 Conditions for the constant discharge test UO26, conducted at Campus Test Site

Abstraction BH	Discharge Rate	Duration of test	Observation Boreholes (Distance to UO26 in Brackets)
UO26	0.71 l/s	780 min	UO27 (7m), UO28 (14m), UO29 (34m)
	Recovery	720 min	

All the boreholes intersected the same Mode I fracture and Figure 6-6 shows the pumping test data in this case. The drawdown values in UO27, UO28 and UO29 were very similar and did not converge to the same drawdown value as the abstraction borehole UO26.

The test data were analysed with different analytical methods to evaluate the aquifer parameter transmissivity T (m^2/d) and storage coefficient S (-). The porous media approach and the GRF-model were used and the results compared.

Porous Media Model

The estimated T-values, using the methods of Cooper-Jacob or Theis, are of the same order of 10 m^2/d, but the estimated S-values differ between 3 E-5 and 2E-3 with a distance dependency (the larger the observation distance, the smaller the estimated S-value). **The reason for this phenomenon is the application of an incorrect method to the real field situation.**

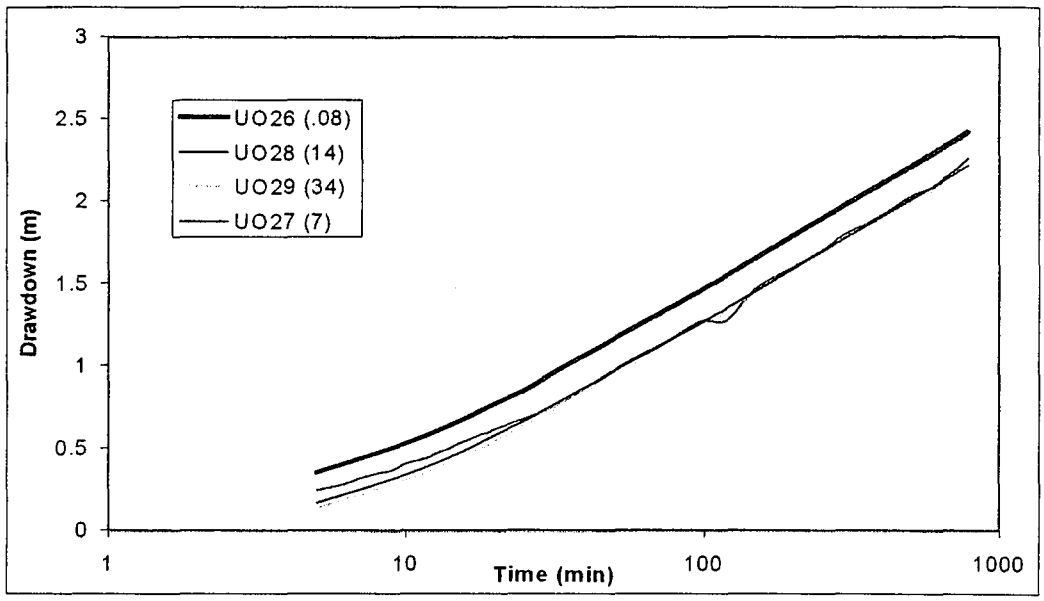

Figure 6-6 Drawdown in the abstraction and observation boreholes during the constant rate test at UO26. The values in parenthesis give the distance between individual boreholes and UO26, which was the abstraction borehole (at 0.7 L/s).

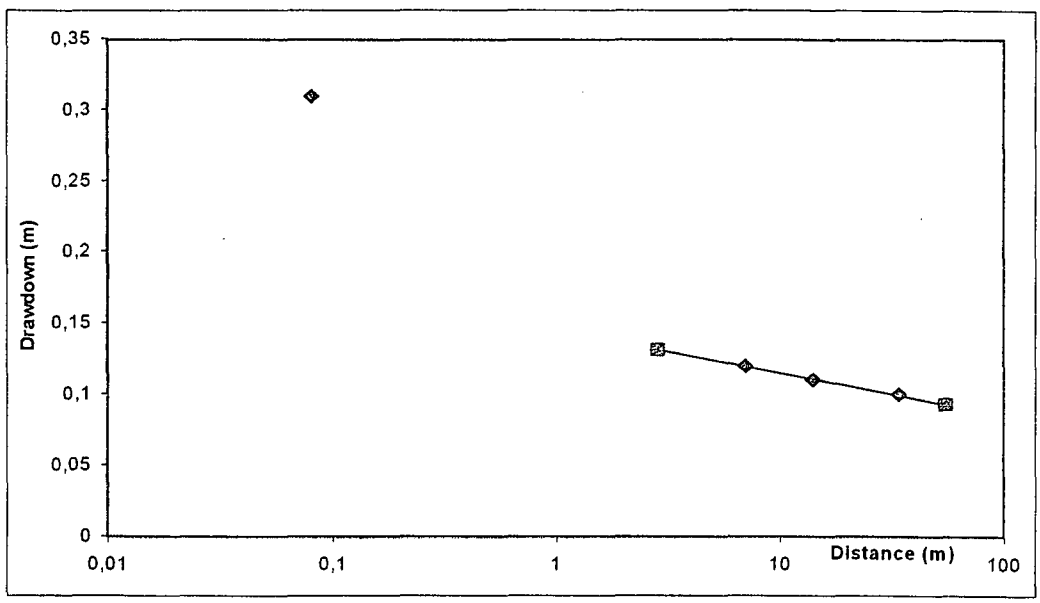

Figure 6-7 Measured drawdown after 2 minutes vs. distance of observation during constant rate test at UO26

By using the distance-drawdown-method (known as Cooper-Jacob II, see Figure 6-7) the estimated T-value is much higher and the S-value much lower than with Cooper-Jacob or Theis. With the method Cooper-Jacob II the estimated values represent the fracture zone, while the estimated values with the other methods represent the whole aquifer (fracture + matrix).

From the graphs and the results it can be seen that the standard methods for estimating aquifer parameters from hydraulic tests (i.e. Theis and Cooper-Jacob) can't be applied correctly to fractured aquifers, because the vertical flux from the matrix to the fracture and the storage of the matrix is nearly neglected in these models. For the numerical model the estimated values are used as initial values of the parameters which have to be verified and recalculated with the inverse modelling technique.

Table 6-4 Results of the evaluated aquifer parameter for the constant rate test UO26

	Cooper-Jacob Method		Theis Method		
Borehole	T (m^2/d)	S (-)	T (m^2/d)	S (-)	Comment
UO26	10.6	2.75 E-5	10	3.30 E-5	S-value calculated with effective BH Radius of 49.7 m
UO27	10.6	2.13 E-3	10	2.45 E-3	T- and S-values valid for whole aquifer (fracture + matrix)
UO28	10.5	5.41 E-4	10	5.80 E-4	
UO29	10.7	8.92 E-5	11	8.60 E-5	
All Boreholes	755	5.87 E-7			Cooper-Jacob II for fracture zone

GRF-Model

Applying the GRF-Model (Barker, 1988) to the test data the type-curve method was used, as it is implemented in the software FC. By forcing the b-value to be between 0.1 and 0.2 m (approximated thickness of the fracture zone, see section 6.1.1) a non-linear least square fit (see Figure 6-8) to the data yield the following parameters. As a comparison Figure 6-8 also shows the fit with a fixed flow dimension of 2.

Table 6-5 Parameter values for the UO26-test obtained from the Barker model

Borehole	K_f (m/d)	S_{sf}	b (m)	n
UO26	199	2.7E-3	0.16	1.85
UO27	187	1.7E-2	0.19	1.80
UO28	201	2.4E-3	0.16	1.84
UO29	200	1.1E-3	0.16	1.85

The flow dimensions estimated for all boreholes are very close together and show, with a value of 1.85, a non-integer, fractional flow dimension. An effective borehole radius of 5m instead of the real radius of 0.0825m was used for the abstraction borehole to estimate the Specific Storage.

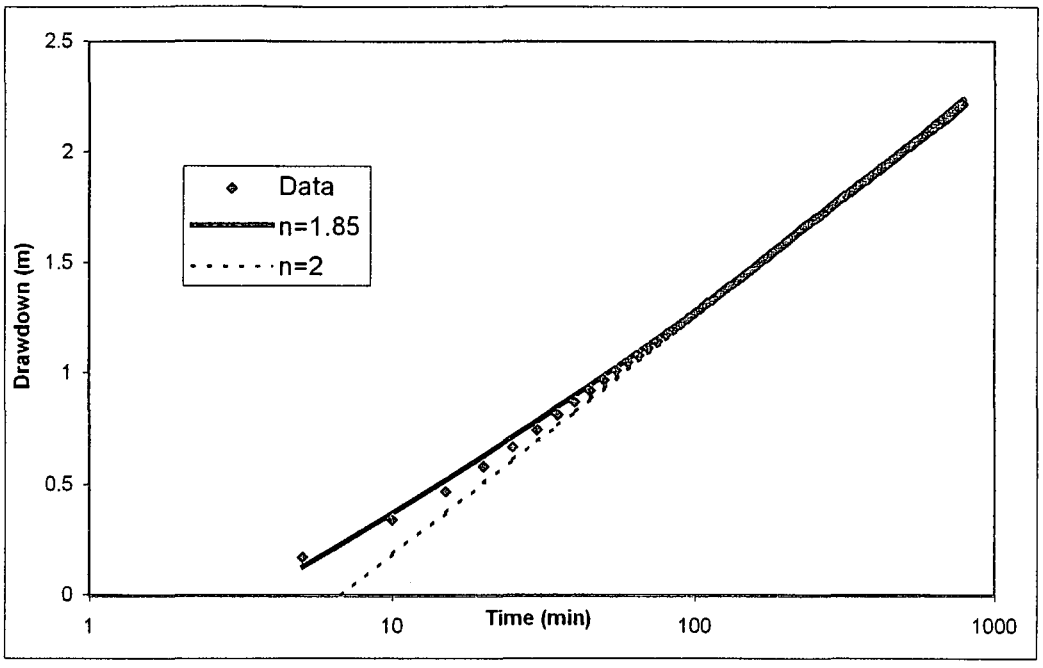

Figure 6-8 Barker-method applied to the abstraction borehole UO26, yielding a flow dimension of 1.85. For comparison the simulated drawdown curve with a flow dimension of 2 is included.

A comparison of both approaches used to estimate the aquifer parameters shows inherent differences due to the different underlying assumptions. Applying the porous media models results in S-values for the aquifer which clearly shows a distance-dependency (i.e. the estimated value decreases with increasing distance of the observation borehole from the abstraction borehole). The GRF-model yields a relative constant S-value for the fracture system, which is of two to three magnitudes larger than the estimates obtained from the porous media model. On the other hand the estimated K_f-value obtained from the GRF-model is far lower than the T-value obtained for the fracture system by applying the Cooper-Jacob II method.

These differences indicate that the various methods relate to different parts of the aquifer. While the porous media model yields estimates representative for the whole aquifer thickness, the GRF-model relates to the thickness of the fracture zone and yields values averaged over the flow domain. The high transmissivity value obtained for the fracture from the Cooper-Jacob II method relates to the single fracture rather than the fracture zone which consists of several fractures and fissures with variable aperture.

(b) UO5 – Test, March 1994

During the UO5-test borehole UO5 abstracted water at a rate of 1.25 l/s and water levels were measured in boreholes UO6 (6m), UP15 (22m), UP16 (32m) which intersected the same bedding plane fracture as UO5. Figure 6-9 shows the measured drawdown values of the test together with the drawdown values measured in borehole UO10 (48m) in which the Mode I fracture does not occur. A very interesting feature is that the water level drawdowns in the boreholes that intersected the same fracture were very similar in form (except in borehole UO10 in which the fracture does not occur). Because the used boreholes are open boreholes, intersecting several aquifers, it was not possible to measure the hydraulic gradient in an accurate way.

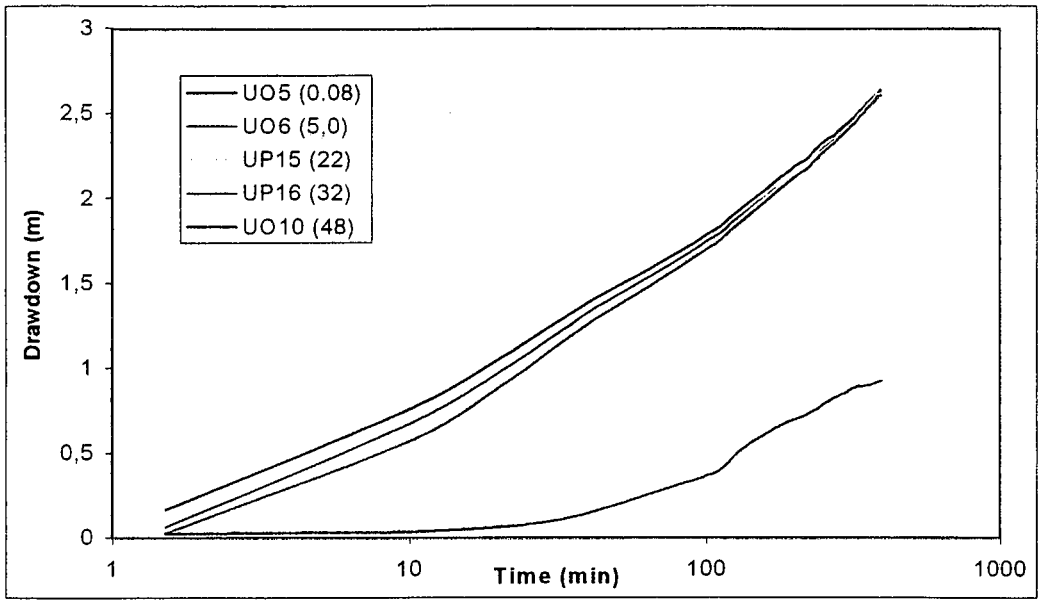

Figure 6-9 UO5 pumping test, showing the drawdown behaviour in boreholes. UO5 was the abstraction borehole (rate of 1.25 l/s).

Several analytical and numerical methods were applied to the test data to estimate the aquifer parameter.

Porous Media Model

Using the straight-line method of Cooper-Jacob the transmissivity of the aquifer was estimated at 10 m^2/day. Drawdown values obtained from the boreholes after 1.5 minutes were used in the Cooper-Jacob II method (distance-drawdown method – see Figure 6-10) and a transmissivity of 700 m^2/d was estimated, which represents the transmissivity of the fracture zone.

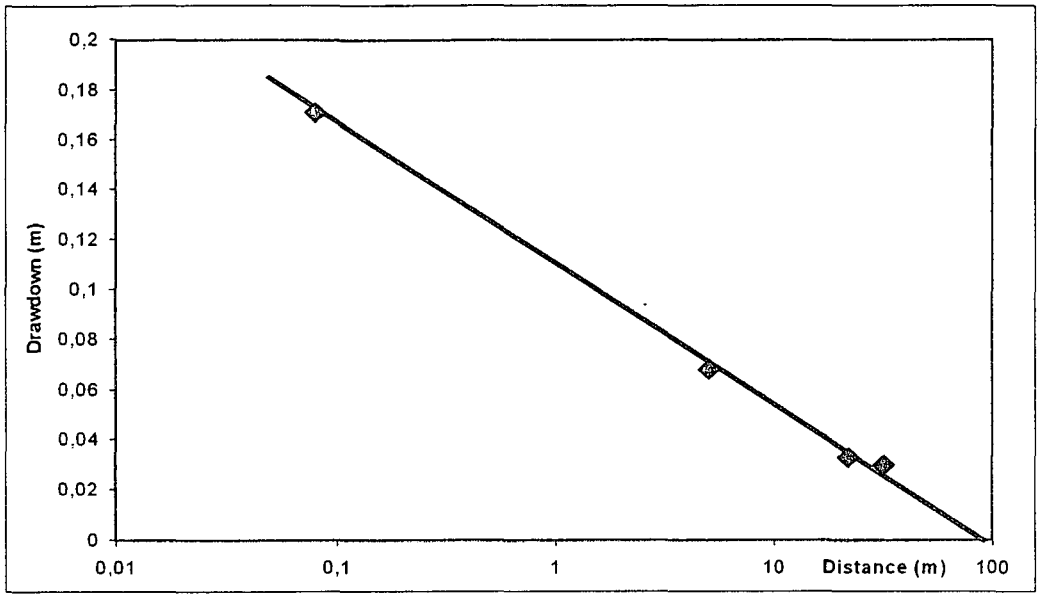

Figure 6-10 Cooper-Jacob II applied to the data of the UO5-test resulting in a T = 700 m^2/d for the fracture zone

GRF-Model

The data of the UO5-test was then analysed with the generalised flow model of Barker (1988). Figure 6-11 and Table 6-6 show the results. From the acoustic scan and borehole video, the thickness of the fracture zone was measured to vary between 0.1 and 0.2m. These values were used as lower and upper values for b in the Barker equation to obtain the solution for the other parameters (only the product $K_f b^{(3-n)}$ and diffusity K_f/S_f can be estimated uniquely with the Barker equation). A non-linear least square method was applied to estimate the parameters shown in Table 6-6.

Table 6-6 Parameter values for the UO5-test obtained from the Barker model

Borehole	Kf (m/d)	Sf	b (m)	n
UO5	653	2.6E-3	0.15	1.75
UO6	645	1.1E-3	0.14	1.75
UP15	651	1.5E-3	0.16	1.75
UO16	657	1.7E-3	0.15	1.74

From previous analysis it can be concluded that the flow prevailing during the UO5-test is partially dimensioned, called a fractional dimension.

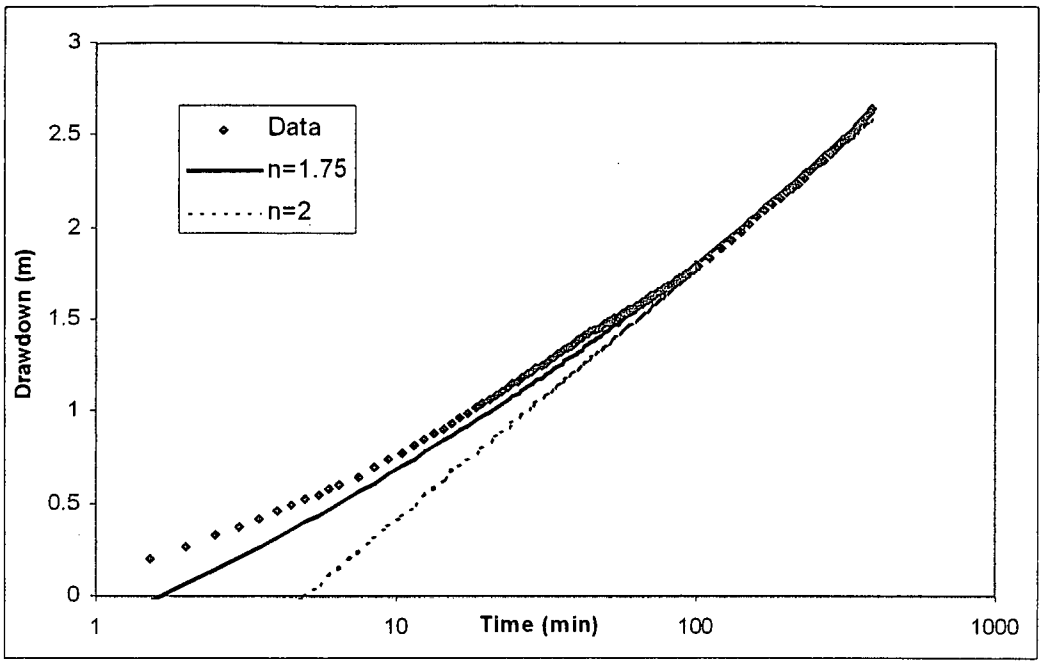

Figure 6-11 Barker-method applied to the abstraction borehole UO5, yielding a flow dimension of 1.75. For comparison the simulated drawdown curve with a flow dimension of 2 is included.

3D-Numerical Model

A numerical model was constructed for the site by using the 3D Modflow program PMWIN (Chiang and Kinzelbach, 2001) and using twenty layers of thickness of 0.5 meters and 1 metres respectively above and below the main fracture layer with thickness of 200 mm. The inverse model PEST (Doherty, 2000) was used to calibrate the data and Table 6-7 shows the results (Van Tonder *et al.*, 2001)

Table 6-7 Hydraulic parameters for the aquifer on the Campus Test Site as estimated with the three-dimensional model (Khm=horizontal matrix K; Kvm=vertical matrix K; Khf=fracture K; Ssm=matrix specific storativity)

Parameter	Estimated values
Khm (m d–1)	0.158
Kvm (m d–1)	5.82·10–3
Ssm (m–1)	5.65·10–5
Khf (m d–1)	3.6·103

The horizontal K-value of the fracture zone was estimated at 3600 m/d and if multiplied with the thickness of the fracture zone of about 0.2m, a T-value of 750 m^2/d is obtained, which is very similar to the value estimated with the analytical method of Cooper-Jacob. The difference in the estimated K_f –value with the Barker method and the numerical model illustrates that there might be a hierarchy of smaller fractures present that possibly forms a fractal system with a lower effective hydraulic conductivity than that of the main fracture.

nSIGHTS - Model

Using the software program nSIGHTS (see section 4.1.2.3(c)) a one-dimensional numerical model was constructed to analyse the hydraulic test data. Two different conceptual models were used:

- Double-porosity aquifer with a volume ratio fracture to aquifer of 0.01
- Leaky aquifer to account for the flow from the matrix to the horizontal fracture

With the model for double-porosity, applied to both the abstraction borehole UO5 and the observation borehole UP16, a good fit for both the drawdown and the derivative of the drawdown could be achieved (see Figure 6-12 and Figure 6-13). From the scaled second derivative of the drawdown in the abstraction borehole a flow dimension of 1.5 is computed, which is less than the value obtained with the GRF-model. The other results are listed in Table 6-8.

Table 6-8 Estimated parameter values for the UO5-test, obtained from applying the nSIGHTS program

Parameter	UO5 data only	UO5 and UP16 data simultaneously
Flow dimension	1.5	1.75
Hydraulic conductivity Fracture	11400 m/day	864 m/day
Specific Storage Fracture	3 E-03	2 E-04
Hydraulic conductivity Matrix	0.03 m/day	0.004 m/day
Specific Storage Matrix	1 E-05	3 E-04
Tubing String Radius (= effective borehole radius)	3.8 m	1.8 m

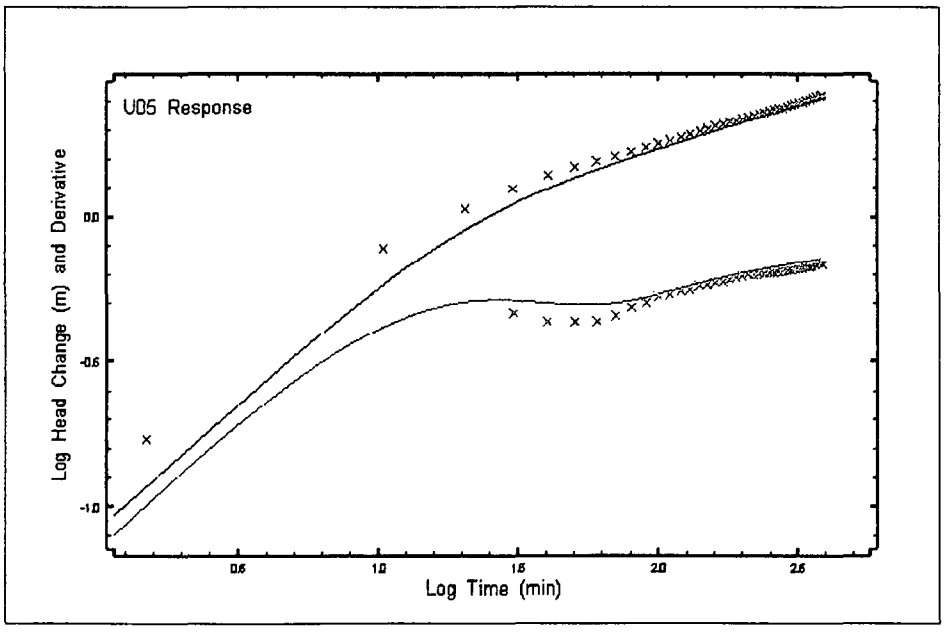

Figure 6-12 Simulation result for UO5-test, using drawdown in abstraction borehole

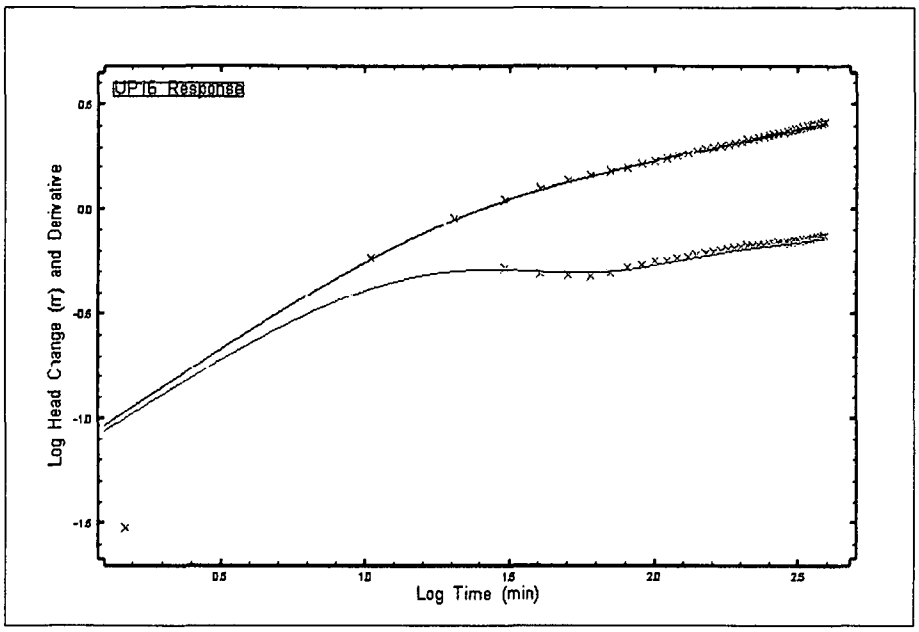

Figure 6-13 Simulation result for UO5-test, using drawdown in observation borehole UP16

The uncertainties in the above-mentioned estimations are calculated in the program by means of the Jacobian Matrix. A Jacobian plot (see Figure 6-14) shows the sensitivity of the match to each data point in constraint with respect to change in a fitting parameter value. If the sensitivity is zero, then the value of the fitting parameter does not affect the match to the constraint. It is obvious from Figure 6-14 that the fit to the data is most sensitive to the estimated flow dimension, followed by the fracture conductivity. Of interest is the fact that the simulated fit is insensitive to the estimate of the matrix conductivity and the storage of both matrix and fracture. These parameters cannot be estimated properly as their values does not affect the match to the data.

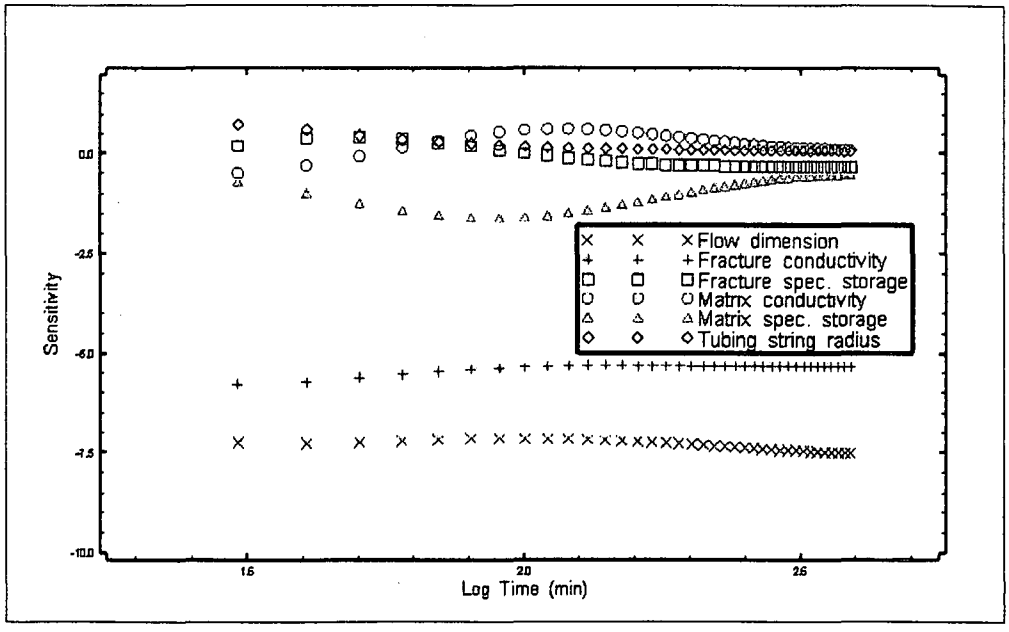

Figure 6-14 Jacobian Matrix for simulation UO5-test for observation borehole UP16

According to the geological settings and the results of other analyses, like diagnostic plots and numerical model, the double-porosity model is not appropriate in this case. The conceptual model for the Campus Test Site, as used for the three-dimensional numerical model, consists of a fracture zone of about 20cm thickness with high conductivity, bounded by a matrix with low conductivity. The matrix can be simulated as a leaky aquitard, as the groundwater stored in the matrix flows towards the fracture, when water is abstracted from the latter.

Using the leaky aquifer model, which is implemented in the nSIGHTS program, the simulation shows a good fit to the drawdown data of observation borehole UP16, but the derivative of the drawdown cannot be matched (see Figure 6-15). At the moment there is no explanation for this phenomenon.

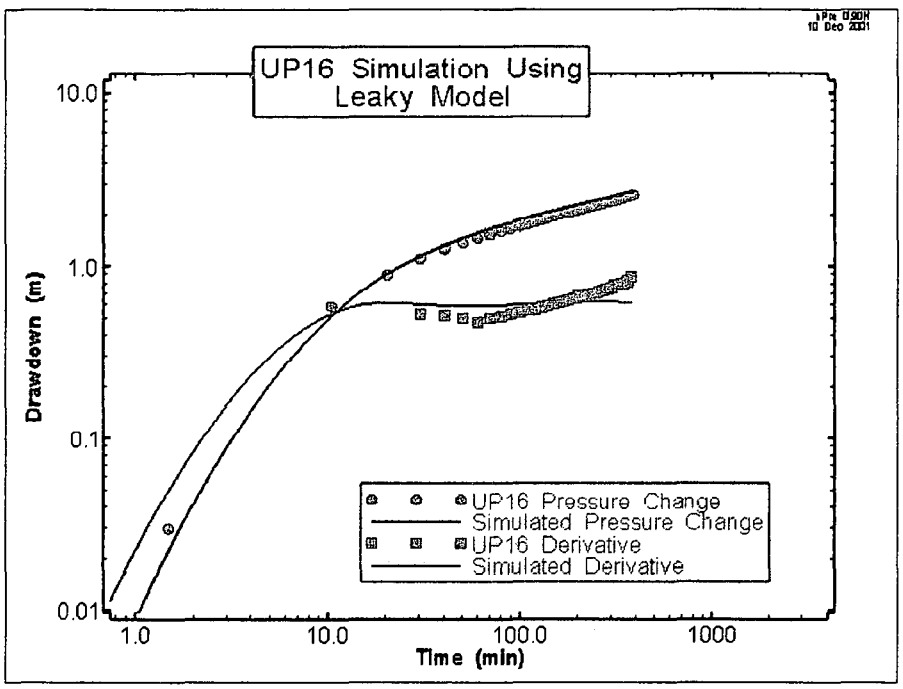

Figure 6-15 Simulation result for UO5-test, using drawdown in observation borehole UP16 and leaky aquifer model

The differences in estimated aquifer parameter values and the accuracy of model fits indicate the influence of the correct conceptual model for the analysing procedure. Although the simulation of the hydraulic test data with the double porosity model shows a proper match, the estimated values are not reliable and cannot compared to the estimations obtained from analytical methods or the three-dimensional numerical model.

(c) UO5 – Test, July 2000

As shown in Table 6-9, the first constant discharge test with installed piezometers on the Campus Test Site was conducted at borehole UO5 for the abstraction with a discharge rate of 0.51 l/s for a period of 67 hours. The piezometers in the boreholes UO23, UO27, UO28 and UO29 were used to observe the water level in the fracture zone, and the rock matrix permanently with a dip meter. The water levels in boreholes UO6, UO7, UO20, UO26 and UO30 were also measured during the period of the test.

Table 6-9 Conditions for the constant discharge test UO5, conducted at Campus Test Site

Abstraction BH	Discharge Rate	Duration of test	Observation Boreholes (Distance to UO5 in Brackets)
UO5	0.5 l/s	4008 min	UO27a, b, c (each 11.5m); UO28a, b, c (each 27.25m); UO29a, b, c (each 75.9m); UO23a, b, c (each 97.9m); UO6a, b (each 5.3m); UO7 (7.0m), UO20 (16.2m), UO26 (16.1m), UO30 (92.5m)
	Recovery	6000 min	

(a: piezometer above the fracture, b: piezometer below the fracture, c: piezometer in the fracture zone)

The drawdown behaviour in the fracture-piezometers and the boreholes are similar to the above-mentioned UO26-test. The water level in all boreholes dropped simultaneously and in the same range as in the abstraction borehole UO5. Figure 6-16 shows the drawdown in the fracture while Figure 6-17 shows the drawdown in the matrix-piezometers.

The behaviour of the groundwater flow during the pumping test conducted in the abstraction borehole UO5 can be described as follows:

- The hydraulic head everywhere in the fracture drops simultaneously
- The hydraulic head in the matrix drops later and less than in the fracture; water from the matrix storage flows into the fracture and from there to the abstraction BH
- After stopping the pumping, the drawdown in the matrix continues while the head in the fracture recovers; water still flows from the matrix toward the fracture to refill the system.

The test data were analysed with different analytical and numerical methods to evaluate the aquifer parameter transmissivity T (m^2/d) and storage coefficient S (-).

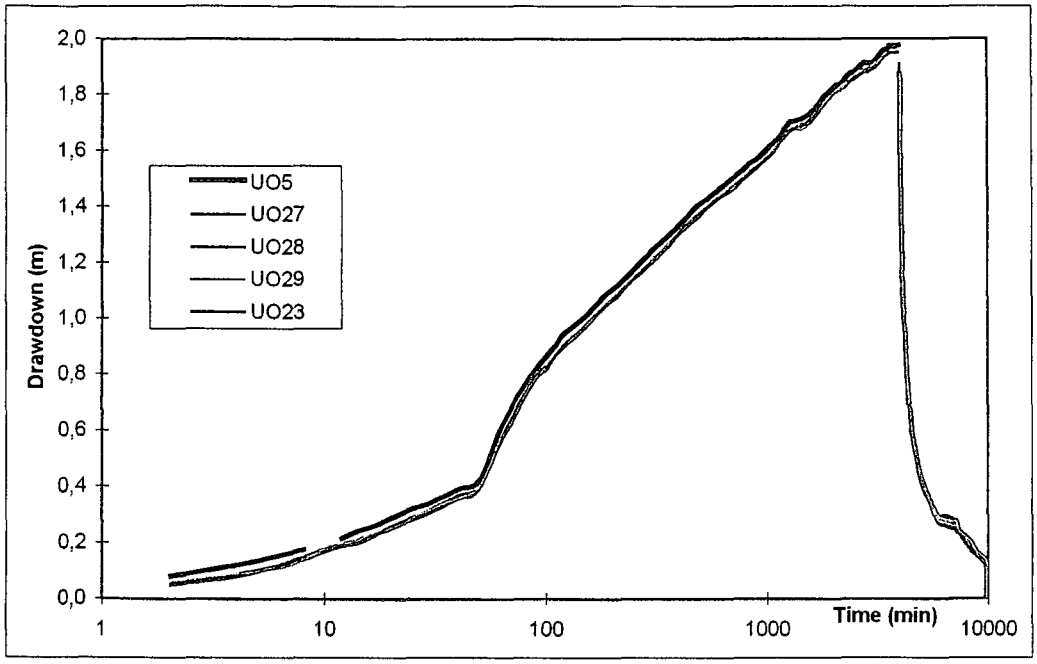

Figure 6-16 Drawdown in the fracture-piezometers during constant discharge test UO5, July 2000

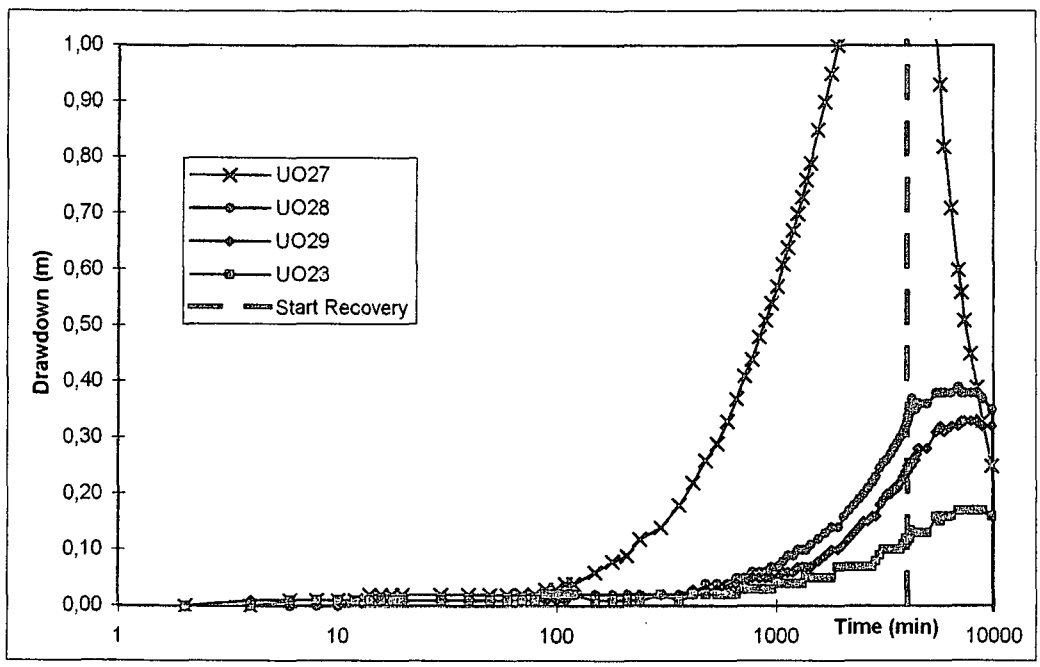

Figure 6-17 Drawdown in the matrix-piezometers below the fracture zone during the constant discharge test UO5, July 2000

Analytical Methods

The estimated T-values, using the methods of Cooper-Jacob or Theis, are of the same order of 10 m^2/d, as estimated for the constant discharge tests UO26 and UO5, March 1994. The estimated S-values differ between 1E-5 and 8E-3 with a distance dependency (the larger the observation distance, the smaller the estimated S-value).

This distance dependency will also occur, when applying the Gringarten-method, which is an analytical solution for a horizontal, uniform flux fracture. The estimated values for the transmissivity and the storage coefficient of the aquifer are of the same order as the values estimated with Cooper-Jacob or Theis (see Table 6-10). In addition to these parameters the thickness of the aquifer, the vertical hydraulic conductivity, the half-length of the fracture and the fracture height have to be estimated (see Table 6-11). Without prior information about the aquifer properties this method is a non-unique solution.

By using the distance-drawdown-method (known as Cooper-Jacob II, see Figure 6-19) the estimated T-value is much higher and the S-value much lower than with Cooper-Jacob or Theis. With the method Cooper-Jacob II, the estimated values represent the fracture zone, while the estimated values with the other methods represent the whole aquifer (fracture + matrix).

Table 6-10 Results of the evaluated aquifer parameter for the constant rate test UO5, July 2000, obtained from the fracture-piezometers

Bore-hole	Cooper-Jacob I		Theis		Gringarten		Comment
	T (m^2/d)	S (-)	T (m^2/d)	S (-)	T (m^2/d)	S (-)	
UO5	10.6	4.4E-03	9	8.0E-03	15	3.0E-03	S-value calculated with effective BH Radius of 5 m
UO27c	10.7	9.1E-04	11	8.3E-04			Distance: 11.5m
UO28c	10.6	1.6E-04	11	1.5E-04			Distance: 27.2m
UO29c	10.6	2.1E-05	11	1.9E-05			Distance: 76m
UO23c	10.6	1.3E-05	10	1.5E-05	10	2.0E-05	Distance: 98m
All BH	743	2.4E-15					Cooper-Jacob II for fracture zone

Table 6-11 Estimated and assumed parameter values from the Gringarten-method for the constant rate test UO5, July 2000

Parameter	UO5 (Abstraction)	UO23 (Observation)	Units
Transmissivity matrix	15	10	m^2/day
Aquifer Thickness	20	20	m
Storage Coefficient	3.0 E-03	2.0 E-05	-
Vertical hydraulic conductivity	3.0 E-03	3.0 E-03	m/day
Fracture half-length	60	60	m
Fracture height	0.2	0.2	m
Fracture Elevation	10	10	m

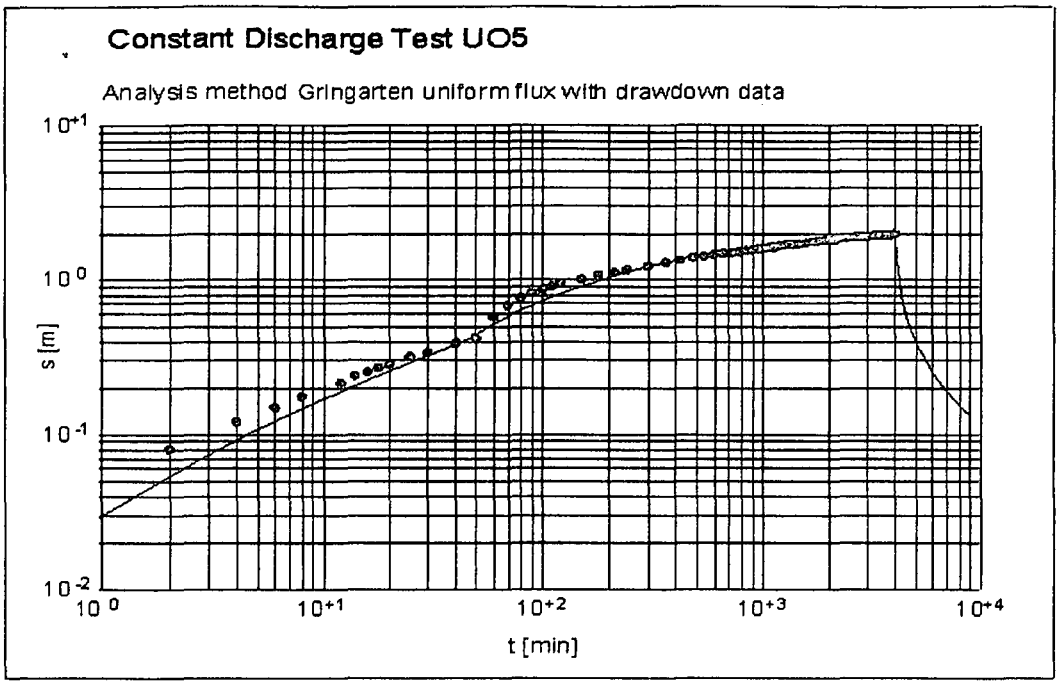

Figure 6-18 Measured drawdown in UO5 (dots) during constant rate test at UO5, July 2000 and fitted curve with Gringarten-method, parameter values from table 3.4.3

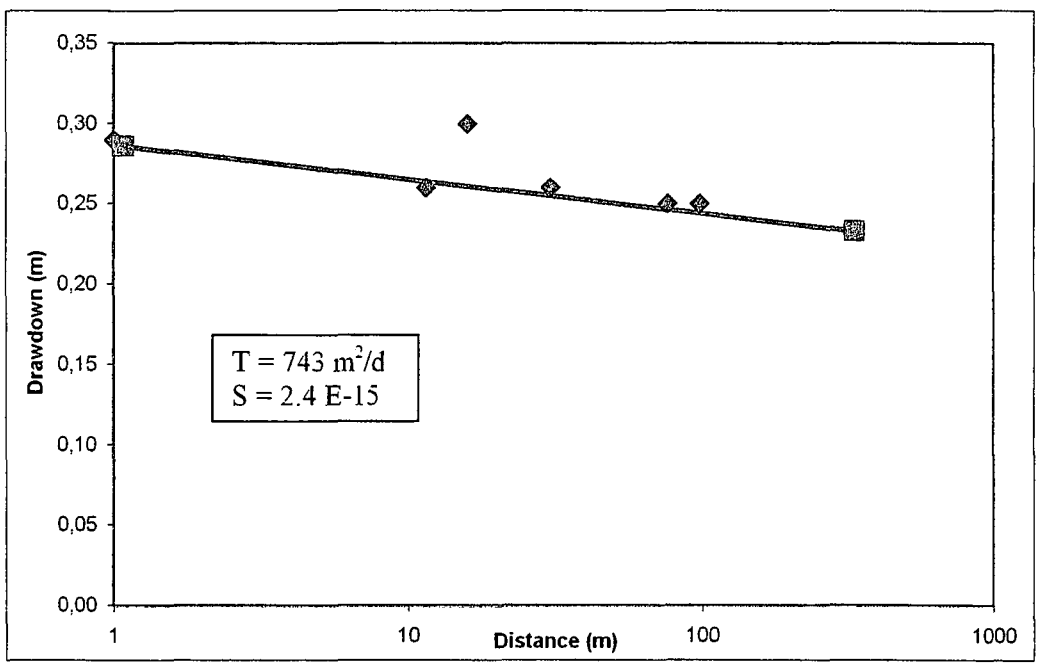

Figure 6-19 Measured drawdown after 20 minutes vs. distance of observation during constant rate test at UO5, July 2000 (The estimated S-value is far too low for the fracture system. If neglecting the abstraction borehole UO5, an S-value of E-10 can be computed, which is even lower than expected)

If applying the above-mentioned methods to the drawdown data obtained from the matrix-piezometers, the estimated values for transmissivity and storage coefficient differ much from the values obtained from the fracture-piezometers and seem too high and unrealistic (see Table 6-12). The Gringarten-method is not applicable to the data from matrix-piezometers.

Table 6-12 Results of the evaluated aquifer parameter for the constant rate test UO5, July 2000, obtained from the matrix-piezometers

	Cooper-Jacob Method		Theis Method		
Borehole	T (m^2/d)	S (-)	T (m^2/d)	S (-)	Comment
UO27a	88.5	3.28E-01	80	3.0E-01	Distance: 11.5m
UO28a	57.5	8.89E-02	60	9.0E-02	Distance: 27.2m
UO29a	80.0	7.39E-03	90	7.0E-03	Distance: 76m
UO23a	12.5 33.7	5.78E-03 9.85E-03	5	7.4E-03	Distance: 98m
UO27b	4.2	2.89E-02	4	3.3E-02	Distance: 11.5m
UO28b	14.1	3.31E-02	11	4.4E-02	Distance: 27.2m
UO29b	11.5	5.43E-03	12	7.6E-03	Distance: 76m
UO23b	34.5	7.06E-03	65	7.5E-03	Distance: 98m
all above	254	2.28E-02			Cooper-Jacob II
all below	50.8 - 162	1.2 E-02			Cooper-Jacob II

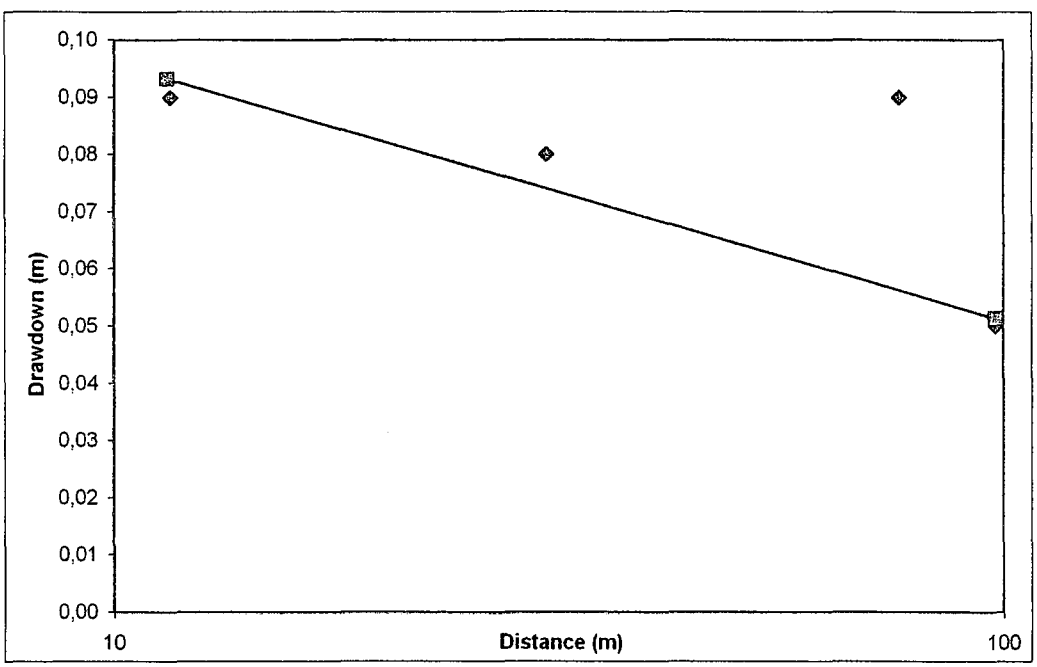

Figure 6-20 Measured drawdown in the matrix-piezometer after 3000 minutes vs. distance of observation during constant rate test at UO5, July 2000

3D-Numerical Model

For this study a numerical model is built by using PMWIN (Chiang and Kinzelbach, 2001), which is a user friendly, graphic pre- and postprocessor and includes MODFLOW for flow modelling and PEST as the inverse modelling technique.

The first step in analysing the groundwater flow in an aquifer with a numerical model is to develop a suitable mesh or grid for the aquifer. The finite difference mesh used in the present model consists of 88 rows, 115 columns and 23 layers of nodes. The horizontal extent of the model chosen was large enough to avoid boundary effects (6200m x 6200m). The grid size varies from 400m at the outer part to 2m in the surroundings of abstraction borehole UO5.

The 12th layer of the model represents the fracture. The other layers represent the sandstone matrix above and below the fracture. The two layers directly above and below the fracture are each assigned a thickness of 0.5 m, and the other layers a thickness of 1 m (see also Figure 4-9). This fine vertical discretisation is necessary to account for the vertical drawdown in the rock matrix.

As mentioned in section 6.1.1, the fracture zone has an aperture of 0.2 m, while its horizontal extent was estimated at 150 m x 200 m, based on the geological profiles of the boreholes. The impact this size has on the estimated parameter values is discussed in section 4.1.2.4(b). The abstraction borehole UO5 and the observation boreholes (UO27, UO28, UO29 and UO23) were also placed in the mesh within the fracture and the matrix respectively.

To calibrate the model with the pumping test data, the inverse model PEST (Doherty, 2000) is used. The criterion for the automatic parameter estimation with inverse modelling techniques is the sum of squared residuals (called phi), where residuals are the differences between the measured and calculated data (e.g. hydraulic head or drawdown).

In this case the drawdown observations during the hydraulic test were used as measured data. Because of the big difference of the values in the fracture and in the matrix, the matrix observations were assigned a weighting factor between 5 and 10, which was calculated from the maximum drawdown in the piezometer vs. maximum drawdown in the fracture (e.g. maximum drawdown in the fracture-piezometers = 2m and maximum drawdown in UO28a = 0.2m, weighting factor for the observation data of UO28a = 10).

To fit the delay of the drawdown in the matrix-piezometer in a better way, the sensitivities of the parameters were tested. There are mainly two parameters responsible for the delay of the drawdown; the storage coefficient of the matrix and the transmissivity of the matrix. While the impact of the storage coefficient on the drawdown curve of the fracture is small, any change of transmissivity value will result in a visible change in the drawdown curve of the fracture.

Therefore the S-value of the matrix was forced to be high for the next calibration runs. By using parameter values obtained from step 5 as initial values, the inverse modelling yields a good fit for both the fracture and the matrix piezometer (see Figure 6-21 and Table 6-13).

a)

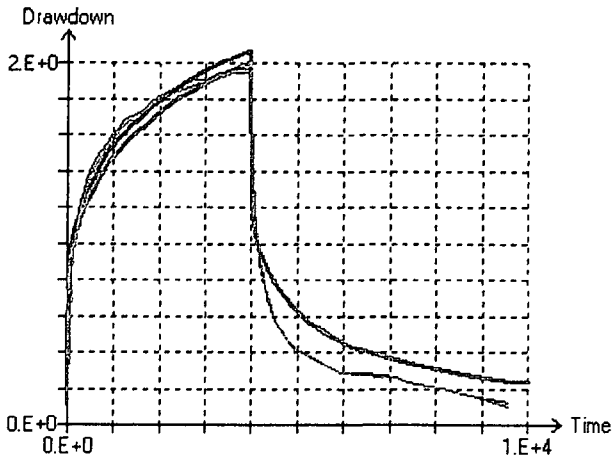

Fracture Piezometer
UO5 and UO23

Bold = calculated
Fine = observed

b)

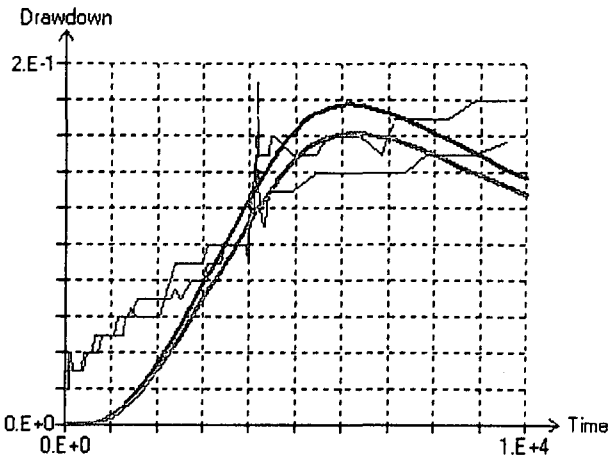

Piezometer Matrix above

UO29a, observed
UO28a, observed
UO28a, calculated
UO29a, calculated

c)

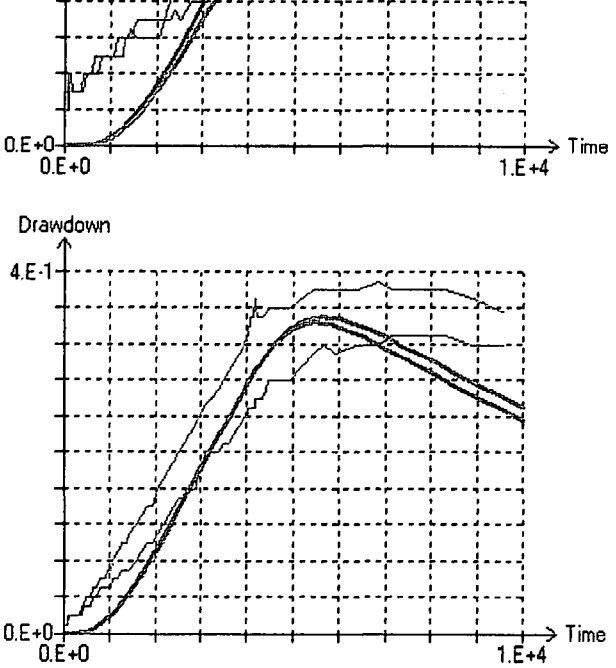

Piezometer Matrix below
UO28b, observed
UO29b, observed

UO28b, calculated.
UO29b, calculated

Figure 6-21 Best result of inverse modelling with observation data of fracture and matrix;

Table 6-13 Estimated parameter values of the best fit of inverse modelling with observation data of the fracture and matrix (comparison of observed and calculated drawdown shown in Figure 6-21)

Parameter (model)	Value	Parameter (aquifer)	Value
Khma = Khmb	3.13E-04 m/min	T matrix (20m)	9.0 m^2/day
Khf	2.14E+00 m/min	T fracture	616 m^2/day
Ssma	3.19E-04 /m	S matrix total (20m)	1.25E-02
Ssmb	9.27E-02 /m		
Ssf	8.55E-05 /m	S fracture	1.71E-05
La	1.07E-07 /min	K vertical matrix a	1.54E-04 m/day
Lb	8.24E-07 /min	K vertical matrix b	1.19E-03 m/day
Laf	4.27E-07 /min		
Lbf	4.78E-07 /min	Fracture Skin	

The estimated parameter values and their relation to each other are reasonable and the statistical data, listed in Table 6-14, validate a good fit. The maximum difference between observed and calculated drawdown is 0.058m, the mean value of all residuals is 2.95E-02, which is close to zero, and the correlation coefficient is close to 1.

Table 6-14 Statistical data for the best fit of inverse modelling

Phi (sum of squared weighted residuals)	34.66
Correlation coefficient	0.9504
Mean value of weighted residuals	2.95E-02
Maximum weighted residual	0.5850
Minimum weighted residual	-0.3871
Standard variance of weighted residuals	4.38E-02
Standard error of weighted residuals	0.2092

(obtained with 800 observations and a maximum weighting factor of 10)

A comparison of all reasonable results from the different calibration runs shows that the range of the parameter values is relatively small (between 2 and 7) and the results of the best fit are inside this range and mostly close to the mean value (see Table 6-15).

Table 6-15 Minimum, maximum and mean values of the estimated parameters, obtained from all reasonable calibration runs compared with the results of the best fit

Parameter	Unit	Best Fit	Min	Max	Mean
T matrix (aquifer)	m^2/day	9.0	7.8	24.8	13.3
T fracture	m^2/day	616	310	876	594
K horizontal matrix	m/day	0.45	0.39	1.24	0.66
K vertical matrix above	m/day	1.54E-4	1.01E-4	3.88E-4	1.86E-4
K vertical matrix below	m/day	1.19E-3	3.83E-4	1.19E-3	6.21E-4
K horizontal fracture	m/day	3080	1550	4381	2969
S matrix (aquifer)		1.25E-2	5.25E-3	1.50E-2	1.03E-2
S fracture		1.71E-5	3.99E-6	2.76E-5	2.21E-5

(d) UO5 – Test, September 2000

As shown in Table 6-16, the second constant discharge test with installed piezometers on the Campus Test Site was conducted at borehole UO5 for the abstraction with a discharge rate of 2 l/s for a period of 24 hours. The piezometers in boreholes UO23, UO27, UO28 and UO29 were used to observe the water level in the fracture zone and the rock matrix permanently with a dip meter. The water levels in boreholes UO6, UO7, UO20, UO26 and UO30 were also measured during the period of the test.

Table 6-16 Conditions for the constant discharge test UO5, conducted at Campus Test Site

Abstraction BH	Discharge Rate	Duration of test	Observation Boreholes (Distance to UO5 in Brackets)
UO5	2.0 l/s	1460 min	UO27a, b, c (each 11.5m); UO28a, b, c (each 27.25m); UO29a, b, c (each 75.9m); UO23a, b, c (each 97.9m); UO6a, b (each 5.3m); UO7 (7.0m), UO20 (16.2m), UO26 (16.1m), UO30 (92.5m)
	Recovery	not permanently measured	

(a: piezometer above the fracture, b: piezometer below the fracture, c: piezometer in the fracture zone)

The drawdown behaviour in the fracture-piezometers and the boreholes are similar to the above-mentioned UO5-test in July 2000. The water level in all boreholes dropped simultaneously and is in the same range as in the abstraction borehole UO5. Figure 6-22 shows the drawdown in the fracture while Figure 6-23 shows the drawdown in the matrix-piezometers.

Analytical Methods

Applying the porous media methods of Cooper-Jacob or Theis, the following parameter estimates are obtained.

Table 6-17 Results of the evaluated aquifer parameter for the constant rate test UO5, September 2000, obtained from the fracture- and the matrix-piezometers

Borehole	Cooper-Jacob Method		Theis Method		Comment
	T (m^2/d)	S (-)	T (m^2/d)	S (-)	
UO5	13.4	1.76E-03	13	2.12E-03	S-value calculated with effective BH Radius of 5 m
UO27c	13.8	3.55E-04	14	3.46E-04	Distance: 11.5m
UO23c	13.7	6.22E-06	13	7.00E-06	Distance: 98.0m
fracture	534	5.73E-40			Cooper-Jacob II
matrix above	1754	2.88E-01			Cooper-Jacob II
matrix below	165	5.67E-03			Cooper-Jacob II

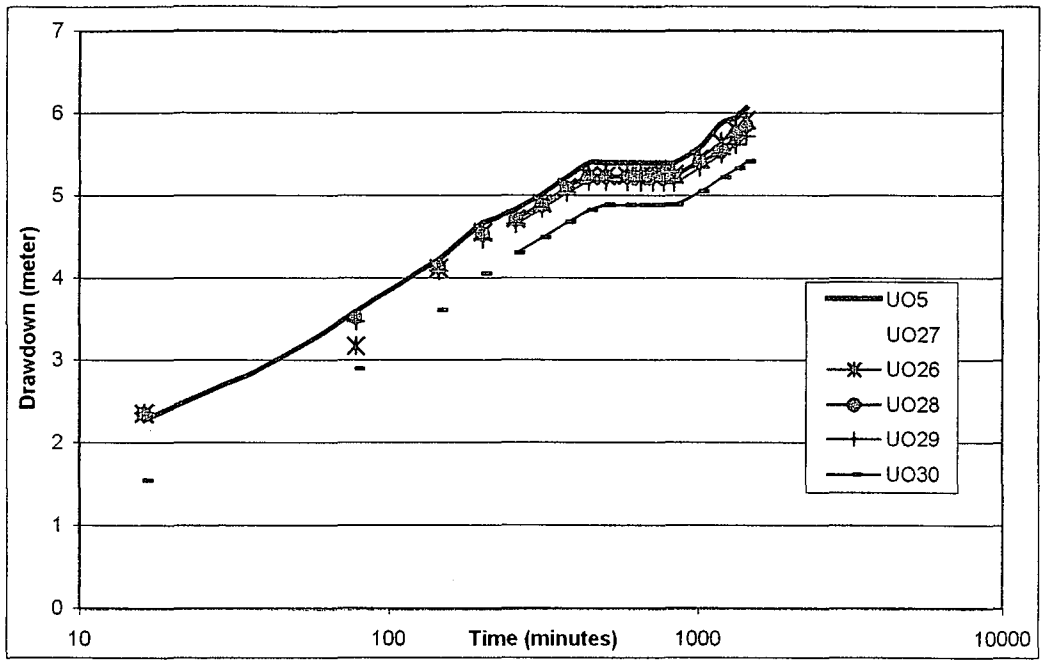

Figure 6-22 Drawdown in the fracture-piezometers during constant discharge test UO5, September 2000

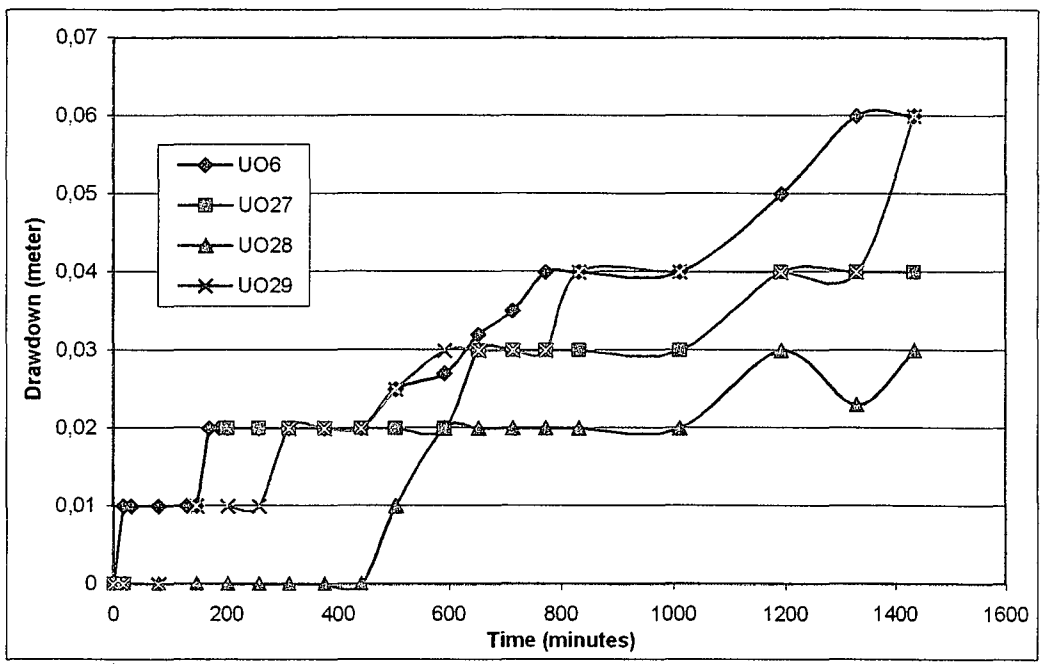

Figure 6-23 Drawdown in the matrix-piezometers during constant discharge test UO5, September 2000

3D-Numerical Model

The UO5 test from July 2000, used for the parameter estimation in section 6.1.2(c), was repeated in September 2000 with an abstraction rate of 2 l/s (see above). Using the parameter values obtained from inverse modelling of the UO5 test, July 2000, the observation data in both the fracture and matrix piezometers don't fit well (see Figure 6-24).

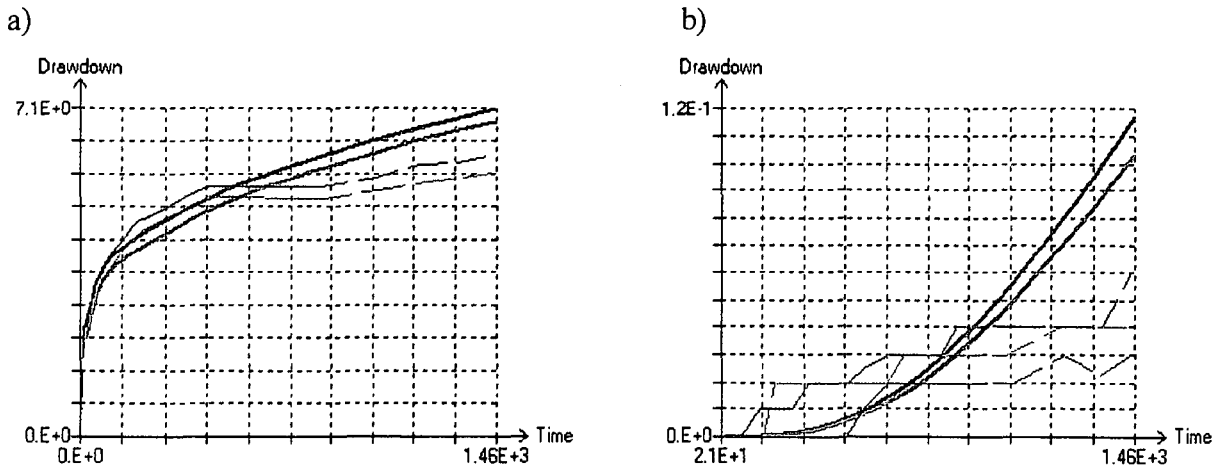

Figure 6-24 Comparison observed and calculated data for the UO5 test September 2000. Forward run with estimated values from UO5 test July 2000 a) Fracture piezometers, b) matrix piezometers above (bold = calibrated, fine = observed)

After calibrating the data with inverse modelling, the fit of the observation data in the matrix piezometers is better, and the estimated parameter values differ from the values obtained as the best fit from the UO5 test in July 2000, but they are still between the minimum and maximum values from the UO5 test in July 2000.

Table 6-18 Comparison of the estimated parameter values for the UO5 tests, July and September 2000, obtained from the best fit of inverse modelling (July 2000) and the geometric mean of reasonable runs of inverse modelling (September 2000)

Parameter	Unit	UO5 Test July 2000 Best Fit	UO5 Test Sept. 2000 Geometric Mean
Discharge Rate	l/s	0.5	2.0
T matrix (aquifer)	m^2/day	9.0	28
T fracture	m^2/day	616	530
K horizontal matrix	m/day	0.45	1.4
K vertical matrix	m/day	1.54E-4	1.8E-4
K horizontal fracture	m/day	3080	2650
S matrix (aquifer)		1.25E-2	8E-3
S fracture		1.71E-5	1.6E-5

6.1.3. Tracer Tests

On the Campus Test Site a number of tracer tests were conducted. While the older tests (van Wyk *et al.*, 2001) were conducted using a packer system to seal off the tested section, recently tracer tests with the proposed system of circulation pumping were conducted. The test data of some of these tests (single-well and multiple-well tests) are analysed with different approaches to compare the methods.

6.1.3.1. Single-Well Tests

The single-well tests, chosen for this case study, were conducted at boreholes UO20 and UO28.

(a) UO20

A point dilution test was performed on borehole UO20 by introducing 1 kg of NaCl in a section from 20.0 to 22.5 m in the borehole. The concentration was continuously mixed by circulating the water in the 2.5-m section with a submersible pump at a rate of 1 l/s and electric conductivity measurements were taken with an EC meter. Figure 6-25 shows the results of the dilution test.

After allowing the tracer to drift away for 90 minutes the tracer was pumped back at a rate of 1 l/s. Figure 6-26 shows the result of the withdrawal phase and Table 6-19 shows the results. The estimated average natural flow velocity by using fractional flow dimensions is two times higher when compared to the standard method.

Table 6-19 Parameter values obtained from the UO20 point dilution and single-well injection-withdrawal tests by using a flow dimension n = 1.75 and n = 2 respectively

	Point dilution (n=1.75)	Point dilution (n=2)	Injection-withdrawal (n=1.75)	Injection-withdrawal (n=2)
Kinematic porosity (from radial convergent test)	0.49	0.07	0.49	0.07
Darcy velocity (m/d)	11.4	0.63		
Seepage velocity (m/d)	23.2	9.28	20.3	10.0

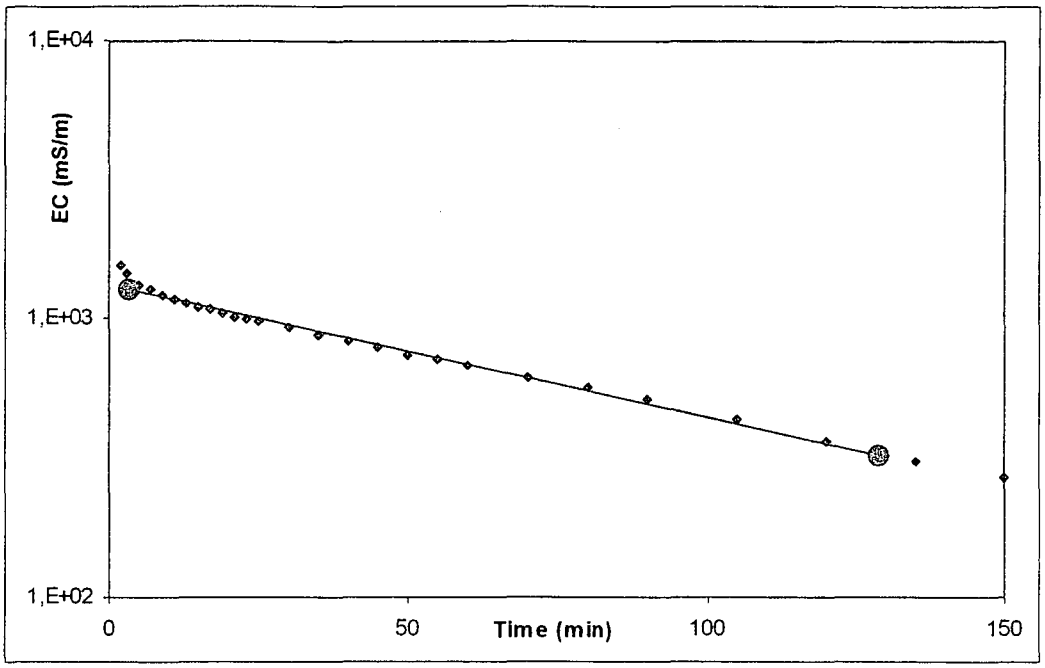

Figure 6-25 Point dilution measurements obtained in borehole UO20 under natural conditions

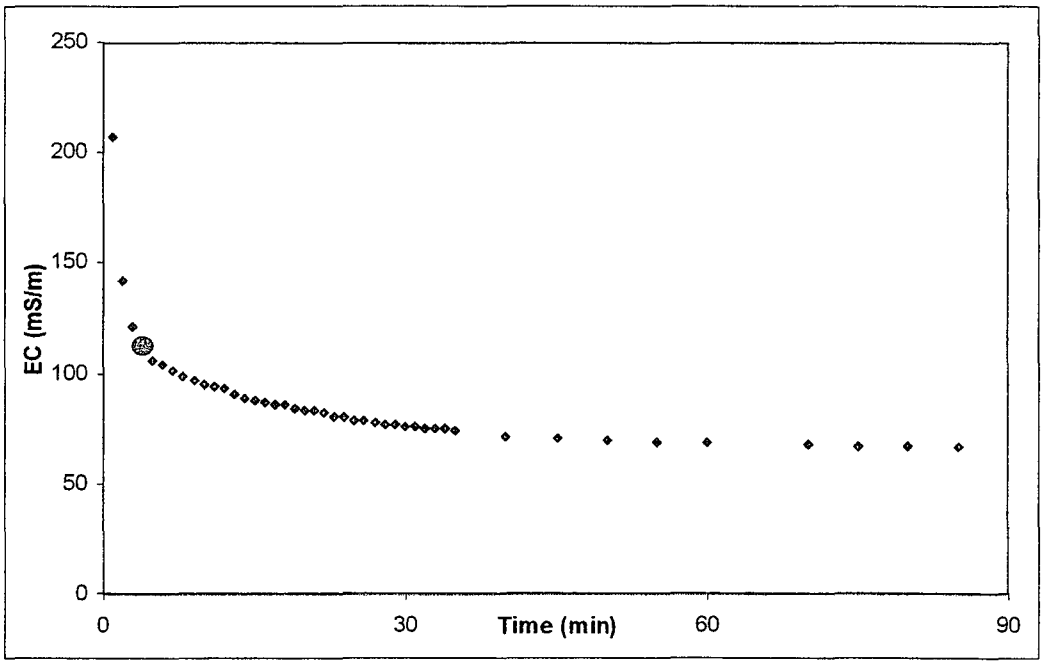

Figure 6-26 Tracer measurements measured during the pump back phase of the single-well injection-withdrawal test in borehole UO20. The large dot shows the tracer mass centre

(b) UO28

A point dilution test was performed on borehole UO28 by introducing 0.1 kg NaCl in a section from 20 to 22 m in the borehole. The concentration was continuously mixed by circulating the water in the 2-m section with a submersible pump at a rate of 0.3 l/s, and electric conductivity measurements were taken with an EC meter. Figure 6-27 shows the results of the dilution test. Using a flow dimension of 1.85, the Darcy velocity was estimated at 4.27 m/d. By using a kinematic porosity of 0.18 as estimated with a radial convergent test (see below), the natural flow velocity was estimated at 23.1 m/d.

The point dilution test was used as the injection part of the injection-withdrawal test. After 300 minutes of allowing the tracer to drift away from UO28, water was abstracted from UO28 at a rate of 0.3 l/s (see Figure 6-28 for the data of the withdrawal phase).

The centre of mass was recovered during the pump back phase after 60 minutes (= t_p) and using t_d = 301 minutes and kinematic porosity of 0.18, yields a seepage velocity of 21.4 m/d which is of the same order as the velocity estimate of 23.1 m/d obtained with the point dilution test. Both the point dilution and the single-well injection-withdrawal tests were also analysed using a flow dimension of 2 and the thickness of the section that was sealed off during the test. By using a flow dimension of 1.85 instead of the standard value of 2, the estimated natural velocity is a factor of two times higher (see Table 6-20).

Table 6-20 Parameter values obtained from the UO28 point dilution and single-well injection-withdrawal tests by using a flow dimension n = 1.85 and n = 2 respectively

	Point dilution (n=1.85)	Point dilution (n=2)	Injection-withdrawal (n=1.85)	Injection-withdrawal (n=2)
Kinematic porosity (from radial convergent test)	0.18	0.02	0.18	0.02
Darcy velocity (m/d)	4.27	0.26		
Seepage velocity (m/d)	23.1	12.9	21.4	11.8

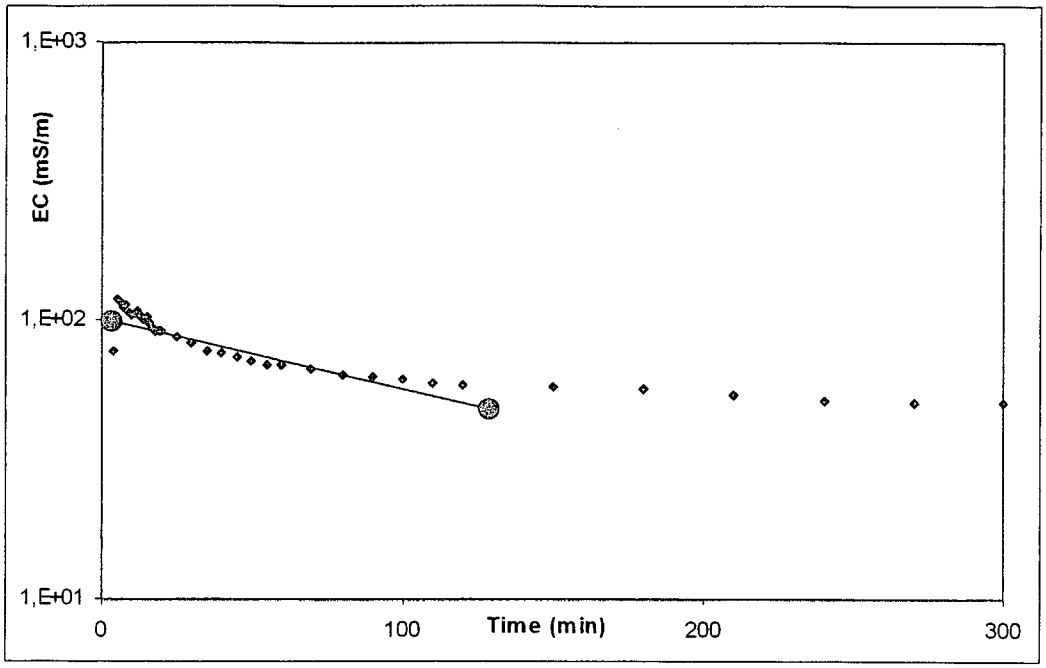

Figure 6-27 Point dilution measurements obtained in borehole UO28 under natural conditions

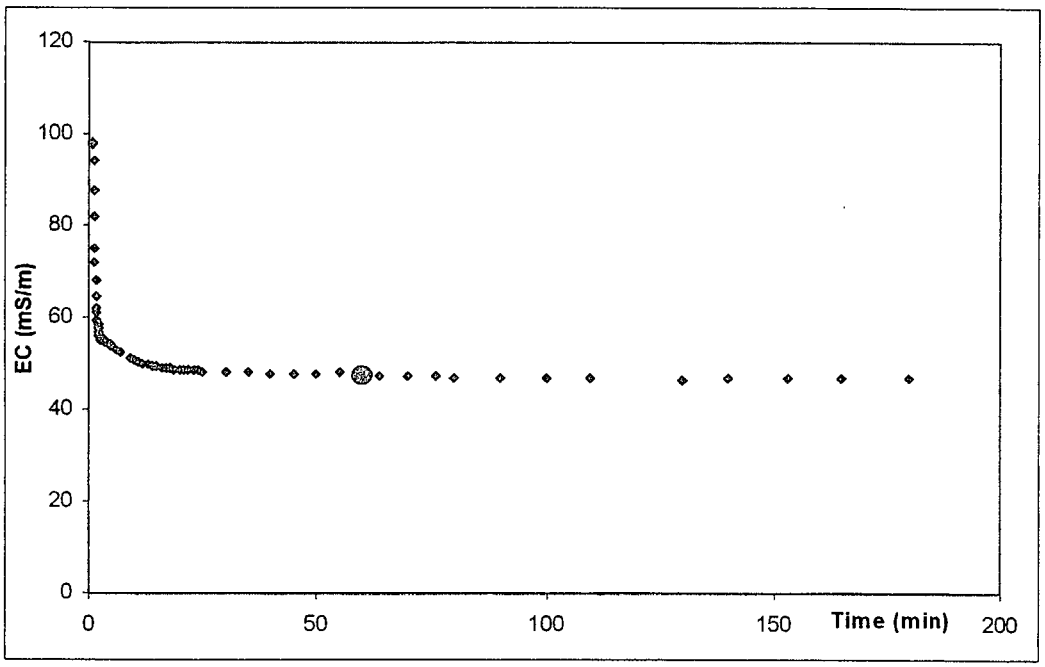

Figure 6-28 Tracer measurements measured during the pump back phase of the single-well injection-withdrawal test in borehole UO28. The large dot shows the tracer mass centre

6.1.3.2. Multiple-Well Tests

The multiple-well tests chosen for this case study were conducted at boreholes UO5 and UO26 as radial convergent tests.

(a) UO5 – Test

Borehole UO20 was used as the source borehole while UO5 was used as the abstraction borehole. Water was abstracted from UO5 at a rate of 1 l/s for 3 hours (until a steady state gradient between UO5 and UO20 existed). A section in borehole UO20 between 20.5-21.5 m below surface was sealed off with packers and NaCl and NaBr was introduced into UO20 (mass of 0.048 kg NaCL and 0.06 kg NaBr). The solution was mixed by circulating the water with a small pump the whole time.

Figure 6-29 and Figure 6-30 show the point dilution and breakthrough curve obtained during the UO5-tracer test. A flow dimension of n = 1.75 was used to estimate the throughflow area, which was used to estimate the Darcy velocity at 24.9 m/d. A fit to the breakthrough data obtained in UO5 yielded a seepage velocity of 51 m/d and an effective fracture zone thickness of 0.15 m between UO20 and UO5. The combination of the estimated Darcy and seepage velocity yielded a kinematic porosity value of 0.49. The standard method (i.e. using n=2 and b = thickness of the sealed-off section) was also used to estimate the parameters. Table 6-21 shows the estimated parameters obtained from the test.

Table 6-21 Parameter values obtained from the UO5-tracer test by using a flow dimension n = 1.75 and n = 2 respectively

Borehole	UO20 (n=1.75)	UO20 (n=2)	UO20 -> UO5 (n=1.75)	UO20 -> UO5 (n=2)
Darcy velocity (m/d)	24.9	3.48		
Forced flow velocity (m/d)	51 (from RCT)	51 (from RCT)	51	51
Thickness of fracture zone (m)	0.15 (b from Barker)	1 (sealed off section*)	0.15 (= fitted)	0.15 (= fitted)
Kinematic porosity	0.49	0.07	0.49	0.12

* The length of the sealed-off section was used in this comparison to illustrate the influence of unknown thickness of the fracture zone

The estimated seepage velocities in the table above are both 51 m/d because the same model was used in both cases. The influence that the flow dimension has on the estimated parameters is revealed by the different values for the Darcy velocity and the effective porosities that were obtained.

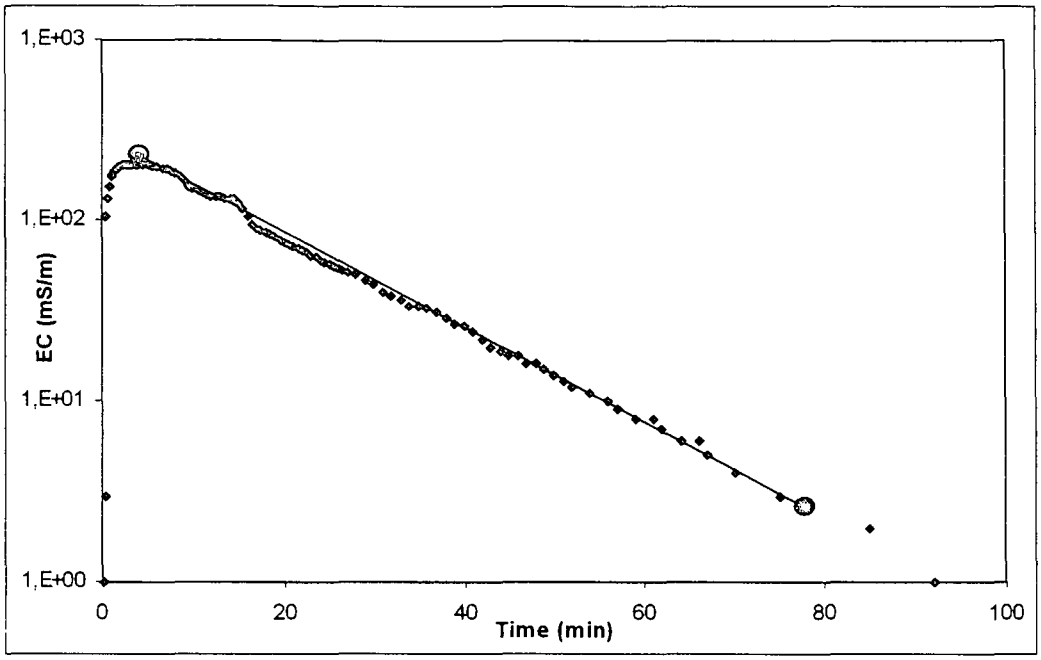

Figure 6-29 Point dilution measurements obtained during the UO5-tracer test in the injection borehole UO20

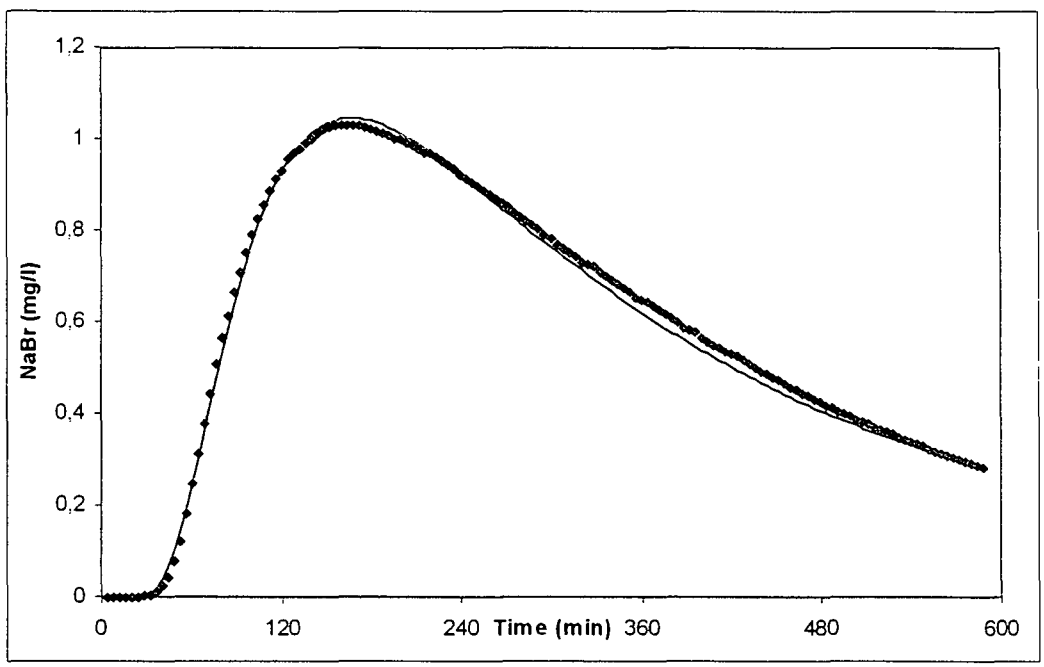

Figure 6-30 NaBr breakthrough curve and best fit obtained in the abstraction borehole (UO5) during the radial convergent UO5-tracer test. Fitted parameters obtained were v=51 m/d, dispersivity = 5.4 m and thickness = 0.15 m.

(b) UO26 – Test

A similar radial convergent test as the UO5-tracer test was conducted between UO26 and UO28, with UO28 as the source borehole and UO26 the abstraction borehole. A pseudo steady state flow was created by abstracting water from UO26 at a rate of 0.7 l/s for three hours. A pulse of 0.2 kg NaCl and 0.02 kg Uranine was introduced in borehole UO28 in the interval 20-22 m below surface and mixing of the solution was obtained by circulating the water continuously. A fluorometer was used to measure the Uranine breakthrough curve in UO26. Figure 6-31 and Figure 6-32 show the point dilution measurements in UO28 and the breakthrough curve in UO26 respectively. The estimated parameters are shown in Table 6-22.

Table 6-22 Parameter values obtained from the UO26-tracer test by using a flow dimension n = 1.85 and n = 2 respectively

Borehole	UO28 (n=1.85)	UO28 (n=2)	UO28 -> UO26 (n=1.85)	UO28 -> UO26 (n=2)
Darcy velocity (m/d)	9.44	0.73		
Forced flow velocity (m/d)	51 (from RCT)	51 (from RCT)	51	51
Thickness of fracture zone (m)	0.16 (b from Barker)	2 (sealed off section)	0.16 (= fitted)	0.16 (=fitted)
Kinematic porosity	0.18	0.02	0.18	0.08

* The length of the sealed-off section was used in this comparison to illustrate the influence of unknown thickness of the fracture zone

The best fit of the breakthrough curve again yielded a flow velocity of 51 m/day, a kinematic porosity of 0.18 and an effective thickness of the fracture zone of 0.16 m. The influence that the flow dimension has on the estimated Darcy velocity and the kinematic porosity can be observed clearly from the table above.

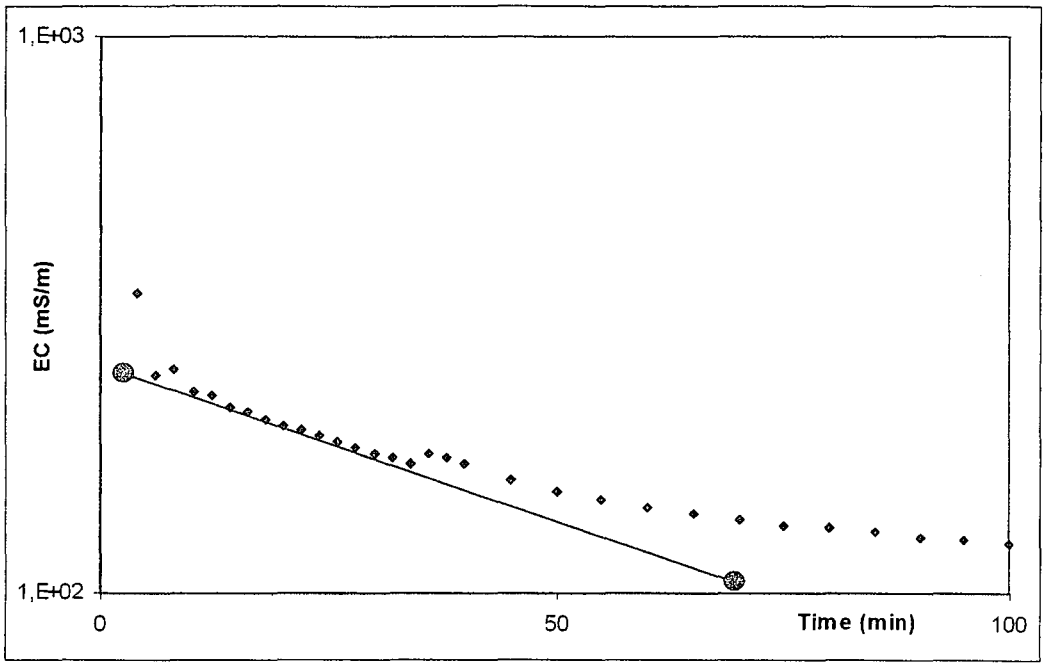

Figure 6-31 Point dilution measurements obtained during the UO26-tracer test in the injection borehole UO28

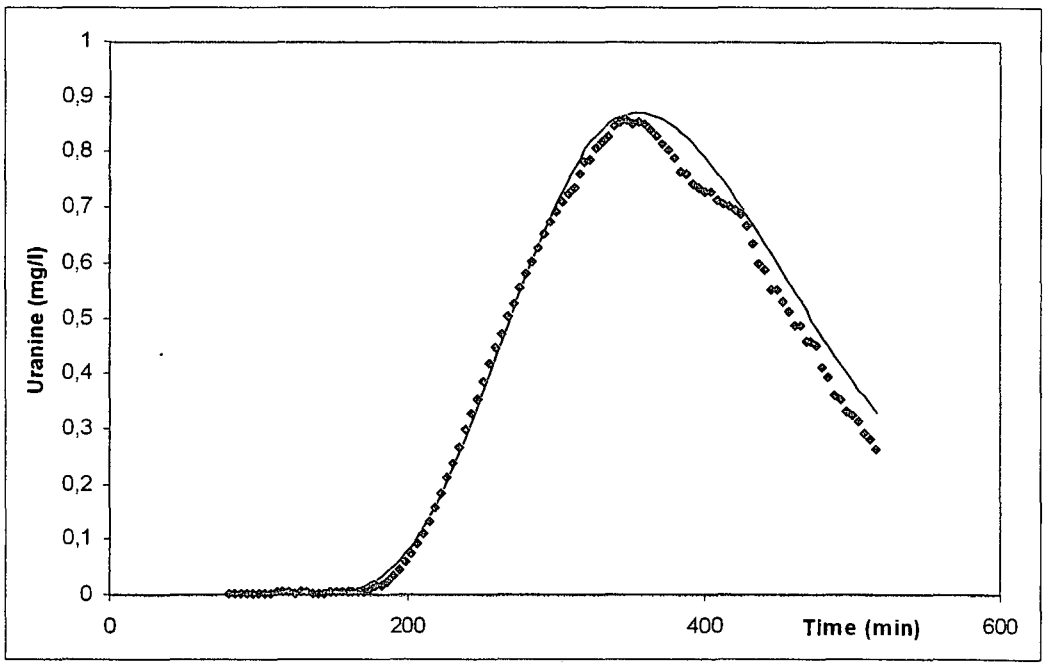

Figure 6-32 Uranine breakthrough curve and fit obtained during the UO26-tracer test (radial convergent). Fitted parameters obtained were v=51 m/d; dispersivity = 0.5 m and thickness = 0.16 m.

6.2. *Meadhurst Test Site*

The Meadhurst Test Site is situated approximately 16 km outside Bloemfontein in the Bainsvlei smallholdings area. Twenty boreholes have been drilled on the site, 12 of which have been equipped with pumps mainly for irrigation or domestic use. The investigation for this project was situated on site A, located in the south of the whole site and consists of 10 boreholes along the dyke and on both sides of the dyke respectively. The locations of the boreholes are shown in Figure 6-33.

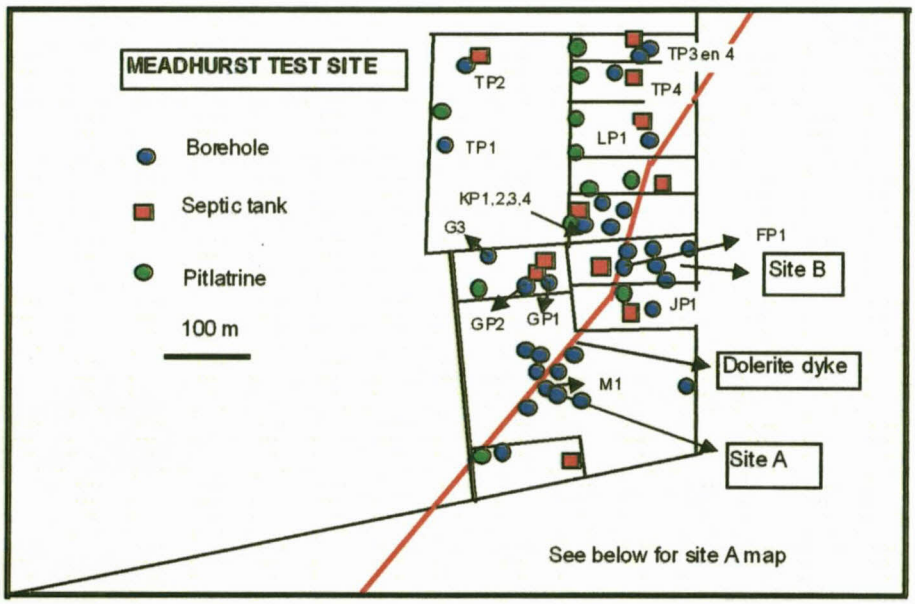

Figure 6-33 Position of boreholes, pitlatrines and septic tanks at Meadhurst test site

6.2.1. Geology

The general geology of the area is made up of Karoo sandstone, dolerite sills, dolerite dykes and mudstone. The intrusion of dolerite caused fracturing in the less elastic layers. The top layer consists of red and orange-red soil and sand with a thickness of approximately 20m. It is underlain by dolerite, which is mostly weathered. Under this aquifer lies a thick layer of mudstone. The mudstone and the dolerite layer are cut by a dolerite dyke, which falls at about 45° towards the south-east. The average water level is 19m below surface and occurs normally in the top soil or in the underlying weathered dolerite sill. Figure 6-34 shows the geological set-up of the Meadhurst Test Site by means of the borehole log for M1.

Water strikes occur in the weathered dolerite (about 0.4 l/s) and in parallel fractures in the dyke and the contact zone between the dyke and mudstone (up to 3 l/s). Due to the width of the dyke the yield of the boreholes directly on the dyke, varies between 0.7 and 3 l/s.

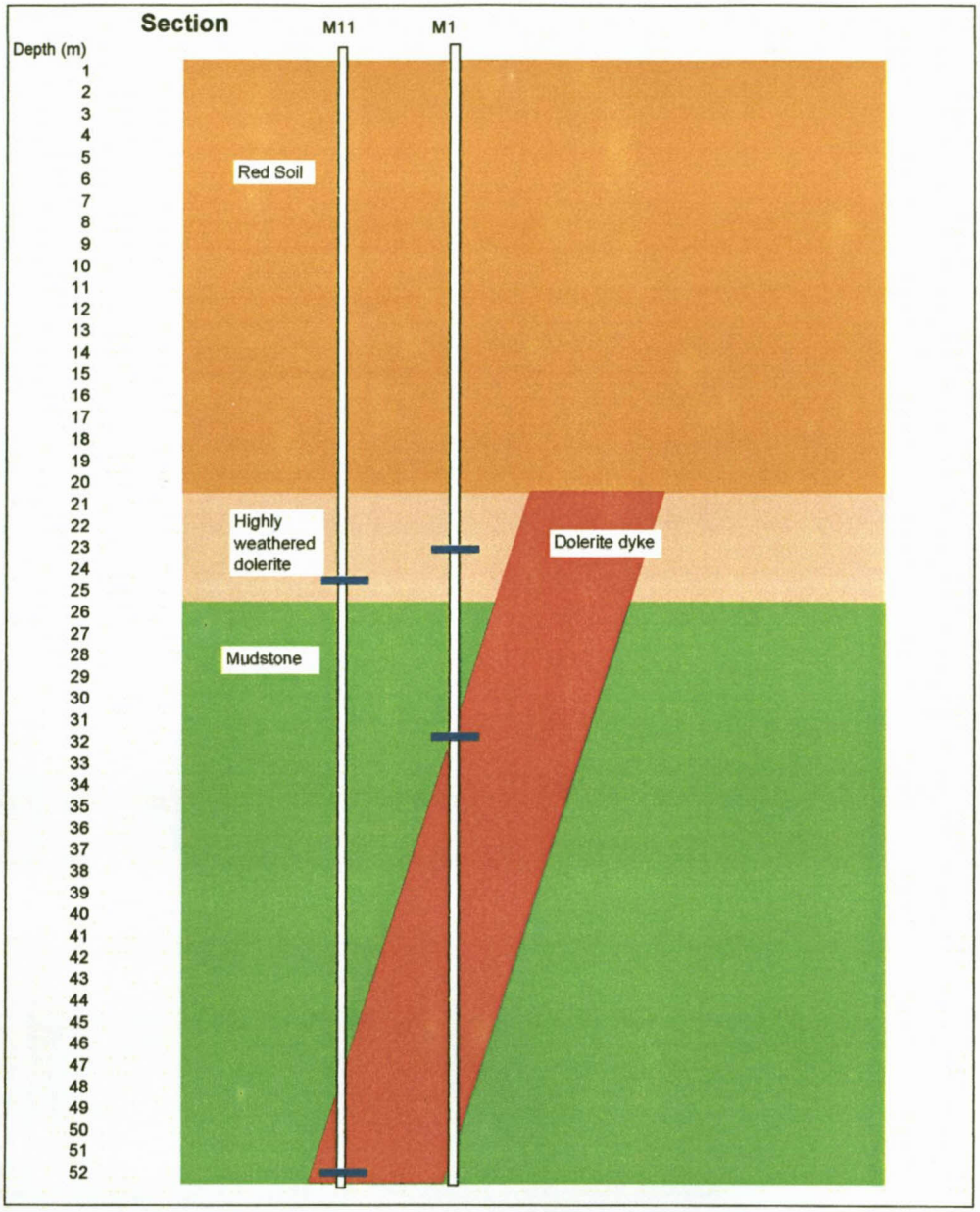

Figure 6-34 Borehole logs of M1 and M11, intersecting the dolerite dyke

The conceptual model for the Meadhurst Test Site bases on the geology and hydrogeology of the site. The main aquifer is situated in a nearly vertical dyke with fractures parallel to the conduct zone (M1) or in the dyke (M11). Other water strikes were found during drilling in the overlying dolerite, high weathered sandstone, and smaller water strikes in fracture zones in the mudstone. The extent and aperture of the fracture zones are unknown. It is also still not clear, whether the water strikes, related to the dyke, are connected with each other.

Compared to the high hydraulic conductivity of the fracture the hydraulic conductivity of the matrix is small. But the storage of the matrix is much higher than that of the fracture.

In a case of a vertical or nearly vertical fracture parallel to a dyke, at least three aquifer systems have to be taken into account when analysing a hydraulic test:

- The vertical fracture zone as the main aquifer
- The matrix of the layer in which the fracture zone occurs (here: mudstone)
- The dyke which can be treated as a barrier

Additionally on the Meadhurst Test Site there is the weathered dolerite layer, which overlies the mudstone but is intersected by the dyke and the main fracture. This dolerite layer has water strikes and therefore has to be treated as a hydraulic part of the aquifer.

During pumping in the fracture, it is assumed that groundwater is released from the matrix, flows horizontally to the fracture or vertically to the weathered dolerite and along the dolerite to the fracture. Finally, groundwater flows along the fracture to the pump.

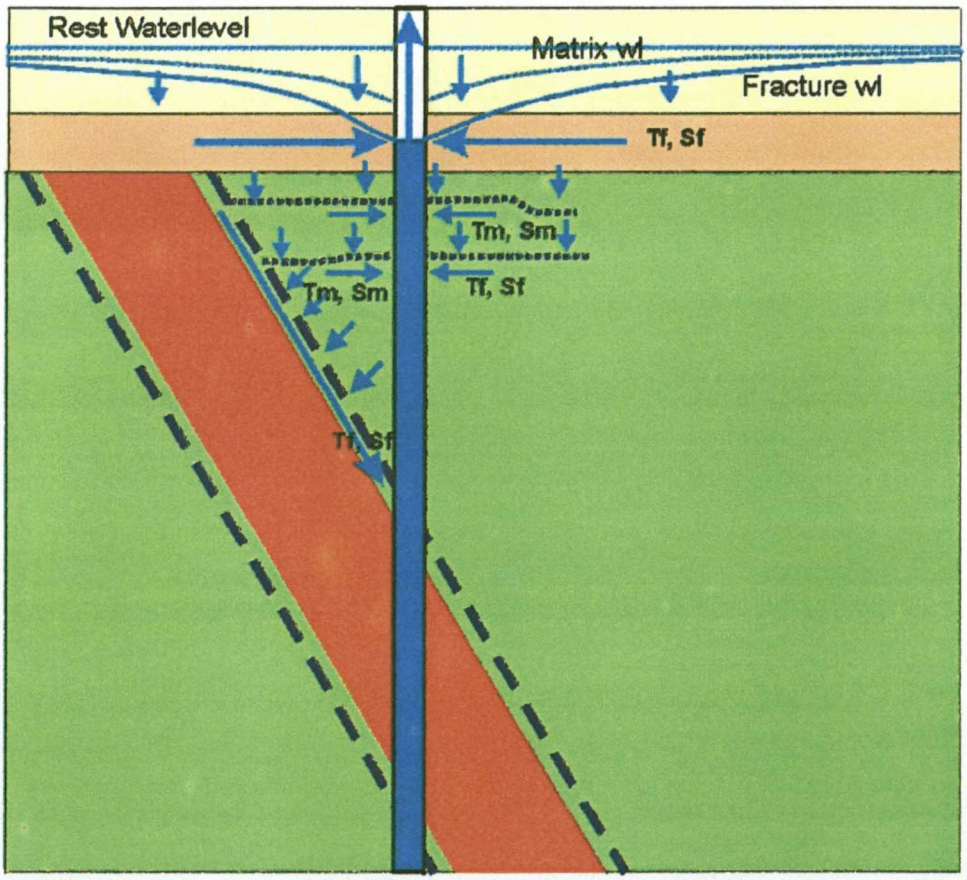

Figure 6-35 Conceptual model of the flow in the Meadhurst aquifer, intersected by an abstraction borehole (after Barnard, 2001)

6.2.2. Hydraulic Tests

The hydraulic tests chosen for this case study were conducted at the boreholes M1 and M11.

(a) M1 – Test

As shown in Table 6-23 the constant discharge tests on the Meadhurst Test Site were conducted at borehole M1 for the abstraction with a discharge rate of 1.4 l/s and 2.0 l/s respectively for a period of 16 and 18 hours. Boreholes M2, M5 and M6 were used for the first test to observe the water level in the aquifer permanently with a pressure transducer and automatic data logger. In the other boreholes listed in Table 6-23 the water levels were measured with a dipmeter over the whole period of the test. During the second test only the water level in the abstraction borehole was measured.

Table 6-23 Conditions for the constant discharge tests, conducted at Meadhurst Test Site

Abstraction BH	Discharge Rate	Duration of test	Observation Boreholes (Distance to M1 in Brackets)
M1	1.4 l/s	960 min	M2 (21.75m), M3 (21.97m), M4 (34.37m), M5 (80.2m), M6 (35.84m), M7 (55m), M8 (77.5m), M9 (86m)
	Recovery	120 min	
M1	2.0 l/s	1080 min	No observation data available
	Recovery	120 min	

Figure 6-36 shows the data and graphs of the first test for the abstraction borehole M1 and the nearest observation borehole M2. The behaviour of the drawdown in both boreholes are very similar, even the jump in the drawdown due to the change of the discharge rate after around 8 minutes is observed easily in both boreholes.

In the other boreholes, intersecting the dyke, the drawdowns reach maximum 25 cm in M3 and less than 10 cm in M5 and M6. In boreholes M8, M9 and M10 outside the dyke which do not intersect the main fracture, no drawdown was observed.

The drawdowns in boreholes M2 and M3, both intersecting the dyke with a distance of 2m from each other and almost the same distance from the abstraction borehole M1, show different behaviour. While drawdown values in M2 and M3 react in the same way as those of the abstraction borehole M1 (Figure 6-36 and Figure 6-37), the drawdown in M3 is much less (Figure 6-37). This shows that hydraulic contact between M1 and M2 is better than between M1 and M3. Similar behaviour can be observed in M6.

To estimate the transmissivity and storativity of the aquifer, analytical methods and a numerical model were applied to the test data, as discussed below.

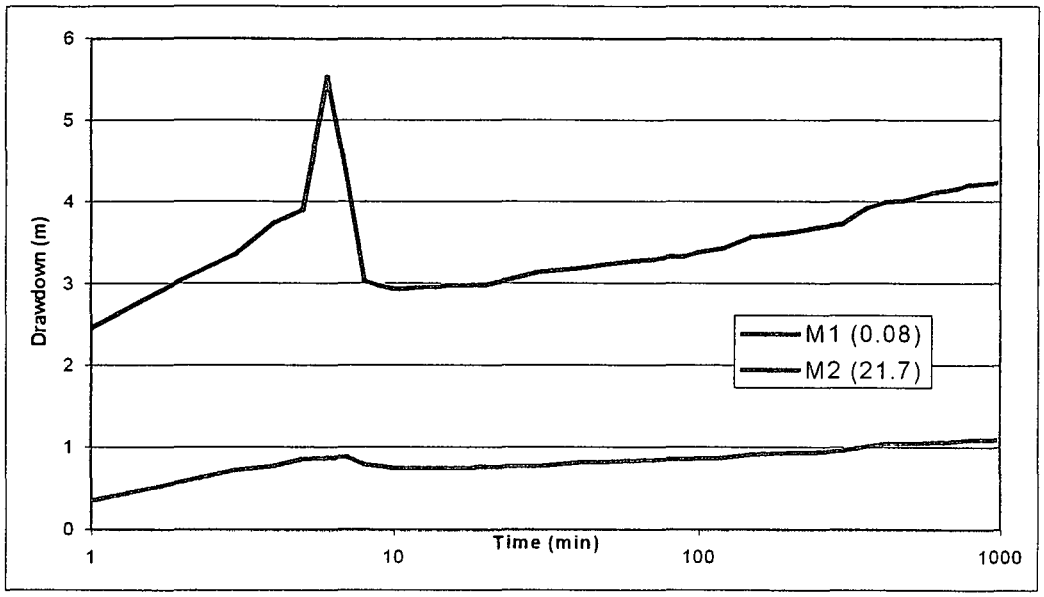

Figure 6-36 Drawdown in the abstraction borehole M1 and the observation borehole M2 during the constant rate test with 1.4 l/s at Meadhurst Test Site

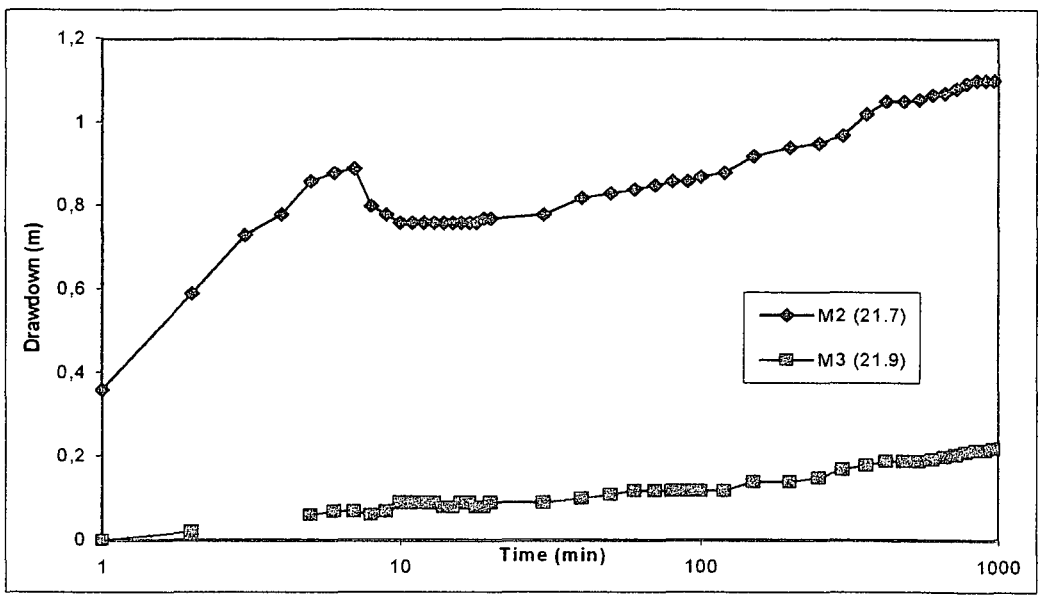

Figure 6-37 Drawdown behaviour of the observation boreholes M2 and M3

Analytical Methods

The estimation of the transmissivity for the different boreholes, using the methods from Theis and Cooper-Jacob, yields values of between 23.8 m^2/d and 294 m^2/d (see Table 6-24). The high values were estimated for boreholes with a small drawdown like M3, M5 and M6. In the same boreholes large values for the storage coefficient of between 3E-3 and 3E-2 were estimated, while the storage coefficient in the boreholes M1 and M2 was estimated at 2E-5, which makes more sense for the fracture system.

Using the drawdown-distance method (Cooper-Jacob II) an average T-value for the fracture is estimated at 35 m^2/d and an average storage coefficient S at 3E-5. From the graph (see Figure 6-38) it can be shown that these values are only valid for boreholes M1, M2 and M5, while the plots of boreholes M3 and M6 lie outside the straight line. This shows that these boreholes do not have good hydraulic contact with the fracture system M1 – M2 – M5.

From the figures and Table 6-24 it can be seen that the application of Cooper-Jacob or Theis methods cannot yield correct values in this case, due to the different behaviour of the fractured aquifer, because these methods are only valid for porous media and under restrictive assumptions.

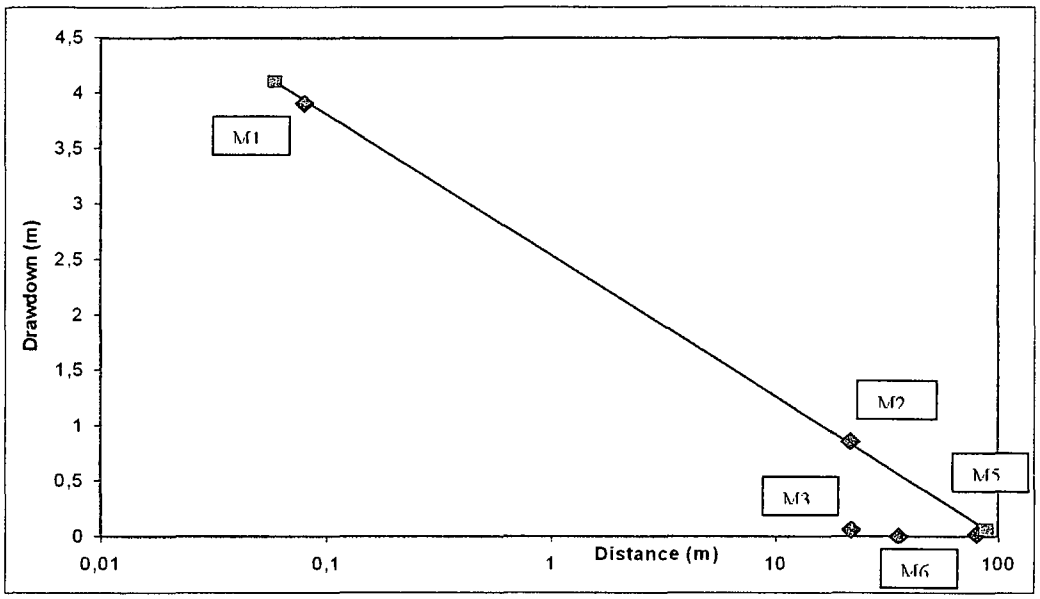

Figure 6-38 Drawdown-distance plot of the constant rate test at Meadhurst Test Site

Table 6-24 Results from the Constant Rate Test at Meadhurst Test Site, using the standard methods of Cooper-Jacob and Theis.

	Cooper-Jacob Method		Theis Method		
Borehole	T (m^2/d)	S (-)	T (m^2/d)	S (-)	Comment
M1, 1st	23.8	2.00 E-5	24	1.70 E-5	S-value calculated with effective BH Radius
M1, 2nd	21.3	1.17 E-6	22	1.00 E-6	
M2	82.1	1.90 E-5	82	1.90 E-5	
M3	167.5	1.09 E-2	182	8.50 E-3	T- and S-values are too high for the system
M5	294.4	3.87 E-3	292	4.40 E-3	
M6	273.7	3.19 E-2	273	3.49 E-2	
all	34.75	3.07 E-5			Cooper-Jacob II for fracture zone

Numerical Model

By using all observation data and the parameter values obtained from step 2 and step 3 as initial parameter values, the drawdown curves were obtained after running PEST and compared with observed curves (Figure 6-39). Except the abstraction borehole M1, which undergoes wellscreen loss, the fit is acceptable and the estimated parameter values are shown in Table 6-25.

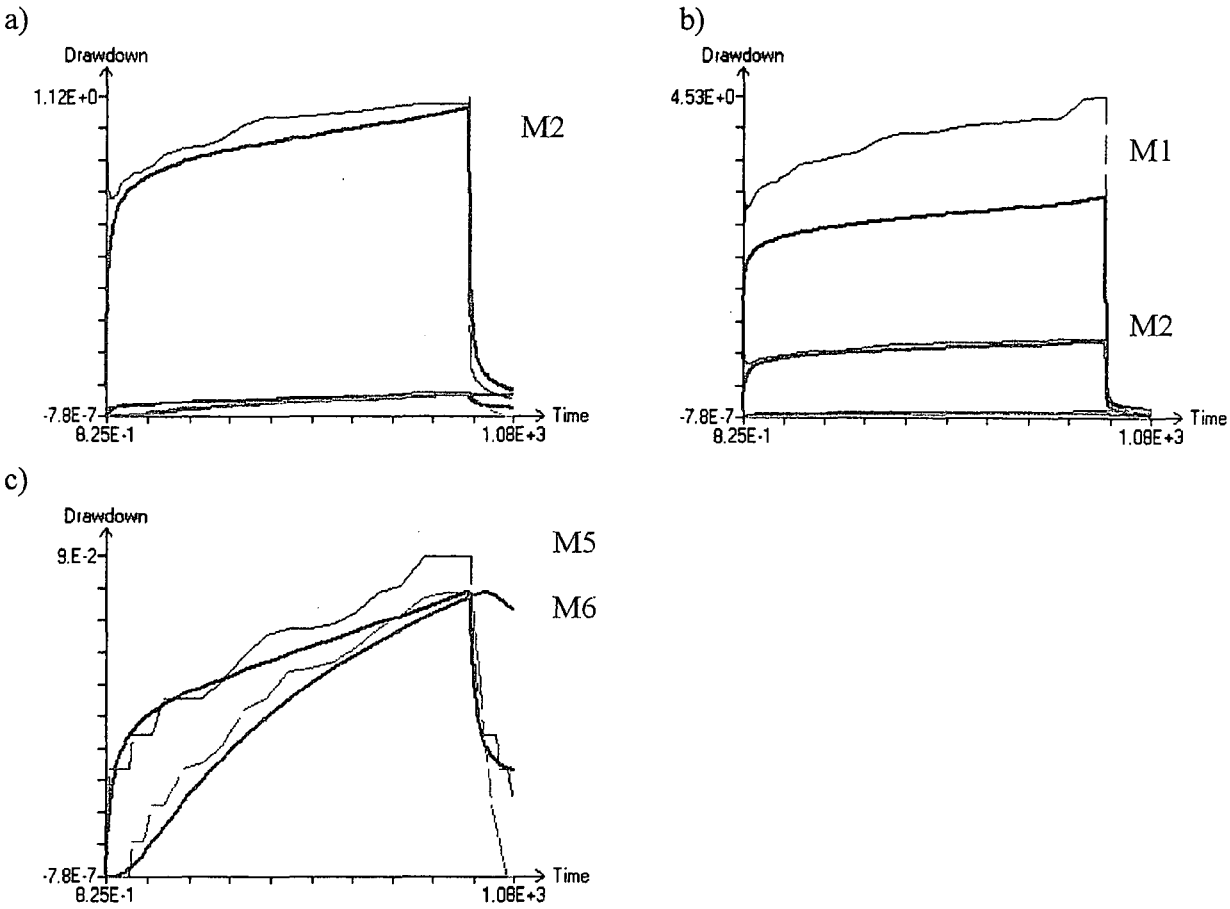

Figure 6-39 Comparison observed (fine line) and calculated drawdown (bold line) of the best fit; using the observation boreholes M2, M5 and M6. a) Observation borehole M2, b) Abstraction borehole M1 (data not used for calibration), c) Observation boreholes M5 and M6

Table 6-25 Estimated parameter values of forward modelling (best fit) with observation data of boreholes M2, M5 and M6 (comparison of observed and calculated drawdown shown in Figure 6-39)

Parameter (model)	Value	Parameter (aquifer)	Value
K dolerite	5.3E-02 m/min	T dolerite (5m)	382 m^2/day
K fracture	2.8E-03 m/min	T fracture (30m)	121 m^2/day
K mudstone	8.0E-06 m/min	T mudstone (25m)	0.3 m^2/day
K dyke	1.0E-06 m/min	T dyke (30m)	0.04 m^2/day
Ss dolerite	1.3E-03 /m	S dolerite (5m)	6.5E-03
Ss fracture	5.0E-05 /m	S fracture (30m)	1.5E-03
Ss mudstone	1.2E-04 /m	S mudstone (25m)	3.0E-03

(b) M11 – Test

Borehole M11 was drilled along the dolerite dyke with the main water strike 30 m below the rest water level, which is situated at 22 m below surface. The dolerite dyke was intersected at 28 m below the rest water level. At 30 m below the rest water level a water strike of 4 L/s was encountered in the dolerite. Two constant rate tests were performed on M11 - one at 3 L/s and the other at 7 L/s. Figure 6-40 shows the pumping test results as well as information on the water strikes.

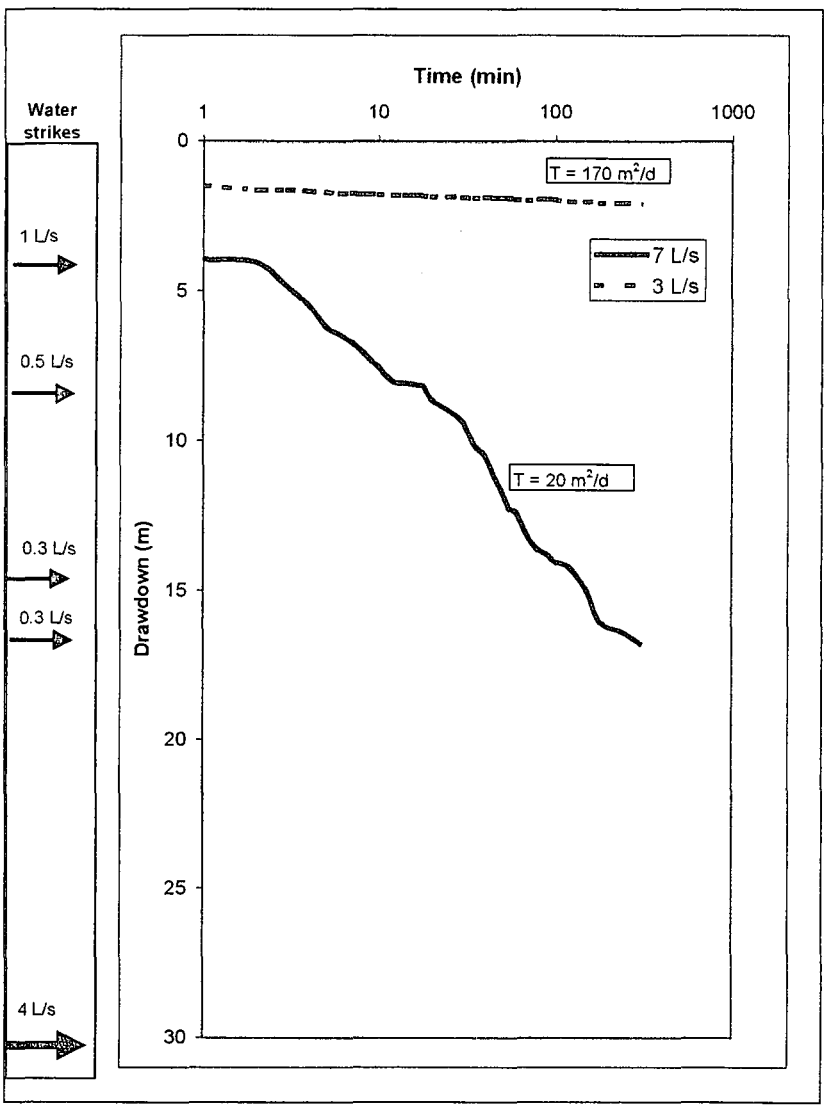

Figure 6-40 Pumping test results and water strike information of borehole M11 on the Meadhurst Test Site

It is obvious that the results from the two abstraction rates produced different drawdown curves. The estimated T-value with the 3 L/s abstraction rate is 170 m^2/d, while the estimated T-value for the 7 L/s abstraction rate is 20 m^2/d. At a rate of 7 L/s, the fractures could not sustain the abstraction rate with the result that the estimated T-value of 20 m^2/d is the formation T-value, while the lower rate gives a T-value more representative of the fractures.

6.2.3. Tracer Tests

During the time of this research no tracer test were conducted at the test site A, because the boreholes were used continuously for irrigation purposes. Van Wyk et al. (2001) conducted several tracer tests at the test site B north of test site A. Since most of these tracer tests were not conducted in the way proposed in Chapter 5, only the multiple-well tracer test at borehole FP1 is chosen for re-interpreting applying the approach of non-integer-flow dimension.

Borehole FP1 was used to abstract water at a constant rate of 0.8 L/s to create a radial flow field. The drawdown data in borehole FP1 are analysed applying the GRF-model of Barker (1988) to estimate the flow dimension and flow domain. A value for the flow dimension of 1.62 is obtained, indicating a bilinear, partially dimensioned flow.

After a steady state situation was established, a mass of 100g fluorescein was introduced into borehole F4, 29 m apart. From the dilution in the injection borehole the Darcy velocity is estimated at 0.41 m/day, using the values for the flow dimension and flow domain, as obtained from the hydraulic test. The obtained breakthrough curve in the abstraction borehole FP1 (see Figure 6-41) shows a behaviour which cannot be analysed with the standard analytical methods, such as Sauty (1980). The shape of the curve can be interpreted as multi peaks caused by different flowpaths of various path lengths and / or flow velocity.

The different simulations shown in Figure 6-41 are calculated with the approach of Sauty (1980) and should indicate the possible different pathways. Because superimposing of the various breakthrough curves of each pathway results in the measured tracer concentration, no analytical method is applicable to analyse multi peak breakthrough curves.

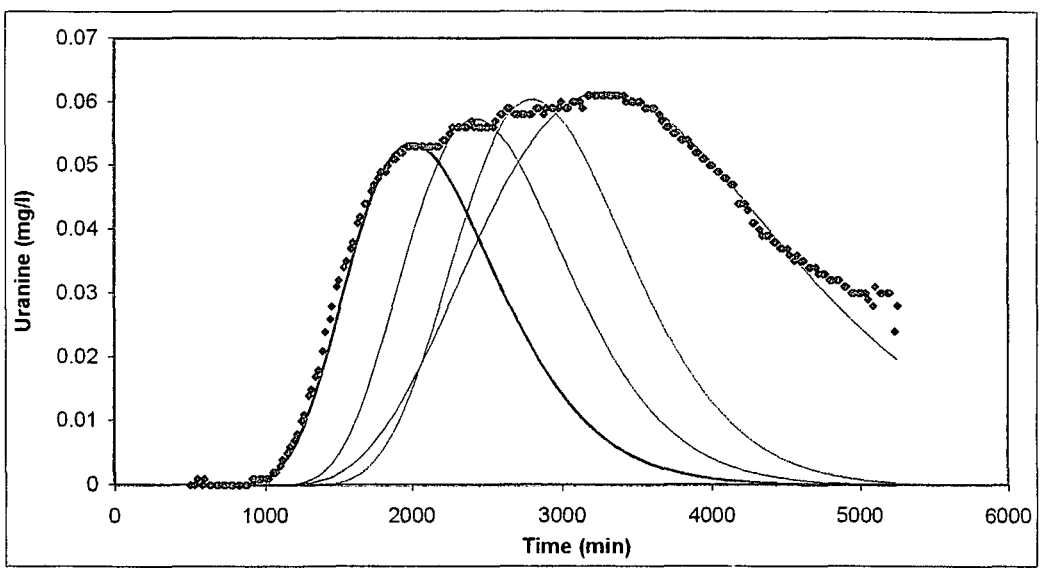

Figure 6-41 Breakthrough curve of fluorescein in borehole FP1 during Radial Convergent Tracer Test, including simulations of various peaks

6.3. Farm Griesel

Besides the main test sites on Campus and Meadhurst, the methods described in this thesis were applied to other sites with different geological and hydrogeological settings.

The test site on the farm Griesel is situated about 30 km west of Bloemfontein. Two boreholes were drilled in the same area where surface geophysical measurements (Nuclear Magnetic Resonance, NMR) were previously conducted by the CSIR (Meyer, 2001). The distance between the boreholes is about 6 m. Below a red and brown soil of about 16 m follows siltstone, which contains the main water strike at 21 m and 22 m, respectively. This siltstone is underlain by black mudstone, which was not drilled through up to the borehole depth of 70 m.

6.3.1. Tracer Tests

The purpose of the tests was to verify the method for estimating the porosity using a single-well tracer test (as described in section 4.2.3.4) and to compare the results with the geophysical measurements of the CSIR. The NMR technique provides direct measurements of the content of mobile water in the subsurface, which should be equal to the kinematic porosity in the saturated zone.

In January and February 2001 several single-well tracer tests were conducted at different depths in borehole BH 2.

Table 6-26 Conducted Tracer Tests at Test Site Griesel

Borehole	Depth	Kind of Test
BH2	19 – 21 m	Point Dilution and Injection Withdrawal
BH2	21 – 23 m	Point Dilution and Injection Withdrawal
BH2	24 – 26 m	Point Dilution and Injection Withdrawal
BH2	26 – 28 m	Point Dilution and Injection Withdrawal
BH2	29 – 31 m	Point Dilution and Injection Withdrawal
BH2	34 – 36 m	Point Dilution and Injection Withdrawal
BH2	39 – 41 m	Point Dilution and Injection Withdrawal
BH2	44 – 46 m	Point Dilution and Injection Withdrawal
BH2	49 – 51 m	Point Dilution and Injection Withdrawal
BH2	54 – 56 m	Point Dilution and Injection Withdrawal

The single-well tests show a high variety of flow velocity over the whole depth of the borehole, which differs mainly in time due to pumping production boreholes nearby. The estimation of the kinematic porosity obtained from single-well tracer tests yield values between 1% and 7%, which compares well to the results of the NMR technique. The test data and analysis are shown in Appendix A. A summary of the results is listed in Table 6-27.

Table 6-27 Results from Single Well Tracer Tests at Test Site Griesel

Depth of tested section	Darcy Velocity (Point Dilution)	Flow Velocity (Inject.-Withdrawal)	Kinematic Porosity
19 – 21 m	0.06 m/day	5.48 m/day	1.1 % ± 0.5 %
21 – 23 m	0.07 m/day	1.97 m/day	3.7 % ± 0.5 %
24 – 26 m	0.39 m/day	11.45 m/day	3.4 % ± 0.5 %
26 – 28 m	0.16 m/day	8.57 m/day	1.6 % ± 0.5 %
29 – 31 m	0.35 m/day	14.11 m/day	2.5 % ± 0.5 %
34 – 36 m	0.30 m/day	13.95 m/day	2.1 % ± 0.5 %
39 – 41 m	0.62 m/day	8.68 m/day	7.1 % ± 2.0 %
44 – 46 m	0.50 m/day	9.76 m/day	5.1 % ± 2.0 %
49 – 51 m	0.66 m/day	4.76 m/day	13.9 % ± 2.0 %
54 – 56 m	2.56 m/day	n.a.	n.a.

The single-well tracer tests, conducted on the test site on the farm Griesel, yield values of the kinematic porosity between 1 % and 7 %, which compares well to the estimation obtained from applying the NMR technique (see Figure 6-42). The variety in the Darcy and flow velocity observed over the whole depth of borehole BH2 depends mainly on the date, when the test was conducted. The tests yielding a Darcy velocity under 0.1 m/day were conducted when no production wells were abstracting water, while the other tests were conducted on days when the production well nearby was abstracting water for irrigation purposes.

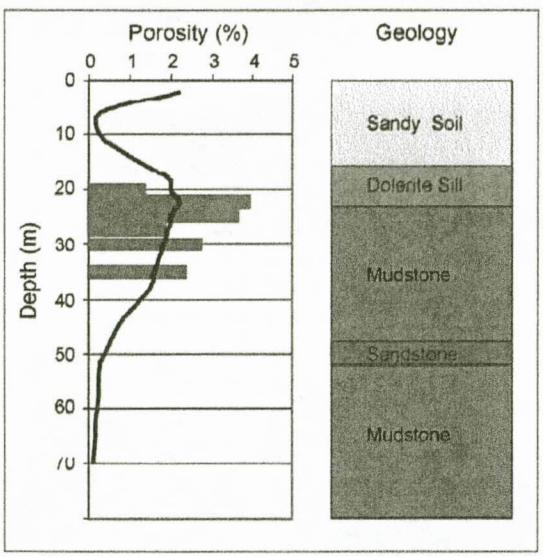

Figure 6-42 Comparison of the porosity estimation from NMR (solid line; after Meyer, 2001) and single-well tracer tests, showing the geology

At the moment there is no explanation for the behaviour in the deeper part of the borehole (between 40 and 60 m). Due to the very high Darcy velocity (up to 2.5 m/day without abstracting at the production well) the possible discharge rate during the pump back phase of the injection-withdrawal test is not high enough to get the tracer back to the injection borehole in sufficient time. Therefore the withdrawal part of the single well test could not be used in this case to estimate the flow velocity and the kinematic porosity.

6.4. Tsabong Botswana

The tests conducted in Tsabong were part of a project of the Resources Services for groundwater investigation, assessment and development in the area of Tsabong and surrounding settlements (Resources Services, 2001). Tsabong is located in the south-western part of Botswana in the Kgalagadi district, close to the Kgalagadi-Transfrontier Park (formerly Gemsbok Nature Reserve), and is the largest city in the study area containing the district headquarters.

6.4.1. Geology

The topography features a gently undulating sand-covered plain, with the ground surface sloping from the north to the south. Four quartzite hills emerge from these sands, twenty to forty metres above the plain, in a ridge running from the southwest to the northeast; namely the Tsabong outcrop, the Maleshe outcrop and the Omaweneno outcrop (see Figure 6-43). The explored and tested aquifers are situated in the quartzite and shale units of the Olifantshoek complex. The following brief description of the geology of the area is taken from Resources Services (2001).

From drill cuttings the argillaceous rocks have been described as phyllite, siltstone, shale and even mudstone. So as not to confuse these rocks with those of the Karoo Supergroup the terms argillite and phyllite are used. The phyllite is often inter-layered with thin silt grade material and quartzite bands. Phyllite is seen to weather to mudstone-like consistency and texture in the vicinity of fractures.

In general the quartzite shows sub-rounded grains with well-preserved primary sedimentary structures and moderate sorting. The rocks are metamorphosed to a low degree without major re-crystallisation and development of metamorphic fabric, hence sedimentary structures are preserved. Any primary pore space is eliminated.

The Olifantshoek Sequence in the outcrops is strongly folded and contains large faults and joints. The folding of the more competent quartzite results in brittle deformation and thus exhibits relatively high secondary porosity and permeability due to jointing. Less competent argillaceous strata, which are prone to plastic deformation rather than brittle fracturing, exhibit significantly lower secondary porosity and permeability.

Several extensive faults cut through the outcrops. In the Tsabong outcrop the fault zones trend southwest-northeast, while the main fault zones in the Omaweneno outcrop trend east-west.

From an evaluation of all data from the Olifantshoek Sequence it is concluded that groundwater occurs in three main geological settings; broad fracture zones in quartzite, discrete fractures within quartzite and in zones of interbedded quartzite and phyllite.

In all outcrops detailed study areas were proposed, boreholes for investigation and production were drilled, and a number of hydraulic tests conducted. During long-term hydraulic tests, conducted at several boreholes, tracer tests were conducted to estimate the kinematic porosity of the fractured zone, a parameter essential for the water balance calculation applying a box model. The long-term hydraulic tests and the combined tracer tests are discussed in detail in the following sections.

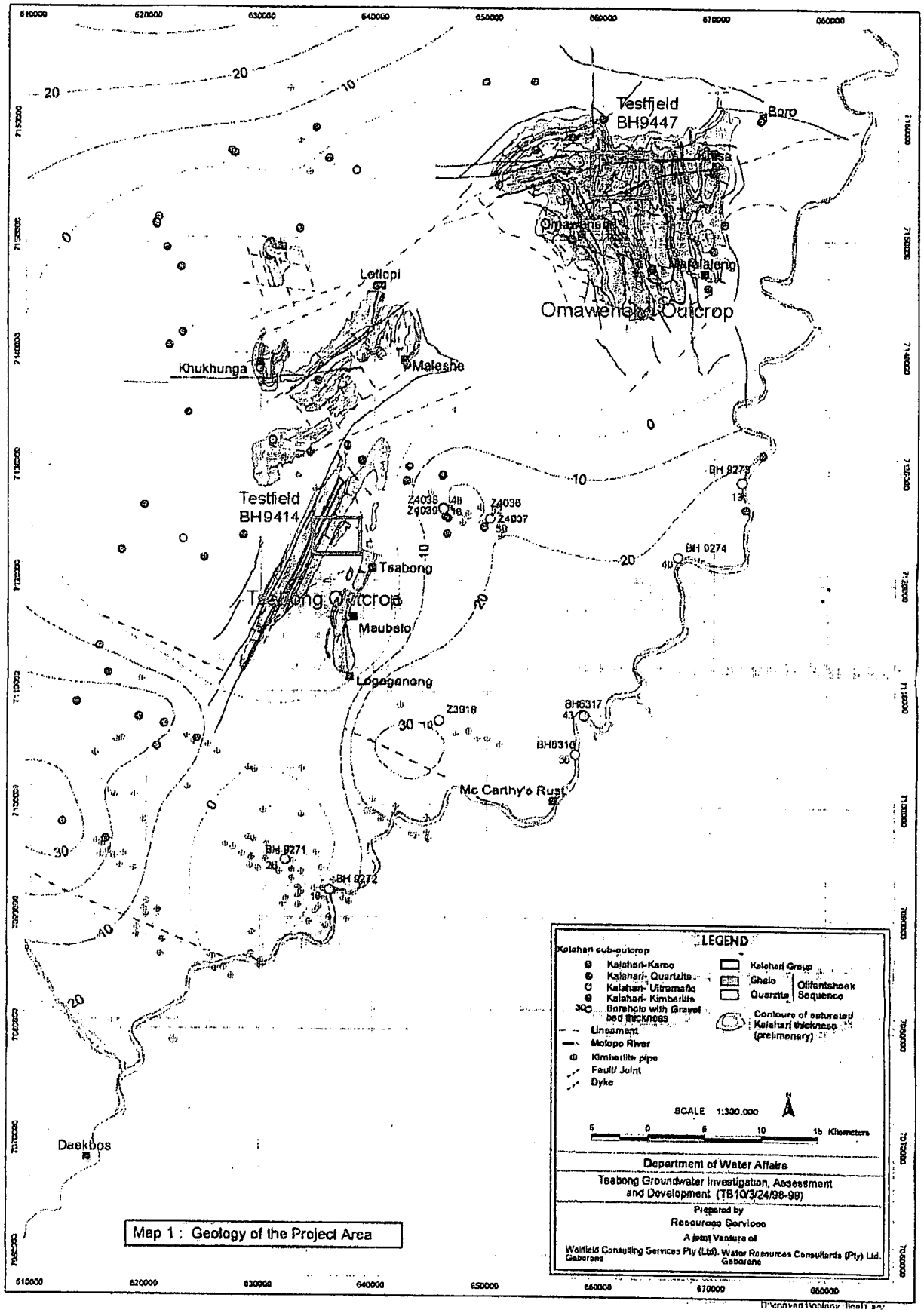

Figure 6-43 Geological map of the Tsabong area with detailed study areas (after Resources Services, 2001)

6.4.2. Hydraulic Tests

For aquifer parameter estimation and conducting the tracer tests, two long-term hydraulic tests were chosen; namely at borehole 9414, located in the Tsabong outcrop and typical for groundwater regime in discrete fractures in quartzite, and at borehole 9447, in the Omaweneno outcrop and typical for broad fracture zones. For both hydraulic tests observation boreholes were available nearby.

(a) 9414 – Test

The first test was conducted at BH 9414 in the Tsabong outcrop. Water was abstracted from BH 9414 at a constant rate of 65 m^3/h for 347 hours, or 14.5 days. Water level measurements were taken at both the abstraction borehole and observation boreholes BH 9276 (15m apart) and BH 9411 (100m apart).

The measured drawdown in the abstraction and observation boreholes is shown in Figure 6-44 to Figure 6-46. Different analytical methods were applied to the field data to estimate the aquifer parameters, such as the Cooper-Jacob straight-line method, the drawdown-distance method of Cooper-Jacob and the GRF-model of Barker. The results are listed in Table 6-28. From the time-drawdown plots and the diagnostic plots it is obvious that no boundary was reached during the test. Puzzling at the moment are the first minutes of the test, which show less drawdown than expected.

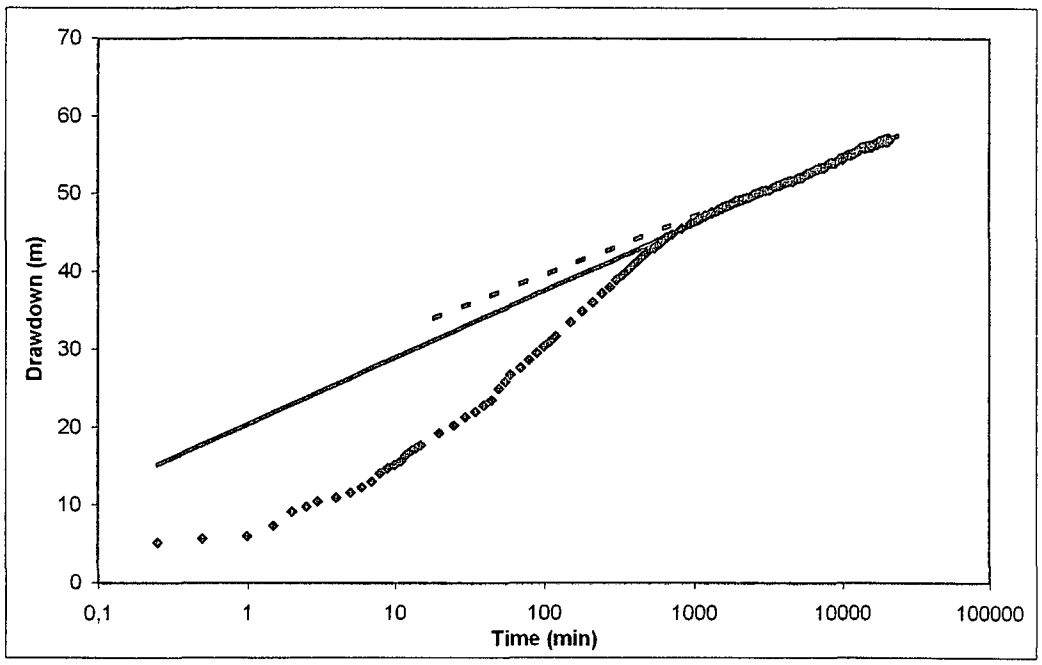

Figure 6-44 Time-Drawdown plot of long-term constant rate test at BH 9414, including simulated drawdown with Barker-method (solid line) and straight-line method of Cooper-Jacob (dashed line)

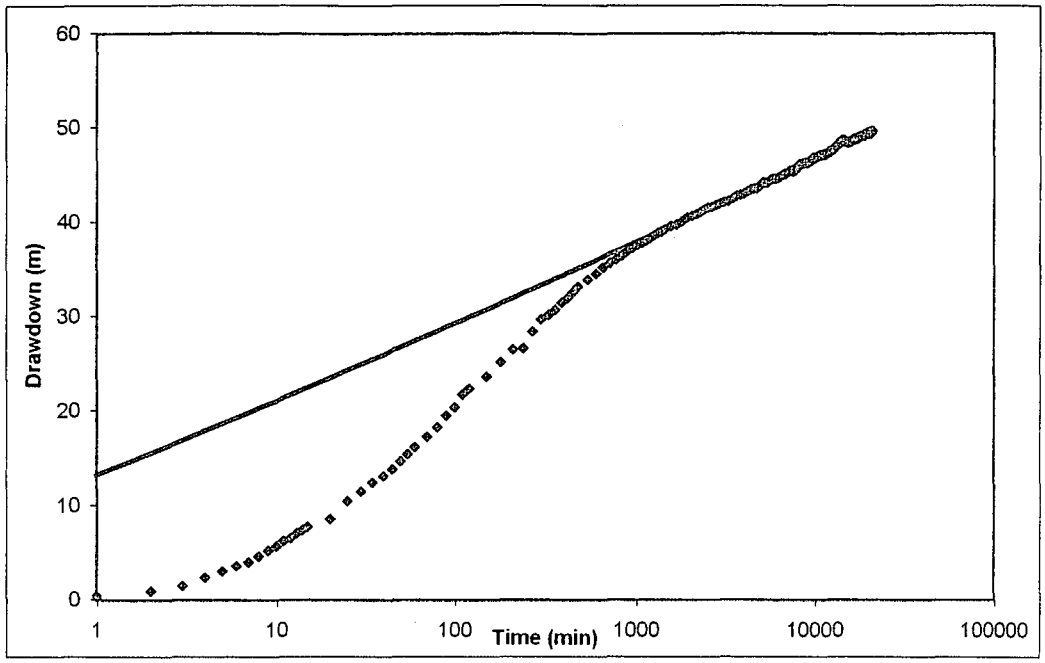

Figure 6-45 Time-Drawdown plot for observation borehole BH 9276 (15m away from abstraction), including simulated drawdown with Barker-method, yielding a flow dimension of 1.96

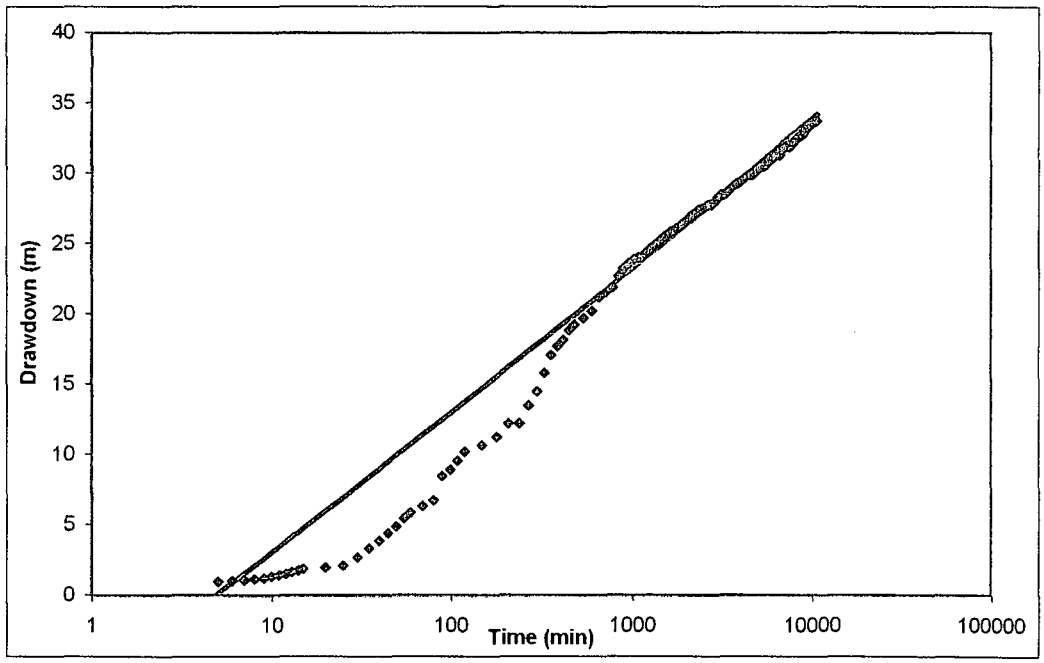

Figure 6-46 Time-Drawdown plot for observation borehole BH 9411 (100m away from abstraction), including simulated drawdown with Barker-method, yielding a flow dimension of 1.97

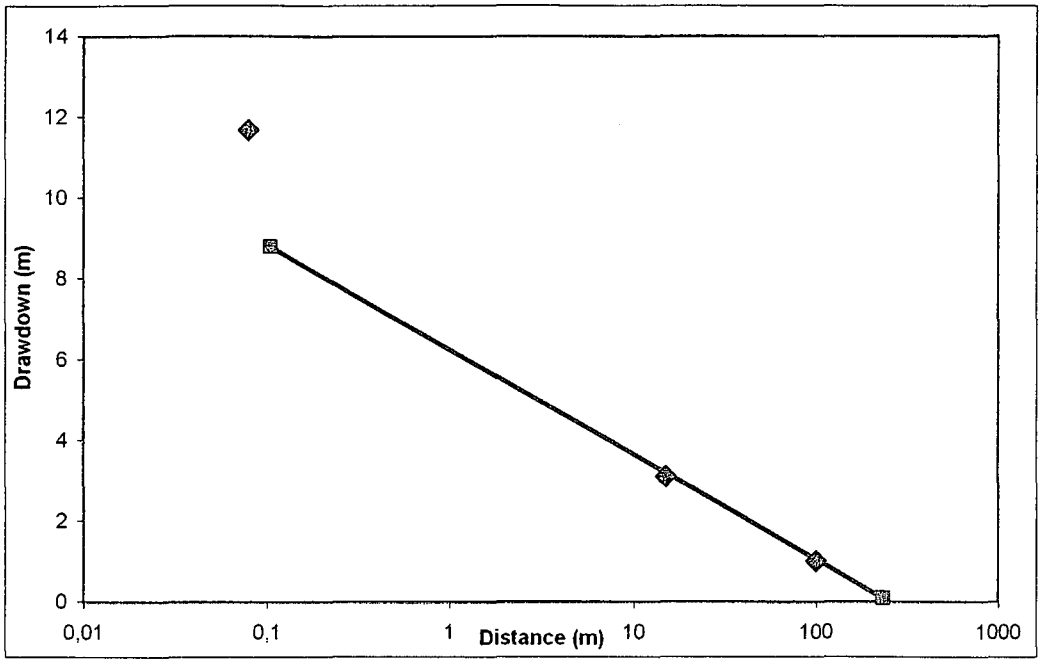

Figure 6-47 Drawdown-Distance method of Cooper-Jacob, applied to long-term constant rate test at BH 9414, yielding a transmissivity value of 220 m2/day and a storativity of 2.8 E-05

Table 6-28 Estimated aquifer parameters for constant rate test at BH 9414, applying the GRF-method and Cooper-Jacob-methods

Parameter		BH 9414	BH 9276	BH 9411	All together
Flow dimension n	[-]	2.0	1.96	1.97	-
Flow thickness b	[m]	0.8	0.8	0.8	-
Conductivity Fracture Kf	[m/day]	42	59	44	-
Sp. Storage Fracture Ssf	[1/m]	4.0E-07	6.3E-06	3.2E-05	-
Transmissivity T	[m^2/day]	37.5	33	30.7	220
Storage Coefficient S	[-]	5.5E-08	9.7E-06	1.4E-05	2.8E-05

The results of the hydraulic test are consistent with the knowledge of the geological set-up. The estimated flow dimension indicates a radial flow system through the fracture zone with a thickness of about 0.8m. The borehole log shows a fracture zone from 227 - 229 m. The transmissivity of the fracture zone is a bit higher than the matrix transmissivity, while the estimated storativity is of the same order for both the fracture zone and matrix.

(b) 9447 – Test

The second test was conducted at BH 9447 in the Omaweneno outcrop. Water was abstracted from BH 9447 at a constant rate of 80 m^3/h for 514 hours, or 21.4 days. Water level measurements were taken at both the abstraction borehole and observation boreholes BH 9391 (5m apart), and BH 9459 (1000m apart).

The measured drawdown in the abstraction and observation boreholes is shown in Figure 6-48 to Figure 6-50. Different analytical methods were applied to the field data to estimate the aquifer parameters, such as the Cooper-Jacob straight-line method, the drawdown-distance method of Cooper-Jacob and the GRF-model of Barker. The results are listed in Table 6-29.

The time-drawdown plot and the diagnostic plots of the abstraction borehole indicate the presence of a double-porosity aquifer with a fracture network that can be considered as continuum. But looking at the time-drawdown and diagnostic plots of the observation boreholes shows a relative decrease of the through-flow area, indicated by a decrease in flow dimension with distance and continuous increase of the derivative. This can be interpreted as a bounded system, whereas the boundary effect does not apply rapidly. Since a double porosity aquifer and a confined aquifer with well-bore storage and one no-flow boundary shows the same drawdown behaviour (van Tonder *et al.*, 2001), it is not possible to distinguish between these cases when using only the drawdown data of the abstraction borehole.

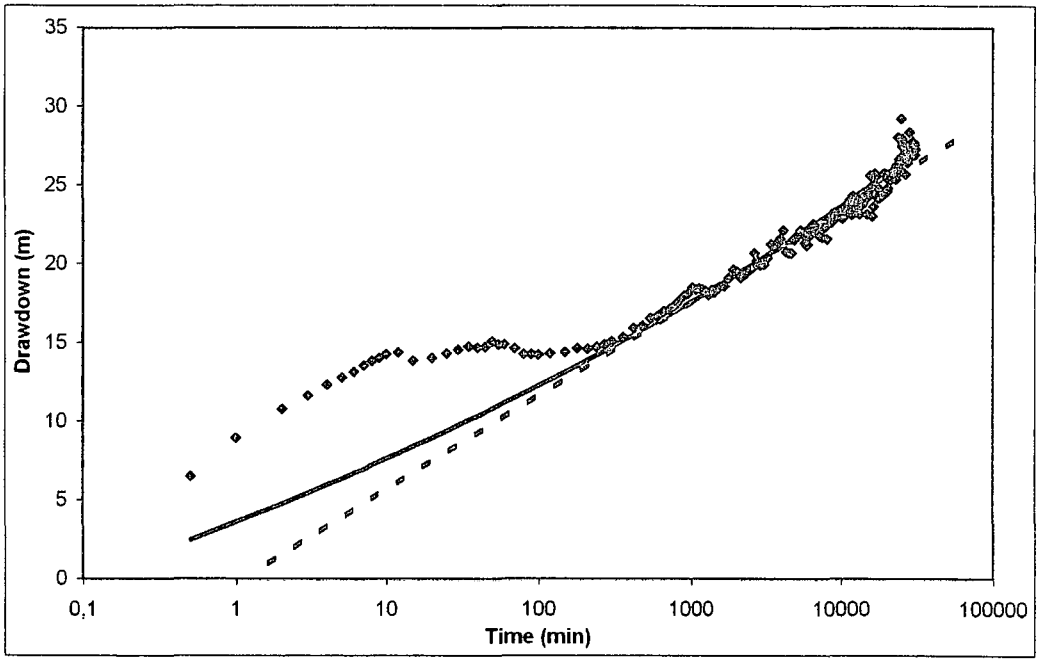

Figure 6-48 Time-Drawdown plot of long-term constant rate test at BH 9447, including simulated drawdown with Barker-method (solid line) and straight-line method of Cooper-Jacob (dashed line)

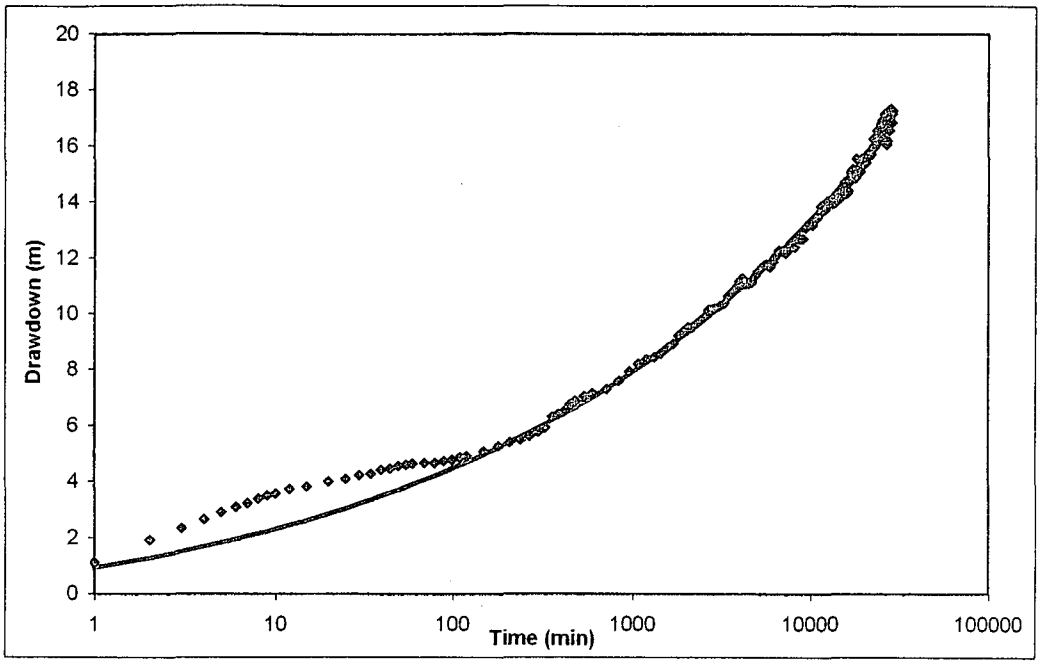

Figure 6-49 Time-Drawdown plot for observation borehole BH 9391 (5m away from abstraction), including simulated drawdown with Barker-method, yielding a flow dimension of 1.6

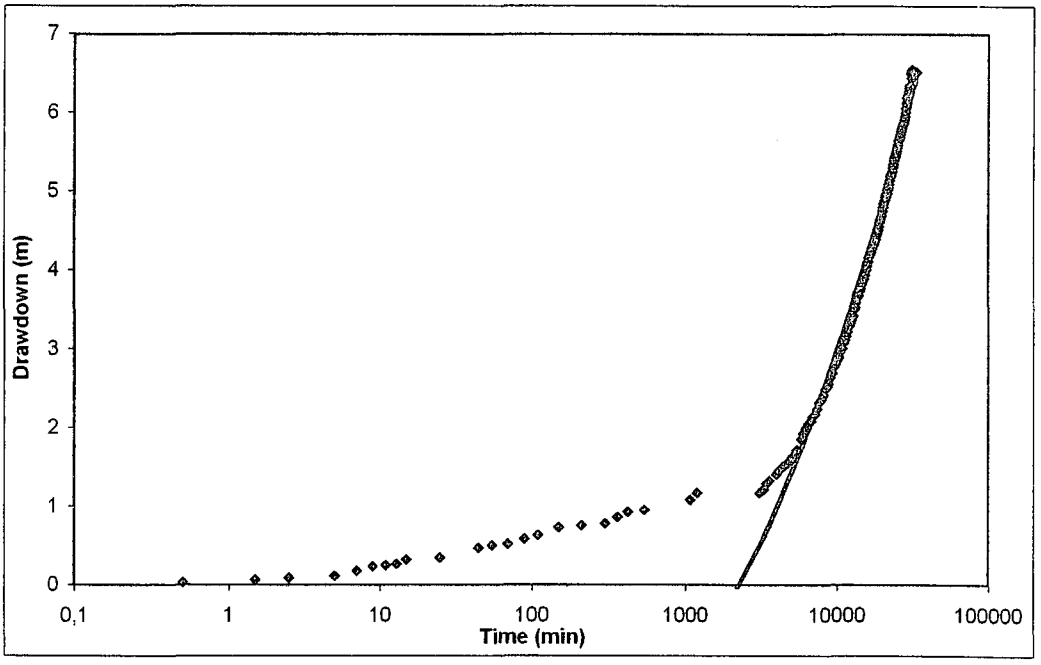

Figure 6-50 Time-Drawdown plot for observation borehole BH 9459 (1km away from abstraction), including simulated drawdown with Barker-method, yielding a flow dimension of 1.47

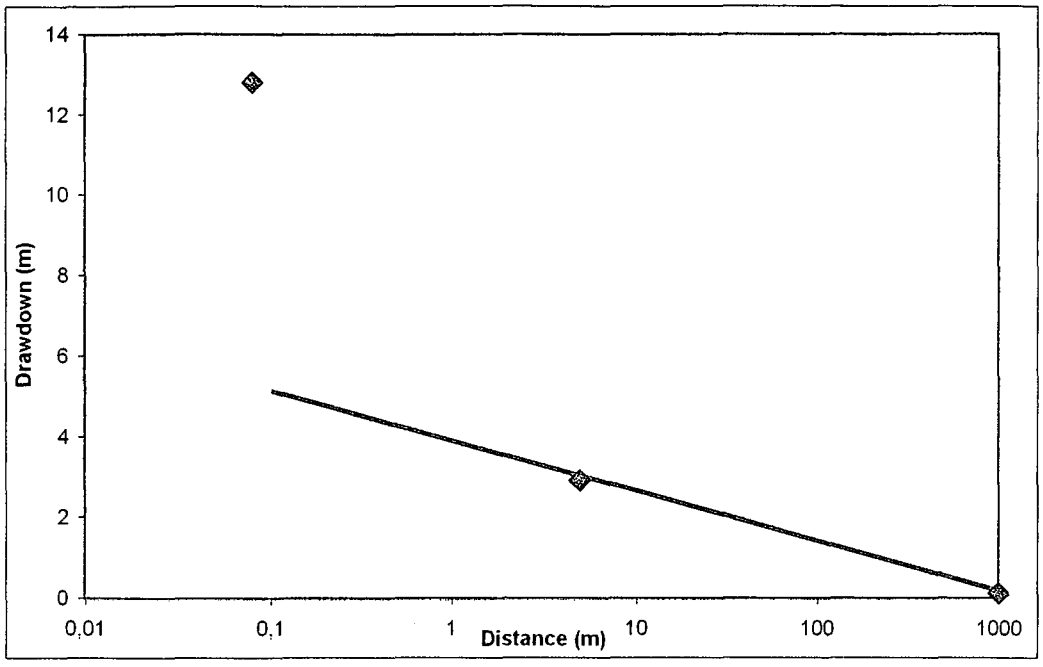

Figure 6-51 Drawdown-Distance method of Cooper-Jacob, applied to long-term constant rate test at BH 9447, yielding a transmissivity value of 555 m^2/day and a storativity of 3,6 E-06

Table 6-29 Estimated aquifer parameters for constant rate test at BH 9414, applying the GRF-method and Cooper-Jacob-method

Parameter		BH 9447	BH 9391	BH 9459	All together
Flow dimension n	[-]	1.88	1.6	1.47	
Flow thickness b	[m]	5.28	5.3	5.3	
Conductivity Fracture Kf	[m/day]	22	149	466	
Sp. Storage Fracture Ssf	[1/m]	1.9E-04	5.6E-04	1.3E-03	
Transmissivity T	[m^2/day]	59	68	47	555
Storage Coefficient S	[-]	7.4E-03	1.3E-01	3.2E-04	3.6E-06

Applying both the GRF-model and Cooper-Jacob method to the intermediate-time data of the hydraulic test will yield distance-dependent values for the transmissivity, equal to the estimates shown in Table 6-29 for the GRF-model applied to the late-time data. The diagnostic plots and this behaviour indicate a double-porosity aquifer with continuously decreasing effective through-flow area. This phenomenon can be caused by decrease in fracturing intensity and fracture opening over a large distance until boundaries are reached. Therefore the estimated transmissivity relates to the matrix rather than to the fracture system, which is contradictory to a classical double-porosity model.

6.4.3. Tracer Tests

During the above-mentioned long-term hydraulic tests, tracer tests in the vicinity of the abstraction boreholes were conducted. In addition one single-well tracer test after the long-term hydraulic test at borehole 9447 was conducted.

(a) Single-well Tests

After the long-term hydraulic test at BH 9447 a single-well tracer test was conducted at observation borehole 9391. The fracture zone was measured from the geological borehole log at 127 to 127.5 m; therefore a tested section from 126 m to 128.3 m depth was used. An amount of 200g NaCl was solved in 10L water and injected into the borehole 9391 at a circulating rate of 3 L/s.

As can be seen from Figure 6-52, the measured data show an oscillation at the beginning of the test due to a too short injection time, compared with the circulating time for the water in the tested section. Applying the straight-line method to the late data yields a Darcy velocity of 10.25 m/day.

Unfortunately the measured data from the withdrawal part cannot be analysed, because no breakthrough of the tracer could be observed. The reason might be insufficient accuracy of the measurement tool (10 μS/cm). Because the dilution was not totally completed before starting the pumping, the measured data during the withdrawal part show a continuous decrease of the concentration before reaching the background value.

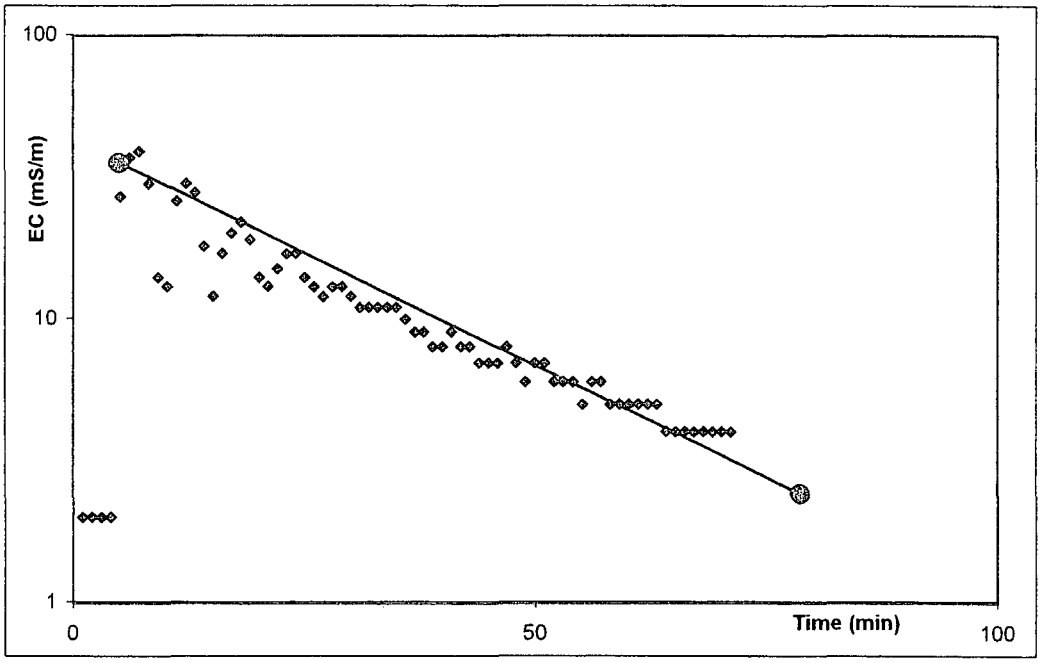

Figure 6-52 Dilution in injection borehole BH 9391 during single-well test at BH 9391

(b) Multiple-well Tests

The multiple-well tests were done at two sites where a pair of boreholes was drilled close to each other. The sites were BH 9447 - BH 9391 in Omaweneno and BH 9414 - BH 9276 in Tsabong on the Tsabong west structure.

9447 Tracer Test

BH 9447 was the abstracting borehole while BH 9391 (5 m away) was used to introduce the tracer. The targeted fracture zone was at 145 - 147.5 and the mixing interval was from 144 - 149.5 m.

Two tests were carried out; the first test with a salt mass of 500 g and fluorescein mass of 15g. The second test had a salt mass of 1000 g and fluorescein mass of 15 g. The tracers were introduced after BH 9447 had been pumped for 48 hours at a constant rate of 40 m^3/hr and the hydraulic gradient between the two boreholes was close to constant.

The circulation discharge was 8.5 m^3/hr with a circulation time 5.2 minutes, thus an injection time of at least 10 minutes was used. The initial calculated EC in the injection borehole was 762 µS/cm. The maximum EC recorded from the circulating water was 600 µS/cm due to dilution and removal by groundwater flowing through the borehole. The background EC before the test was 100 µS/cm. The EC decreased in 50 minutes close to the background value, which was then reached after 105 minutes (see Figure 6-53).

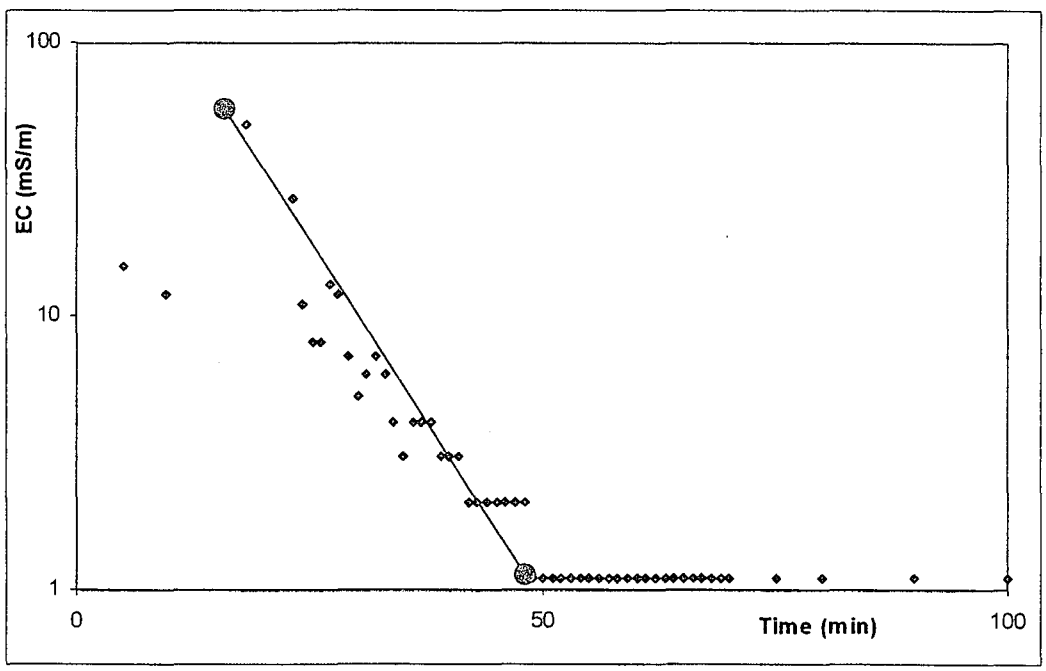

Figure 6-53 Dilution in injection borehole BH 9391 during first radial convergent tracer test at BH 9447

The second test was done at the same circulation discharge. The initial calculated EC was 1524 µS/cm; the maximum-recorded EC was 1100 µS/cm. The second test was started with the same background EC as in the first test and the EC decreased again in 50 minutes close to the background value, which was then reached after 155 minutes (see Figure 6-54).

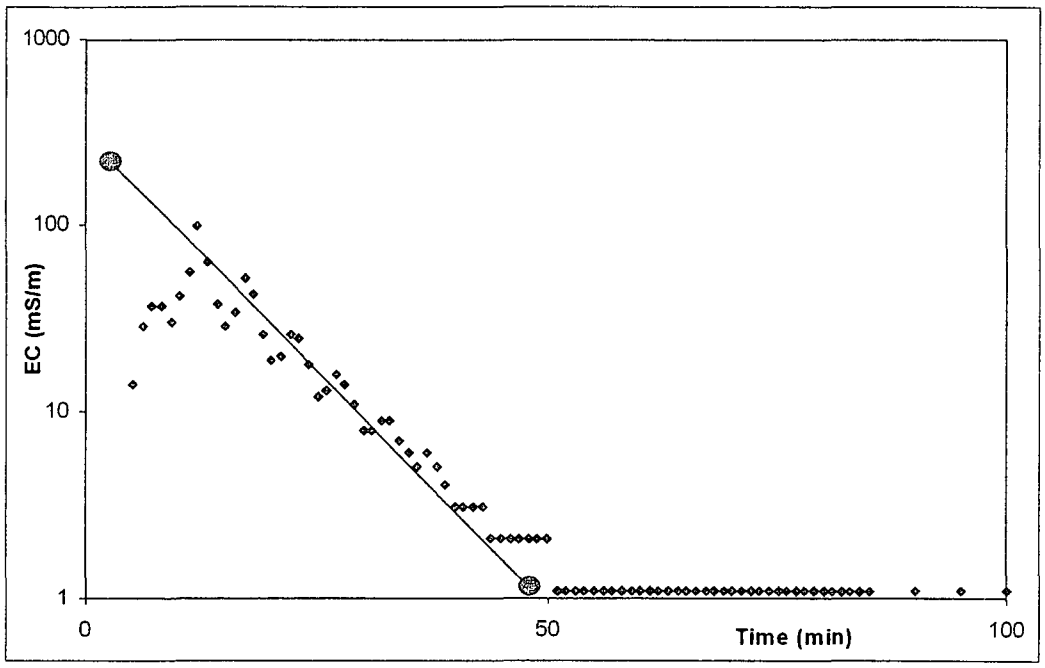

Figure 6-54 Dilution in injection borehole BH 9391 during second radial convergent tracer test at BH 9447

The analysing procedure for the two dilution tests yields a Darcy velocity of 6.32 m/day and 6.0 m/day, respectively. A flow thickness of 5.3 m and a flow dimension of 1.89 and 1.95, respectively, were used, as estimated from the radial-convergent test (see below).

In the abstraction borehole the breakthrough curve of both salt and fluorescein were measured. The background value for EC was 100 µS/cm. During the first test the EC changed to 120 µS/cm. In the second test the highest EC measured was 130 µS/cm. In both tests the measurements were stopped after the EC had fallen back to the background value. The accuracy of the measurement and the increase of tracer concentration are not sufficient for analysing these test data.

The breakthrough curves for fluorescein are shown in Figure 6-55 and Figure 6-56. The maximum measured concentration was 18.7 ppm for the first test and 16.8 ppm for the second test. The peak arrival time for the breakthrough curve was at 61.5 minutes for both tests.

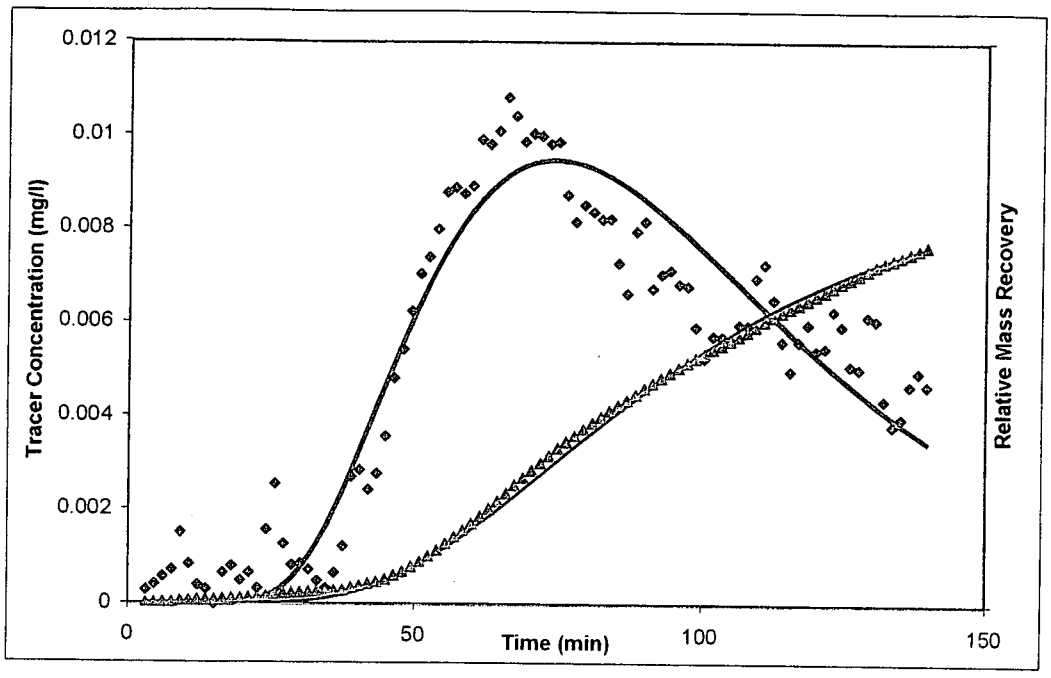

Figure 6-55 Breakthrough curve for fluorescein during first radial convergent tracer test at BH 9447

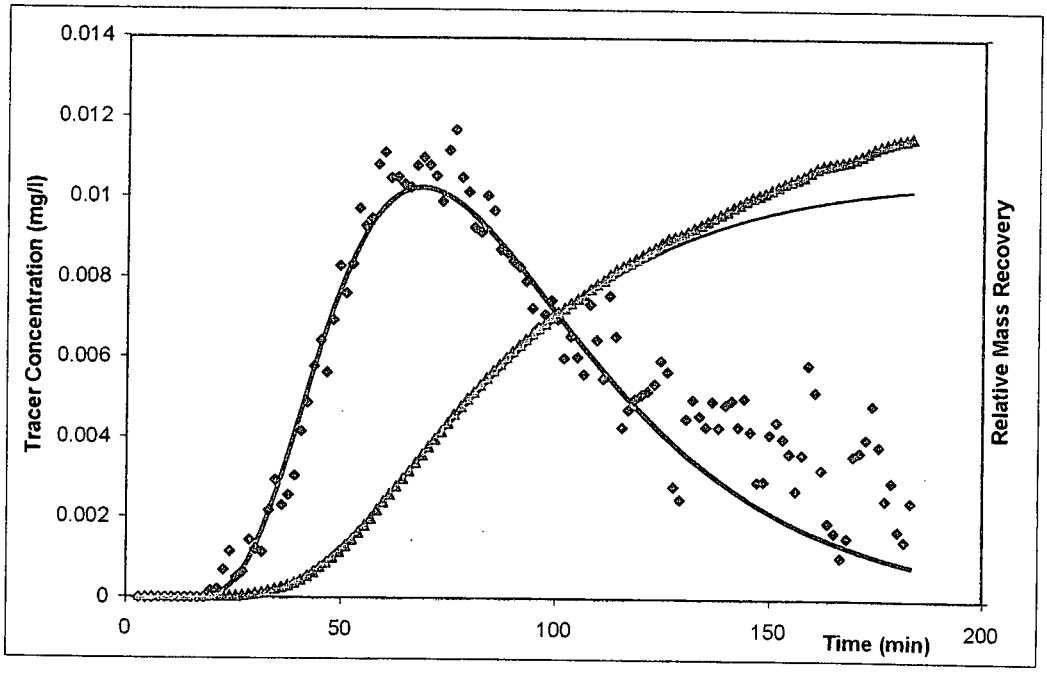

Figure 6-56 Breakthrough curve for fluorescein during second radial convergent tracer test at BH 9447

Both the dilution and the radial convergent test data were analysed using the program TRACER. From the first test, the test data yield a forced flow velocity of 72m/day, with a Darcy velocity of 6.32 m/d. A flow thickness of 5.3 m was interpreted with a fracture porosity of 9 %. In the second test a forced flow velocity of 78 m/d was interpreted with a Darcy velocity of 6 m/d.

The estimated flow thickness was 5.3 m with a fracture porosity of 8 %. The results for both tests are close together, indicating that a sufficient steady state condition was established before introducing the tracer.

Table 6-30 Results of radial convergent tracer tests at BH 9414

	Test 1	Test 2
Flow dimension [-]	1.89	1.95
Flow thickness [m]	5.3	5.3
Darcy velocity [m/day]	6.32	6.0
Flow velocity [m/day]	72	78
Dispersivity [m]	0.5	0.5
Porosity [%]	9	8

9414 Tracer Test

BH 9414 was the abstracting borehole with BH 9276, 15 m away, used to introduce the tracer. Two tracers were used; fluorescein and salt. The tracers were introduced after BH 9414 had been pumped for 24 hours at a constant rate of 50 m^3/hr and the hydraulic gradient between the two boreholes was close to constant. The targeted fracture zone was from 227 - 229 m. The mixing section was from 226.5 to 230.3 m.

Two tests were carried out, the first test with a salt mass of 500 g and fluorescein mass of 15g. The second test had a salt mass of 900 g and a fluorescein mass of 15 g.

The circulation discharge was 8.5 m^3/hr with a circulation time 6.82 minutes; thus an injection time of at least 14 minutes was used. Initial calculated EC was 582 µS/cm. The maximum EC recorded from the circulating water was 590 µS/cm. The background EC before the test was 310 µS/cm. The EC fell back to the background value after 40 minutes (see Figure 6-57).

The second test was done at the same circulation discharge. The initial calculated EC was 1047 µS/cm; recorded EC was 990 µS/cm. The second test was started with the same background EC as in the first test. At the end of the test after 1hr 20 min, the EC was 320 µS/cm (see Figure 6-58).

The analysing procedure for the two dilution tests yields a Darcy velocity of 27.24 m/day and 17.05 m/day, respectively. A flow thickness of 0.72 m and 0.88 m and a flow dimension of 1.89 and 1.96, respectively, were used, as estimated from the radial-convergent test (see below).

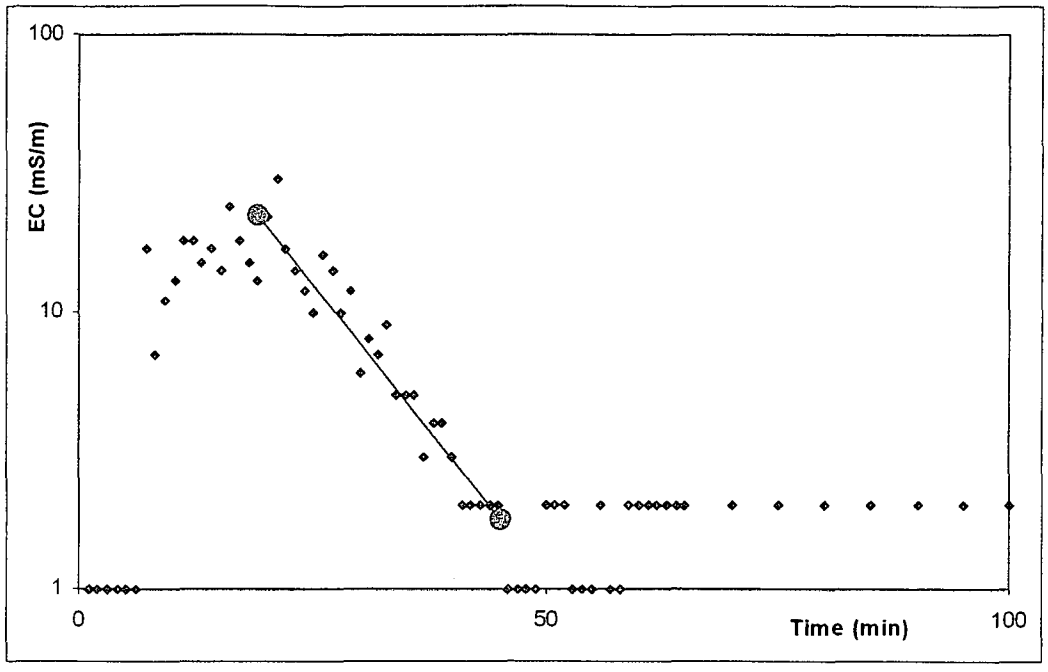

Figure 6-57 Dilution in injection borehole BH 9276 during first radial convergent tracer test at BH 9414

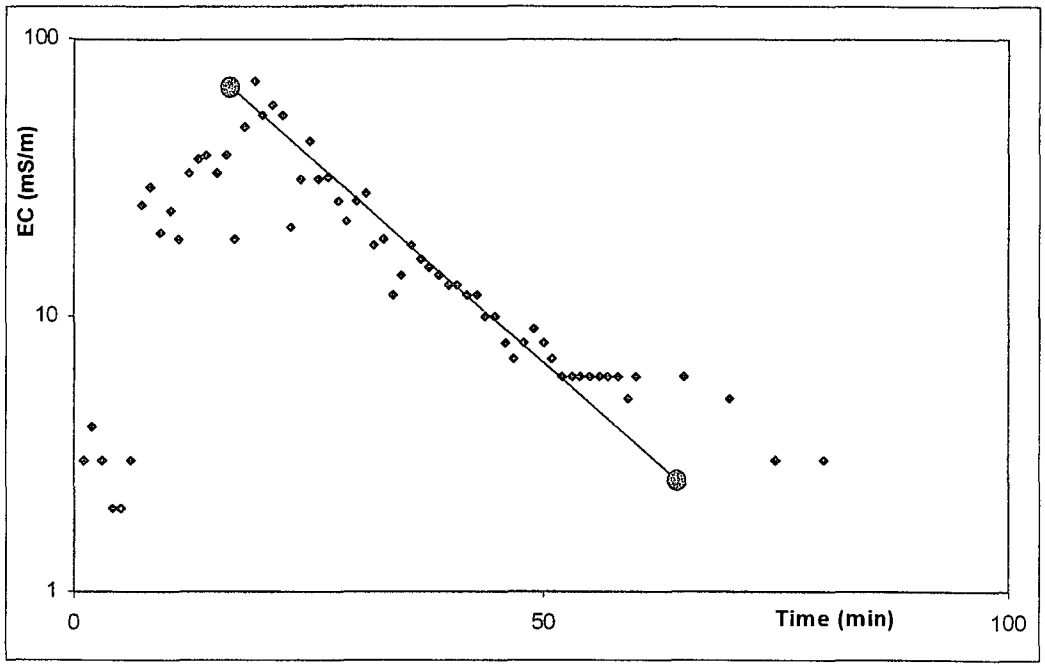

Figure 6-58 Dilution in injection borehole BH 9276 during second radial convergent tracer test at BH 9414

In the abstraction borehole the breakthrough curve of both salt and fluorescein were measured. The breakthrough curves for fluorescein are shown in Figure 6-59 and Figure 6-60. The peak arrival time for the breakthrough curve was 32 minutes in the first test and 26 minutes in the second test.

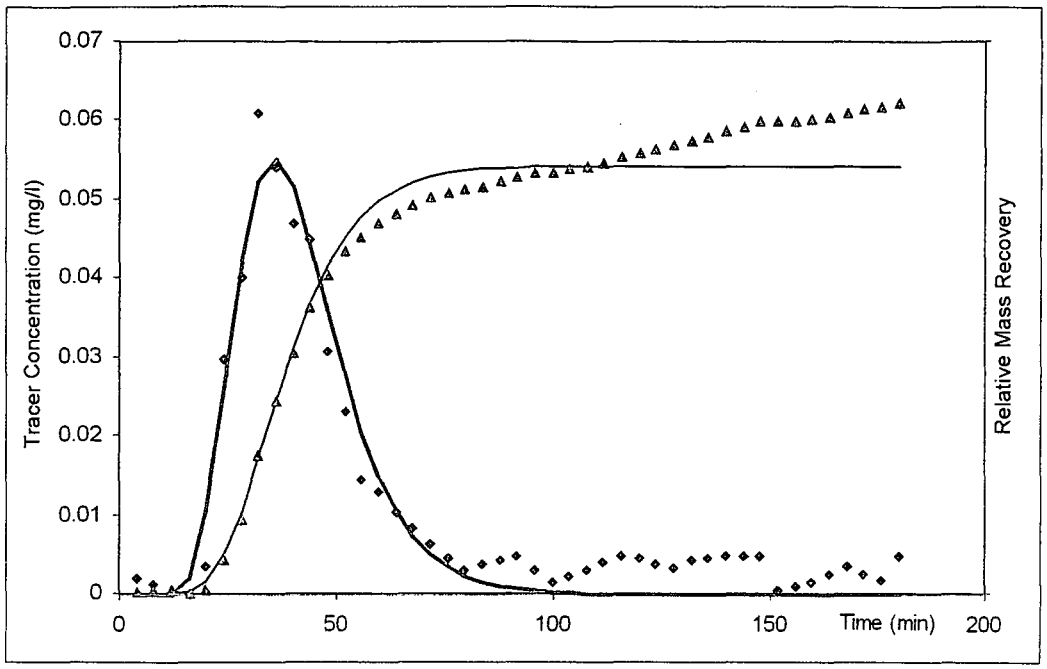

Figure 6-59 Breakthrough curve for fluorescein during first radial convergent tracer test at BH 9414

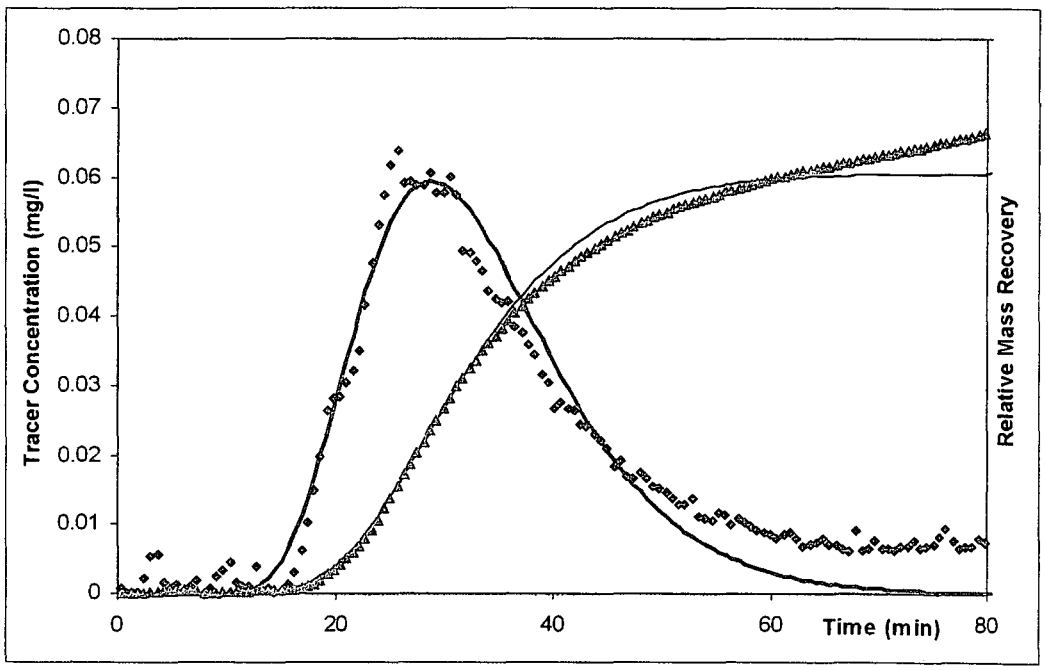

Figure 6-60 Breakthrough curve for fluorescein during second radial convergent tracer test at BH 9414

From the first test, the test data yield a forced flow velocity of 519m/day, with a Darcy velocity of 27.24 m/d. A flow thickness of 0.72 m was interpreted with a fracture porosity of 5 %. In the second test, a forced flow velocity of 650 m/d was interpreted with a Darcy velocity of 17.05 m/d. A flow thickness of 0.88 m was estimated with a fracture porosity of 3 %.

The difference in the results of both tests is obvious, indicating that the steady state condition was not established completely before the tracer tests were conducted. The increase of the flow velocity from the first to the second test verifies this finding.

Table 6-31 Results of radial convergent tracer tests at BH 9414

	Test 1	Test 2
Flow dimension [-]	1.89	1.96
Flow thickness [m]	0.72	0.88
Darcy velocity [m/day]	24.24	17.05
Flow velocity [m/day]	519	650
Dispersivity [m]	0.8	0.7
Porosity [%]	5	3

As mentioned above, the double tracing method was applied with a combination of salt and fluorescein. The background measurement for the salt concentration was 320 µS/cm. During the first test, the EC changed to 370 µS/cm. In the second test the highest EC measured was 410 µS/cm from a background value of 360 µS/cm. The accuracy of the measurement and the increase of tracer concentration are not sufficient for analysing these test data, but a comparison of the measurement with the fluorescein data indicates the conformity between both tracers (see Figure 6-61).

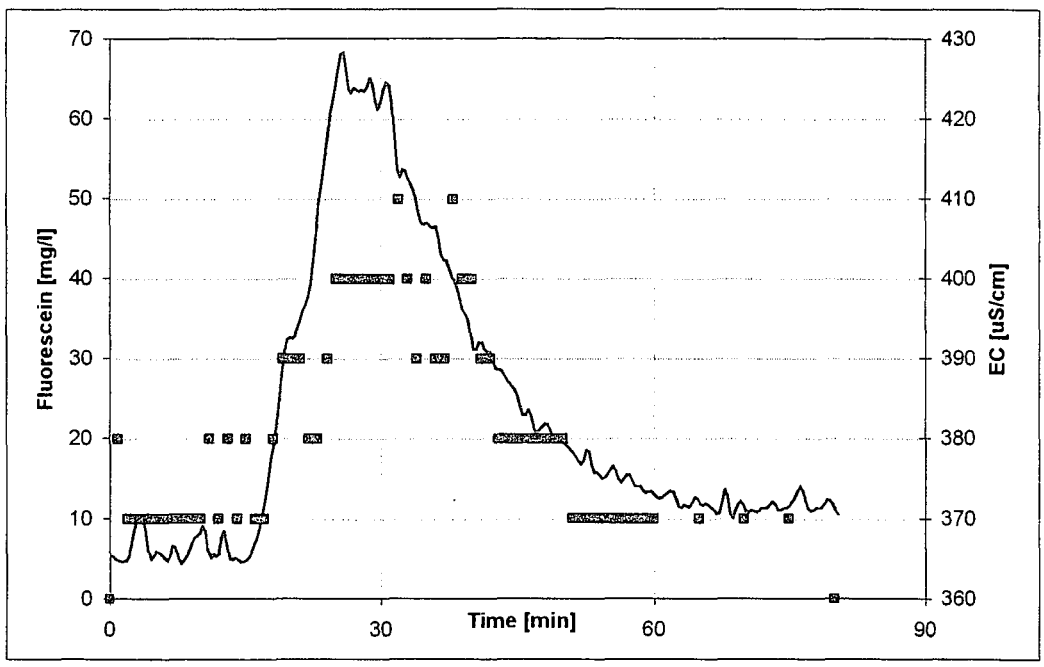

Figure 6-61 Comparison of measurements of fluorescein (solid line) and salt (dots) during second radial convergent tracer test at borehole BH 9414

Chapter 7 Conclusion and Recommendation

7.1. Conclusion

A guideline for aquifer parameter estimation in fractured rocks is derived, based on a combination of hydraulic and tracer tests. The methods included account for the unknown flow geometry and the resulting uncertainty by introducing the non-integer flow dimension, which can be calculated from hydraulic and / or tracer test data.

While the approaches for estimating the hydraulic parameters from pumping test data are commonly used methods, which are adapted to the situation in Southern Africa, new approaches to analyse tracer test data are developed, which account in a more general way for the unknown geometry.

The proposed methods were used in case studies with different geological settings and compared to each other. From the results of the case studies and theoretical models it can be concluded that

- analytical methods for estimating the hydraulic properties of fractured rock aquifers must be used with precaution, when the correct conceptual model is chosen,
- for more accurate estimation numerical models, preferable a three-dimensional numerical model, should be used,
- the developed methods for analysing tracer test data, using the concept of fractional flow dimension, will yield more accurate and normally higher values for the flow velocity than the common methods, using the length of the tested section and a flow dimension of 2,
- the developed methods for analysing tracer test data, using the concept of fractional flow dimension, are applicable in different geological settings,
- the developed method for estimating the kinematic porosity from a single-well tracer test is generally applicable in both the fracture zone and the matrix, but the accuracy depends upon the correct conducting procedure,
- the validity and accuracy of the results depends mainly on the quality of the conducting procedure and the correct conceptual model for the analysing procedure.

A combination of hydraulic and tracer tests including analysing procedure is proposed, which enables the hydrogeologist to estimate important hydraulic and transport parameters from the results of one test rather than conducting different tests. Depending on the purpose of the investigation, two types of combined tests are developed. As minimum requirement conducting and analysing a single-well test in the following manner is suggested:

- Inject the tracer in a single borehole, using the principle of circulation for sufficient mixing of the tracer solution
- Apply the dual tracer approach, e.g. salt and fluorescein
- Measure the dilution of the tracer in the borehole until background value is reached (complete dilution), while mixing is continued
- Pumpback the tracer plume with a sufficient flow rate
- Measure the tracer concentration in the abstracted water
- During pumpback measuring the drawdown in source borehole
- If available the drawdown in an observation borehole should be recorded
- The pump phase should be long enough to reach radial acting flow phase (normally longer than necessary for tracer recovery)
- Analyse the test data applying the approach of non-integer flow dimension

If an observation borehole in the vicinity is available, a multiple-well test should be conducted, as recommended

- Abstract water at a constant discharge rate until a steady state condition is reached
- Record the water level or drawdown in the abstraction and observation boreholes
- Continue pumping at constant rate until tracer test is completed
- Inject the tracer in a borehole in the vicinity of the abstraction borehole, using the principle of circulation for sufficient mixing of the tracer solution
- Apply the dual tracer approach, salt and fluorescein
- Measure the dilution of the tracer in the borehole until background value is reached (complete dilution), while mixing is continued
- Measure the tracer concentration in the abstracted water from the start of tracer injection
- The pump phase should be long enough to reach radial acting flow phase (normally longer than necessary for tracer recovery)
- Analyse the test data applying the approach of non-integer flow dimension

For best results and comparison a single-well test and a radial-convergent test should be conducted using the same source borehole for tracer injection.

The following points for conducting and analysing hydraulic and tracer test data in fractured aquifers are given as recommendation:

- The duration of a hydraulic test should be long enough to reach the radial acting flow phase, when analytical methods are intended to be used.
- The discharge rate must be chosen in such a way that no fracture will be dewatered during the test. Neither with analytical nor with numerical models is it possible to analyse such a test.
- The discharge rate should be kept constant over the whole period of abstraction. Otherwise no analytical method should be used to estimate the parameter values unless the drawdown is corrected. Tracer tests with variable discharge rates cannot be analysed analytically. When using a numerical model, every change in the discharge rate must be considered (in another stress period).
- The measurement of the drawdown must have an accuracy of at least 1cm.
- The measurement of tracer concentration should have an accuracy of at least 1 ppm, or 1% of maximum concentration
- The time intervals of measurement in the beginning of the test should be small, at least less than 1 minute (recommended 10 seconds).
- For estimating vertical hydraulic conductivity, piezometers with short wellscreen should be installed at different depths.
- Parameter r, i.e. the effective borehole radius or half-length of the fracture, must be calculated from early hydraulic test data.
- To estimate the storage coefficient of the aquifer in an accurate way, piezometers in the matrix should be used and the hydraulic test data should be analysed with a numerical model.
- Observation boreholes used for the hydraulic test should never intersect more than one reacting aquifer system, to avoid a mix of observation.

The requirement for the analysing procedure can be summarised as:

- From the hydraulic test data the conceptual model should be derived, using diagnostic plots and derivatives, as integrated in the software TRACER or in other software programs such as FC and TPA
- The hydraulic data should be analysed applying the approach of non-integer flow dimension, as integrated in the software TRACER.
- If necessary numerical models should be used for complete parameter estimation.
- The tracer test data should be analysed, applying the approach of non-integer flow dimension, as integrated in the software TRACER.

7.2. Recommendation

From the findings of this research, the results of the case studies and theoretical models it becomes obvious that there is a need for further research, as recommended below:

- The effect of matrix diffusion on solute transport in fractured aquifers is immanent, but no existing method is able to simulate it properly. Further research in estimating the impact of matrix diffusion on the plume movement and in developing a suitable method to simulate and quantify its effect is therefore strongly recommended.

- The combination of a Point-Dilution tracer test and an Injection-Withdrawal tracer test has been proved as a powerful tool for estimating the transport parameter, such as kinematic porosity and flow velocity, when it is conducted in a proper way. Both mathematical models to analyse the tracer test data obtained from an Injection-Withdrawal test have inherent problems and should be revised for more accuracy in the analysing procedure.

- The developed methods for analysing tracer test data, using the concept of fractional flow dimension, are applicable in different geological settings and independent from the conceptual flow model. It yields more accurate and normally higher values for the flow velocity than the common methods. Nevertheless the relative impact of the flow dimension and the flow thickness on the estimated values should be studied further.

- Because the validity and accuracy of the results depends mainly on the quality of the conducting procedure and the correct conceptual model for the analysing procedure, the impact of both should be quantified in a comparative study.

Chapter 8 References

Acuna, J.A. and Y.C. Yortsos (1995). Application of fractal geometry to the study of networks of fractures and their pressure transient. Water Resources Research, Vol. 31(3), pp. 527-540

Aydin, A. (1997). Theory of single-well tests in acute fracture – wellbore systems. Journal of Hydrology 194, pp.201-220

Bangoy, L.M., P. Bidaux, C. Drogue, R. Plegat, and S. Pistre (1992). A new method of characterizing fissured media by pumping test with observation wells. Journal of Hydrology 138, pp. 77-88.

Bardenhagen, I., (1999). TPA software, Test Pumping Analysis for fractured and non fractured aquifers. Published in Van Tonder *et al.* (2001)

Barenblatt, G.I., Yu.P. Zheltov, and I.N. Kochina (1960). Basic Concepts in the Theory of Seepage of Homogeneous Liquids in Fissured Rocks. In Well Testing in Heterogeneous Formations. An Exxon Monograph. T.D. Streltsova. John Wiley & Sons, New York, 413 p.

Barker, J.A., (1988). A Generalized Radial Flow Model for Hydraulic Tests in Fractured Rock. Water Resources Res., Vol. 24, No. 10, pp. 1796 – 1804

Barnard, S. (2001). Geohydrological Investigation of the Meadhurst Test Site. Unpublished Practical Examination in the course "Aquifer Mechanics", Institute for Groundwater Studies, University of the Free State, Bloemfontein. S.A.

Becker, M.W. and A.M. Shapiro (2000). Tracer transport in fractured crystalline rock: Evidence of nondiffusive breakthrough tailing. Water Resources Res., Vol. 36, No. 7, pp. 1677-1686

Benson, D.A., S.W. Wheatcraft, and M.M. Meerschaert (2000). Application of a fractional advection-dispersion equation. Water Resources Res., Vol. 36, No. 6, pp. 1403-1412

Black, J.H., (1994). Hydrogeology of fractured rocks – a question of uncertainty about geometry. *Applied Hydrogeology,* Vol. 2, No. 3, pp. 56 – 70.

Borowczyk, M, J. Mairhofer, and A. Zuber (1966). Single-well pulse technique. In Proceedings, Symposium on Isotopes in Hydrology, 1966, Vienna, pp. 507-518.

Botha, J.F., J.P. Verwey, I. Van der Voort, J.J.P. Vivier, W.P. Colliston, and J.C. Loock, (1998). *Karoo Aquifers. Their Geology, Geometry and Physical Behaviour*. WRC Report No 487/1/98. Water Research Commission, P.O. Box 824, Pretoria 0001.

Chang, J. and Y.C. Yortsos (1990). Pressure-transient analysis of fractal reservoirs. SPE Form Eval., 5, 631

Chao, H.-C., H. Rajaram, and T. Illangasekare (2000). Intermediate-scale experiments and numerical simulations of transport under radial flow in a two-dimensional heterogeneous porous medium. Water Resources Res., Vol. 36, No. 10, pp. 2869-2884

Chen, J-S, C-S Chen, H-S Gau, and C-W Liu (1999). A two-well method to evaluate transverse dispersivity for tracer tests in a radially convergent flow field. Journal of Hydrology 223, pp. 175-197

Chiang, W.H. and W. Kinzelbach (2001). 3D-Groundwater Flow and Transport Modeling with PMWIN, A Simulation System for Modeling Groundwater Flow and Pollution. Berlin, Heidelberg, New York: Springer

Chiang, W.H. and K. Riemann (2001). Guidelines for aquifer parameter estimation with computer models. WRC Report No. 1114/1/01. Water Research Commission, Pretoria

Cinco-Ley, H. and F. Samaniego (1977). Determination of the Orientation of a Finite Conductivity Vertical Fracture by Transient Pressure Analysis. SPE 6750. Society of Petroleum Engineers of AIME. Paper presented at the 52nd Annual Fall Technical

Conference and Exhibition of the Society of Petroleum Engineers of AIME held in Denver, Colorado, 9 – 12 October 1977.

Cinco-Ley, H. and F. Samaniego (1981). Pressure Transient Analysis for Naturally Fractured Reservoirs. SPE 11026. Society of Petroleum Engineers of AIME. Paper presented at the 57th Annual Fall Technical Conference and Exhibition of the Society of Petroleum Engineers of AIME held in New Orleans, Luisiana, 26 – 29 September 1982.

Cinco, H., F. Samaniego, and N. Dominguez (1978). Transient pressure behaviour for a well with a finite-conductivity vertical fracture. *Society of Petroleum Engrs Jl*, August 1978, pp. 253-264.

Cooper H.H. and C.E. Jacob (1946). A Generalized Graphical Method for Evaluating Formation Constants and Summarizing Well Field History. Am. Geophys. Union Transactions, Vol. 27, pp. 526 – 534.

Cushman, J.H. and T.R. Ginn (1993). On Dispersion in Fractal Porous Media. Water Resources Res., Vol. 29, No. 10, pp. 3513-3515

De Lange, S.S. (1999). Environmental impact of point pollution sources. Unpublished M.Sc.thesis, University of the Free State, Bloemfontein, South Africa.

Detwiler, R.L., H. Rajaram, and R.J. Glass (2000). Solute transport in variable-aperture fractures: An investigation of the relative importance of Taylor dispersion and macrodispersion. Water Resources Res., Vol. 36, No. 7, pp. 1611-1625

Doe, T.W. (1991). Fractional dimension analysis of constant-pressure well tests. SPE paper 22702, pp. 461-467. presented at the 66th Annual Technical Conference and Exhibition of the Soc. of Pet. Eng., Dallas, Tex., 1991

Doherty, J. (2000). PEST—Model-independent Parameter Estimation, User's Manual. Watermark Computing, Australia.

Drost, W., D. Klotz, A. Koch, H. Moser, F. Neumaier, and W. Rauert (1968). Point Dilution Methods of Investigating Ground Water Flow by Means of Radioisotopes. Water Resources Res., Vol. 4, No. 1, pp. 125-146

Drost, W. and F. Neumaier (1974). Application of single borehole methods in groundwater research. In Proceedings, Symposium on Isotope Techniques in Groundwater Hydrology, 1974, Vienna, pp. 241-254.

Fetter, C.W. (1999). Contaminant Hydrogeology. Second Edition. Prentice Hall, Upper Saddle River, N.J., 500 pp.

Freeze, R.A. and J.A. Cherry (1979). Groundwater. Prentice-Hall, Englewood Cliffs, N.J., 604 pp.

Gelhar, L.W. (1986). Stochastic subsurface hydrology from theory to applications. Water Resources Res., Vol. 22, No. 9, pp. 135S-145S

Grenier, C., E. Mouche, and E. tevissen (1998). Influence of variable fracture aperture on transport of non-sorbing solutes in a fracture: a numerical investigation. Journal of Contaminant Hydrology 35, pp. 305-313

Gringarten, A. C. (1984). Interpretation of tests in fissured and multilayered reservoirs with double porosity behavior: theory and practice. *Jl Petroleum Technology,* Vol. 36, No. 4, pp. 549-564.

Gringarten, A.C. and H.J. Ramey Jr. (1974). Unsteady-State Pressure Distribution Created by a Well With a Single Horizontal Fracture, Partial Penetration, or Restricted Entry. Society of Petroleum Engineers of AIME. Transactions, Vol. 257, pp. 413 – 426.

Gringarten, A.C., H.J. Ramey, and R. Raghavan (1974). Unsteadv-state pressure distributions created by a well with a single infinite-conductivity vertical fracture. *Society of Petroleum* Engrs *Jl*, August, pp. 347-360.

Hall, S.H., S.P. Luttrell, and W.E. Cronin (1991). A method for estimating effective porosity and groundwater velocity. Groundwater, Vol. 29(2), pp.171-174.

Horne, R.N. (1997). *Modern well test analysis: A computer-aided approach* . Petroway Inc., Palo Alto, USA.

Johns, R.A. and P.V. Roberts (1991). A Solute Transport Model for Channelized Flow in a Fracture. Water Resources Res., Vol. 27, No. 8, pp. 1797-1808

Kazemi, H. (1969). Pressure Transient Analysis of Naturally Fractured Reservoirs with Uniform Fracture Distribution. SPE 2156A. Society of Petroleum Engineers. Paper Presented at the 43rd Annual Fall Meeting held in Houston, Texas, 29 September – 2 October 1969.

Kinzelbach, W. (1992). Numerische Methoden zur Modelliering des Transports von Schadstoffen im Grundwasser. Schriftenreihe gwf Wasser – Abwasser. Band 21, R.Oldenbourg Verlag Muenchen Wien

Kirchner, J and G.J. van Tonder (1995). Proposed guidelines for the execution, evaluation and interpretation of pumping tests in fractured-rock formations. Water SA, Vol. 21(3), South Africa.

Kruseman, G.P. and N.A. de Ridder (1991). Analysis and Evaluation of Pumping Test Data. Second Edition. International Institute for Land Reclamation and Improvement. Publication 47. Wageningen, the Netherlands. 377 p.

Leap, D.I. and P.G. Kaplan (1988). A single-well tracing method for estimating regional advective velocity in a confined aquifer: Theory and Preliminary laboratory verification. Water Resources Research, Vol. 24 (7), pp. 993-998.

Long, J.C.S. and P.A. Witherspoon (1985). The Relationship of the Degree of Interconnection to Permeability in Fracture Networks. J. of Geophysical Research, Vol. 90, No. B4, pp. 3087 – 3098.

Louis, C. (1967). Stroemungsvorgaenge in klueftigen Medien und ihre Wirkung auf die Standsicherheit von Bauwerken und Boeschungen im Fels. Ph.D. Thesis at Fakultaet fuer Bauingenieur- und Vermessungswesen der Technischen Hochschule Karlsruhe, Germany

Maloszewski, P. and A. Zuber (1985). On the theory of tracer experiments in fissured rocks with a porous matrix. Journal of Hydrology 79, pp. 333-358

Maloszewski, P. and A. Zuber (1993). Tracer Experiments in Fractured Rocks: Matrix Diffusion and the Validity of Models. Water Resources Res., Vol. 29, No. 8, pp. 2723-2735

Meyer, R. (2001). Status report on the magnetic resonance sounding (MRS) technique for ground water exploration with examples from South African fractured rock aquifers,- unpublished report to the Water Research Commission on the project "Evaluation of Nuclear Magnetic Resonance (NMR) as a new geophysical technique for ground water exploration in fractured rocks"

Moench, A.F. (1984). Double-Porosity Models for a Fissured Groundwater Reservoir with Fracture Skin. Water Resources Res., Vol. 20, No. 7, pp. 831 – 846.

Moench, A.F. (1995). Convergent radial dispersion in a double-porosity aquifer with fracture skin: Analytical solution and application to a field experiment in fractured chalk. Water Resources Res., Vol. 31, No. 8, pp. 1823 – 1835

Nordqvist, A.W., Y.W. Tsang, C-Fu Tsang, B. Dverstorp, and J. Andersson (1996). Effects of high variance of fracture transmissivity on transport and sorption at different scales in a discrete model for fractured rocks. Journal of Contaminant Hydrology 22, pp. 39-66

Novakowski, K.S. (1992). The Analysis of Tracer Experiments Conducted in Divergent Radial Flow Fields. Water Resources Research, Vol. 28(12), pp. 3215-3225

Novakowski, K.S., P.A. Lapcevic, J.W. Voralek, and G. Bickerton (1995). Preliminary interpretation of tracer experiments conducted in a discrete rock fracture under conditions of natural flow. Geophysical Research Letters, Vol. 22(11), pp. 1417-1420.

Novakowski, K.S. (1996). "Course in fractured rock aquifers", presented at the Institute for Groundwater Studies, Bloemfontein.

Painter, S. and G. Mahinthakumar (1999). Prediction uncertainty for tracer migration in random heterogeneities with multifractal character. Advances in Water Resources 23, pp. 49-57

Raven, K.G., K.S. Novakowski, and P.A. Lapcevic (1988). Interpretation of field tests of a single fracture using a transient solute storage model. Water Resources Res., Vol. 24, No. 12, pp. 2019-2032

Resources Services (2001). Tsabong Groundwater Resources Investigation, Assessment and Development, Exploration phase review report – Volume 1,- unpublished report to the Department of Water Affairs, Republic of Botswana, March 2001

Riemann, K. (2001) Estimation of the effective porosity from single-well tracer tests,- unpublished report to the CSIR Pretoria

Riemann, K. and G.J. van Tonder. (2001a). Interpretation of tracer tests in fractured aquifers using fractional flow dimensions. In Proceedings, Fractured Rock 2001, 2001, Toronto

Riemann, K. and G.J. van Tonder. (2001b). The fractional flow dimension of fractured aquifers, obtained from and used with single-well and multiple-well tracer tests. In Proceedings, New approaches to characterizing groundwater flow, XXXI. IAH Congress, 2001, Munich

Roberts, R.M. and R.L. Beauheim (2001). Hydraulic-Test Interpretation in Systems with Complex Flow Geometries. Submitted for publication to Water Resources Research.

Roberts, R.M., R.L. Beauheim, and J.D. Avis (2001). nSIGHTS (n-dimensional Statistical Inverse Graphical Hydraulic Test Simulator), software for hydraulic test interpretation in low permeable aquifers. Unpublished beta-version. Sandia National Laboratory, Albuquerque

Sabet, M.A. (1991). Well Test Analysis. Contributions in Petroleum Geology and Engineering, Volume 8. Gulf Publishing Company, Houston. 460 p.

Sauty, J-P (1980). An Analysis of hydrodispersive transfer in aquifers. Water Resources Research, Vol. 16(1), pp. 145-158.

Shapiro, A.M. (2001). Effective matrix diffusion in kilometer-scale transport in fractured crystalline rock. Water Resources Res., Vol. 37, No. 3, pp. 507-522

Shapiro, A.M. and J.R. Nicholas (1989). Assessing the Validity of the Channel Model of Fracture Aperture under Field Conditions. Water Resources Res., Vol. 25, No. 5, pp. 817-828

Stober, I. (1986). Strömungsverhalten in Festgesteinsaquiferen mit Hilfe von Pump- und Injektionsversuchen. Geol. Jb., C42, pp. 3 – 204.

Sutton, D.J., Z.J. Kabala, D.E. Schaad and N.C. Ruud (2000). The dipole-flow test with a tracer: a new single-borehole tracer test for aquifer characterization. Journal of Contaminant Hydrology 44, pp. 77-101

Theis, C.V. (1935). The Relation Between the Lowering of the Piezometric Surface and the Rate and Duration of Discharge of a Well Using Ground-Water Storage. American Geophysical Union, Transactions. Reports and Papers, Hydrology – 1935.

Tidwell, V.C., L.C Meigs, T. Christian-Frear, and C.M. Boney (2000). Effects of spatially heterogeneous porosity on matrix diffusion as investigated by X-ray absorption imaging. Journal of Contaminant Hydrology 42, pp. 285-302

Tsang, Y.W. (1992). Usage of "Equivalent Apertures" for Rock Fractures as Derived From Hydraulic and Tracer Tests. Water Resources Research. 28(5): 1451-1455

Van der Voort, I. and G.J. Van Tonder (2000). Analysing the geometry of South African fractured rock aquifers. In: Proceedings of the *XXXth IAH Congress on Groundwater: Past achievements and Future Challenges.* O. Sililo (eds.) Cape Town, South Africa. A.A. Balkema, Rotterdam.

Van der Voort (2001). Risk based decision tool for managing and protecting groundwater resources. Ph.D. Thesis, University of the Free State, Institute for Groundwater Studies, Bloemfontein, S.A.

Van Tonder G.J., H. Kunstmann, and Y. Xu (1998). Estimation of the Sustainable Yield of a Borehole Including Boundary Information, Drawdown Derivatives, and Uncertainty Propagation, Technical Report, University of the Orange Free State, Institute for Groundwater Studies, Bloemfontein, S.A.

Van Tonder, G.J., I. Bardenhagen, K. Riemann, J. van Bosch, P. Dzanga, and Y. Xu (2001). Manual on Pumping Test Analysis in fractured-Rock Aquifers. Final Report, WRC Project, Pretoria

Van Tonder, G.J. and K Riemann (2001). Non-linear relationship between drawdown and discharge rate, observed in fractured rocks of South Africa. In Proceedings, Fractured Rock 2001, 2001, Toronto

Van Wyk, AE, Y. Xu, S.S. De Lange, G.J. Van Tonder, and W-H Chiang (2001). Utilization of tracer experiments for the development of rural water supply management strategies for secondary aquifers. WRC Report, Pretoria, South Africa.

Van Wyk, A.E. (1998). Tracer experiments in fractured-rock aquifers. Unpublished M.Sc. Thesis, Institute for Groundwater Studies at the University of the Orange Free State, Bloemfontein, South Africa

Verweiji, H.J.M. and J.A. Barker (1999). Well Hydraulics and Yield Analysis. In Water Resources of hard rock aquifers in arid and semi-arid zones. UNESCO Publication 58, Edited by J.W. Lloyd, Paris.

Verwey, J.P., W. Kinzelbach, and G.J. van Tonder (1995). Interpretation of pumping test data from fractured porous aquifers with numerical models. Technical Report, University of the Orange Free State, Institute for Groundwater Studies, Bloemfontein, S.A.

Warren, J.E. and P.J. Root (1963). The behavior of naturally fractured reservoirs. *Society of Petroleum Engrs Jl,* Vol. 3, pp. 245-255.

Wei, L. and C. Chakrabarty (1996). Evaluation of a self-consistent approach to fractured crystalline rock characterisation. European Commission Report EUR16936EN.

Wei, L., J. Hadwin, E. Chaput, K. Rawnsley, and P. Swaby (1998). Discriminating Fracture Patterns in Fractures Reservoirs by Pressure Transient Tests. SPE 49233. Society of Petroleum Engineers. Paper presented at the 1998 SPE Annual Technical Conference and Exhibition held in New Orleans, Luisiana, 27 – 30 September 1998.

Welty, C. and L.W. Gelhar (1994). Evaluation of longitudinal dispersivity from nonuniform flow tracer tests. Journal of Hydrology 153, pp. 71-102

Wheatcraft, S.W. and S.W. Tyler (1988). An explanation of scale-dependent dispersivity in heterogeneous aquifers using concepts of fractal geometry. Water Resources Res. Vol. 24, No. 4, pp. 566-578

Zlotnik, V.A. and J.D. Logan (1996). Boundary conditions for convergent radial tracer tests and effect of well bore mixing volume. Water Resources Res., Vol. 32, No. 7, pp.2323-2328

Appendices

Appendix A: Data of unpublished Tracer Tests

Appendix B: Data Sheets for Field Measurements

Appendix C: Software Packages TRACER and TRACER-PLAN

APPENDIX A

DATA OF UNPUBLISHED TRACER TESTS

- SINGLE-WELL TRACER TESTS, FARM GRIESEL

BH 2 **19 - 21 m**

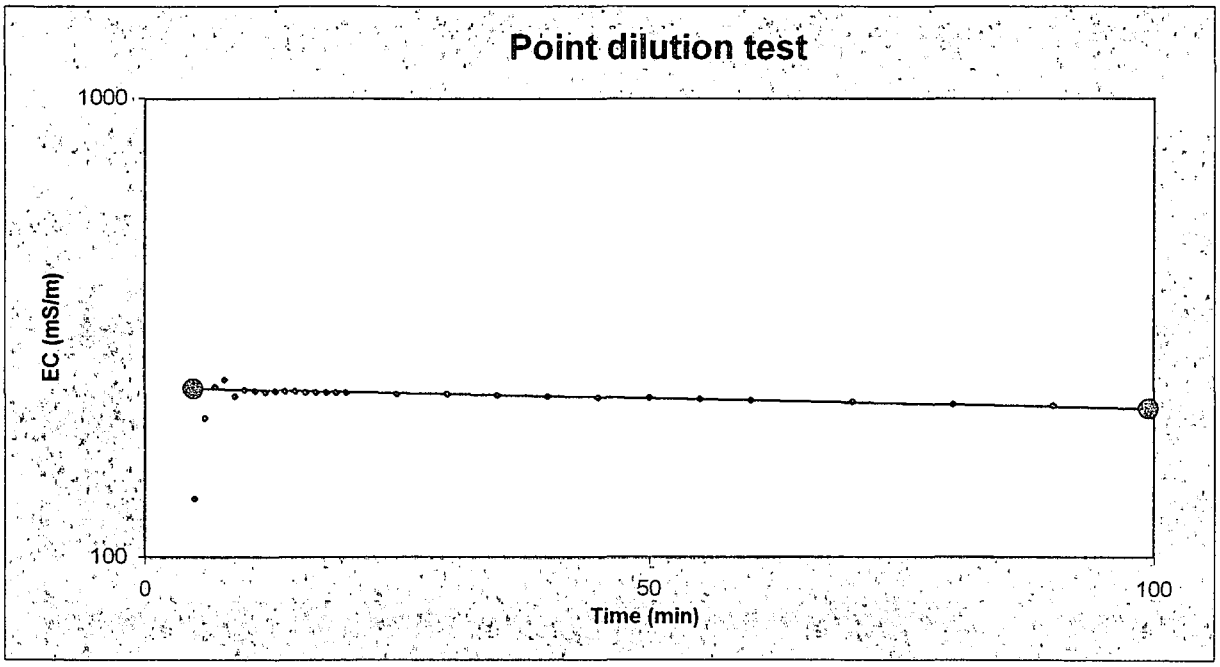

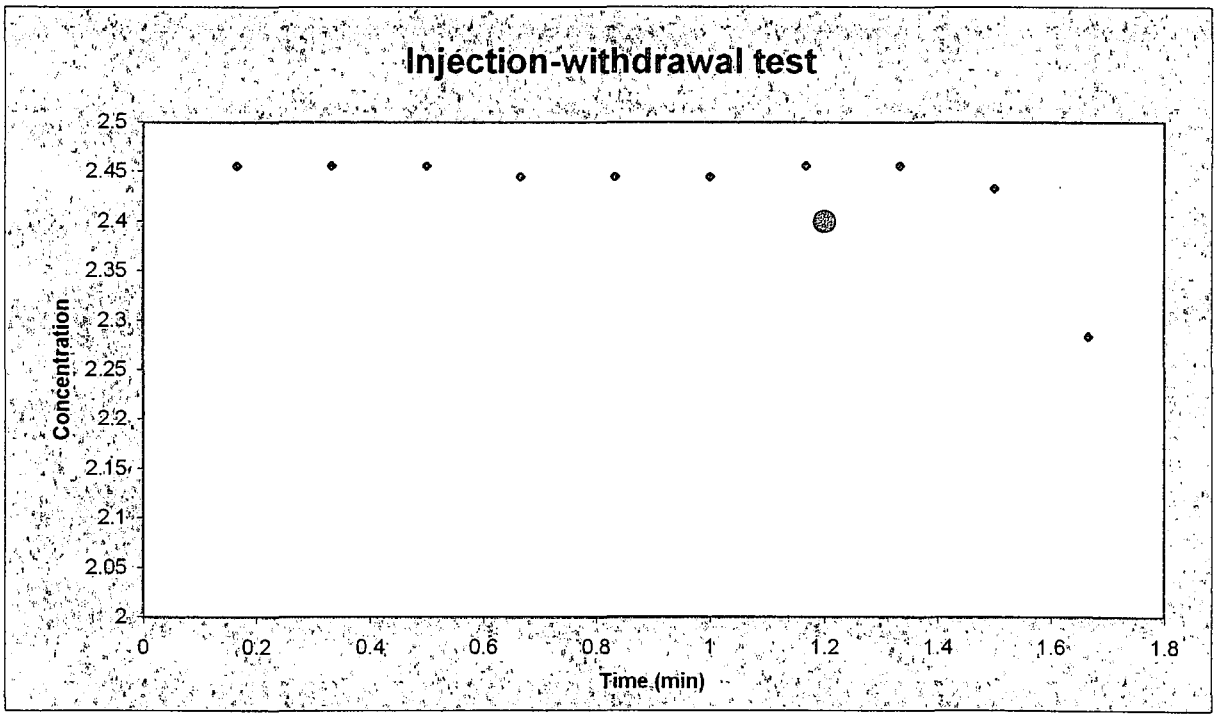

Duration of Dilution Test	120 min
Discharge Rate of Pump Back Phase	0.2 l/s
Darcy-Velocity (from Point Dilution Test)	0.06 m/day
Seepage Velocity (from Withdrawal Test)	5.48 m/day
Kinematic Porosity	1.1 %

BH 2 **21 - 23 m**

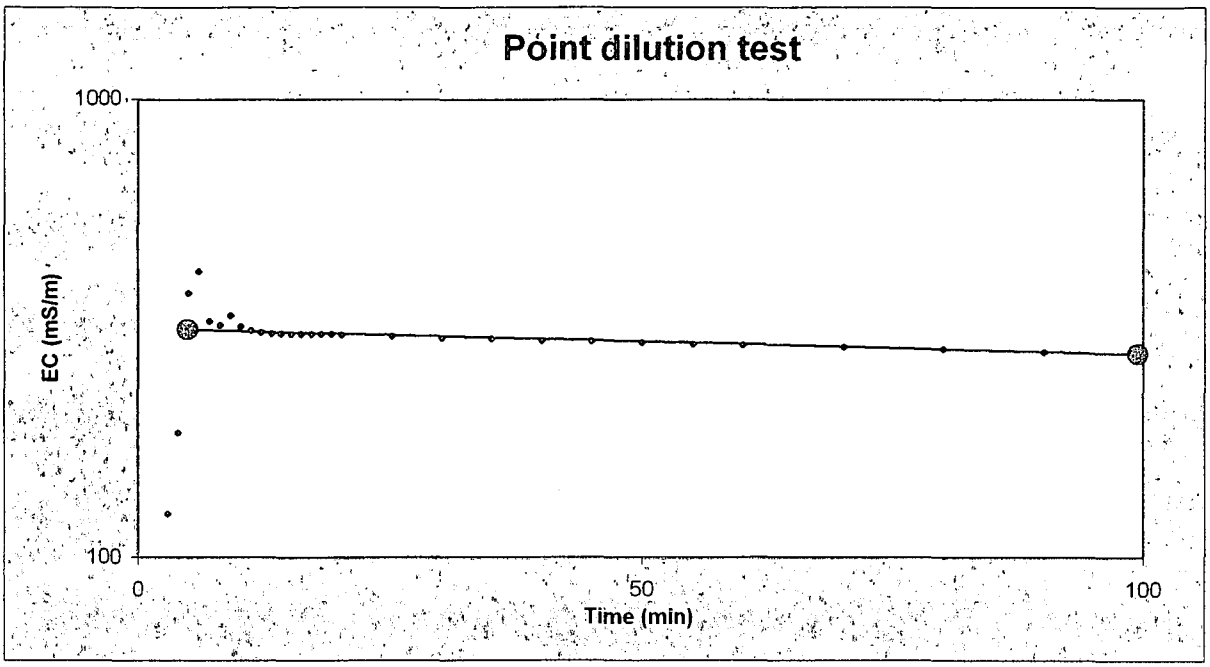

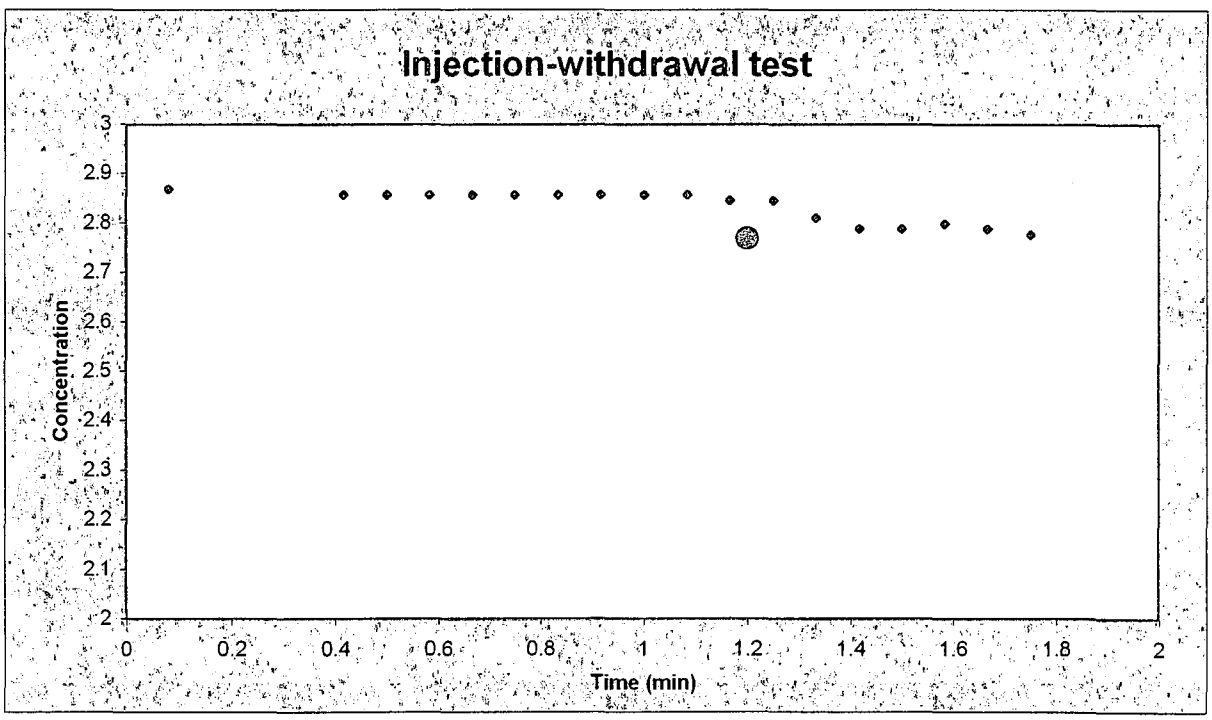

Duration of Dilution Test	180 min
Discharge Rate of Pump Back Phase	0.2 l/s
Darcy-Velocity (from Point Dilution Test)	0.07 m/day
Seepage Velocity (from Withdrawal Test)	1.97 m/day
Kinematic Porosity	3.7 %

BH 2 **24 - 26 m**

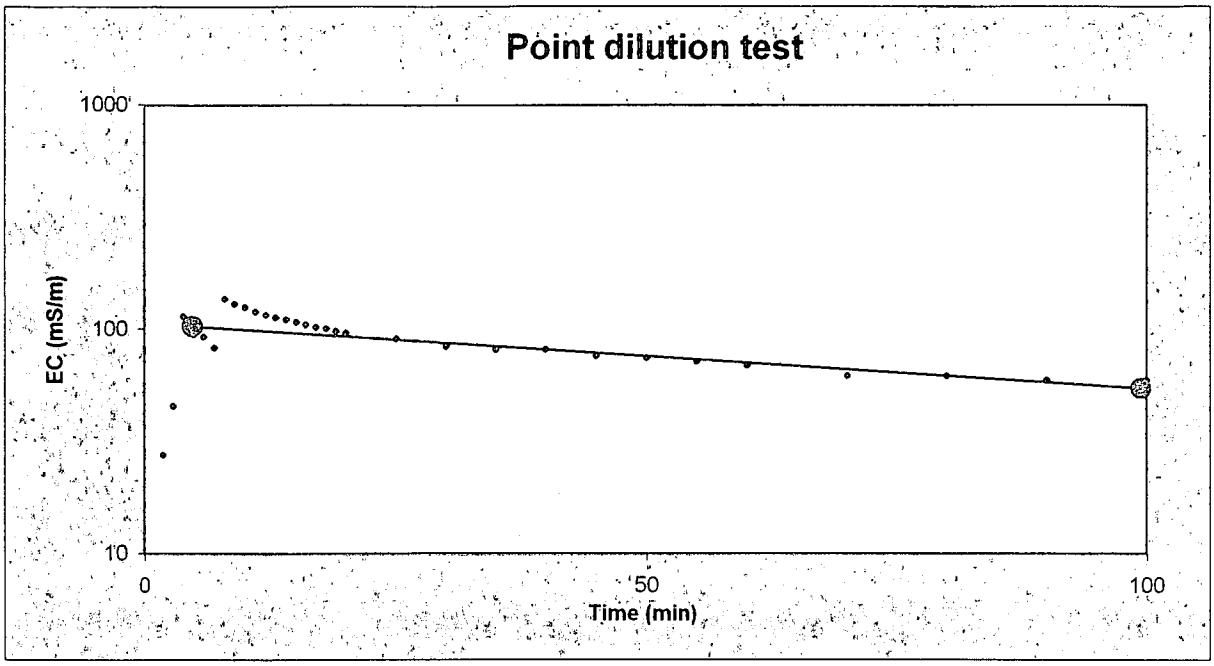

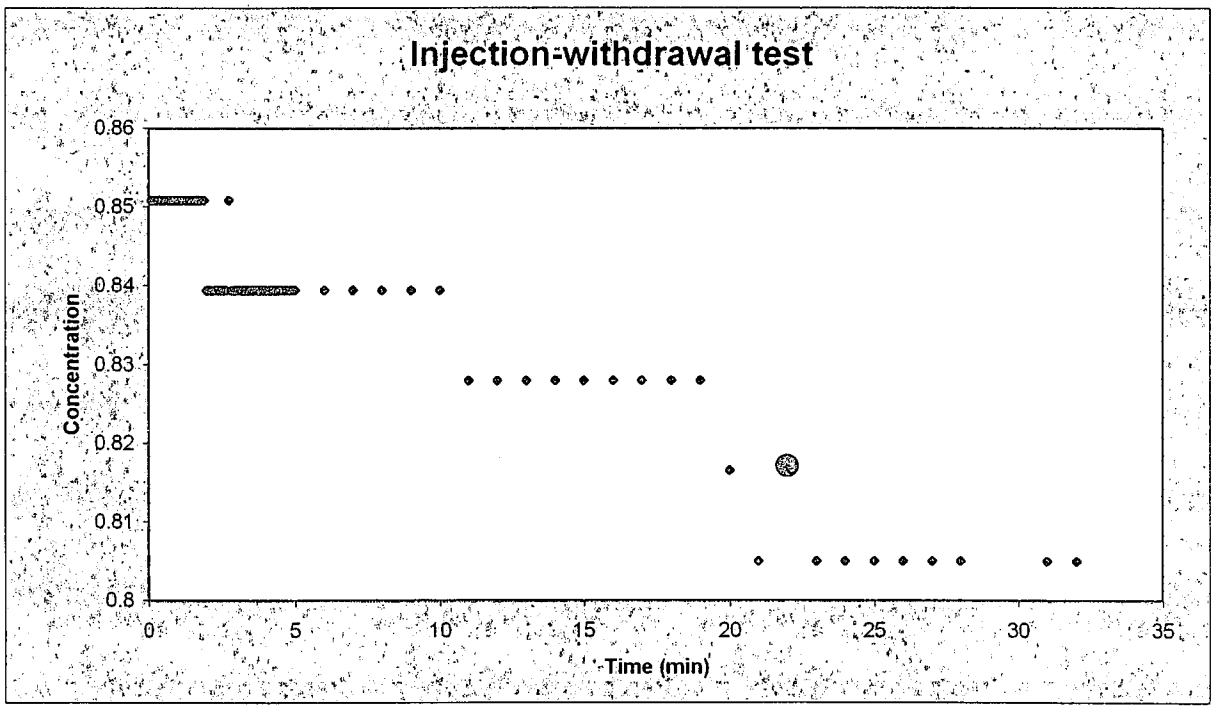

Duration of Dilution Test	140 min
Discharge Rate of Pump Back Phase	0.2 l/s
Darcy-Velocity (from Point Dilution Test)	0.39 m/day
Seepage Velocity (from Withdrawal Test)	11.45 m/day
Kinematic Porosity	3.4 %

BH 2 **26 - 28 m**

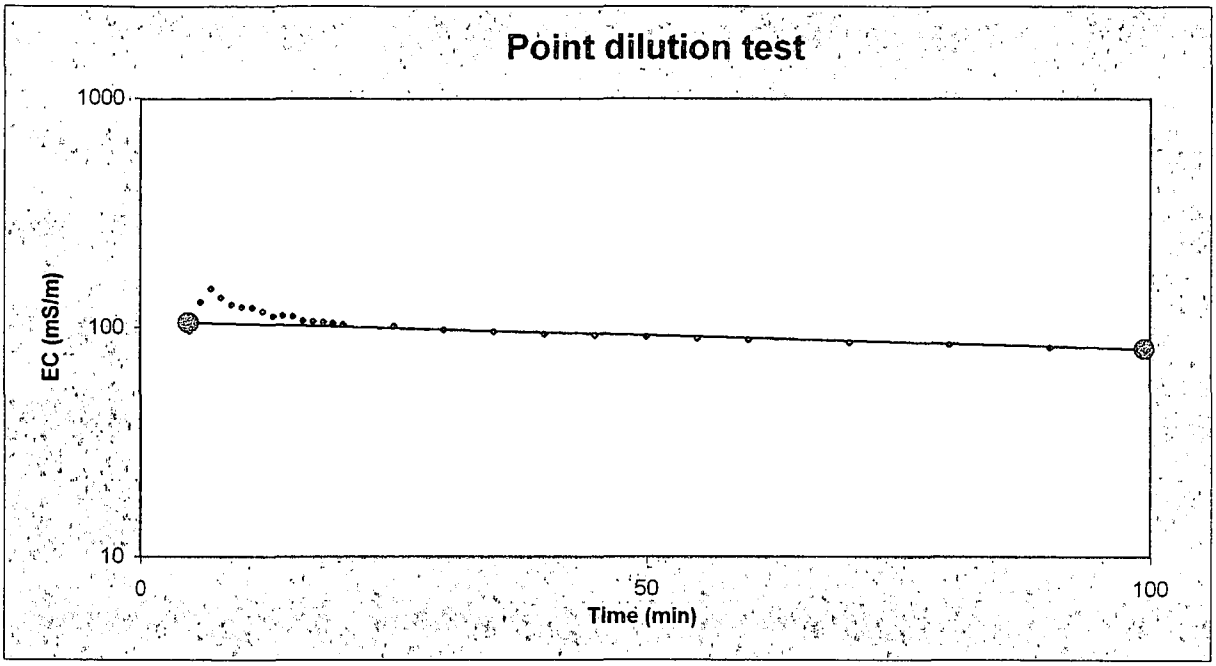

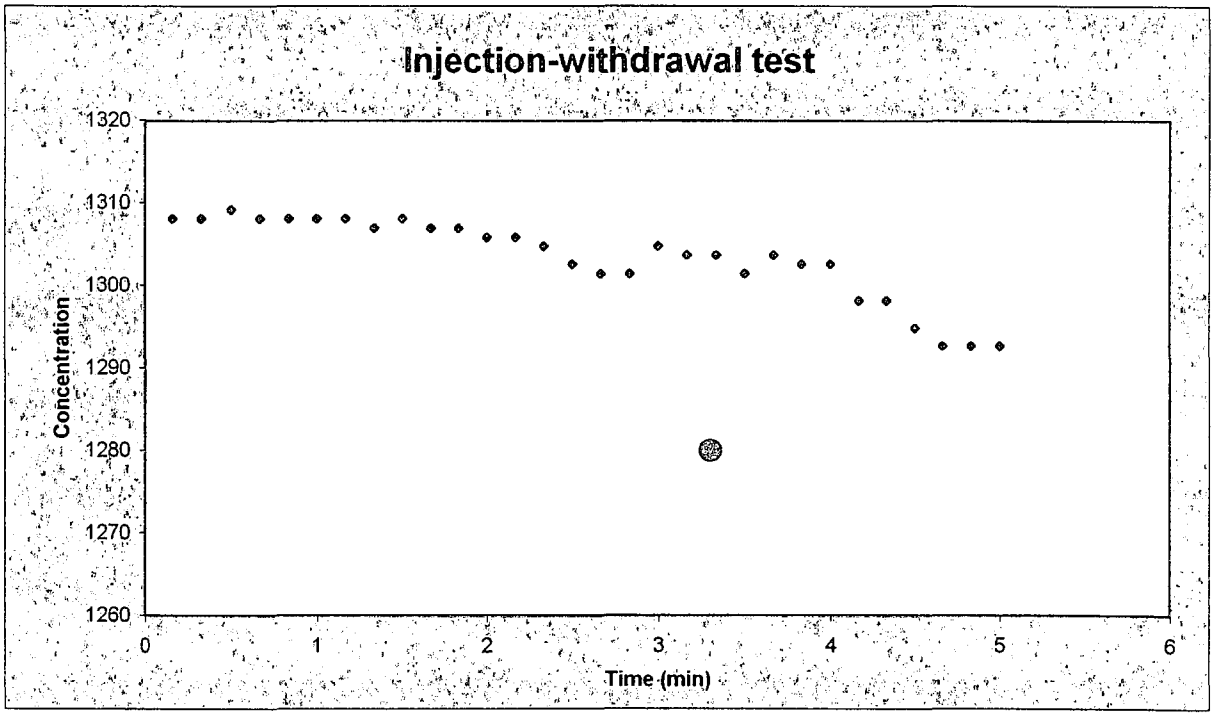

Duration of Dilution Test	90 min
Discharge Rate of Pump Back Phase	0.2 l/s
Darcy-Velocity (from Point Dilution Test)	0.16 m/day
Seepage Velocity (from Withdrawal Test)	10.01 m/day
Kinematic Porosity	1.6 %

BH 2 **29 - 31 m**

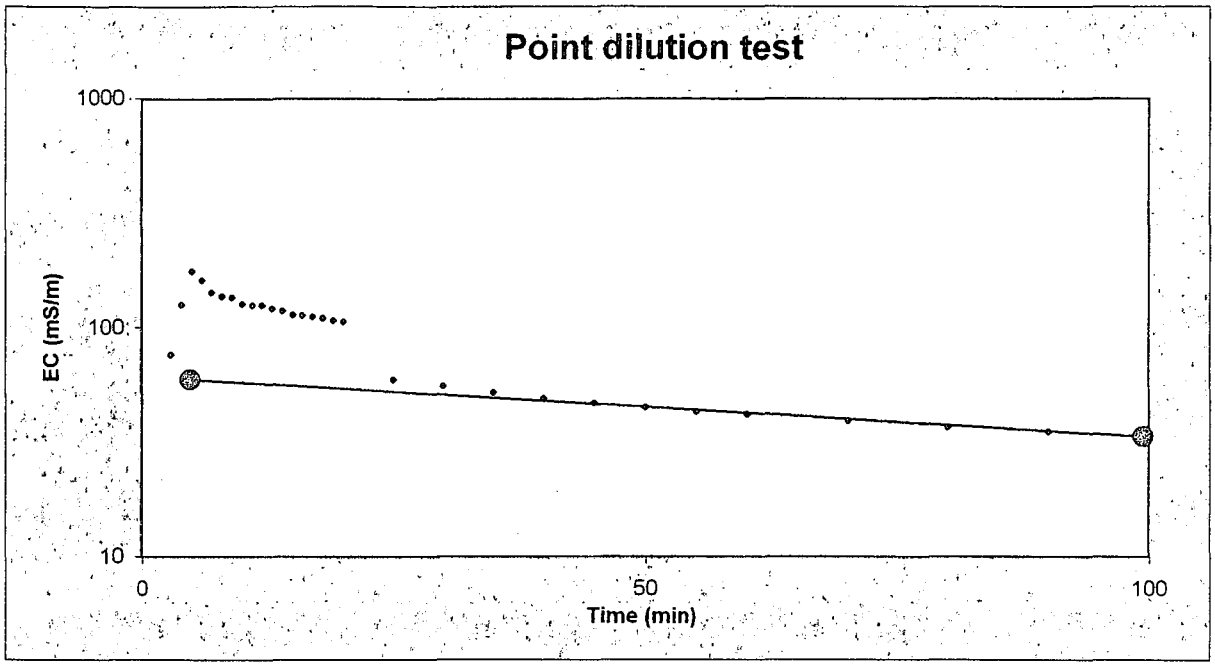

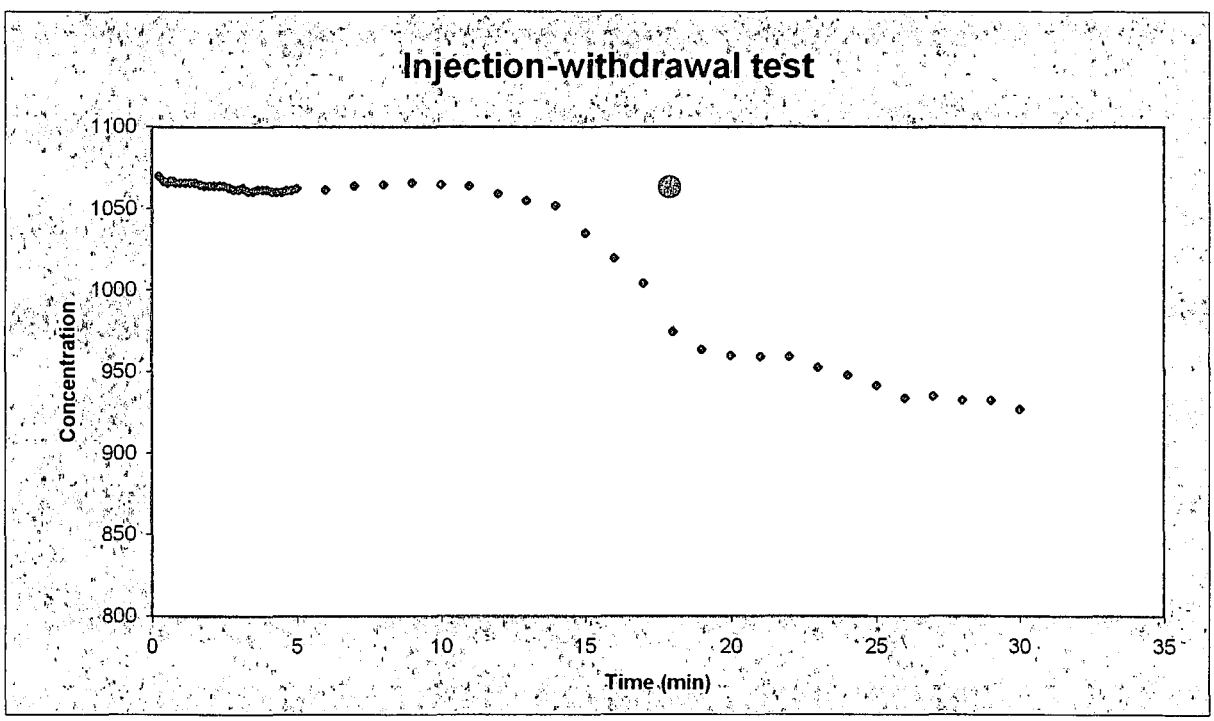

Duration of Dilution Test	120 min
Discharge Rate of Pump Back Phase	0.2 l/s
Darcy-Velocity (from Point Dilution Test)	0.35 m/day
Seepage Velocity (from Withdrawal Test)	14.11 m/day
Kinematic Porosity	2.5 %

BH 2 **34 - 36 m**

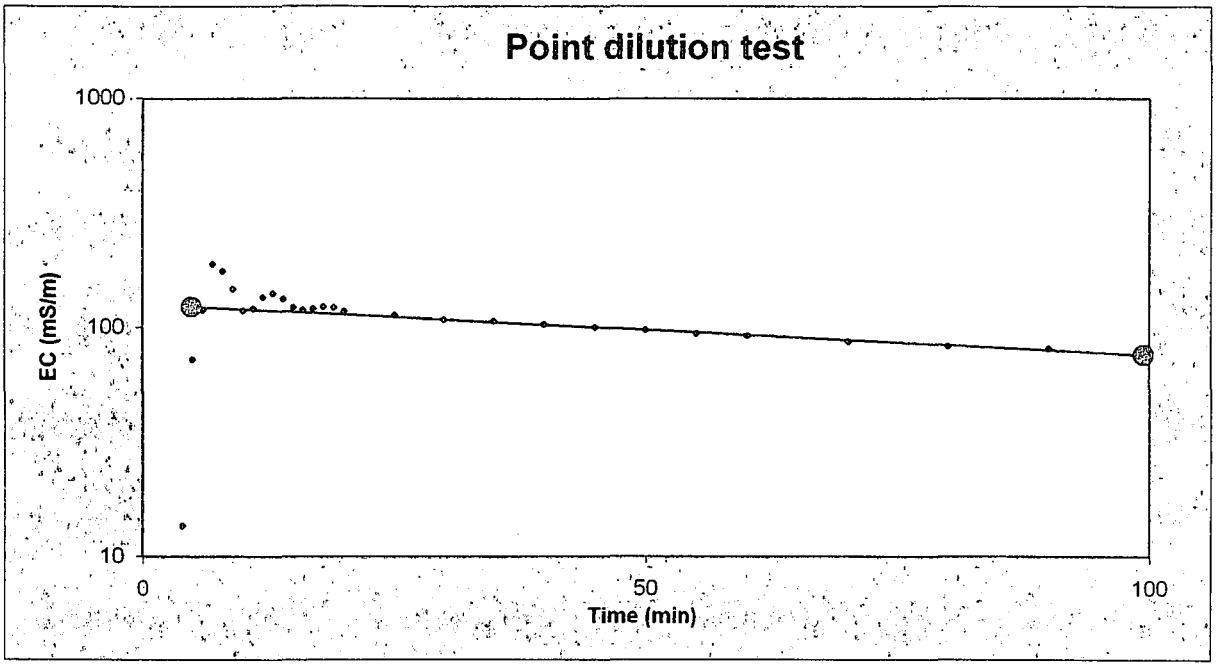

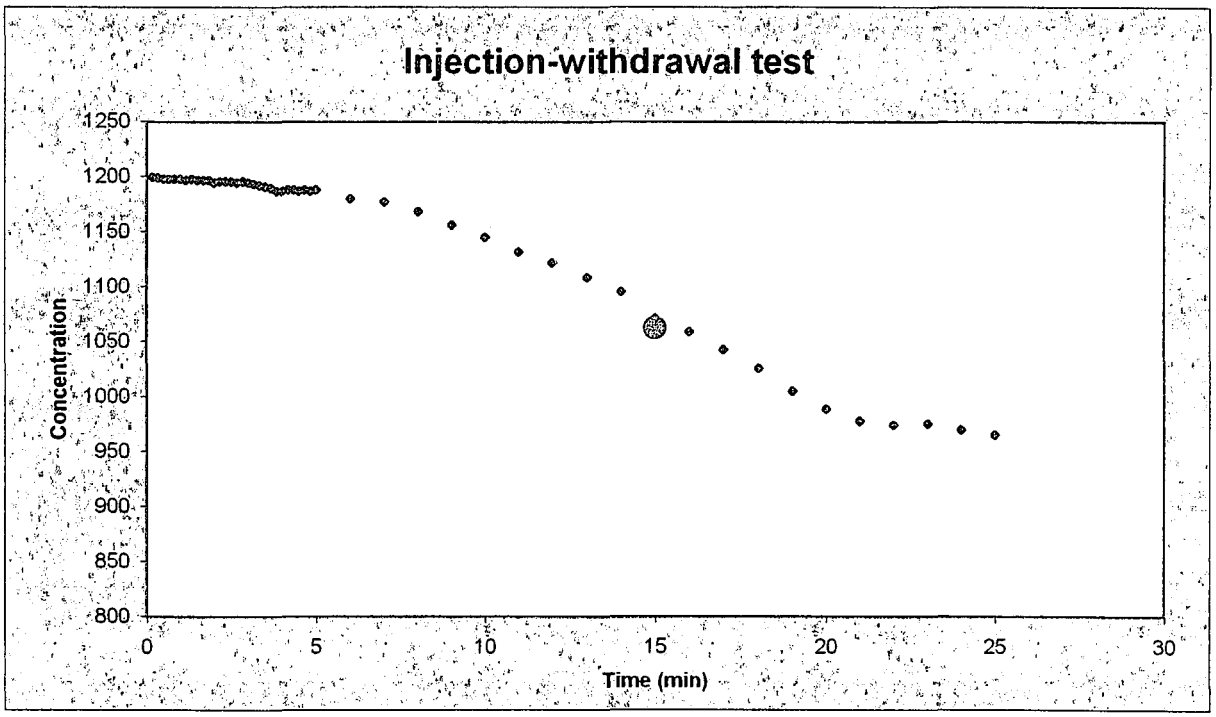

Duration of Dilution Test	120 min
Discharge Rate of Pump Back Phase	0.2 l/s
Darcy-Velocity (from Point Dilution Test)	0.3 m/day
Seepage Velocity (from Withdrawal Test)	13.95 m/day
Kinematic Porosity	2.1 %

BH 2 **39 - 41 m**

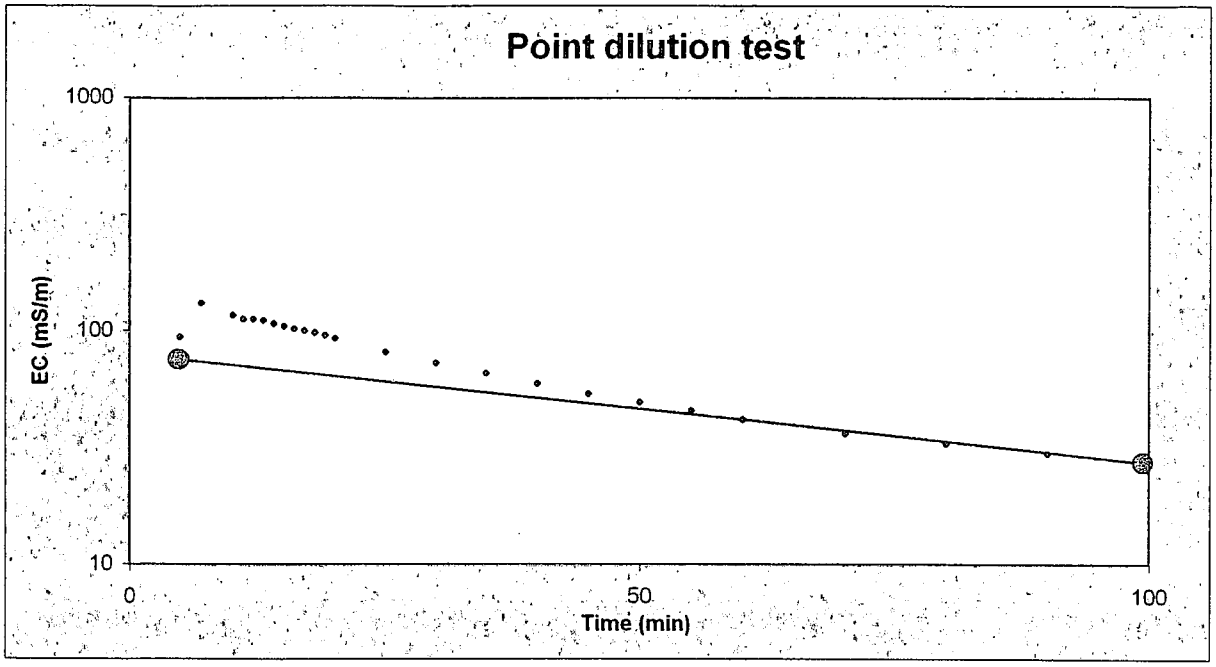

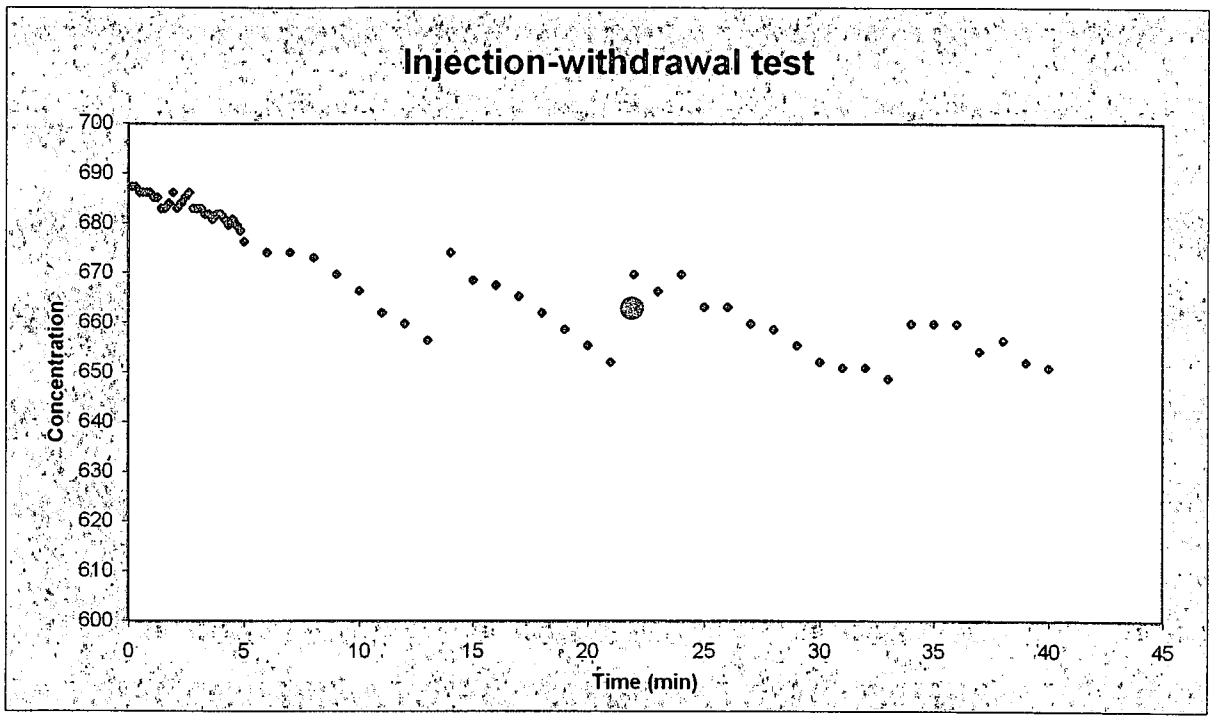

Duration of Dilution Test	90 min	
Discharge Rate of Pump Back Phase	0.1 l/s	
Darcy-Velocity (from Point Dilution Test)	0.62 m/day	
Seepage Velocity (from Withdrawal Test)	8.68 m/day	?
Kinematic Porosity	7.1 %	?

BH 2 **44 - 46 m**

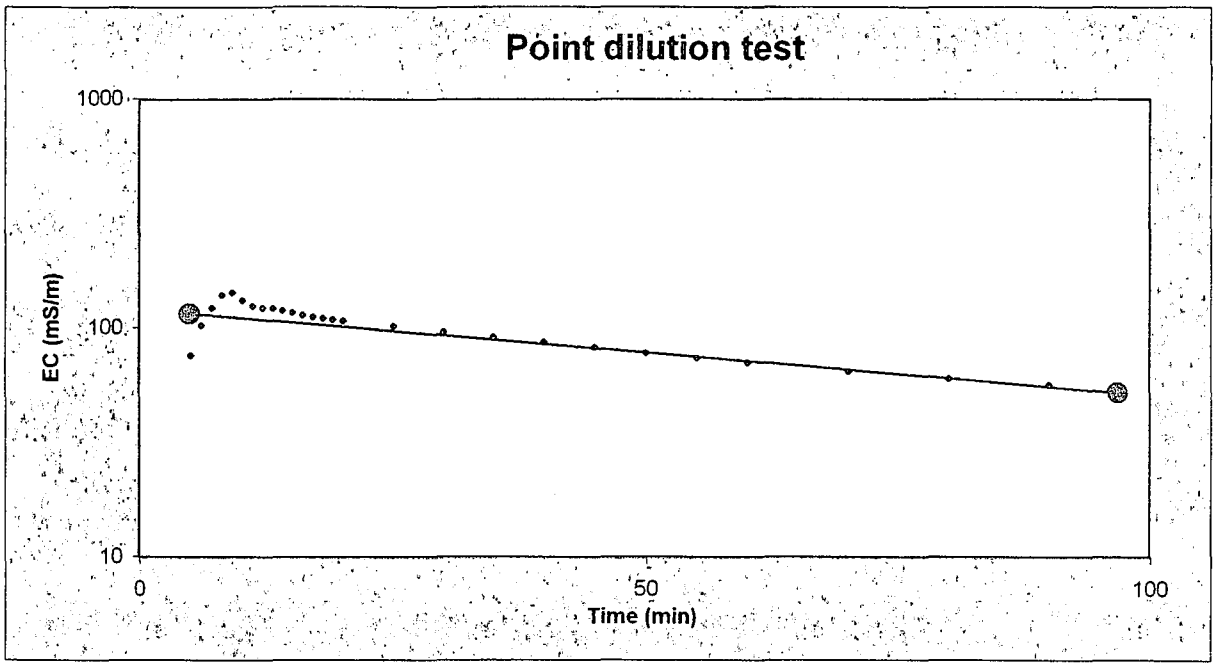

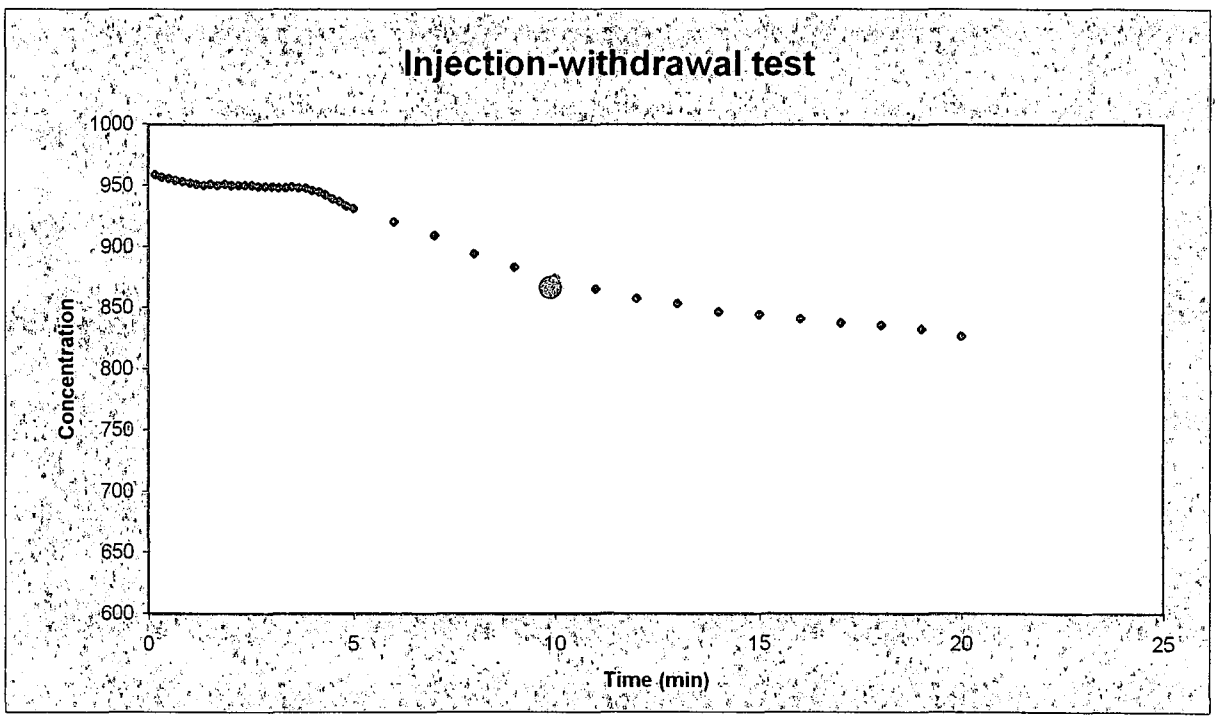

Duration of Dilution Test	90 min
Discharge Rate of Pump Back Phase	0.2 l/s
Darcy-Velocity (from Point Dilution Test)	0.5 m/day
Seepage Velocity (from Withdrawal Test)	9.76 m/day
Kinematic Porosity	5.1 %

BH 2 **49 - 51 m**

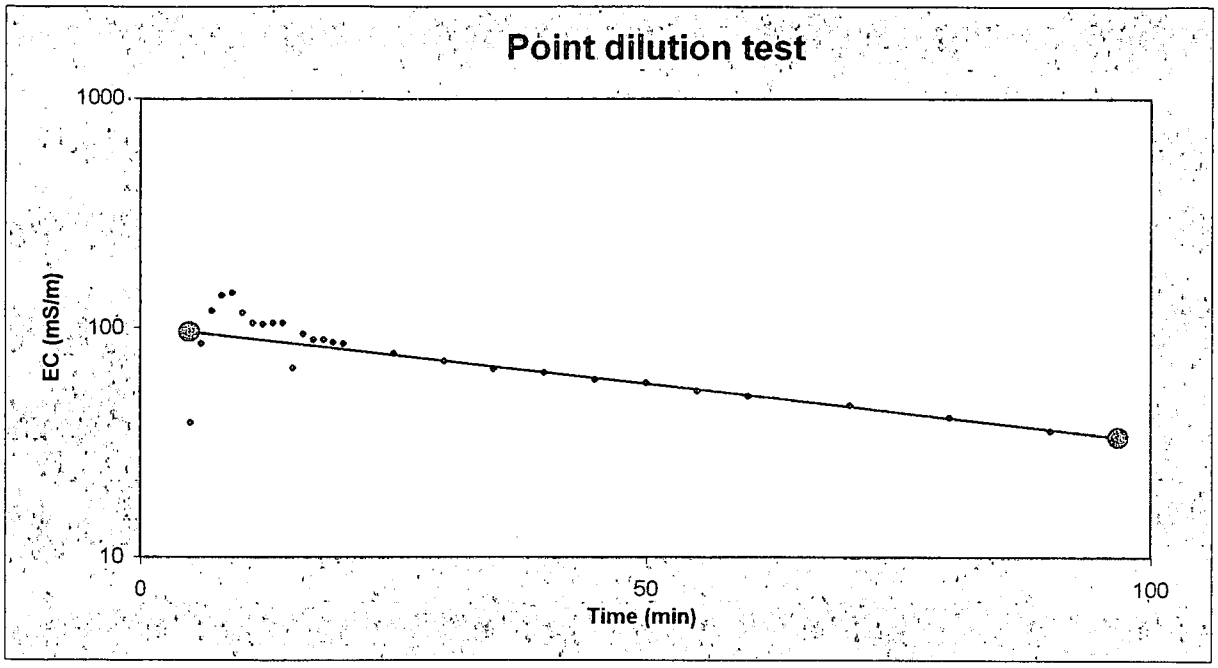

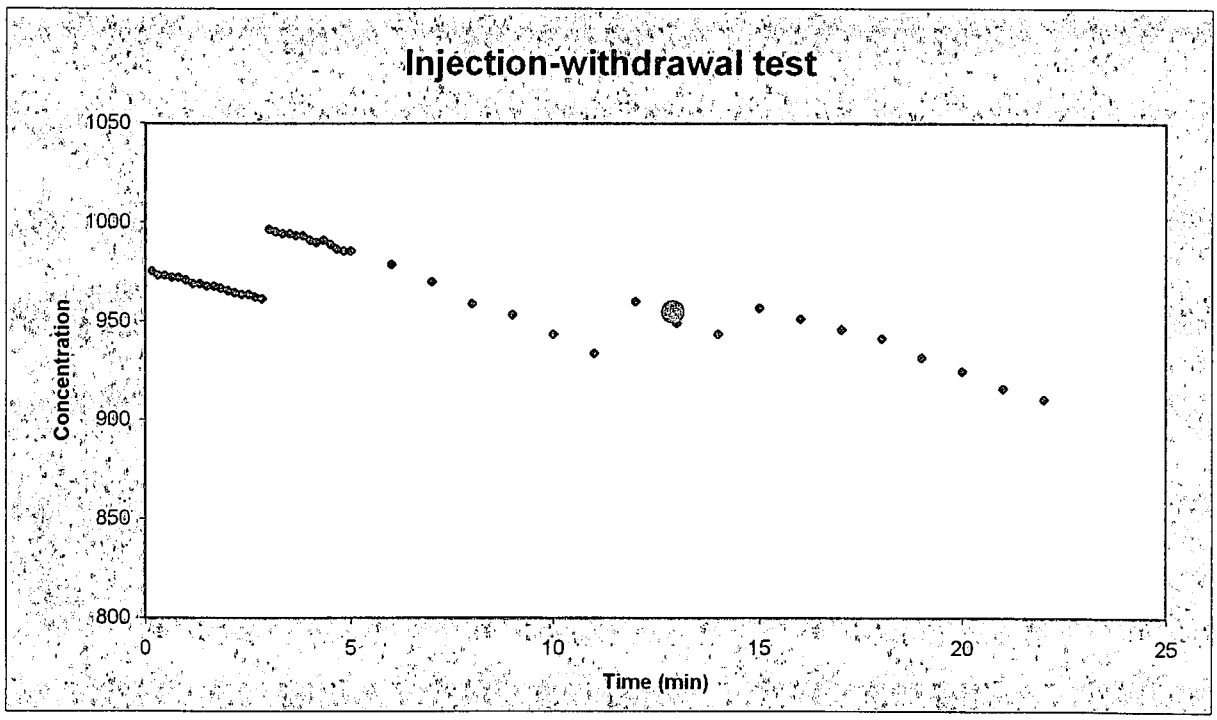

Duration of Dilution Test	90 min	
Discharge Rate of Pump Back Phase	0.1 l/s	
Darcy-Velocity (from Point Dilution Test)	0.66 m/day	
Seepage Velocity (from Withdrawal Test)	4.76 m/day	?
Kinematic Porosity	13.9 %	?

BH 2 **54 - 56 m**

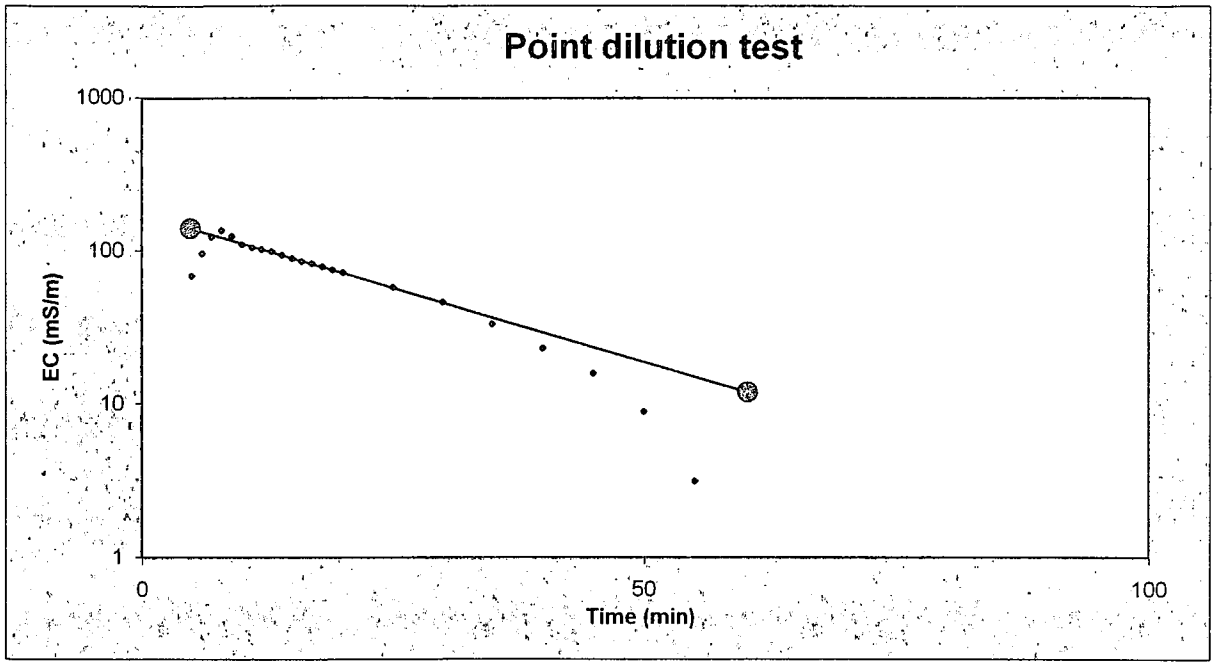

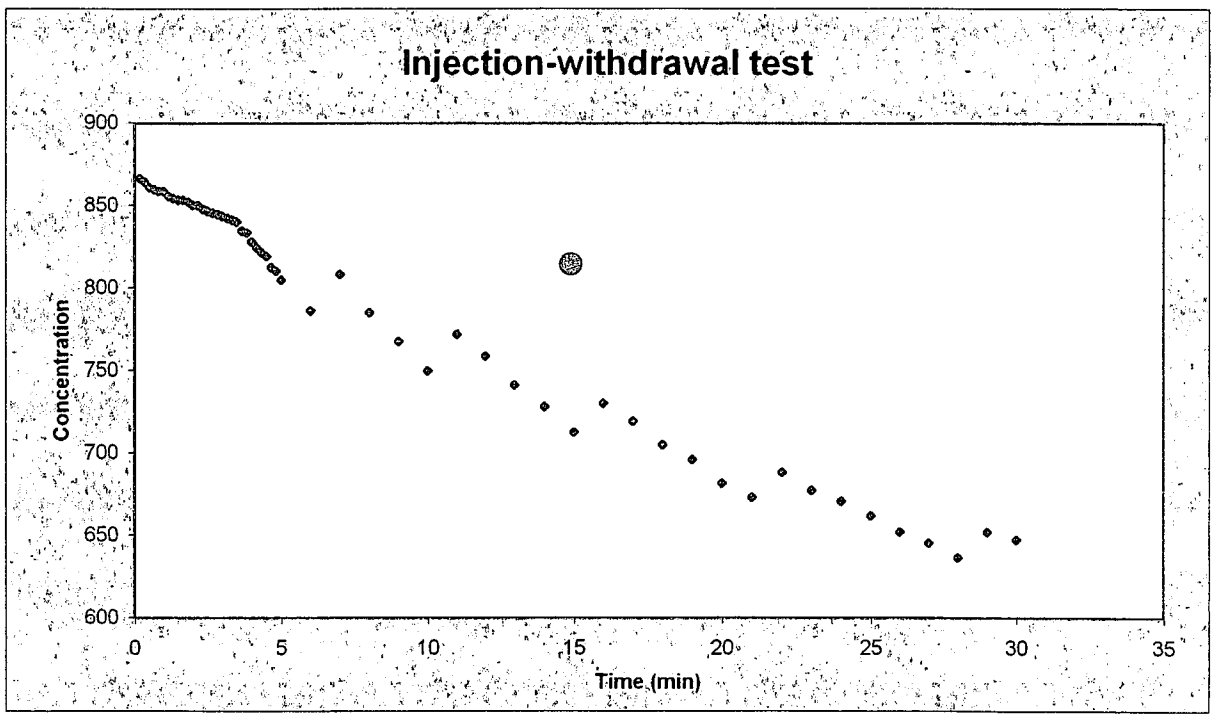

Duration of Dilution Test	60	min
Discharge Rate of Pump Back Phase	0.2	l/s
Darcy-Velocity (from Point Dilution Test)	2.56	m/day
Seepage Velocity (from Withdrawal Test)	n.a.	m/day
Kinematic Porosity	n.a.	%

APPENDIX B

DATA SHEETS FOR FIELD MEASUREMENTS

Measurement of Tracer Tests — Date: — Page: 1

Single Well Test with Point Dilution and Injection Withdrawal

	Name	BH Radius (m)	Type of Pump	Depth of Pump (m)	Depth of Inject. (m)	Depth of Circul. (m)	Length of Test (m)	Discharge (l/s)	Used Tracer	Mass of Tracer (kg)
Inject./Abstr. BH										
Observation BH										

Distance Abstract.- Observ.		Circulating Water in Borehole (l)		Circulatingtime (sec.)	
Natural Hydraulic Gradient		Added Volume by Injection (l)		Injectionduration (sec.)	
Forced Hydraulic Gradient		Complete Volume (l)		Mixingtime bef. Injection (min.)	

Point Dilution

Start of Injection (tj = 0)

Time tp (min.)	Conc. of Tracer 1 ( )	Conc. of Tracer 2 ( )	Flowmeter Discharge (l or l/s)
Instrum.			
tj = 0			
1			
2			
3			
4			
5			
6			
7			
8			
9			
10			
11			
12			
13			
14			
15			
16			
17			
18			
19			
20			
25			
30			
35			
40			
45			
50			
55			
60			
70			
80			
90			
100			
110			
120			
150			
180			
210			
240			
270			
300			
330			
360			
390			
420			
450			
480			
510			
540			

Pump Back Phase

tp = tj + **min.**

Time tj (min.)	Water Level (m) Abstract.	Water Level (m) Observ.	Flowmeter Discharge (l or l/s)
Instrum.			
tp = 0			
0.5			
1			
1.5			
2			
2.5			
3			
4			
5			
6			
7			
8			
9			
10			
11			
12			
13			
14			
15			
16			
17			
18			
19			
20			
25			
30			
35			
40			
45			
50			
55			
60			
70			
80			
90			
100			
110			
120			
130			
140			
150			
160			
170			
180			
190			
200			
210			
220			
230			

Constant Rate Pumping

Start of Pumping (tp = 0)

Time tj (min.)	Water Level (m) Abstract.	Water Level (m) Observ.	Flowmeter Discharge (l or l/s)
240			
250			
260			
270			
280			
290			
300			
310			
320			
330			
340			
350			
360			
370			
380			
390			
400			
410			
420			
430			
440			
450			
460			
470			
480			
490			
500			
510			
520			
530			
540			
550			
560			
570			
580			
590			
600			
610			
620			
630			
640			
650			
660			
670			
680			
690			
700			
710			
720			
END			

Measurement of Tracer Tests — Date: — Page: 2

Single Well Test with Point Dilution and Injection Withdrawal

	Name	BH Radius (m)	Pump	Depth of Pump (m)	Depth of Inject. (m)	Depth of Circul. (m)	Length of Test (m)	Discharge (l/s)	Used Tracer	Mass of Tracer (kg)
Inject./Abstr. BH										
Observation BH										

Pump Back Phase = Injection Withdrawal — Start of Pumping (tp = — tp = tj + min.

Time tp (sec.)	Conc. of Tracer 1 ( )	Conc. of Tracer 2 ( )	Time tp (min.)	Conc. of Tracer 1 ( )	Conc. of Tracer 2 ( )	Time tp (min.)	Conc. of Tracer 1 ( )	Conc. of Tracer 2 ( )	Time tp (min.)	Conc. of Tracer 1 ( )	Conc. of Tracer 2 ( )
Instrum.			6			62			185		
tp = 0			7			64			190		
5			8			66			195		
10			9			68			200		
15			10			70			205		
20			11			72			210		
25			12			74			215		
30			13			76			220		
35			14			78			225		
40			15			80			230		
45			16			82			235		
50			17			84			240		
55			18			86			245		
60			19			88			250		
65			20			90			255		
70			21			92			260		
75			22			94			265		
80			23			96			270		
85			24			98			275		
90			25			100			280		
95			26			102			285		
100			27			104			290		
105			28			106			295		
110			29			108			300		
115			30			110			310		
120			31			112			320		
125			32			114			330		
130			33			116			340		
135			34			118			350		
140			35			120			360		
145			36			122			370		
150			37			124			380		
155			38			126			390		
160			39			128			400		
165			40			130			410		
170			41			132			420		
175			42			134			430		
180			43			136			440		
185			44			138			450		
190			45			140			460		
195			46			142			470		
200			47			144			480		
205			48			146			490		
210			49			148			500		
215			50			150			510		
220			51			153			520		
225			52			156			530		
230			53			159			540		
240			54			162			550		
250			55			165			560		
260			56			168			570		
270			57			171			580		
280			58			174			590		
290			59			177			600		
300			60			180			Remark		

Measurement of Tracer Tests — Date: — Page: 1

Multiple Well Test with Point Dilution and Radial Convergence

	Name	BH Radius (m)	Type of Pump	Depth of Pump (m)	Depth of Inject. (m)	Depth of Circul. (m)	Length of Test (m)	Discharge (l/s)	Used Tracer	Mass of Tracer (kg)
Injection BH										
Abstraction BH										

Distance Inject. - Abstract.		Circulating Water in Borehole(l)		Circulatingtime (sec.)	
Natural Hydraulic Gradient		Added Volume by Injection (l)		Injectionduration (sec.)	
Forced Hydraulic Gradient		Complete Volume (l)		Mixingtime bef. Injection (min.)	

Constant Rate Pumping bef. and while Radial Convergent

Point Dilution

Start of Pumping (tp = 0)

tj = tp + **min.**

Start of Injection (tj = 0)

Time tp (min.)	Water Level (m) Abstract.	Water Level (m) Inject.	Flowmeter Discharge (l or l/s)	Time tp (min.)	Water Level (m) Abstract.	Water Level (m) Inject.	Flowmeter Discharge (l or l/s)	Time tj (min.)	Conc. of Tracer 1 ( )	Conc. of Tracer 2 ( )	Flowmeter Discharge (l or l/s)
Instrum.				570				Instrum.			
tp = 0				600				tj = 0			
1				630				1			
2				660				2			
3				690				3			
4				720				4			
5				750				5			
6				780				6			
7				810				7			
8				840				8			
9				870				9			
10				900				10			
11				930				11			
12				960				12			
13				990				13			
14				1020				14			
15				1050				15			
16				1080				16			
17				1110				17			
18				1140				18			
19				1170				19			
20				1200				20			
25				1230				25			
30				1260				30			
35				1290				35			
40				1320				40			
45				1350				45			
50				1380				50			
55				1410				55			
60				1440				60			
70				1470				70			
80				1500				80			
90				1530				90			
100				1560				100			
110				1590				110			
120				1620				120			
150				1650				150			
180				1680				180			
210				1710				210			
240				1740				240			
270				1770				270			
300				1800				300			
330				1830				360			
360				1860				420			
390				1890				480			
420				1920				540			
450				1950				600			
480				1980				660			
510				2010				720			
540				2040				780			

Measurement of Tracer Tests — Date: — Page: 2

Multiple Well Test with Point Dilution and Radial Convergence

	Name	BH Radius (m)	Type of Pump	Depth of Pump (m)	Depth of Inject. (m)	Depth of Circul. (m)	Length of Test (m)	Discharge (l/s)	Used Tracer	Mass of Tracer (kg)
Injection BH										
Abstraction BH										

Radial Convergence | Start of Injection (tj = C | **tj = tp +** **min.**

Time tj (min.)	Conc. of Tracer 1 ( )	Conc. of Tracer 2 ( )	Time tj (min.)	Conc. of Tracer 1 ( )	Conc. of Tracer 2 ( )	Time tj (min.)	Conc. of Tracer 1 ( )	Conc. of Tracer 2 ( )	Time tj (min.)	Conc. of Tracer 1 ( )	Conc. of Tracer 2 ( )
Instrum.			270			545			820		
tj = 0			275			550			825		
5			280			555			830		
10			285			560			835		
15			290			565			840		
20			295			570			845		
25			300			575			850		
30			305			580			855		
35			310			585			860		
40			315			590			865		
45			320			595			870		
50			325			600			875		
55			330			605			880		
60			335			610			885		
65			340			615			890		
70			345			620			895		
75			350			625			900		
80			355			630			905		
85			360			635			910		
90			365			640			915		
95			370			645			920		
100			375			650			925		
105			380			655			930		
110			385			660			935		
115			390			665			940		
120			395			670			945		
125			400			675			950		
130			405			680			955		
135			410			685			960		
140			415			690			965		
145			420			695			970		
150			425			700			975		
155			430			705			980		
160			435			710			985		
165			440			715			990		
170			445			720			995		
175			450			725			1000		
180			455			730			1005		
185			460			735			1010		
190			465			740			1015		
195			470			745			1020		
200			475			750			1025		
205			480			755			1030		
210			485			760			1035		
215			490			765			1040		
220			495			770			1045		
225			500			775			1050		
230			505			780			1055		
235			510			785			1060		
240			515			790			1065		
245			520			795			1070		
250			525			800			1075		
255			530			805			1080		
260			535			810			1085		
265			540			815			1090		

APPENDIX C

SOFTWARE PROGRAMS

- **TRACER PLAN**

- **TRACER**

The developed software programs can be purchased for free from both the Institute for Groundwater Studies, University of the Free State, Bloemfontein and the author.

- www.uovs.ac.za/faculties/igs
- gerrit@igsnt.uovs.ac.za
- kornelius@umvoto.com

SUMMARY

Water resources in South Africa are already being stressed and the country is slowly becoming a water-scarce country. This presents a challenge to all water resource managers to ensure that the basic water needs of every South African are met. A good estimation of the aquifer parameters is the basis of managing groundwater resources and understanding groundwater flow and transport processes. Because most of the suitable groundwater resources in Southern Africa occur in fractured rock aquifers, this thesis focuses on aquifer parameter estimation in fractured rock aquifers.

A guideline for aquifer parameter estimation in fractured rocks is derived, based on a combination of hydraulic and tracer tests. The methods included account for the unknown flow geometry and the resulting uncertainty by introducing the non-integer flow dimension, which can be calculated from hydraulic and / or tracer test data. The guideline includes:

- New methods for conducting and analysing tracer tests accounting for non-integer flow dimension prevailing during the tests in fractured aquifers.
- A new method for estimating the kinematic porosity from single-well tracer tests.
- Description and comparison of the use of a three-dimensional numerical model for aquifer parameter estimation.
- The software TRACER-PLAN to enable the geohydrologist to conduct effective tracer tests. Depending on the type of test and the geological structure the test set-up, such as discharge rates, amount of tracer and duration of the test, can be optimised.
- To simplify and unify the analysing procedure the software TRACER enables the user to choose the correct analysing method depending on the test set-up and the conceptual model of groundwater flow. Most of the analysing procedures mentioned in this thesis are included.

While the approaches for estimating the hydraulic parameters from pumping test data are commonly used methods, which are adapted to the situation in Southern Africa, new approaches to analyse tracer test data are developed, which account in a more general way for the unknown geometry.

A combination of hydraulic and tracer tests including analysing procedure is proposed, which enables the hydrogeologist to estimate important hydraulic and transport parameters from the results of one test rather than conducting different tests. Depending on the purpose of the investigation, two types of combined tests are developed. As minimum requirement conducting and analysing a single-well test is suggested. If an observation borehole in the vicinity is available, a multiple-well test should be conducted.

The proposed methods were used in case studies with different geological settings and compared to each other. From the results of the case studies and theoretical models it can be concluded that

- analytical methods for estimating the hydraulic properties of fractured rock aquifers must be used with precaution, even when the correct conceptual model is chosen,
- for more accurate estimation numerical models, preferable a three-dimensional numerical model, should be used,
- the developed methods for analysing tracer test data, using the concept of fractional flow dimension, will yield more accurate and normally higher values for the flow velocity than the common methods, using the length of the tested section and a flow dimension of 2,
- the developed methods for analysing tracer test data, using the concept of fractional flow dimension, are applicable in different geological settings,
- the developed method for estimating the kinematic porosity from a single-well tracer test is generally applicable in both the fracture zone and the matrix, but the accuracy depends upon the correct conducting procedure,
- the validity and accuracy of the results depends mainly on the quality of the conducting procedure and the correct conceptual model for the analysing procedure.

The requirement for the analysing procedure can be summarised as:

- From the hydraulic test data the conceptual model should be derived, using diagnostic plots and derivatives, as integrated in the software TRACER or in other software programs such as FC and TPA
- The hydraulic data should be analysed applying the approach of non-integer flow dimension, as integrated in the software TRACER.
- If necessary numerical models should be used for complete parameter estimation.
- The tracer test data should be analysed, applying the approach of non-integer flow dimension, as integrated in the software TRACER.

The effect of matrix diffusion on solute transport in fractured aquifers is immanent, but no existing method is able to simulate it properly. Further research in estimating the impact of matrix diffusion on the plume movement and in developing a suitable method to simulate and quantify its effect is therefore strongly recommended.

OPSOMMING

Waterbronne in Suid Afrika is onder redelike groot druk, omdat Suid Afrika stadig maar seker 'n waterskaars land raak. Dit bied dus 'n uitdaging aan alle waterbronbestuurders om te verseker dat daar aan die basiese waternood in Suid Afrika voldoen word. 'n Goeie bepaling van die akwifeerparameters vorm die basis van bestuur van 'n grondwaterbron, asook die verstaan van grondwatervloei en vervoerprosesse. Omdat meeste van die bruikbare grondwaterbronne in Suid Afrika in fraktuur akwifere voorkom, fokus die tesis op akwifeerparameter bepaling in 'n fraktuur akwifeer.

Die afleiding van riglyne vir akwifeerparameter bepaling in fraktuur akwifere is gebasseer op 'n kombinasie van hidrouliese en spoorder toetse. Die metodes ingesluit in die tesis dien as beskrywing vir die onbekende vloeigeometrie asook die gevolglike onsekerheid, deur die bekendstelling van die fraksionele vloeidimensie wat bereken kan word vanaf die hidrouliese en/of spoorder toets data. Riglyne sluit in:

- Nuwe metodes vir uitvoering en analisering van spoorder toetse om fraksionele vloeidimensie te bepaal, is verkry deur toetse op die fraktuur akwifeer.
- 'n Nuwe metode vir die bepaling van die kinetiese porositeit vir 'n enkel boorgat spoorder toets.
- Beskrywing en vergelyking van die gebruik van 'n drie-dimensionele numeriese model vir akwifeerparameter bepaling.
- Die sagteware TRACER-PLAN, wat die geohidroloog in staat stel om effektiewe spoorder toetse uit te voer. Afhangende van die tipe toetse wat gedoen word en die geologiese struktuur kan die toetsopset, soos byvoorbeeld onttrekkings tempos, die hoeveelheid tracer en die duurte van die toets, geoptimeer word.
- Om die analiseringsprosedure te vereenvoudig en te unifiseer kan die sagteware TRACER die gebruiker instaat stel om die regte analiseringsmetodes te kies, afhangende van die toetsopstelling en die konsepsieële model van die grondwater vloei. Meeste van die analiseringsprosedure wat in die tesis genoem word, is ingesluit.

Terwyl die aanvoering vir die bepaling van die hidroliese parameters vir die pomptoets data eenvoudige metodes is, wat geskik is vir situasies in Suider Afrika, word nuwe maniere ontwikkel om spoorder toetse te analiseer, wat meer algemeen die onbekende geometrie bepaal.

'n Kombinasie van hidroliese en spoorder toetse, insluitend analiseringsprosedure, word voorgestel, wat die geohidroloog instaat stel om die belangrike hidrouliese en transport parameters vanaf die resultate van een toets te verkry eerder as om verskillende toetse uit te voer. Afhangende van die doel van die ondersoek, is twee tipes gekombineerde toetse ontwikkel. As 'n minimum vereiste, word uitvoering en analisering van 'n enkel boorgat toets voorgestel. As 'n observasie boorgat in die omgewing beskikbaar is, moet 'n veelvoudige boorgat toets op die boorgat uitgevoer word.

Die voorgestelde metodes is gebruik in veldondersoeke met verskillende geologiese omgewings en word ook vergelyk met mekaar. Vanaf die resultate van die veldondersoeke en die teoretiese modelle, kan die volgende gevolgtrekkings gemaak word.

- Analitiese metodes vir die bepaling van hidrouliese eienskappe van die fraktuur akwifeer moet gebruik word met voorsorg, selfs al word die regte konsepsieële model gebruik.
- Baie meer akkurate numeriese berekeningsmodelle, by voorkeur 'n drie-dimensionele numeriese model, moet gebruik word.
- Die ontwikkelde metodes vir die analisering van spoorder toets data, deur gebruik te maak van die konsep van fraksionele vloeidimensies, sal meer akkurate en normaalweg hoër waardes gee vir die vloeisnelheid as met die gewone metodes, deur gebruik te maak van die getoetste seksie en 'n vloeidimensie van 2.
- Die ontwikkelde metodes vir analisering van spoorder data, deur gebruik te maak van fraksionele vloeidimensies, is toepaslik in verskillende geologiese omgewings.
- The ontwikkelde metode vir die bepaling van kinetiese porositeit vir 'n enkel boorgat tracer toets is algemeen toepaslik in beide die fraktuur sone en die matriks, maar die akkuraatheid hang af van die korrekte prosedure.
- Die geldigheid en akkuraatheid van die toetse hang hoofsaaklik af van die gehalte van die prosedure en die korrekte konsepsieële model vir die analiseringsprosedure.

Die vereistes vir die analiseringsprosedure kan soos volg opgesom word:

- Vanaf die hidroliese toets data kan die konsepsieële model afgelei word, deur gebruik te maak van die diagnostiese grafiek en afgeleides, soos geintegreer in die sagteware TRACER of in ander sagteware programme, soos byvoorbeeld, FC en TPA.
- Die hidroliese data moet geanaliseer word deur gebruik te maak van die benadering van nie-integrale getalvloei, soos geintegreer in die sagteware TRACER.
- Indien nodig, moet numeriese modelle gebruik word vir volledige parameter berekening.
- Die spoorder toets data moet geanaliseer word, deur gebruik te maak van die benadering van fraksionele vloeidimensie, soos geintegreer in die sagteware TRACER.

Die effek van matriks diffusie op oplosbare vervoering in gefraktueerde akwifere is inwonend (innerlik), maar geen bestaande metode is daartoe instaat om dit behoorlik te simuleer nie. Verdere navorsing in die bepaling van die impak van matriks diffusie op die pluim in beweging en ontwikkeling, asook 'n geskikte metode vir die simulering en kwantifisering van die effek word ten sterkste aanbeveel.